UNIVERSITÀ DEGLI STUDI FIRENZE

PhD in

Chemical Sciences

CYCLE XXXIII

COORDINATOR Prof. PIERO BAGLIONI

Synthesis of Alkylated Azasugars and their Therapeutic Potential Against Lysosomal Storage and Neurological Disorders: the Gaucher-Parkinson Case

Academic Discipline CHIM/06

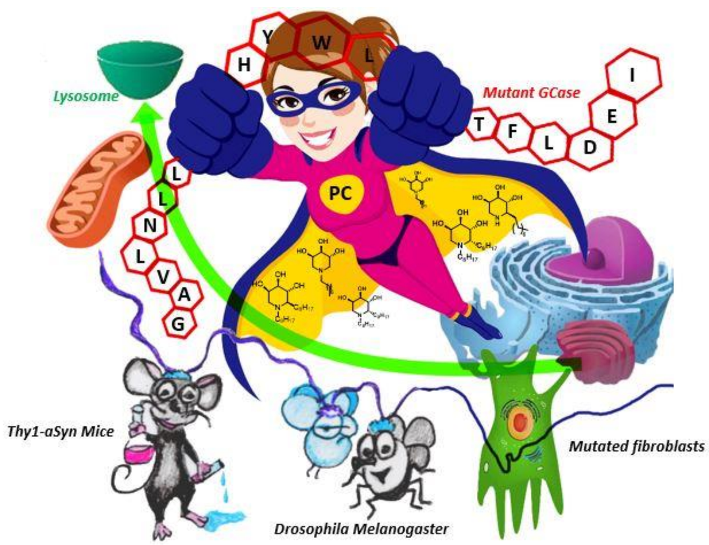

Doctoral Candidate
Dr. Francesca Clemente

Supervisor
Prof. Francesca Cardona

Years 2017/2020

UNIVERSITÀ DEGLI STUDI FIRENZE

PhD in
Chemical Sciences
CYCLE XXXIII

COORDINATOR Prof. PIERO BAGLIONI

Synthesis of Alkylated Azasugars and their Therapeutic Potential Against Lysosomal Storage and Neurological Disorders: the Gaucher-Parkinson Case

Academic Discipline CHIM/06

Doctoral Candidate
Dr. Francesca Clemente

____

Supervisor
Prof. Francesca Cardona

____

Coordinator
Prof. Piero Baglioni

____

Years 2017/2020

SUMMARY

Preface

Pharmacological chaperones (PCs) are small molecules that bind and stabilize enzymes. They can rescue the enzymatic activity of misfolded or deficient enzymes when they are used at subinhibitory concentration, thus with minimal side effects. Pharmacological Chaperone Therapy (PCT) is an emerging treatment for many Lysosomal Storage Disorders (LSDs) including Gaucher disease, the most common, which is characterized by a deficiency in the lysosomal enzyme acid β-glucosidase (GCase). Structurally, the most promising PCs for LSDs are nitrogen glycomimetics with a nitrogen atom replacing the endocyclic oxygen or the anomeric carbon of sugars, also known as iminosugars, or azasugars, respectively. As inhibitors of the carbohydrate-processing enzymes, imino- or azasugars, and other substrate analogues which behave as competitive glycosidase inhibitors, are good PC candidates.
This PhD thesis deals with straightforward synthetic strategies aimed at affording alkylated trihydroxypiperidine azasugars with different alkyl chains in different positions of the cyclic skeleton and with different configurations, starting from low cost D-mannose as starting material. The target compounds have a potential as PCs for LSDs and also for Parkinson's Disease (PD). PD is the second most common neurological disorder characterized by aggregates of α-synuclein, affecting approximately 1% of people over 60-65 years and more than 5-6% over 80-85 years. Recently, GCase mutations were shown to be a major risk factor for PD. In particular, the risk to develop the disease increases from 1% to 5% for *GBA* heterozygous patients over 60-65 years, and from 5-6% to 15% for *GBA* heterozygous patients over 80-85 years.

This doctorate is part of the doctorate research programs funded by the ''University Strategic Plan (2018-2020)''. Due to the multidisciplinary approach of this doctorate, this thesis reports not only the synthetic strategies, but also the biological evaluation towards human lysosomal enzymes, the *ex-vivo* activity on cell lines and *in-vivo* assays on animal Parkinson animal models carried out by the candidate thanks to the collaboration with national and international groups.

Chapter 1 describes the pathogenesis and current available treatments for LSDs, with particular emphasis on Gaucher disease, and the role of GCase in the pathogenesis of PD together with the main applications of azasugars as potential PCs.

Chapter 2 describes relevant examples of synthetic strategies involving the Reductive Amination (RA) step as the key ring-closure step to obtain polyhydroxypiperidines and their derivatives. It is organized according to the nitrogen containing functional moiety which takes part in the key RA ring-closing reaction. Since there is not a unified RA procedure for all type of carbonyl compounds and amines, and both reducing agent and reaction conditions can considerably vary, particular emphasis is given to these aspects. In addition, the biological properties of the most promising polyhydroxypiperidines are also reported. The content of this chapter has been published as a Minireview (**F. Clemente**, C. Matassini, F. Cardona, "The Reductive Amination Routes to the Synthesis of Piperidine Iminosugars". *Eur. J. Org. Chem.* **2020**, 4447–4462. DOI: 10.1002/ejoc.201901840.)

Chapter 3 reports the synthetic strategies developed by our group at the University of Florence to synthesize trihydroxypiperidine azasugars alkylated in different positions (and with different configurations) and their biological evaluation towards commercial and human lysosomal enzymes, and the *ex-vivo* activity on fibroblasts derived from Gaucher patients bearing the N370/RecNcil and L444P/L444P mutations. The biological evaluation towards commercial glycosidases were carried out by the research group of Prof. I. Robina, (Departamento de Química Orgánica, Facultad de Química, Universidad de Sevilla). Instead, the biological evaluation towards human lysosomal enzymes and the *ex-vivo* activity on cell lines are carried out by the candidate in the Lab of Prof. A. Morrone (Paediatric Neurology Unit and Laboratories, Neuroscience Department, Meyer Children's Hospital, and Department of Neurosciences, Pharmacology and Child Health, University of Florence (NEUROFARBA)).This work has been partially published (**F. Clemente** , C. Matassini, A. Goti, A. Morrone, P. Paoli, F. Stereoselective synthesis of C-2 alky lated trihydroxypiperidines: effect of the chain length and the configuration at C-2 on their activity as Pharmacological Chaperones for Gaucher Disease", *ACS Med. Chem. Lett* , **2019** *10*, 621 626. DOI: 10.1021/acsmedchemlett.8b00602. **F. Clemente**, C. Matassini, C. Faggi, S. Giachetti, C. Cresti, A. Morrone, P. Paoli, A. Goti, M. Martínez Bailén, F. Cardona, "Glucocerebrosidase (GCase) activity modulation by 2 alkyl trihydroxypiperidines: inhibition and pharmacological chaperoning". *Bioorg. Chem*. **2020**, *98*, 103740 103763. DOI: 10.1016/j.bioorg.2020.103740. M. G. Davighi, **F. Clemente**, C. Matassini , A. Morrone, A. Goti, M. Martínez Bailén, F. Cardona, Molecules. **2020**, 25, 4526-4549. The last results will be the object of a manuscript which will be submitted to *The Journal of Organic Chemistry*.)

Chapter 4 describes the biological evaluation of our best PCs on an animal Parkinson model, resulting from the presence of human *GBA* alleles mutated in the fruit fly (*Drosophila Melanogaster*), with the aim of reducing parkinsonian signs. *Drosophila Melanogaster*, as a non-mammalian animal, provides a simple, yet powerful, *in vivo* system for studying Gaucher Disease associated with PD. This work has been achieved thanks to a three-months period during the PhD Course spent in the Laboratory of Cell Research and Immunology (Tel Aviv University (Israel)) as a result of a nascent collaboration with Prof. M. Horowitz. The evidence in the literature that targeting GCase, also in the absence of GD mutations, has become a valid therapeutic strategy for sporadic forms of PD, has led us to testing our best PC on mouse models thanks to the collaboration with Prof. G. Mannaioni, (Department of Neurosciences, Psychology, Drug Research and Child Health (NEUROFARBA), Division of Pharmacology and Toxicology, University of Florence). The final goal is to assay our best compound on Thy1-aSyn Mice, a mouse model that overexpresses α-synuclein and mimics the characteristics of sporadic PD. Chapter 4 reports the preliminary biological results obtained on WT mice (wild type mouse-WTC57) in order to evaluate the dose, the vehicle of administration *per os* and the ability to increase the activity of the GCase in the brain.

Chapter 5 reports the synthesis of two *divalent multivalent* *polyhydroxypiperidines* exploiting the Double Reductive Amination (DRA) approach and their biological screening towards GCase and others human lysosomal glycosidases. The *chapter* also describes the role of the DRA reaction starting from dicarbonyl compounds as a straightforward tool to efficiently access polyhydroxipiperidines. Part of the content of this chapter has been published as a Chapter in a scientific Volume (TARGETS IN HETEROCYCLIC SYSTEMS Chemistry and Properties (THS): C. Matassini, **F. Clemente**, F. Cardona, THE DOUBLE REDUCTIVE AMINATION APPROACH TO THE SYNTHESIS OF POLYHYDROXYPIPERIDINES", THS Volume 23 **2019**, *14*, 283-301. Editor: Orazio A. Attanasi, Pedro Merino, Domenico Spinelli; published by Società Chimica Italiana. DOI: https://www.soc.chim.it/it/libri _collane/ths/vol_23_2019.)

Chapter 6 describes the exploitation of the synthetic strategy described in the chapter 3 in order to obtain C-2 pentyl trihydroxypiperidines with both configurations of the hydroxy group at C-3, in order to access new alkylated azasugars as potential PCS for GM1 gangliosidosis and Morquio B diseases, two other LSDs.

Chapter 1:
Azasugars: therapeutic potential against Lysosomal Storage and Neurological Disorder

1.1 Lysosomal Storage Disorders

Lysosomal storage diseases (LSDs) are a group of hereditary metabolic diseases (to date more than 70 different diseases have been described), with an overall prevalence estimated to be 1:1500-1:7000 live births, caused by mutations in genes that encode proteins involved in different lysosomal functions, in most cases acidic hydrolases. [1] [2] Mutations of these genes result in the defect of one or more functions of the lysosomes, subcellular organelles devoted to the turnover and recycling of a wide range of complex molecules, including sphingolipids, glycosaminoglycans, glycoproteins and glycogen. In the most severe forms of LSDs there is a complete loss of a lysosomal enzyme due to protein truncations (deletion and insertion mutations causing frameshifts) and non-sense mutations (premature stop codons). In addition, for some LSDs, functional mRNA generation is blocked due to splice site mutations resulting in almost complete loss of the enzyme or very low residual activity when a small amount of the transcript is normally processed and translated. [3] Missense mutations are very frequent in LSDs but their effects are the most difficult to establish. Missense mutations effects depend mostly on the site of change at the protein level. Amino acid substitution changes in the enzyme active site are believed to be the most deleterious leading to almost complete loss of residual enzyme activity. [4]-[6] Missense mutations occurring outside the active site may affect the folding properties and trafficking of the mutated protein. In both cases, the mutated enzyme does not successfully reach lysosomes to perform its function. [5] The total absence of a protein or the synthesis of a non-functional protein, modified in its tertiary structure, leads to the storage of complex non-metabolized molecules in the lysosome. Generally, accumulation is observed in different tissues and organs. As a result, the phenotypic manifestations of these disorders are complex and characterized by the variable association of visceral, ocular, haematological, skeletal and neurological manifestations. These events are in most cases responsible for physical and neurological handicaps. [1] LSDs are generally classified on the basis of the type of disorder and the age of onset of the clinical signs as congenital or infantile (which usually have the most severe presentation), late- infantile, juvenile and adult types. [7] Lysosomal enzymes are glycoproteins synthesized in the endoplasmic reticulum (ER) (Figure 1.1). Like many other proteins, lysosomal enzymes, during their synthesis, are co-translationally assisted by molecular chaperones and folding factors (e.g., heat-shock proteins, BiP, calnexin, calreticulin, thiol-disulfide oxidoreductases, and protein disulfide isomerase) that interact with partially folded, aggregation-prone structural motifs of the nascent protein. These molecular chaperones recognize common structural features, which may include exposed hydrophobic regions, unpaired cysteine residues, or aggregation, to distinguish stable, native protein conformations from unstable. [8]-[10] Upon recognition and binding to the nascent polypeptide, molecular chaperones can stabilize protein conformation, inhibit premature misfolding, and prevent aggregation. Enzymes that are correctly folded and stable pass the quality control (QC) of ER, exit the ER efficiently, and move to Golgi. Once in the Golgi, most lysosomal enzymes undergo a phosphotransferase and diesterase enzymatic processes to acquire a mannose 6-phosphate (M6-P) moiety that is important for protein translocation into lysosomes via M6-P receptors expressed on lysosomal membranes.

The protein-receptor complex dissociates under lysosomal acidic environment where receptors are recycled back to Golgi for another round leaving the enzyme within lysosomes. [11] Proteins that fail to fold properly in ER, may aggregate disrupting cellular haemostasis in a condition known as endoplasmic reticulum stress (ERS)(Figure 1.1).

A cell under ERS activates various signalling pathways and processes including unfolded protein response (UPR) to restore its normal state through the expression of various genes functioning as chaperones to enhance protein folding, translational inhibitors to stop protein flux into ER, and activators of endoplasmic-reticulum-associated protein degradation (ERAD) machinery. In the case of chronic UPR, when a cell fails to reach haemostasis, specific apoptotic pathways are activated leading to cell death. UPR gene expression initiates the activation of three signalling pathways in the ER membrane; inositol-requiring protein 1 (IRE1), protein kinase R (PKR)-like endoplasmic reticulum kinase (PERK), and activating transcription factor 6 (ATF6). The activation of IRE1 pathway by self-oligomerize and phosphorylation initiates the expression of the ERAD components. The PERK pathway on the other hand inhibits mRNA translation resulting in less protein flux to ER. ATF6 is an ER transmembrane transcription

factor that is transported to Golgi where its cytosolic peptide gets cleaved by the site-2 protease (S2P) to be translocated to the nucleus and activates the transcription of ER protein folding chaperones. As part of the UPR system, degradation of misfolded proteins that failed to fold properly is carried out by the ERAD machinery. ERAD is a highly orchestrated protein machinery for ubiquitination and subsequent degradation by a protein-degrading complex, called the proteasome. The recognition of misfolded or mutated proteins depends on the detection of substructures within proteins such as exposed hydrophobic regions, unpaired cysteine residues and immature glycans. [12]
In the case of LSDs, the ER quality control recognizes mutant forms of lysosomal enzymes that retain catalytic activity or that have only modestly compromised function, due to slight modifications in their stability or conformation. This recognition may prevent trafficking through the secretory pathway and results in loss of function due to premature degradation or ER aggregation. [13]

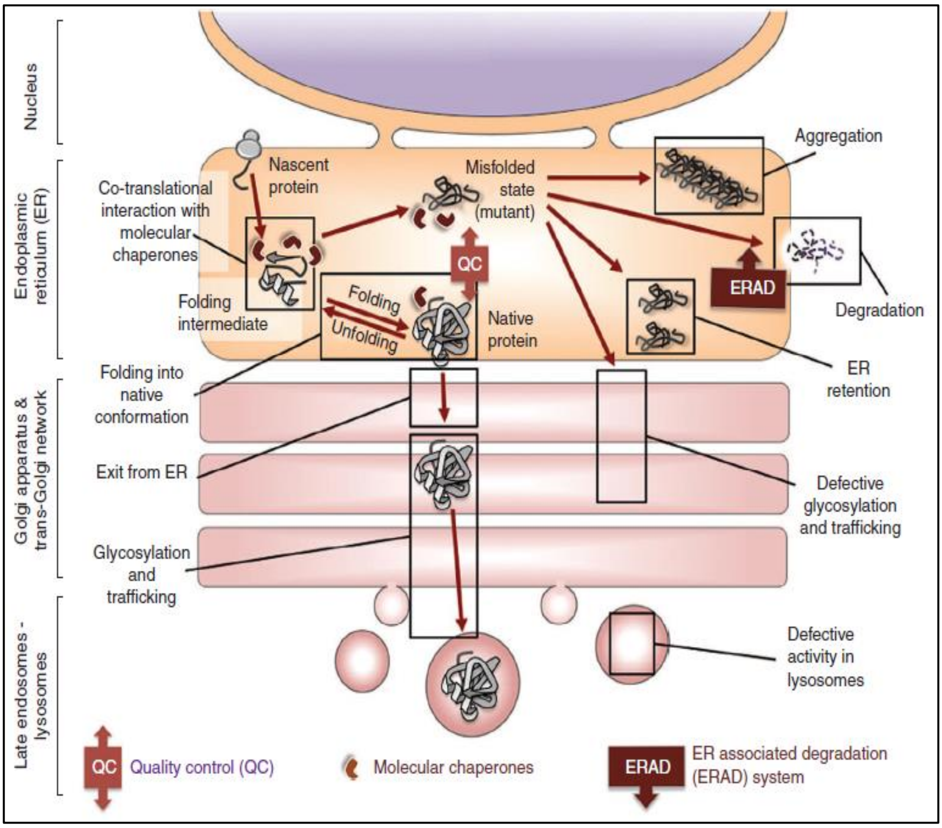

Figure 1.1: The cellular pathways that control folding of lysosomal enzymes. [13]

LSDs diagnosis is based on three major stages including preliminary clinical screening, biomedical testing, and genetic molecular testing. [14] Patients are first assigned for clinical screening of the presented signs and symptoms. There are some common diagnostic features that have been clinically associated with specific disorders. The second stage involves the measurement of residual enzymatic activities of different lysosomal enzymes. Enzymatic assays can be performed in various types of tissues expressing the targeted enzyme like serum, leukocytes, fibroblasts, and urine. Such assays are mostly fluorometric or colorimetric using artificial tagged substrates. The complete or excessive loss of enzymatic activity is enough to confirm the underlying diagnosis but in cases with normal enzymatic activities that are presented with clinical symptoms genetic testing is needed. Analysis of DNA or RNA for mutations is required to confirm the results obtained from the enzymatic activity measurements and to identify LSDs with non-enzymatic lysosomal protein defects. [14]

1.2 Therapeutic approaches to Lysosomal Storage Disorders

During the past two decades, the research in the field of LSDs has made significant progress, particularly in the development of a variety of innovative therapeutic approaches. These include strategies aimed at increasing the hydrolysis of the accumulated substrate by infusing a recombinant enzyme (the enzyme replacement therapy, ERT), or reducing the synthesis of the stored substrate by inhibiting its biosynthesis with small compounds (the so-called substrate reduction therapy, SRT). More recently, an alternative therapeutic strategy has emerged, namely the pharmacological chaperone therapy (PCT). It consists in the identification of specific ligands that selectively bind and stabilize otherwise unstable mutant enzymes, increasing total cellular levels and improving lysosomal trafficking and activity. [7]

1.2.1 Enzyme replacement therapy

The primary therapeutic approach for several lysosomal storage disorders is ERT. ERT is based on the periodic intravenous administration of the missing lysosomal enzyme produced and purified by recombinant DNA technologies. The resulting glycoproteins present M6P residues on the oligosaccharide chains. This allows specific binding of the enzyme to M6P receptors on the cell surface, thus enabling the enzymes to enter the cell and to be targeted to lysosomes, with subsequent catabolism of accumulated substrates. [15] The disadvantages of ERT is the large size of the delivered recombinant enzymes which do not diffuse easily into all affected tissues such as bone, cartilage, and skeletal muscle and cannot cross the blood-brain barrier (BBB). Furthermore, most of the current ERTs are immunogenic, eliciting immune responses that can limit tolerability and efficacy. In addition, ERT requires lifelong intravenous infusion, with frequent hospital admissions, needs for central venous devices (and related risk of infections), and high costs. [16]

1.2.2 Substrate reduction therapy

SRT approach aims to reduce substrate synthesis using small molecular inhibitors that bind and inhibit enzymes involved in substrate biosynthesis. SRT has been approved for Gaucher and Niemann–Pick Type C diseases using ZAVESCA® (Miglustat, *N*-Butyldeoxynojirimycin, **NB-DNJ**) inhibitor. The **NB-DNJ** inhibits ceramide glucosyltransferase (Ki, 7.4 μM), which catalyses the initial step in the synthesis of glycosphingolipids [17], and showed effective clinical improvements in both diseases. [18] [19] Unfortunately, **NB-DNJ** did not have any appreciable effect on the neurological manifestations of neuronopathic Gaucher disease type 3. [20] Recently, Eliglustat (Cerdelga) has been approved for adults with Gaucher disease type 1. [21]

1.2.3 Pharmacological chaperone therapy

PCT is considered a promising new therapeutic approach for LSDs. PCs are low molecular weight compounds able to physically interact with the mutated protein, favouring its proper conformation, improving its stability in the ER, preventing its aggregation and premature degradation (Figure 1.2). PCs are compounds which act as competitive inhibitors of the enzyme. When they are used in subinhibitory amounts (with consequent minimal side effects) they can correct the folding and/or stabilize the catalytic activity. In addition, PCs are reversible inhibitors, and therefore can be replaced by the enzyme natural substrate which is accumulated in the lysosomes. Indeed, once the PC-enzyme complex reaches the lysosome, the large amounts of stored substrates is believed to displace the PC and to be at least partially hydrolysed by the restored enzyme. Moreover, PCs present several advantages with respect to the previously mentioned therapies, such as oral administration and the possibility to cross the BBB. [22]-[26]

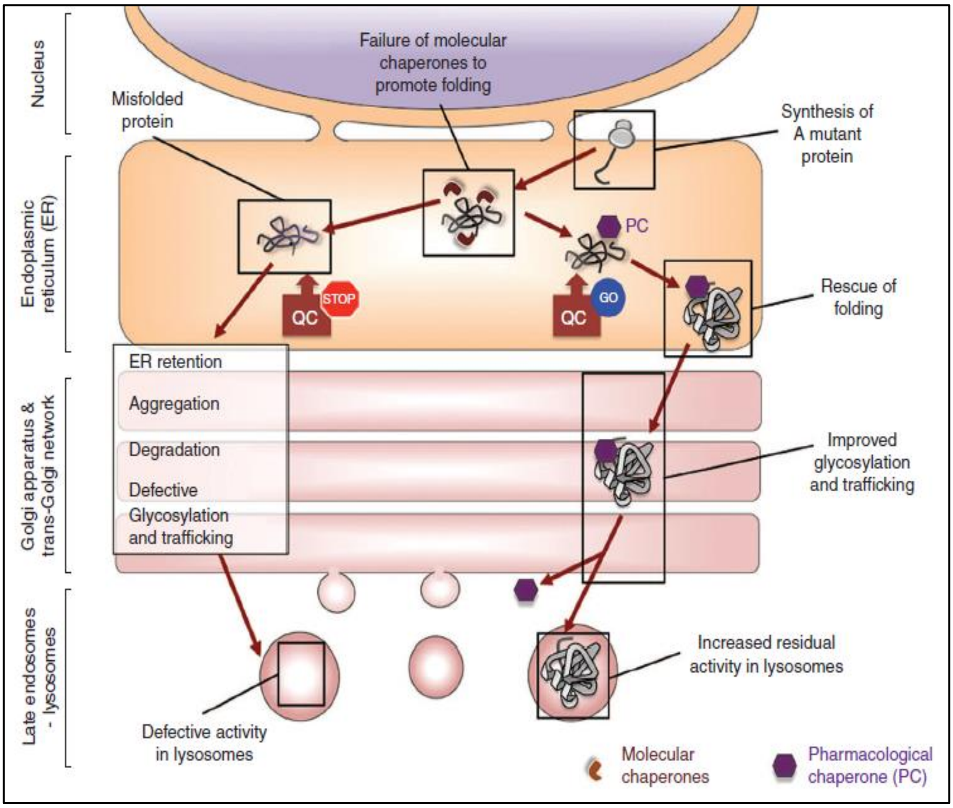

Figure 1.2: Mechanism of action of pharmacological chaperones. [13]

An important evolution in pharmacological chaperone therapy was the demonstration that some chaperones not only are able to rescue the endogenous, mutant, misfolded proteins, but can also improve the physical stability and delivery to lysosomes and possibly the efficacy, of the wild-type recombinant enzymes that are commonly used for ERT. This effect, at the basis of the so-called combined PC/ERT therapy, was demonstrated in preclinical *in vitro* and *in vivo* studies for Pompe, Fabry, and Gaucher diseases. [27]-[31]

1.3 β-Glucosidase: Gaucher Disease

Gaucher disease (GD) is the most common LSD of glycosphingolipids. It occurs at a frequency of between 1 in 40,000 to 1 in 60,000 in the general population, and of 1 in 500 to 1 in 1,000 among Ashkenazi Jews. [32] GD is caused by mutations in the *GBA* gene (mapped on chromosome: 1q21-22), which encodes for the lysosomal enzyme acid β-glucosidase (glucocerebrosidase, also known as GCase, EC 3.2.1.45, MIM*606463). [33] GCase hydrolyses the β-glucosyl linkage of glucosylceramide (GlcCer) in the lysosomes (Figure1.3) and requires the coordinated action of saposin C and negatively-charged lipids for maximal activity. [34] The active site of the enzyme contains at least three domains with differing specificities: (i) the catalytic site, a hydrophilic pocket that recognizes glucosyl moieties; (ii) an aglycon binding site that is hydrophobic and has affinity for the alkyl chains of GlcCer; and (iii) a hydrophobic domain that interacts with negatively charged lipids to increase hydrolytic rates. [35]

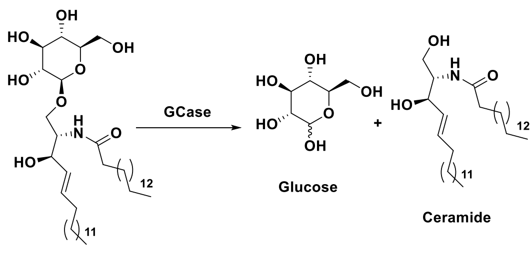

Figure 1.3: Hydrolysis of glucosylceramide (GlcCer) by the lysosomal enzyme acid β-glucosidase (GCase).

Symptoms associated with GD are due to the progressive accumulation of GlcCer in various organs. Thus, GD is a multisystemic disorder with clinical manifestations at all ages, which is dependent on the subtype of GD. Three clinical forms of GD can be distinguished depending on the degree of neurological involvement. Type 1, the most common form (OMIM#230800), which was considered non-neuronopathic until recent discoveries; Type 2, acute neuronopathic (OMIM#230900), the rarest and most severe form; Type 3, subacute chronic neuronopathic (OMIM#231000), with later onset and a slower progressive course. [36] At present, more than 500 *GBA* gene mutations have been reported in Gaucher patients (data from Human Gene Mutation Database

(HGMD®professional) 2019.2; http://www.hgmd.cf.ac.uk/ac). Gaucher patients affected by the non-neuronopathic form of Gaucher disease are treated with ERT through infusion of the recombinant enzyme [e.g. Imiglucerase (Cerezyme®), Genzyme; velaglucerase alfa (VPRIV®), Shire and taliglucerase alfa (Elelyso®), Pfizer]. However, this therapy has a high cost, requires the patients' frequent hospitalization and is not effective for the neuronopathic forms of the disease. An alternative option for GD is the SRT by treatment of patients with drugs (such as miglustat (ZavescaTM), Actelion and the most recently approved eliglustat (CerdelgaTM), Sanofi/Genzyme]), which are able to inhibit the enzyme that produces the glycosphingolipid accumulating during the disease. [18]-[21]

1.3.1 The role of β-Glucosidase in Parkinson's Disease pathogenesis

Parkinson's Disease (PD) is the second most common neurodegenerative disorder affecting approximately 1% of the population over 60 and 5% of the population over 80-85. [37] People with PD typically present with cardinal motor symptoms including bradykinesia, muscular rigidity, rest tremor, or gait impairment but often also develop nonmotor symptoms, such as cognitive impairment and psychiatric symptoms. Many but not all of the symptoms associated with PD result from loss of the dopaminergic neurons of the *substantia nigra pars compacta*. [38] PD is treated pharmacologically, by enhancing dopamine tone (e.g. dopamine replacement with L-dopa) and, surgically, by deep brain stimulation. PD is currently treated also with NMR guided thermal ablation by ultrasounds without invasive surgery. [39] Pathologically, PD is characterized by the presence of proteinaceous intracellular aggregates composed primarily of α-synuclein, termed Lewy pathology (Lewy bodies). Missense mutations and multiplications of the SNCA gene, which encodes for α-synuclein (α-Syn), cause heritable forms of PD and enhance the propensity of α-Syn to self-aggregate thus implicating α-Syn aggregation in the pathogenesis of the disease. [40] [41] Mutations in the *GBA* gene are numerically the most important risk factor for developing PD. PD has an incidence greater than 1% among population over 60-65 years and more than 5-6% over 80-85 years. The presence of *GBA* mutations dramatically affects these percentages. In particular, the risk to develop the disease increases from 1% to 5% for *GBA* heterozygous patients over 60-65 years, and from 5-6% to 15% for *GBA* heterozygous patients over 80-85 years (www.gauchergenova2020.it). Furthermore, loss of GCase activity is found in sporadic PD forms.

1.3.1.1 The links between Gaucher Disease and Parkinson's Disease

Mutations in the *GBA* gene are associated with Parkinson's disease. This association has been established in patients with mutations in two *GBA* alleles (i.e. patients with Gaucher disease) [42] [43] and in carriers of a single *GBA* mutation (i.e. *GBA* heterozygotes). [43]-[50] The two most common *GBA* mutations associated with PD are N370S and L444P mutations. [51]

The exact mechanism through which GCase deficiency contributes to PD pathogenesis is still unclear, but may include the accumulation of α-Syn, impaired lysosomal function and ER associated stress and may differ according to genotype (e.g. GD versus heterozygote *GBA* mutations). Impairment of the autophagy-lysosomal pathway plays a principal role in PD pathogenesis and in particular its effect on abnormal accumulation of α-Syn with formation of oligomers and fibrils. [52] Various markers of lysosomal dysfunction such as altered lysosomal content, abnormal lysosomal morphology and increased lysosomal pH have all been reported in cellular and animal models where GCase is knocked down, knocked out or which express pathogenic mutations or where GCase enzyme is inhibited by conduritol B epoxide (CBE), an specific and covalent GCase inhibitor (irreversible inhibitor). [53]-[59]

Normally, GCase is synthesized in the ER and transported via Golgi to lysosomes, by the lysosomal integral membrane protein (LIMP)-2 that it binds the M6PR, where GCase interacts with its substrate GlcCer as well as monomers of α-Syn in lysosomes. This interaction, physiologically, promote the degradation of α-Syn through lysosomal autophagy (Figure 1.4a). In GD patients and *GBA* mutation carriers, a loss of GCase activity was observed, which can lead to lysosomal dysfunction and consequent α-Syn buildup. It has also been suggested that accumulation of GlcCer in lysosomes may contribute to lysosomal dysfunction for homozygous *GBA* mutations. This might alter the homeostasis of α-Syn in the lysosomes, but no evidence of glucosylceramide accumulation in PD brains with heterozygous *GBA* mutations has been reported (Figure 1.4b). [60]

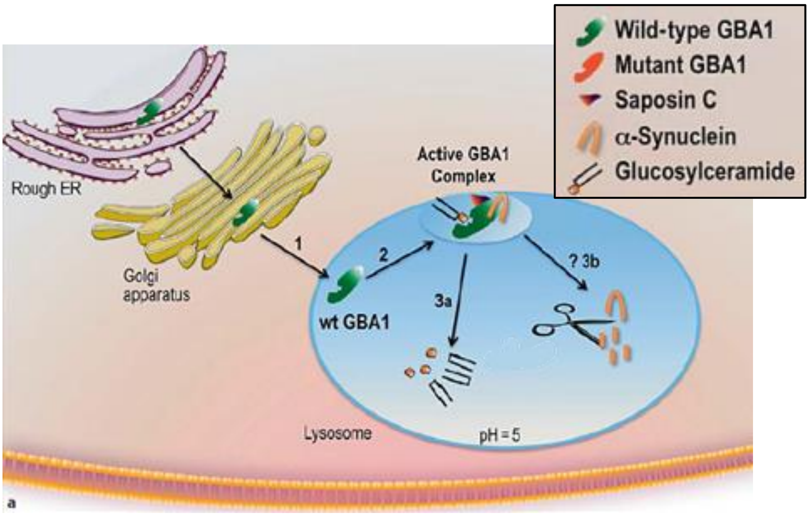

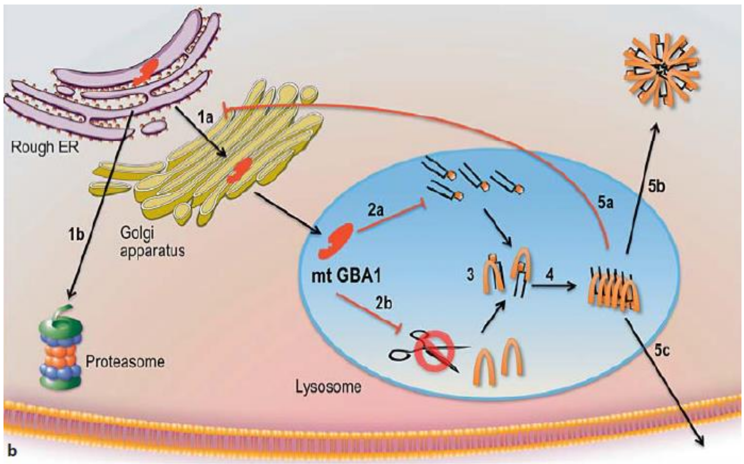

Figure 4: Proposed model for the interaction between wild-type (wt) (a) and mutant (mt) (b) *GBA*1 and α-Syn. a) Wild-type *GBA*1 (green) is trafficked to the lysosome (1). For optimal enzymatic function, *GBA*1 requires the sphingolipid activator protein saposin C, low lysosomal pH, and interaction with membrane-associated phospholipids (2). The active *GBA*1 complex represents proper interactions between wild-type *GBA*1, saposin C, and α-Syn, which might act by bringing the lipid glucosylceramide to *GBA*1. *GBA*1 catalyzes the hydrolysis of glucosylceramide to glucose and ceramide (3a). *GBA*1 can also stimulate α-Syn degradation by still undefined mechanisms resulting in proper degradation of α-Syn (3b). **b**) Mutant *GBA*1 proteins (red) are trafficked to the lysosome (1a). Mutant *GBA*1 can also be tagged for endoplasmic reticulum-associated degradation and directed to the proteasome (1b). Through a loss of (hydrolytic) function effect, mutant *GBA*1 causes accumulation of its lipid substrates (glucosylceramide) (2a). Through a gain-of-toxic-function effect, mutant *GBA*1 inhibits α-Syn degradation via unknown mechanism/s, resulting in impaired degradation α-Syn (2b). Both accumulation

of glucosylceramide and inhibition of α-Syn degradation promote buildup of α-Syn monomers that can associate with glucosylceramide-containing lipids (3). Accumulation of these α-Syn monomers eventually leads to formation of neurotoxic soluble α-Syn oligomers (4). Soluble α-Syn oligomers can inhibit ER maturation of *GBA*1 proteins (5a), form insoluble α-Syn Lewy bodies or be secreted through exocytosis (5c). [61]

In *GBA* mutation carriers, misfolded GCase trapped in the ER leads the UPR and/or ERAD activate. [5] Markers of ER stress are elevated in PD brains with *GBA* mutation carriers. Dysregulation of ER calcium stores and damage lysosomal have been reported in cell models and animal models containing *GBA* mutations associated with PD. [62] Lysosomes show impaired autophagy due to ER stress, build up of substrate and/or α-Syn oligomers and fibrils, which implies that α-Syn cannot undergo degradation, resulting in an increased accumulation of α-Syn in the cytoplasm. Accumulation of α-Syn in cytoplasm, on the other hand, may block the ER-Golgi trafficking of WT-GCase, resulting in reduced GCase activity and therefore in reduced α-Syn degradation, thus creating a vicious circle of neurotoxicity. [63] Moreover, autophagy-lysosomal pathway inhibition has also been implicated with mitochondrial dysfunction (Figure 1.4b). [64]-[66]

1.3.1.1 Sporadic (non-familial) forms of Parkinson's Disease

Experimental evidence show that GCase activity in the sporadic PD brain decreases with aging. Aging is the major risk factor contributing to decreased activity and protein expression of GCase enzyme in sporadic PD brains. Studies in humans, monkeys and mice showed that GCase activity decreases with age in regions of the midbrain such as the *substantia nigra*, *striatum* and *putamen*.
The decrease in GCase activity in the *striatum* and *hippocampus* of monkeys coincided with an increase in α-Syn oligomers in the same compartments. [67] [68] [69] Analysis suggested that the lysosomal maturation of GCase was decreased in brains with higher amounts of α-Syn. [70] A correlation between increased α-Syn levels and decreased GCase activity was demonstrated in sporadic PD brains. Increased levels of intracellular α-Syn are also known to induce ER stress and this could be another mechanism by which GCase transport to the lysosome is affected. Mitochondrial dysfunction and oxidative stress may also play a role in the loss of GCase activity in human dopaminergic neurons. [65] [71] [72]

1.4 Imino- and Azasugars as Pharmacological Chaperones

Structurally, the most promising PCs for LSDs are nitrogen glycomimetics with a nitrogen atom replacing the endocyclic oxygen (such as deoxynojirimycin, DNJ (**1**), Figure 1.5) or the anomeric carbon of sugars (e.g. isofagomine, IFG (**2**) or 1,5-dideoxy-1,5-iminoxylitol, DIX (**3**), Figure 1.5), also known as iminosugars, or azasugars, respectively. [73] As inhibitors of carbohydrate-processing enzymes, imino- or azasugars, and other substrate analogues which behave as competitive glycosidase inhibitors, are good PC candidates. [73] The first oral PC drug has recently been commercially developed for the treatment of Fabry disease (another LSD) in Europe (Migalastat, Galafold, Amicus Therapeutics), (https://www.ema.europa.eu/ and https://www.fda.gov/) but no PC for Gaucher disease has reached the market yet. IFG (Figure 1.4) reached the most advanced stage of development (Phase III clinical trials in a combined therapy with recombinant GCase). IFG showed remarkable *in vivo* effects in a neuronopathic Gaucher disease mouse. [74] However, it was not effective in reducing the accumulation of lipid substrates; it is believed that its high hydrophilicity hampers an efficient transport to the cells. For this reason, several alkylated imino- or azasugars were synthesized and investigated as PCs for GD, showing better metabolic properties. [23]

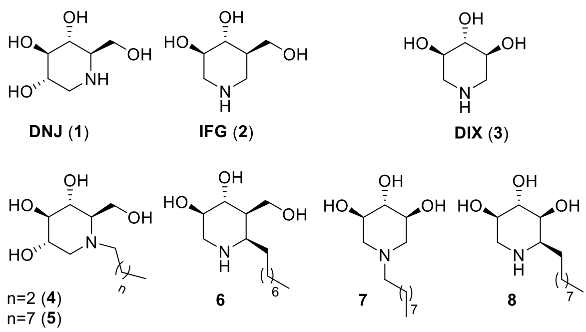

Figure 1.5: Some natural polyhydroxypiperidines and their alkylated analogues active as PCs for Gaucher Disease.

The *N*-alkylation of iminosugars has been one of the most widely explored structural changes that resulted in increased activity as PC. In this context, *N*-

alkylated derivatives of DNJ (**1**) such as *N*-butyl-deoxynojirimycin (**4**) and *N*-nonyl-deoxynojirimycin (**5**) (Figure 1.5) showed to be highly potent PCs for the potential treatment of GD by correcting the folding and stabilizing the catalytic activity of mutant GCase. *N*-butyl-DNJ (**4**) is an inhibitor of the ceramide-specific glucosyltransferase (CSG) and catalyzes the first step of glycosphingolipids biosynthesis; it was currently approved as SRT in the oral treatment of type 1 GD. In addition, it worked as a PC, increasing the activity of mutant GCase bearing N370S mutations. [75]

N-Nonyl-DNJ (**5**) was a potent inhibitor of lysosomal GCase with an IC_{50} value of 1 µM, and showed a 2-fold increase in the activity of mutant GCase in N370S fibroblasts after 9 days of incubation at 10 µM. However, it did not enhance the intracellular activity of the L444P variant. [76] [77] Azasugars are monosaccharide analogues with a nitrogen atom that replaces the anomeric carbon of sugar, such as isofagomine, IFG (**2**) and 1,5-dideoxy-1,5-iminoxylitol, DIX (**3**). [73] IFG is a competitive inhibitor of human lysosomal GCase (K_i = 0.016+0.009 µM; IC_{50} = 0.06 µM) [78]-[80] and increased mutant GCase activity to 3-fold at 30 µM after 5 days of incubation in fibroblasts with the N370S missense mutations. [81] [82]

Unfortunately, IFG reached only Phase III clinical trials due to high hydrophilicity, which prevented an efficient transport of the compounds in the ER and in the lysosome. [23] In order to avoid this drawback, less hydrophilic IFG derivatives were investigated. In case of azasugars, such as IFG, *N*-alkylation of IFG produced less potent inhibitors. [80] Instead, the shift of the alkyl chain from the N-atom to the adjacent C-atom led to potent GCase inhibitors with GCase chaperoning properties. Fan and co-workers reported IFG analogues bearing an alkyl chain at the C6 position, such as 6-nonyl IFG (**6**), which displayed a remarkable GCase inhibition and PC activity (IC_{50} value of 0.6 nM, 1.5-fold GCase activity enhancement at 3 nM in N370S GD fibroblasts). [80] [83] [84] A comparable trend, moving the alkyl chain from the N-atom to the adjacent C-atom, was found with *N*-nonyl-DIX (**7**), which showed an IC_{50} of 1.5 µM, and with α-1-C-nonyl-DIX (**8**), which showed a remarkable IC_{50} of 6.8 nM and 1.8-fold activity increase in N370S mutated fibroblasts at 10 nM. [85] Therefore, the position of the alkyl chain seems to be crucial for the pharmacological chaperoning activity in dependence on the peculiar hydroxypiperidine skeleton. Indeed, while for DNJ analogues the *N*-alkylation gave good PCs for GCase, in the case of azasugars the alkylation of the carbon adjacent to nitrogen furnished better PCs for GD.

1.4.1 Pharmacological Chaperones as novel drugs for Parkinson's Disease

Small-molecule chaperones for GCase bind mutant GCase in the ER, helping them to refold, and thus facilitating trafficking to the lysosome. This type of therapy for PD has two effects: 1) improve lysosomal function and thus degradation of α-synuclein 2) reduce ER stress. Several drug screens have identified a number of candidates, including already known drugs (drug repositioning or drug repurposing strategy), [86] such as ambroxol, a drug used in the treatment of respiratory diseases, or IFG, under clinical phase trials for the treatment of Gaucher disease. [87] The fruit fly *Drosophila melanogaster* shows that development of PD in carriers of GD mutations results from the presence of mutant *GBA* alleles. Expression of mutated *GBA* in *Drosophila* resulted in dopaminergic neuronal loss, a progressive locomotor defect and increased levels of the ER stress. In *Drosophila* model, both ambroxol and IFG have been shown to effectively reduce the ER stress and the locomotor deficit. [88] [89] [59] Oral administration of ambroxol to transgenic mice expressing the heterozygous L444P mutation in the murine glucocerebrosidase gene increased GCase activity in the brain stem, midbrain, striatum and cortex. [90]

The treatment with ambroxol and IFG also increased wild-type GCase activity in the brain of transgenic mouse expressing human α-synuclein inducing a decrease of α-Syn accumulation in dopaminergic neurons of the *substantia nigra* and improving motor and non-motor functions. [91] The observation that these two chaperones increase wild-type GCase activity *in vivo* suggests that small molecule chaperones could also be used as a treatment for sporadic PD.

Considering the potential benefits of discovering an effective PC for GCase not only for GD but also for GD-related PD and for the sporadic forms of PD that do not have the *GBA* mutation, there is an urgent need to develop new small compounds with the ability of modulating the GCase enzyme activity. Azasugars are of great synthetic interest as potential PCs against Lysosomal Storage and Neurological Disorders.

Chapter 2:
The Reductive Amination Routes to the Synthesis of piperidine Iminosugars and Azasugars

Introduction

The Reductive Amination (RA) reaction is one of the most common ways to introduce a nitrogen atom in a compound through the conversion of a carbonyl group, and one of the most important methods to synthesize amines. [92] [93] The RA reaction is a two-step procedure that first involves the condensation of ammonia, a primary or a secondary amine with a carbonyl compound (aldehyde or ketone), to form imines or iminium ion intermediates (in equilibrium with the enamine forms). The latter are subsequently reduced by an appropriate reducing agent to form a primary, a secondary or a tertiary amine compound (Scheme 2.1). [94] The first condensation step is reversible and is best done under mildly acidic conditions (pH 4-5), which increase the electrophilic properties of the carbonyl compound. If the solution is too acidic, however, the amine nucleophile is completely converted into its non-nucleophilic conjugate acid and no reaction will occur. Addition of a dehydrating agent to adsorb the water generated in the condensation reaction improves the yields of imines which form slowly. [95]

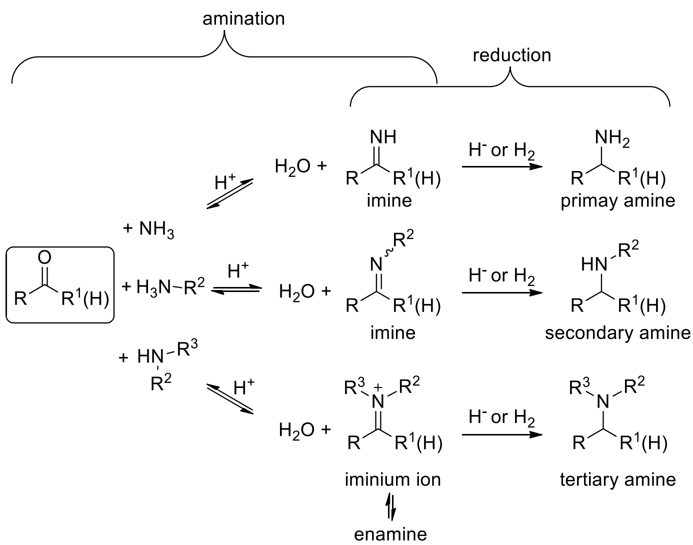

Scheme 2.1: The reductive amination reaction.

The two steps can be performed in one-pot, thus minimizing the use of solvents for intermediate purification. This is mandatory when ammonia is employed as the amination reagent, due to the low stability of the corresponding imine. The

in situ reaction can be achieved by waiting the formation of the imine intermediate before adding the reducing agent or, alternatively, using reagents selective towards the C=N bond (over the C=O bond) such as sodium cyanoborohydride ($NaBH_3CN$) or sodium triacetoxyborohydride ($NaBH(OAc)_3$), or H_2 in the presence of a suitable Pd-based catalyst. The advantage of using such reagents [96] is that they are not strong enough to reduce aldehydes and ketones (such as $NaBH_4$ or $LiAlH_4$), but they can reduce imines or iminium ions. In this way, all reagents are added at the beginning of the reaction in a tandem process. While $NaBH_3CN$ [97] and $NaBH(OAc)_3$ [98] are selective towards imines, catalytic hydrogenation is a commonly employed procedure for the reduction of many nitrogen containing functional groups to the corresponding amines (e.g. azides, nitro compounds, hydroxylamines, nitrones and cyano groups).
This further expands the scope of the RA reaction by increasing the number of steps that can be performed in one-pot. RA is therefore a powerful and reliable tool for synthetic organic chemists (both from academia and industry) in the construction of carbon–nitrogen bonds.
Indeed, very recently, Chusov and co-workers reported that at least a quarter of C-N bond forming reactions in the pharmaceutical industry are performed *via* RA. [99] In its intramolecular version, RA allows the synthesis of cyclic amines. In this regard, carbohydrates are particularly suited as starting materials for the RA approach, since they possess the anomeric carbon, as well as primary and secondary hydroxyl groups, which can be converted into nitrogen containing moieties. This method found enormous application in the synthesis of iminosugars, and this Minireview aims to describe relevant examples in this field.
Iminosugars are small natural or synthetic glycomimetics characterized by the presence of an amine that replaces the carbohydrate endocyclic oxygen. [100] [73] The protonation of the amine at physiological pH is generally considered responsible for the high affinity of iminosugars towards carbohydrate receptors. Indeed, iminosugars can interfere with carbohydrate processing enzyme (glycosidases or glycosyltransferases) by mimicking the transition state involved in the glycosidic bond hydrolysis or formation. [101] [102]
Inhibition of the oligosaccharide processing enzymes results in modification of the oligosaccharide portion of glycoproteins on the surfaces of cells and thus

interferes with a number of cellular recognition processes. In particular, glycosidase inhibitors are of interest for the treatment of cancer, viral infections and parasitic diseases. [103]-[106] Inhibition of α-glucosidase enzymes in the brush border of the small intestine delays glucose absorption and decreases postprandial hyperglycaemia, as demonstrated by the deoxynojirimycin (DNJ) derivative miglitol, which is a commercially available drug (Figure 2.1). [107] Iminosugars have also found applications as therapeutic agents for metabolic disorders. For instance, the ability of the iminosugar miglustat (Zavesca^{TM}, Figure 2.1) to inhibit the biosynthesis of glycosylceramide is used to treat type 1 Gaucher Disease (GD1), the most common lysosomal storage disorder (LSD), and Niemann-Pick type-C disease, in the substrate reduction therapy (SRT). [108]-[110] More recently, it was recognized that the ability of iminosugars to bind to mutant lysosomal hydrolases makes them excellent candidates as Pharmacological Chaperones (PCs) for LSDs and other protein misfolding diseases.

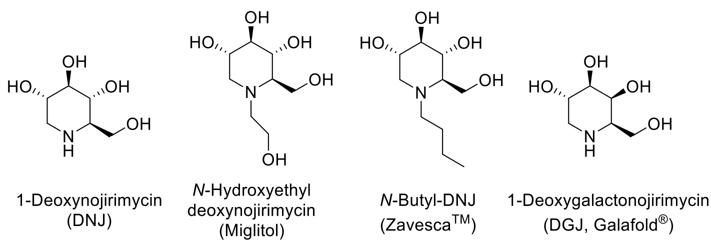

Figure 2.1: Examples of some biologically relevant iminosugars.

PCs are small molecules that bind and stabilize mutant lysosomal enzymes, thereby allowing proper cellular translocation and restoring enzyme activity. PCs often act as competitive inhibitors of the enzyme. However, when they are employed in sub-inhibitory amount, they can correct the folding and/or stabilize the catalytic activity. [24] [23] [26]

The first iminosugar PC oral drug for the treatment of Fabry diseases was recently approved in Europe with the name of Galafold® (DGJ, Figure 2.1). [111] Due to the importance of iminosugars for their potential therapeutic applications, great efforts have been devoted to the development of general strategies for their synthesis in a pure form and that of non-natural analogues for structure-activity relationship, and many important reviews on this topic have been reported.

[112]-[122] This Minireview focuses in particular on the exploitation of the RA approach to the synthesis of piperidine iminosugars. In particular, the interesting biological activity of trihydroxypiperidines has been recently reviewed. [123] This review describes relevant examples of synthetic strategies involving the RA step as the key ring-closure step to obtain polyhydroxypiperidines and their derivatives. It is organized according to the nitrogen containing functional moiety which takes part in the key RA ring-closing reaction. The last section covers examples in which an amine is directly employed as the nitrogen source, the following sections describe synthetic strategies in which other nitrogen containing precursors are exploited to access the target compounds. Since there is no unified RA procedure for all type of carbonyl compounds and amines and both reducing agent and reaction conditions can considerably vary, [96] particular emphasis is given to these aspects. In addition, the biological properties of the most promising polyhydroxypiperidines are also reported.

2.1 The amine route

In the present section the nitrogen is introduced as an amine group, eventually protected, that undergoes the RA reaction upon deprotection. Dhavale and co-workers reported an efficient synthetic access to 3,4,5 trihydroxy-4-hydroxyethyl piperidine **14a** and of a series of *N*-alkyl derivatives **14b–f** via RA and the evaluation of their glycosidase inhibitory and immunosuppressive activity (Scheme 2.2). [124] C-3-Allyl-α-D-ribofuranodialdose (**9**) was prepared in five steps starting from D-glucose and employed as a substrate of a RA with benzylamine and $NaBH_3CN$ in methanol followed by amine protection to access compound **10** in 85% yield**.** Dihydroxylation of **10** with catalytic $K_2OsO_4\cdot 2H_2O$ and *N*-methylmorpholine *N*-oxide followed by oxidative cleavage with sodium metaperiodate afforded aldehyde **11**, which was reduced to alcohol **12** with $NaBH_4$ in good overall yield over three steps (64%). After acetylation of the primary hydroxy group (compound **13**) and acetonide deprotection to free the hemiacetal moiety, an intramolecular RA using 10% Pd/C in methanol under hydrogen pressure (200 psi) provided **14a**. Notably, these four steps (amine deprotection, formation of the six-membered cyclic iminium ion and *in situ* reduction with concomitant deacetylation) occurred in one-pot with high yield

(81%). *N*-Alkylation was performed using appropriate alkyl bromides in DMF-K_2CO_3 in good yields (60–70%). The whole set of the newly synthesized iminosugars showed moderate inhibition towards commercially available α-glycosidases. The best inhibitory activity was observed for compound **14e** showing IC_{50} = 112 μM towards α-mannosidase. In addition, iminosugar **14e** showed weak activity (IC_{50} = 15 μM) in the B-cell assay performed to target one of the two major components of the immune response. [124]

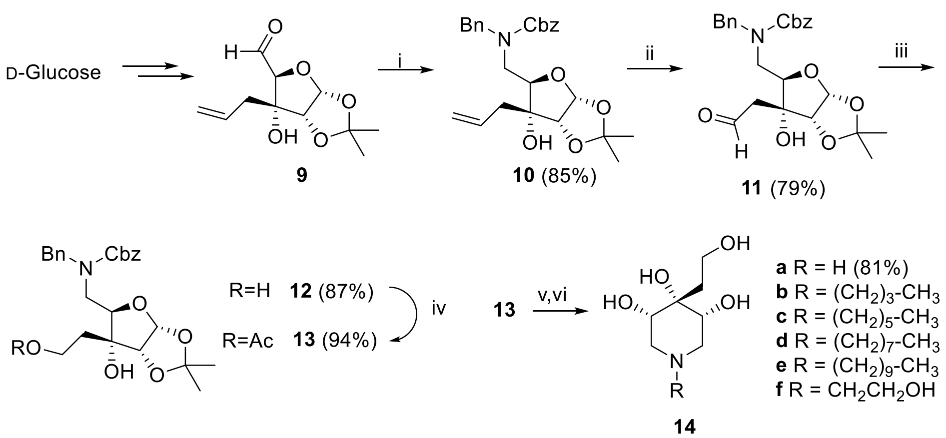

Scheme 2.2: Reactions and conditions i) (a) $BnNH_2$, $NaBH_3CN$, MeOH, -20°C to r.t., (b) CbzCl, $NaHCO_3$, MeOH:H_2O, r.t., ii) (a) K_2OsO_4 $2H_2O$, *N*-Methylmorpholine *N*-oxide, Acetone:H_2O, 0°C to r.t., (b) $NaIO_4$, Acetone:H_2O, 0°C to r.t., iii) $NaBH_4$,THF:H_2O, 0°C to r.t., iv) Ac_2O, Py, 0°C to r.t., v) (a) TFA:H_2O, 0°C to r.t., (b) H_2, Pd/C, 200 psi, r.t., vi) R-Br, K_2CO_3, DMF, 80°C.

The same group also developed an efficient methodology where the amino moiety was introduced as an aziridine group, which is a highly reactive nitrogen heterocycle that enables the preparation of amines by reaction with a broad range of nucleophiles (Scheme 2.3). [125] A Wittig reaction performed on D-glucose-derived aldehyde **15** furnished compound **16**, which underwent conjugate addition of benzylamine and *in situ* intramolecular nucleophilic substitution leading to the more stable *trans*-aziridine **17** as the only isolable product in 70% yield. The regioselective aziridine ring-opening with trifluoroacetic acid (TFA) (1 equiv.) provided the α-hydroxy-β-aminoester **18** in 82% yield, which represented a promising chiral precursor to the synthesis of six-membered iminosugars. Reduction of ester **18** and selective amine protection followed by oxidative cleavage of **19** furnished an unstable aldehyde, which was immediately reduced to primary alcohol **20**. Acetonide removal and intramolecular RA (ammonium formate, 10% Pd/C, MeOH) afforded the corresponding 1-deoxy-L-ido-nojirimycin **21** in 58% yield. When intermediate **18** was reduced but not subjected to oxidative cleavage compound **22** was obtained**,** and afforded 1,5-dideoxy-1,5-imino-6-hydroxy-β-L-glycero-L-ido-heptitol (**23**) in good yield (75%) through hydrogenation under high pressure (80 psi) in the presence of Pd/C catalyst. [125]

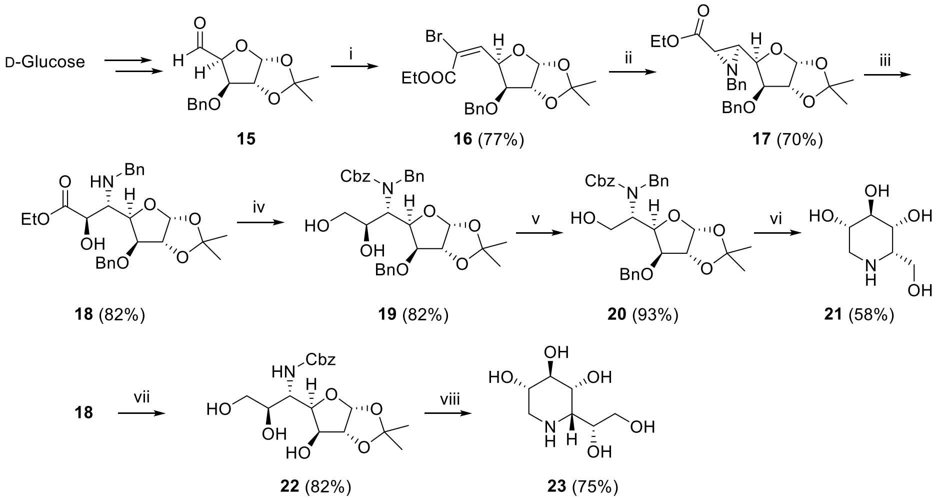

Scheme 2.3: Reactions and conditions: i) PPh_3=CBrCOOEt, CH_2Cl_2, 25℃, 12 h, ii) $BnNH_2$, benzene, 10 to 20℃, 6 h, iii) TFA (1 equiv.), Acetone:H_2O (2:1), 25℃, 24 h, iv) (a) $LiAlH_4$, THF, 0 to 25℃, 2 h, (b) CbzCl, $NaHCO_3$, MeOH:H_2O, 0 to 25℃, 6 h, v) (a) $NaIO_4$, Acetone:H_2O (3:1), 0 to 15℃, 1.5 h, (b) $NaBH_4$, EtOH, 15℃, 15 min, vi) (a) TFA: H_2O (6:4), 0 to 25℃, 3 h, (b) $HCOONH_4$, 10% Pd/C, MeOH, reflux, 1.5 h, vii) (a) $LiAlH_4$, THF, 0 to 25°C, 2 h, (b) $HCOONH_4$, 10% Pd/C, MeOH, reflux, 2 h, (c) CbzCl, MeOH:H_2O (9:1), 0 to 25°C, 3.5 h, viii) (a) TFA:H_2O (2:1), 0 to 25°C, 4 h, (b) H_2, 10% Pd/C, 80 psi, 24 h.

Enzymatic procedures followed by intramolecular RA were employed for the synthesis of six-membered iminosugars using aldolases, which catalyze reversible formation of C-C bonds with high enantioselectivities. In particular, fructose 6-phosphate aldolase (FSA) has the ability to stereoselectively catalyze the aldol addition using dihydroxyacetone (DHA), hydroxyacetone (HA), and hydroxybutanone (HB) as donors with a variety of Cbz-amino aldehyde acceptors, not showing any phosphate dependency on its donor molecule. The first example of the synthetic capabilities of FSA was reported for the synthesis of D-fagomine (**25**) and some of its *N*-alkylated derivatives (Scheme 2.4). [126] Catalytic hydrogenation of ketoamine **24** under high pressure (50 psi) promoted amine deprotection and intramolecular RA providing **25** in excellent yield (89%). Additionally, *N*-Alkylated derivatives (**26a-f**) were obtained by intermolecular RA on **25** with different aldehydes in the same experimental conditions. More interestingly, the synthesis of **26** could also take place directly from **24** in a one-pot reaction. The isolated yields obtained by this procedure were similar to those achieved starting from **25**. [126]

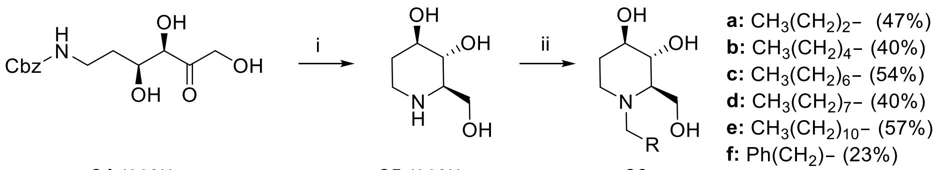

24 (69%) **25** (89%) **26**

Scheme 2.4: Reactions and conditions: i) H_2, Pd/C, 50 psi, H_2O:EtOH 9:1, r.t., 24 h, ii) R-CHO, H_2, Pd/C, 50 psi, MeOH, r.t., 24 h.

The wide substrate tolerance of FSA and the ability to circumvent the need for phosphorylated substrates, allowed the synthesis of DNJ, 1-deoxymannojirimycin (DMJ) [127] and other known and novel polyhydroxypiperidines [128] in good yields (Figure 2.2), through this cascade reaction approach.

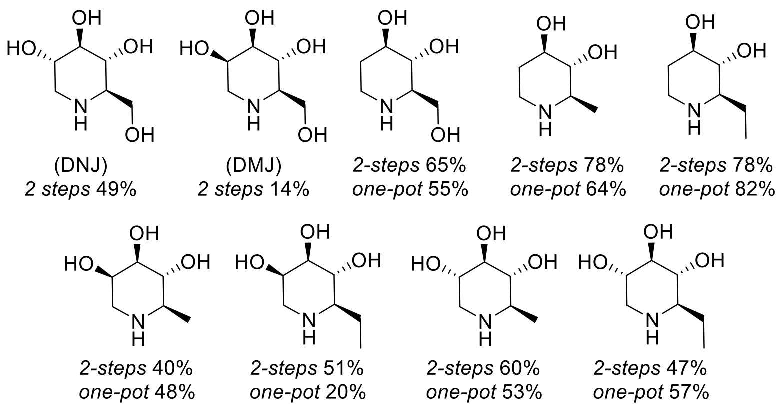

Figure 2.2: FSA mediated chemoenzymatic syntheses of polyhydroxypiperidines.

A non-enzymatic protocol for the synthesis of analogous iminosugars **30** and **31** was more recently reported by Martin et al. exploiting stereoselective aldol reactions between optically pure Cbz-protected (*S*)-isoserinal acetonide **27** and appropriate hydroxyketones **28** (Scheme 2.5). [129] [130] The stereoselective *syn* aldol reaction was achieved successfully by using tertiary amines proline based [129] or Zn/prophenol complexes [130] as aldol catalysts, thus presenting two parallel routes to get optically pure products with good yields and high diastereoselectivity. The corresponding adducts **29** were transformed into iminosugars **30** and **31** in a two-step protocol, involving deprotection with an acidic ion-exchange resin, followed by intramolecular RA using catalytic hydrogenation in acidic medium. Iminosugars **30** and **31** were obtained in excellent yields (85 – 99%) and high diastereoselectivity (only β-isomer). The stereochemical outcome was rationalized invoking thermodynamic control obtained in acidic medium, which accelerated the formation of an isomer with the aliphatic substituent in the preferred equatorial position. [129] [130]

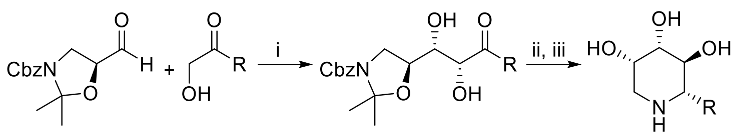

27 **28** **29** **30**: R=CH_3 (85%)
31: R=$(CH_2)_5CH_3$ (99%)

Scheme 2.5: Reactions and conditions: i) 20 mol% catalyst, ii) DOWEX 50WX8, iii) H_2, Pd/C, HCl, MeOH, 60 h.

2.2 The imine route

In this section the nitrogen atom is introduced into the scaffold as an imine functional group. The imine, thanks to its electrophilic properties, allows to introduce further structural diversity in the final polyhydroxy piperidines skeleton through nucleophilic addition reactions, using the wide library of organometallic or heteroatomic nucleophiles available. A careful choice of the reaction conditions can give selectively one of the two possible epimers at the newly formed stereocentre. The last steps of the synthetic strategy rely on the intramolecular RA to afford the target iminosugar. Following this approach, Martin *et al.* reported on the access to α- or β- 1-C-substituted 1-deoxynojirimycin derivatives through organometal addition reactions to an L-sorbose-derived imine followed by intramolecular RA. Imine **33** was synthesized in quantitative yield from L-sorbose-derived aldehyde **32** (Scheme 2.6). [131] [132] Careful choice of the reaction conditions during the organometal addition allowed to control the α- *vs* β-configuration at the pseudoanomeric centre in the final products **35a-d** and **36b-c** (Scheme 2.6). The addition of different organometallic reagents was initially investigated in a cooled solution (-78 or 0°C) of the *N*-benzylimine **33** in diethyl ether without Lewis acid. The reaction turned out to be highly diastereoselective both with organolithium and with organomagnesium reagents (*Re*-face addition) and afforded amines **6(*R*)-34** in good yields (65-90%).

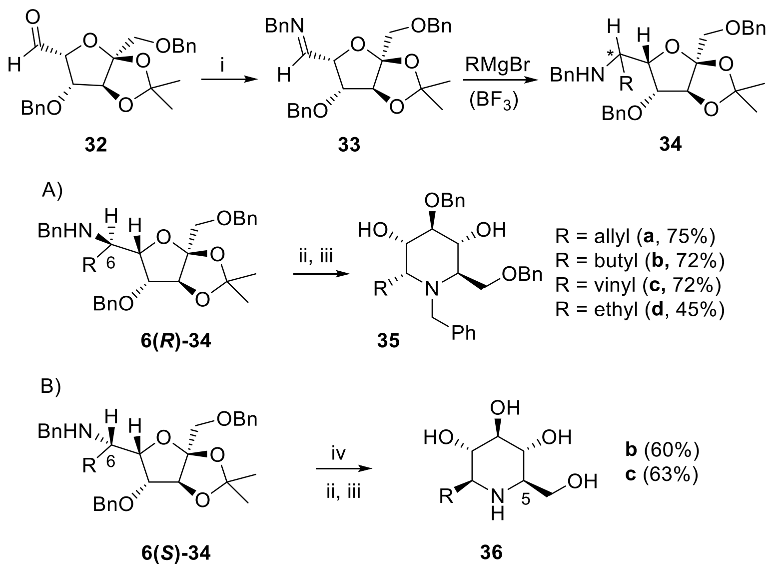

Scheme 2.6: Reactions and conditions i) $BnNH_2$ (1.05 equiv.), 4Å MS, CH_2Cl_2, 4°C, 16 h, ii) TFA:H_2O (9:1), 30 h, iii) $NaBH_3CN$ (3 equiv.), AcOH (1 equiv.), MeOH, 24 h, r.t., iv) H_2, Pd/C, HCl, MeOH, r.t., 48 h.

The presence of Lewis acid during the organometal addition reaction, in case of BuLi and vinylmagnesium bromide, completely reversed the selectivity in favor of the amines **6(*S*)-34** with good yields (69-72%) and high stereoselectivity (*Si*-face addition). The next step of the strategy was the intramolecular RA of **34**, which was first subjected to hydrolysis using CF_3COOH at room temperature. The crude intermediate was treated with $NaBH_3CN$, AcOH in MeOH for 24 h at room temperature affording diastereomerically pure **35a-d** in good yields (Scheme 2. 6A). Starting from the **6(*S*)-34**, the presence of the phenyl group produced partial destabilization of the cyclic iminium ion intermediate with complete loss of stereoselectivity at C5. Therefore, it was necessary to remove the benzyl protecting groups through hydrogenolysis prior to the RA step to afford the β-C-glycosides **36b-c** (Scheme 2.6B). The hydrogenolysis was carried out with Pd/C in MeOH and allowed the cleavage of the isopropylidene group, while the RA was carried out under the same conditions.

This efficient and versatile synthetic strategy developed by Martin and co-workers was successfully applied also to the synthesis of the first example of a 1-phosphonate iminosugar, (1*S*)-1-*C*-diethylphosphono-1-deoxynojirimycin. Following this approach, Asano et al. described the first synthesis of enantiomerically pure 1,6-dideoxy-L-nojirimycin in nine steps from L-xylose with an overall yield of 15%. [133]

Godin and co-workers synthesized iminosugar *C*-glycosides with a great degree of structural diversity *via* cross-metathesis reactions of *N*-protected α-1-*C*-allyl-1-deoxynojirimycin derivatives and a large series of different alkenes. [134] Condensation of aldehyde **32** with 2-naphthalenemethylamine ($NAPNH_2$) followed by reaction with vinylmagnesium bromide gave the diastereomerically pure amine **37** (Scheme 2.7).

Acetonide hydrolysis and intramolecular RA with $NaBH_3CN$ and AcOH in MeOH, followed by acetylation afforded the protected nojirimycine *C*-glycosides **38** in good yields and high diastereoselectivity. The *N*-naphthalenemethyl protective group was selectively and efficiently removed and the resulting secondary amine **39** was formylated or protected with a Troc group. The following cross-metathesis step afforded the expected iminosugar *C*-glycosides **40**-**51** in 45-96% yield and excellent *E*/*Z* selectivity (*E*/*Z* > 20/1) (Scheme 2.7).

Martin and collaborators developed the synthesis of α- and β- 1-C-alkyl iminosugars using nucleophilic addition to different pentodialdofuranose-derived imines generated using enantiopure *t*-butanesulfinamides. Depending on the pentafuranose configuration, the stereoselectivity of this reaction was controlled either by the sugar moiety or by the stereogenic sulfur center on the *t*-butanesulfinamide. [135] The same authors used a similar approach to access

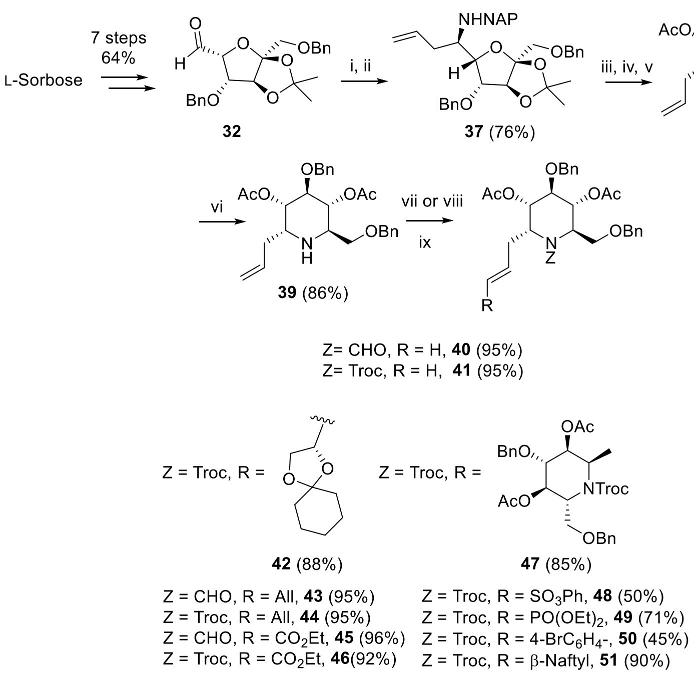

Scheme 2.7: Reactions and conditions i) $NAPNH_2$ (1.05 equiv.), CH_2Cl_2, MS, 4°C, 2 h, ii) VinylMgBr (3 equiv.), Et_2O, 0 to 20°C, 24 h, iii) TFA:H_2O (9:1), 30 h, iv) $NaBH_3CN$ (4 equiv.), AcOH (1 equiv.), MeOH, 30 h, v) Ac_2O (6 equiv.), Py, 5 h, vi) DDQ (3 equiv.), CH_2Cl_2:MeOH, 1 h, vii) HCOONa (2.5 equiv.), PivCl (2.5 equiv.), CH_2Cl_2, 8 h, viii) TrocCl (1.5 equiv.), Py, 2 h, ix) $RCH=CH_2$ (2-3 equiv.), 5-10 mol% Grubbs catalyst, CH_2Cl_2, reflux, 20 h.

D-galacto configured α- and β- 1-C-hexyl derivatives **59** and **60** as potential drugs for the treatment of lysosomal diseases. As shown in Scheme 2.8, L-sorbose-derived aldehyde **52** was transformed into *N*-*t*-butanesulfinyl imines **54-S$_R$** and **54-S$_S$** with racemic *t*-butanesulfinamide (**53**) and the two epimers could be separated easily (Scheme 2.8).An extensive study on the addition of Grignard reagents to imines **54** in different reaction conditions was carried out. In particular, careful choice of co-solvents (diethyl ether or THF) allowed to obtain both diastereoiseomers **55** and **56** from the same imine **54-S$_R$** (Scheme 2.8).
The formation of the piperidine ring was achieved by removing the sulfinyl group using methanolic HCl and the resulting amines were individually submitted to a diazo transfer reaction followed by cleavage of the isopropylidene *via* treatment with acidic ion exchange resin, to yield **57** and **58**, respectively. The conversion of amines to azides at this stage was necessary since the free 6-aminoketoses,

which were in principle capable of intramolecular RA, revealed unstable and underwent degradation in all attempts. The final RA step was performed on azides **57** and **58** under hydrogenation conditions affording the final compounds **59** and **60** in 64% and 71% yields, respectively. [136]

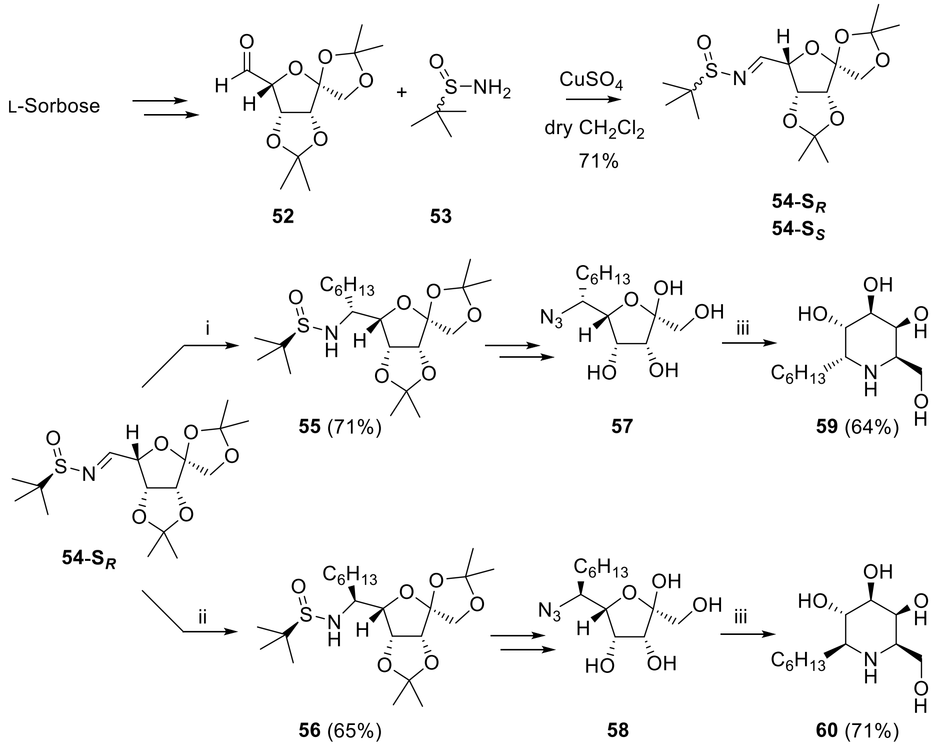

Scheme 2.8: Reactions and conditions: i) HexylMgBr 2 M in Et_2O, -78°C, ii) HexylMgBr 0.8 M in THF, -78°C, iii) H_2 , 10 bar, 10% Pd/C, MeOH, r.t., 4 h.

2.3 The azide route

Formation of azides has been extensively employed in organic synthesis as one of the most useful and practical tools for the synthesis of nitrogen-containing compounds. In this section, we will discuss examples in which an azido moiety is introduced onto a carbohydrate as the amine precursor. Sodium azide displaces an appropriate leaving group (e.g., Br, I, OTs) to give the corresponding azido compound. This latter is converted to the desired piperidine through azide reduction/intramolecular RA *via* a two steps procedure or in one-pot.

Ichikawa and co-workers synthesized iminosugars **63, 66, 67, 70, 71** and **73** starting from the available carbohydrates D-lyxose, D-ribose, D-arabinose, and Dmannofuranose (Scheme 2.9). [137]-[139] The synthetic strategy involved regioselective tosylation of protected carbohydrates followed by azidation to afford **61**, **64**, **68** and **72**, respectively. Removal of benzyl protecting groups and tandem azide reduction/intramolecular RA using catalytic hydrogenation over palladium (Pearlman's catalyst or Lindlar catalyst) afforded the corresponding iminosugar precursors **62**, **65** and **69** which were finally deprotected to yield the final compounds. In case of azide **72**, the RA directly afforded iminosugar **73**. [139]

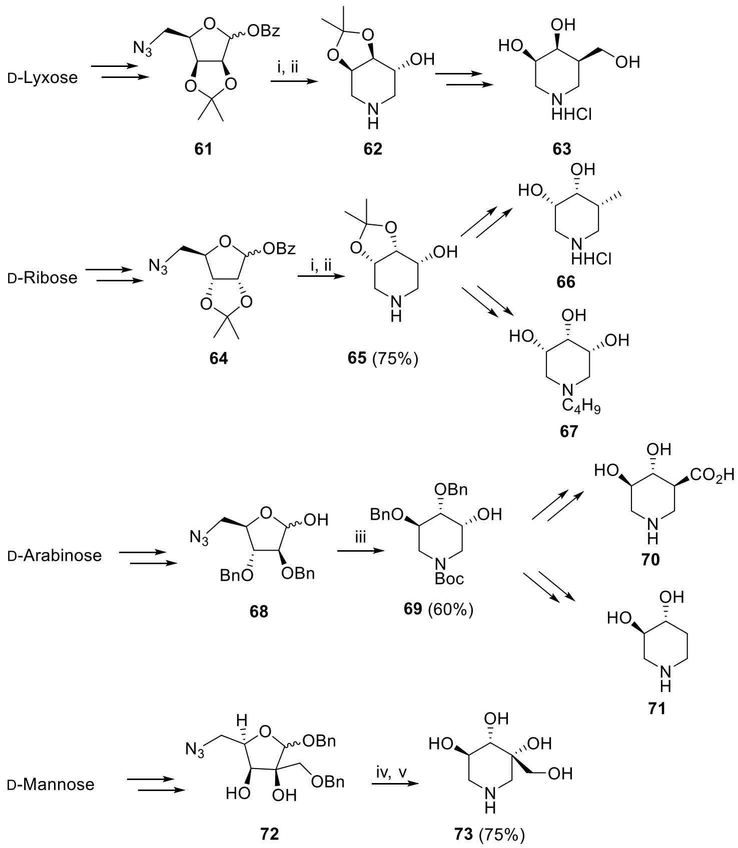

Scheme 2.9: Reactions and conditions: i) NaOMe, MeOH, r.t., ii) H_2, $Pd(OH)_2/C$, MeOH, r.t., 12 h, iii) H_2, Lindlar catalyst, MeOH, r.t., 24 h, iv) H_2, $Pd(OH)_2/C$, H_2O:HCl (pH 3), r.t., 16 h, v) DOWEX 50WX8.

These compounds are also known as 1-*N* azasugars, since they have a nitrogen at the anomeric carbon of common sugars, while iminosugars are commonly

defined as compounds in which the nitrogen atom replaces the ring oxygen of sugars. The inhibitory potencies of the 1-*N*-azasugars shown in Scheme 2.9 were evaluated against several α- and β-glycosidases. For example, **63** inhibited β-galactosidase with an IC_{50} = 19 nM and α–galactosidase with an IC_{50} = 200 µM. This showed for the first time that 1-*N*-azasugars selectively inhibit β-glycosidases over α-glycosidases, in contrast to conventional DNJ-type iminosugars, which are more active towards α-glycosidases. [137] Moreover, compound **66** was found to inhibit α-fucosidase (K_i = 8.4 µM). [138]
Greck and co-workers described a synthetic strategy to obtain 1-deoxyhomonojirimycin **77** from the protected 1,2:5,6-di-*O*-isopropylidene-α-D-glucofuranose in 10 steps with an overall yield of 13%. Moreover, the two 1,5,6-trideoxy-1,5-iminoheptitols **81** and **84** were obtained from the protected 1,2:5,6-di-*O*-isopropylidene-α-D-allofuranose, with overall yields of 19% and 9%, respectively (Scheme 2.10). [140]

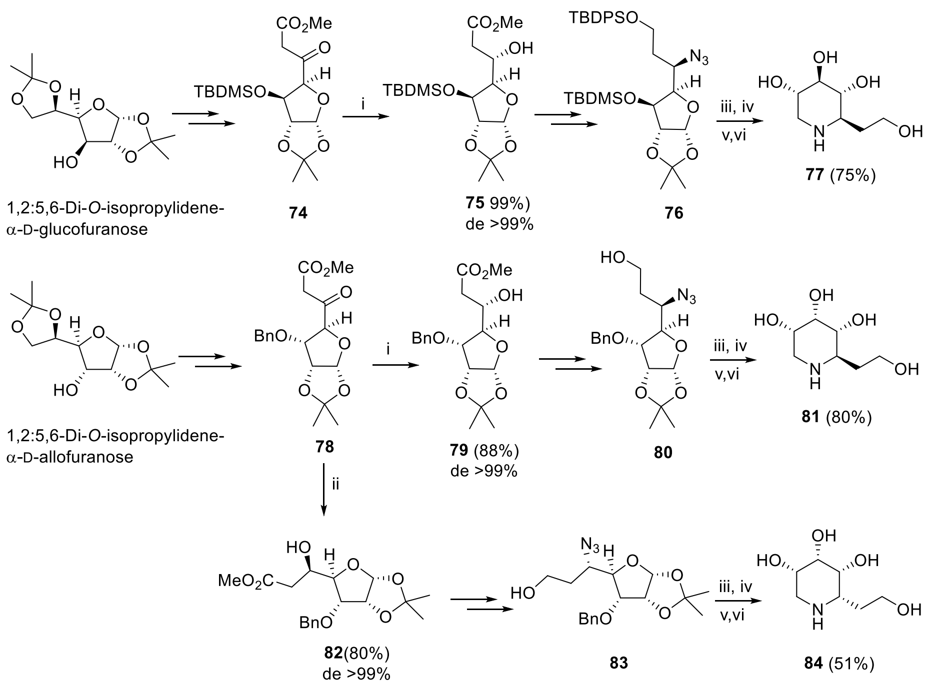

Scheme 2.10: Reactions and conditions: i) H_2, [(*R*)-BinapRuBr$_2$], 1 atm, 45°C, 24 h, ii) H_2, [(*S*)-BinapRuBr$_2$], 1 atm, 45°C, 24 h, iii) TBAF, THF, r.t., 1 h, iv) TFA:H_2O (3:2), 40°C, 2 h, v) H_2, PtO_2, 1 atm, 12 h, r.t., vi) Amberlyst A26.

The key step was the catalytic hydrogenation of β-ketoesters **74** and **78** in the presence of chiral ruthenium complexes, which guaranteed total control of the configuration at the newly formed C-5 stereogenic centre, thus affording the corresponding β-hydroxyesters **75**, **79** and **82** with excellent diastereoselectivity. The secondary alcohols in **75**, **79** and **82** were activated as the corresponding methyl sulfonate esters and directly converted into azides **76**, **80** and **83** through sodium azide displacement with inversion of configuration. The tandem azide reduction/intramolecular RA process was run under acidic conditions affording concomitant deprotection of the diol moiety. The following reaction with hydrogen under atmospheric pressure at room temperature in the presence of platinum oxide (Adam's catalyst) gave a crude product whose further purification over Amberlyst A26 exchange resin afforded **77**, **81** and **84** in 75%, 80% and 51% yields, respectively, over three steps. [140]

Bols and Pedersen, with the aim of studying the effects of different substituents on the basicity of iminosugars (pK_a), synthesized epimeric 2-phenyl iminoxylitols having a phenyl group as a conformational anchor and thus hydroxy groups in the axial or equatorial position, respectively. [141] The synthetic approach relied on the Grignard addition using phenyl magnesium bromide onto the D-glucose-derived aldehyde **15** to give a 12:1 ratio of epimers **85** and **86**. Since both were required, a two-step oxidation/reduction protocol was employed to obtain epimer **86** as the major compound (Scheme 2.11).

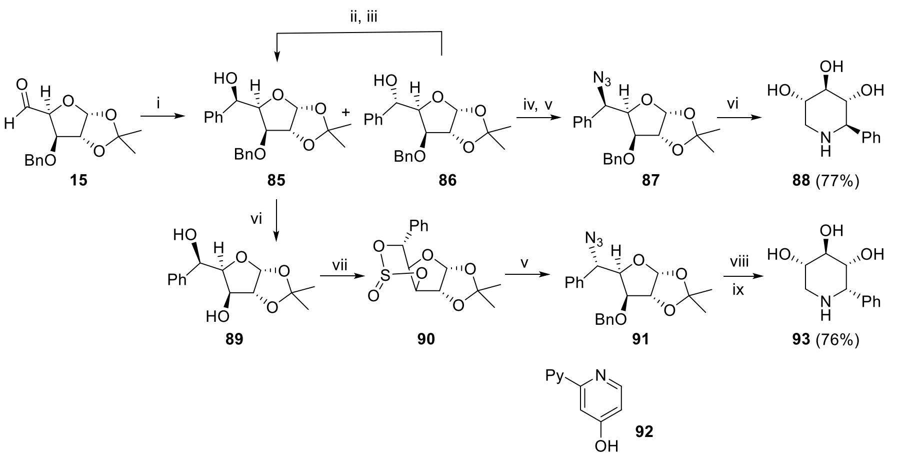

Scheme 2.11: Reactions and conditions: i) PhMgBr, ii) PDC, CH_2Cl_2, iii) $NaBH_4$, MeOH, iv) TsCl, Py, v) NaN_3, DMF, vi) H_2, Pd/C, vii) $SOCl_2$, Et_3N, CH_2Cl_2, 0°C, viii) AcOH, reflux, ix) Pd/C, TESH.

The synthesis proceeded differently for the two isomers. Tosylation of **86** followed by nucleophilic substitution with NaN_3 gave **87** (Scheme 2.11).
Removal of the isopropylidene group and hydrogenation over Pd/C afforded compound **88**. The same approach could not be applied to epimer **85** since it did not undergo tosylation probably due to steric hindrance. Therefore, the benzyl group in **85** was removed by hydrogenolysis to give **89** and the cyclic sulfite **90** was prepared with thionyl chloride and converted into the desired azide **91**. Acidic treatment followed by hydrogenolysis with Pd/C and triethylsilane (TESH) afforded **93**. The hydrogenation/hydrogenolysis step was sluggish and use of more forcing conditions resulted in formation of the pyridine derivative **92** as the dominant side product in the final RA. The use of different catalysts such as Pearlman's catalyst ($Pd(OH)_2$) or Raney-Ni did not improve the reaction. [141]
Davis and co-workers reported a novel procedure [142] to synthesize L-rhamnomimetic iminosugars as inhibitors of rhamnosyltransferase (RhamT), an important enzyme involved in the biosynthesis of the bacterial cell wall in Mycobacterium. [143] The authors described a dual stereodivergent synthetic strategy to access libraries of both α- and β-pseudoanomers based on the L-rhamno-aza-*C*-glycoside scaffold from the azidolactone intermediate **94** (Scheme 2.12). [142] Azidolactone **94** was prepared from D-gulonolactone in six steps. The synthesis of derivatives **96** involved the selective addition of organometallic reagents to intermediate **94**, followed by reduction of the azido group in **95** and subsequent intramolecular RA. Isopropylidene deprotection with TFA, followed by treatment with ion-exchange resin, gave novel aza-*C*-β-rhamnomimetics **96** with good yields (70–98%) (Scheme 2.12). The RA performed directly on the intermediate **94** under these conditions provided 5-dideoxy-1,5-imino-L-rhamnitol **97** in good yield. Taking advantage of these conditions for the RA, also S. Dharuman *et al.* reported a convenient synthesis of **97** in seven steps and 17% overall yield from L-rhamnose. [144] A Staudinger aza-Wittig reaction performed on **98** afforded partially protected cyclic imine **99**. [142] The latter was subjected to diastereoselective (de>98%) addition of Grignard reagents, which afforded the corresponding aza-*C*-α-mimetics **100** in good yield (85-95%) after acetonide deprotection with TFA. Interestingly, among the whole set of compounds, **97** was the most potent inhibitor of mycobacterial system (38% at 100 μM). Moderate

inhibition (19-30% at 100 μM) was also exhibited by some of the aza-*C*-β-rhamnomimetics **96** (namely those bearing Me, Bu, Et, octyl, MeOPhCH and naphthyl pseudoanomeric substituents).

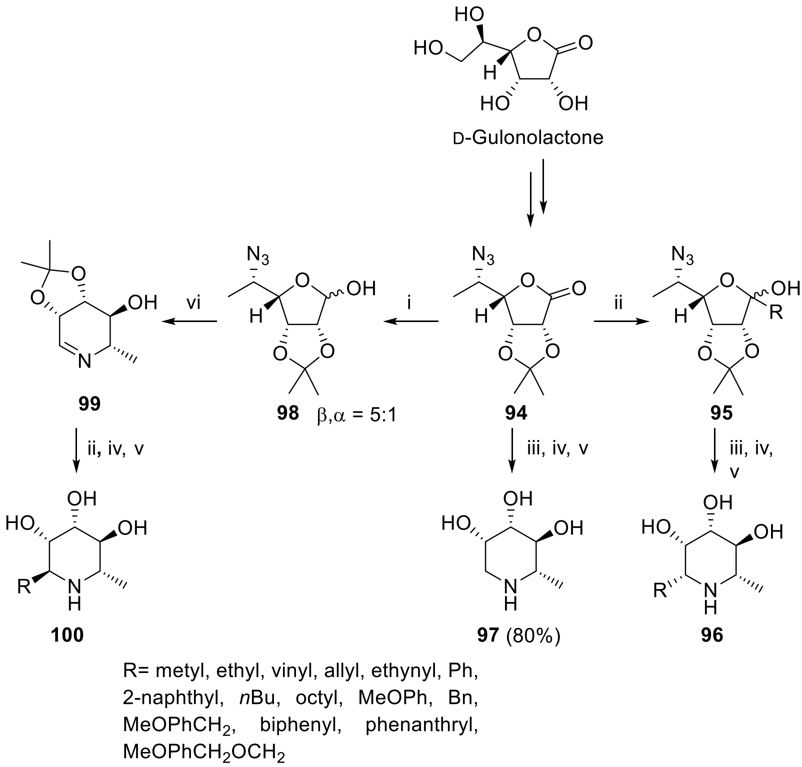

Scheme 2.12: Reactions and conditions: i) DIBAL-H, THF, -78°C, 2 h, ii) organometallic reagents (1.2-1.3 equiv.), -78 to -60°C, THF, iii) H_2, Pd/C, EtOH, r.t., 24-48 h, iv) TFA:H_2O (1:1), r.t., 24 h, v) Amberlite IR120, vi) $Ph_2P(CH_2)_2PPh_2$, THF, 50°C, 15 min.

In order to investigated the glycosidase inhibition profiles of the enantiomers of the naturally occurring glycosidase inhibitors (the so-called "looking glass inhibitors"), Fleet and co-workers reported a convenient large-scale synthesis of 1,6-dideoxygalactostatin **105** (D-DFJ), the enantiomer of the potent fucosidase inhibitor deoxyfuconojirimycin (L-DFJ), from the readily available 2,3-*O*-isopropylidene-D-gulonolactone, in five steps and 54% overall yield. [145] The straightforward synthesis involved introduction of azide moiety through sulfonylation of the free hydroxy group in compound **101** with trifluoromethanesulfonic anhydride in dichloromethane, followed by

nucleophilic displacement of the resulting triflate with sodium azide in DMF to afford the corresponding azidolactone **102** (Scheme 2.13). Addition of methyl lithium to azidolactone afforded azidolactol **103** as a single stereoisomer in good yield (91%). Hydrogenation of **103** in the presence of palladium black in EtOH resulted in tandem azide reduction/intramolecular RA to obtain the corresponding protected iminosugar **104** in 84% yield. The stereochemistry of the reduction of the transient imine was controlled by the adjacent isopropylidene group. Final deprotection with TFA yielded the target **105** (D-DFJ) in 96% yield. This compound was evaluated as inhibitor of several plant and human α- and β-galactosidases (K_i = 1.36 µM towards coffee been α-galactosidase) and naringinase (IC_{50} = 90 µM), a glycosidase that targets L-rhamnose containing saccharides.
The authors also reported the synthesis of L-DFJ from L-gulonolactone in analogy with the synthetic approach used to obtain D-DFJ. [145]

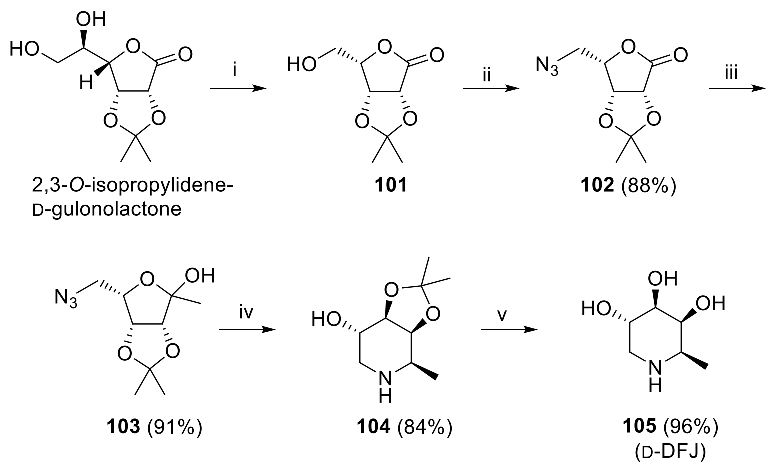

Scheme 2.13: Reactions and conditions: i) $NaIO_4$, $NaBH_3CN$, THF, ii) Tf_2O, Py, CH_2Cl_2 then NaN_3, DMF, iii) MeLi, THF, 4Å MS, -78°C, iv) H_2, Pd black, EtOH, v) TFA:H_2O (1:1).

Dhavale and co-workers introduced on several D-hexoses a keto functionality at C-5, which was subjected to the Jocic−Reeve and Corey−Link type reaction. This strategy allowed introduction of an hydroxymethyl group and an azide moiety at C-5, thus forming 5-azido-5-hydroxylmethyl substituted hexofuranoses **106**, **108** and **110** (Scheme 2.14). [146]

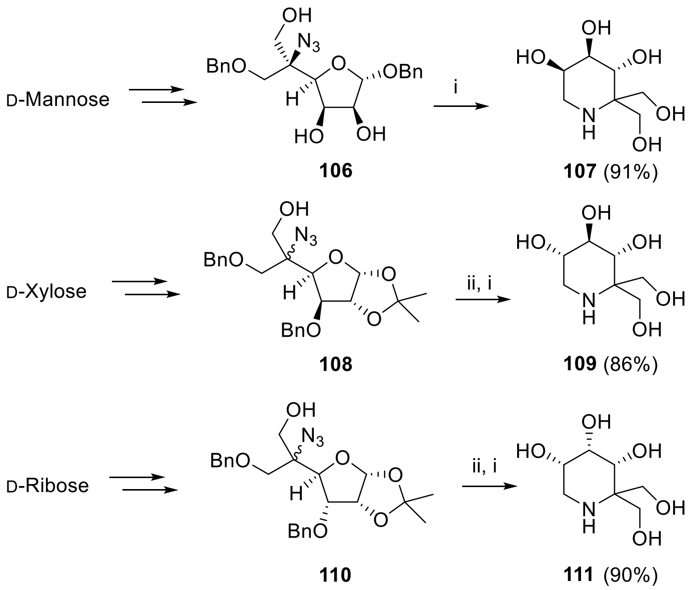

Scheme 2.14: Reactions and conditions: i) H_2, 10% Pd/C, MeOH, 200 psi, 24 h, ii) TFA:H_2O (3:1), 0 °C, 3 h.

Removal of protecting groups and conversion of the C-1 anomeric carbon into the free hemiacetal followed by intramolecular RA afforded the corresponding 5C-dihydroxymethyl piperidine iminosugars **107**, **109** and **111**. The reaction conditions for the RA step employed H_2 as the reducing agent at high pressure (200 psi), in the presence of Pd/C (10%) catalyst in MeOH, and allowed to obtain the piperidines in good yields (86-91%) after 2 days. Compounds **109** and **111** behave as potent inhibitors of rice α-glucosidase (IC_{50} = 32 nM and IC_{50} = 52 nM, respectively), while **107** was less potent (IC_{50} = 4 μM). Moderate inhibition was also found for the three new compounds towards the microbial α-galactosidase from *Geobacillus sp.* (IC_{50} = 15-22 μM) and for compound **103** towards β-galactosidase from bovine liver (IC_{50} = 40 μM). [146]

The same authors also reported an efficient route for the synthesis of trihydroxypipiperidines **123**, **124**, and **125**, starting from D-glucose derived pentodialdoses **15, 112** and **113** (Scheme 2.15). [147]

The exocyclic aldehyde of these compounds was reduced to the corresponding alcohol, which was subsequently tosylated to give compounds **114**, **115** and **116**. The nucleophilic displacement of the tosyl group by NaN_3 in DMF led to the formation of azido compounds **117**, **118** and **119**. Catalytic hydrogenation and protection gave *N*-Cbz protected compounds **120**, **121** and **122**, which upon removal of the acetonide moiety and hydrogenation afforded the corresponding 1-*N*-azasugars **123**, **124** and **125** in good overall yields. Compounds **124** and **125** revealed more potent inhibitors of β-glucosidase (IC_{50} = 3.18 µM and 4.97 µM, respectively), than **123** (IC_{50} = 1.40 mM), showing that either inversion of configuration at C-4 or substitution of an OH group with a hydroxyethyl functionality resulted in increased potency towards β-glucosidase with high specificity. [147]

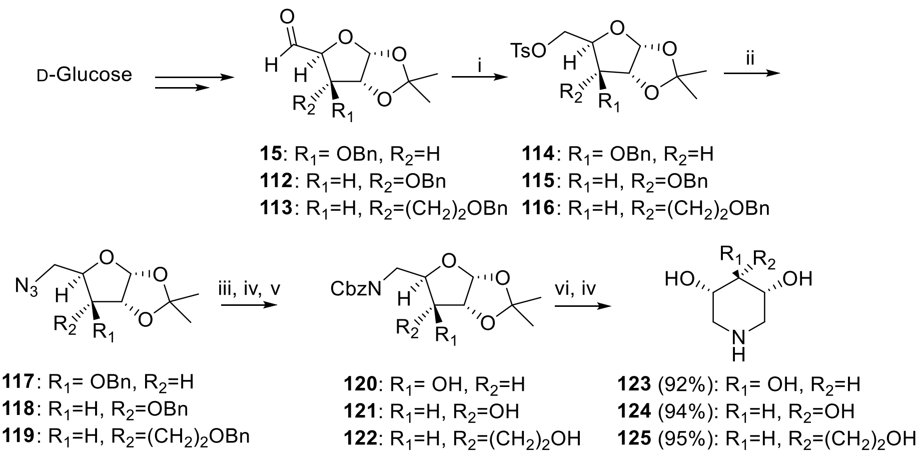

Scheme 2.15: Reactions and conditions: i) $NaBH_4$, MeOH, r.t., 15 min, ii) TsCl, Py, r.t., 12 h, iii) NaN_3, DMSO, 100°C, 6 h, iv) 10% Pd/C, H_2, 80 psi, MeOH, 12 h, v) CbzCl, $NaHCO_3$, EtOH:H_2O (4:1), r.t., 2 h, vi) TFA:H_2O (3:2), r.t., 2 h.

Fleet and co-workers exploited the kinetic and thermodynamic azide displacement of sugar-derived triflates to access azido-γ-lactones as key intermediates in the synthesis of homonojirimycin (HNJ) analogues, employing a biotechnological approach *via* the Izumoring techniques. [148]

We report in detail the synthetic strategy starting from D-glucoheptonolactone (**126**), which was transformed into the kinetic *ido*-azido-γ-lactone derivative **127** (Scheme 2.16). *Gluconobacter thailandicus* NBRC 3254 was able to recognize selectively the *R*,*R* configuration of the diol adjacent to the terminal alcohol in compound **128** leading to the azido-ketose **129**, which was recognized by the D-tagatose-3-epimerase to obtain epimeric **132**. The azido-ketose derivatives **129** and **132** underwent RA using Raney-Ni in water under hydrogen affording a mixture of isomers **130** and **131** in 1:11 ratio and **133** and **134** in 14:1 ratio, respectively. The selectivity of the reductions were explained by the presence of torsional strain and axial substituents in the imine intermediate. [148]

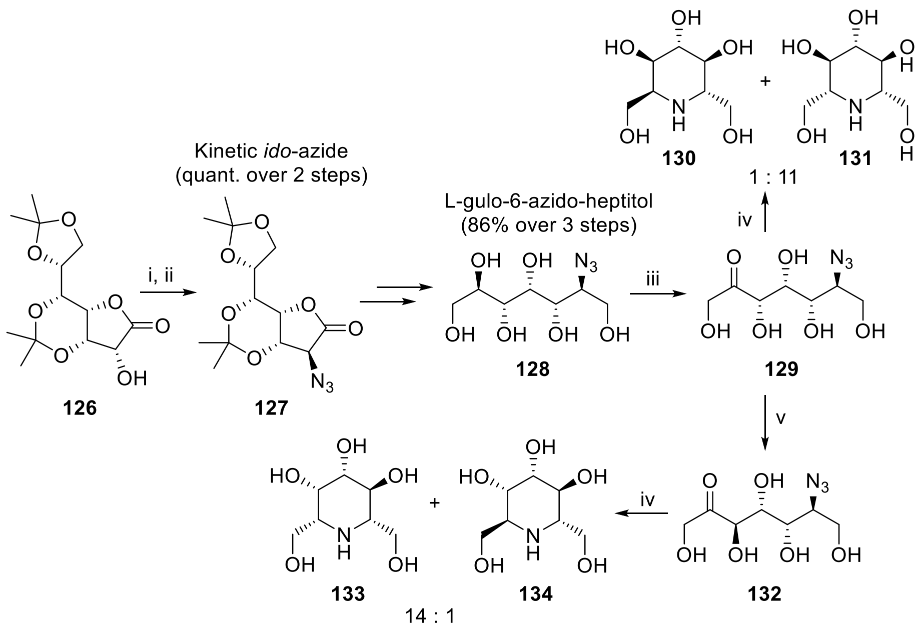

Scheme 2.16: Reactions and conditions: i) Tf_2O, CH_2Cl_2, Py, −30°C, 30 min, ii) NaN_3 (1.5 equiv.), DMF,−15 to 6°C, 15.5 h, iii) *Gluconobacter thailandicus* NBRC 3254, H_2O, 30°C, iv) H_2, Ni, H_2O, v) D-tagatose-3-epimerase, H_2O.

In 2017, our group reported the synthesis of C-2 (*S*) substituted piperidine **139** (Scheme 2.17). [149] The procedure involved Grignard addition to the carbohydrate-derived aldehyde **135** followed by azide insertion with inversion of configuration and final intramolecular RA. Aldehyde **135** was accessed in four steps from D-mannose on gram scale. The addition of MeMgBr to **135**, performed at -78°C, afforded the corresponding alcohols **136** in excellent yield (92%) and good stereoselectivity (dr = 5:1). The alcohol with the (*R*) absolute configuration at the newly formed stereocentre was obtained as the major diastereoisomer. Modification of the reaction conditions (time, temperature, Grignard reagents) or Lewis acids addition in the presence of a higher excess of Grignard reagent did not lead to any improvement or reversal of selectivity. The nitrogen installation was attempted through direct displacement from alcohols **136** via a Mitzunobu reaction with inversion of configuration. The reaction allowed the one-pot synthesis of the major azide **137a** in good yield (67%). The final RA step was performed with Pearlman's catalyst under hydrogen atmosphere and afforded **138** with 91% yield. Acetonide deprotection gave piperidine **139** with the (*S*) absolute configuration at C-2 (Scheme 2.17). [149]

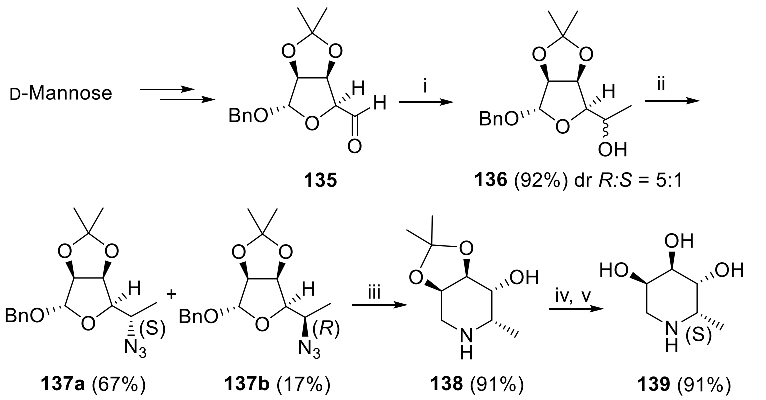

Scheme 2.17: Reactions and conditions: i) MeMgBr (1.8 equiv.), THF, -78°C, 1.5 h, ii) PPh_3, DIAD, DPPA, THF, r.t., 24 h, iii) H_2, $Pd(OH)_2/C$, MeOH, r.t., 5 d, iv) 12 M HCl, MeOH, r.t., 16 h, v) DOWEX 50WX8.

2.4 The nitrone/hydroxylamine route

As part of our longstanding interest in the synthesis and biological evaluation of iminosugars, [150]-[156] we recently synthesized a library of C-2 substituted trihydroxypiperidine iminosugars with different alkyl chains through the stereoselective Grignard reagent addition onto nitrone **140**, followed by RA reaction (Scheme 2.18). [157] [158] In particular, in this project we were interested in the synthesis of compounds able to interact with the glucocerebrosidase (GCase) enzyme, for their potential use as Pharmacological Chaperones (PCs) for Gaucher Disease. [23]

Due to the outstanding activity as PCs found for some *C*-alkylated trihydroxypiperidines, [85] [84]we reasoned that the activity of our previously reported *N*-alkylated trihydroxypiperidines [159]could be improved by shifting the alkyl chain onto the C-2 position.

To this scope, we explored the nitrone approach. Grignard additions to carbohydrate-derived nitrones have been extensively studied by Merino and co-workers, demonstrating that the diastereoselectivity of the addition can be finely tuned by Lewis acids and is also dependent on the particular Grignard employed. [160]-[164]

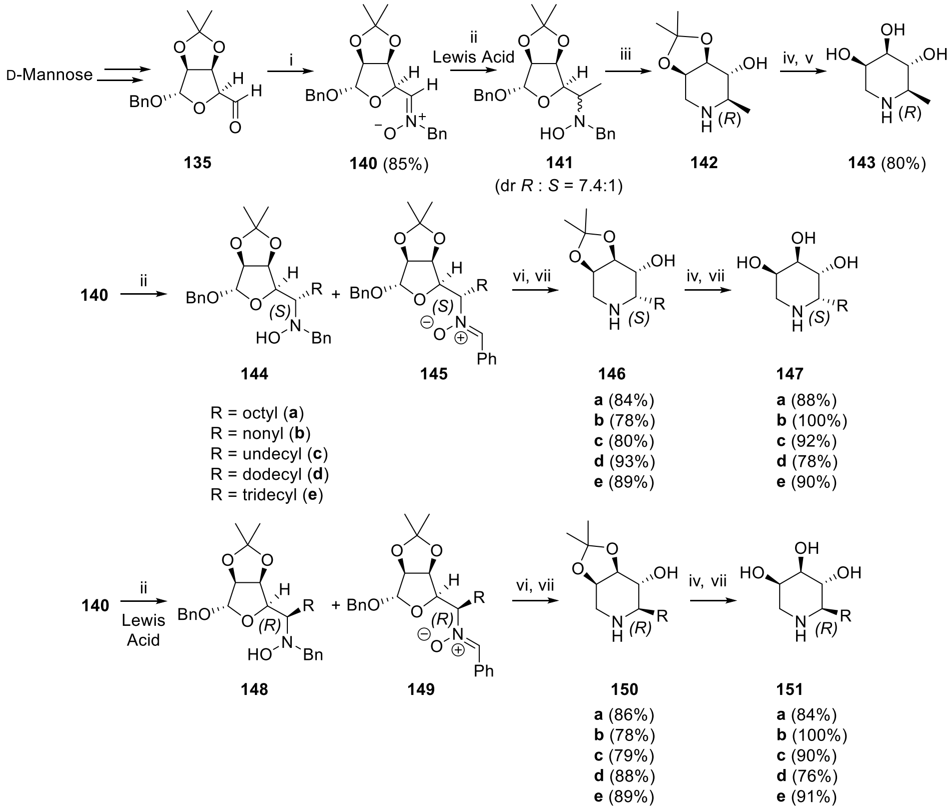

Scheme 2.18: Reactions and conditions: i) BnNHOH·HCl, Et_3N, dry CH_2Cl_2, r.t., 16 h, ii) Grignard reagents, THF, iii) H_2, $Pd(OH)_2/C$, MeOH, r.t., 4 d, iv) 12 M HCl, MeOH, r.t., 18 h v) DOWEX 50WX8, vi) H_2, Pd/C, AcOH, MeOH, r.t., 2 d, vii) Ambersep 900-OH.

Nitrone **140** was synthesized starting from aldehyde **135** in 85% yield by reaction with *N*-benzyl hydroxylamine in dry CH_2Cl_2. [165] The addition of MeMgBr to **140** afforded two diastereoisomeric hydroxylamines **141** with almost no stereoselectivity. [149] To our delight, in the presence of Lewis acids, a good stereoselectivity (dr = 7.4:1) in favor of the hydroxylamine **141** with the (*R*) absolute configuration at the newly formed stereocenter was observed (Scheme 2.18). The hydroxylamine **141** was directly employed for the final cyclization reaction using Pd catalyzed hydrogenation. This synthetic strategy afforded, after deprotection of **142**, the trihydroxypiperidine **143**, epimeric at C-2 with respect to **139**, which had been obtained in the previous approach *via* the azido route (see Scheme 2.17). [149] We then applied this protocol employing several long chain Grignard reagents to access iminosugars bearing lipophilic moieties at C-2, able in principle to better mimic glucosylceramide, the natural substrate of the GCase enzyme. In this case, the Grignard addition on **140** afforded (*S*) hydroxylamines **144** as the major diastereoisomers, while addition of Lewis Acid completely reversed the selectivity in favor of (*R*) hydroxylamines **148** (Scheme 2.18). Both hydroxylamines **144** and **148** underwent to oxidation to air to give the corresponding nitrones **145** and **149**. The hydroxylamine/nitrone mixtures were directly subjected to the RA key step, with H_2 as a reducing agent, Pd/C as catalyst and MeOH as solvent, and in the presence of 2 equiv. of CH_3COOH, affording piperidines **146** and **150** with excellent yields. The overall efficiency of this one-pot reaction is remarkable, considering that it results from a cascade of several synthetic steps (*N*- and *O*- debenzylation, hydyroxylamine/nitrone reduction, condensation with sugar aldehyde and C=N reduction). Deprotection of the acetonide protecting groups under acidic conditions led to the synthesis of the final trihydroxypiperidines **147** and **151**.

All the newly synthesized trihydroxypiperidines showed β-glucocerebrosidase inhibitory activity higher than 80%, and the (*R*)-configured trihydroxypiperidines **151** were more active than epimeric trihydroxypiperidines **147**. The compounds with the dodecyl alkyl chain imparted the best inhibitory activity to the final compounds for both series. Overall, compound **151d** was the best inhibitor (with IC_{50} = 1.5 μM). The ability of the C-2 alkylated trihydroxypiperidines **147** and **151** to enhance the activity of GCase was next assayed in human fibroblasts derived from Gaucher patients bearing the N370/ RecNcil mutation.

Nearly all new compounds showed an increase in GCase activity from 1.2-fold to 1.9 –fold. In particular, compound **151a** was able to induce a remarkable 1.8-fold in GCase activity at 100 μM in fibroblasts carrying the L444P/L444P mutation, [157] which is particularly notable since fibroblasts bearing the homozygous L444P mutation are resistant to most PCs. A small rescue towards wild-type human fibroblasts was also observed, which is important for the development of treatments for sporadic forms of Parkinson disease without the mutations typical of Gaucher Disease. [158] Indeed, recent studies highlighted that the loss of glucocerebrosidase function contributes to the pathogenesis of Parkinson disease, and the modulations of GCase activity is emerging as the key therapeutic target for both pathologies. [166]

2.5 The nitro route

A distinguished example in which the amino moiety was introduced in the molecule through reduction of a nitro compound was reported by Withers and co-workers. [167]

They employed a β-xylosidase-derived glycosynthase to catalyze the glycoside bond formation using activated glycosyl donors, in order to prepare xylanase inhibitors. [168] The xylose-configured iminosugar acceptor **154** was prepared from 1,2:5,6-di-*O*-isopropylidene-α-D-glucofuranose through aldehyde **15**, which was subjected to Henry reaction with nitrometane, followed by dehydration and reduction to give nitro compound **152** (Scheme 2.19). Acetonide removal and treatment with $NaIO_4$ gave the unstable aldehyde **153**, which was immediately subjected to hydrogenation and *N*-Cbz protection to afford **154** in overall good yield.

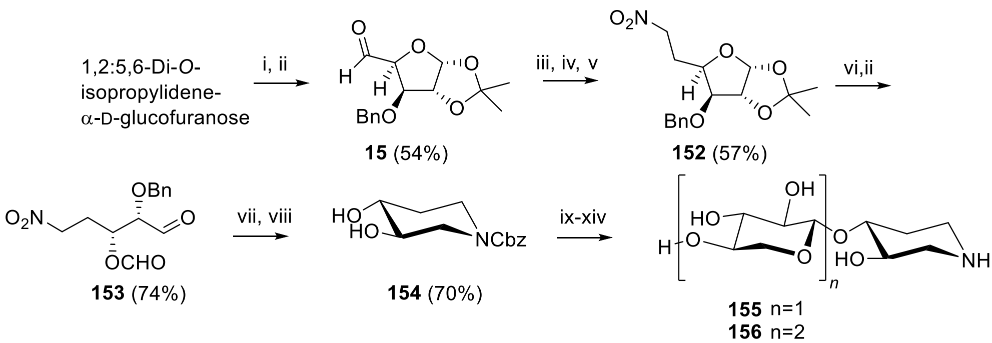

Scheme 2.19: Reactions and conditions: i) (a) NaH, BnBr, DMF, (b) AcOH:H_2O (9:1), ii) $NaIO_4$, MeOH, H_2O, iii) $MeNO_2$, 1N NaOH, EtOH, iv) MsCl, Et_3N, CH_2Cl_2, v) $NaBH_4$, EtOH, vi) 6N HCl, THF, vii) H_2 (3 atm), Pd/C, HCl, MeOH, viii) CbzCl, K_2CO_3, H_2O:MeOH (1:1), ix) xylopyranosyl fluoride, E334G Bhx mutant, exo-β-xylosidase, pH 7, r.t., 1 d, x) Ac_2O, DMAP, Py, xi) NaOMe, MeOH, xii) Amberlite IR120, xiii) H_2 (1 atm), Pd/C, MeOH, xiv) 1N HCl.

The xylose like acceptor **154** took part in the reaction with the E334G mutant of a *B. halodurans* xylosidase (Bhx), which efficiently catalyzed the glycosylation

with a donor substrate (α-D-xylopyranosyl fluoride) forming the β-(1→4)-linked di- and trisaccharides **155** and **156** in excellent yield. Kinetic studies revealed that the trisaccharide iminosugars are better inhibitors than the corresponding disaccharides for two xylanases of different GH families. [169] In particular, the trisaccharide **156** was the most potent competitive inhibitor of xylanase from *Cellulomonas fimi* (Cex), a GH10 family enzyme (IC_{50} = 0.018 µM), and xylanase from *Bacillus circulans* (Bcx), belonging to the GH11 family (IC_{50} = 63 µM). [167]
Also Martin and co-workers reported a nice example in which the nitrogen atom was introduced as nitro moiety, to access the two epimeric derivatives of 4-*epi*-isofagomine carrying a pentyl group at C-5a **161** and **163** (Scheme 2.20). [170]

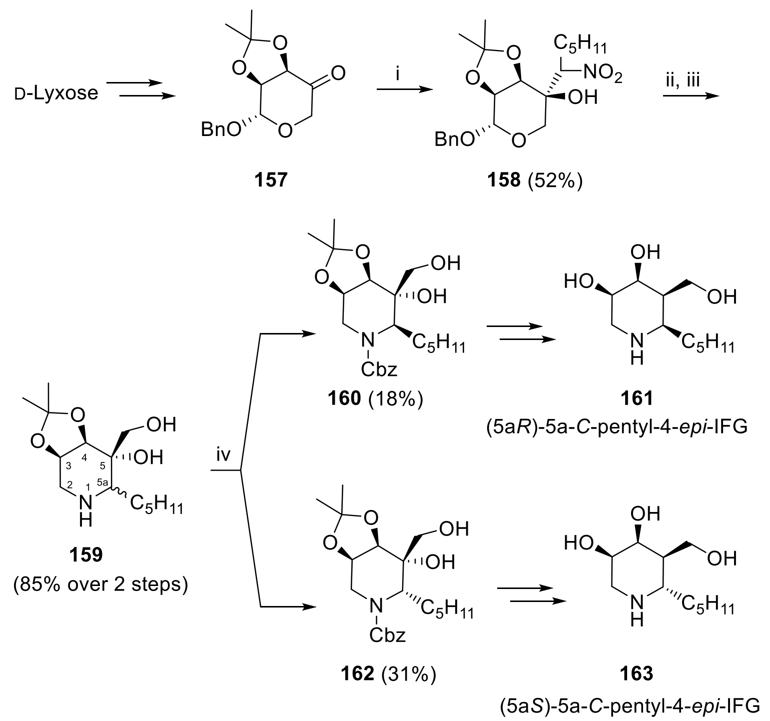

Scheme 2.20: Reactions and conditions: i) 1-nitrohexane, NEt_3, r.t., 4 d, ii) H_2, Raney®-Ni, AcOH, iPrOH, r.t., 5 d, iii) H_2, $Pd(OH)_2$/C, AcOH, iPrOH, r.t., 3 d, iv) CbzCl, DIPEA, EtOH, r.t., 16 h.

The addition of 1-nitrohexane to ketopentopyranoside **157,** in turn obtained from D-lyxose, afforded derivative **158** as a 7:3 mixture of epimers.
Two consecutive catalytic hydrogenations (performed in the presence of Raney®-

Ni and $Pd(OH)_2/C$, respectively) promoted the reduction of the nitro moiety, cleavage of the benzyl group and intramolecular RA, providing in good yield (85% over two steps) iminosugar **159** as a not separable mixture of two epimers at C-5a. Protection of the nitrogen atom as a benzyl carbamate allowed separation of **160** and **162,** which were further converted into the final compounds (5a*R*)-5a-*C*-pentyl-4-*epi*-isofagomine **161** and (5a*S*)-5a-*C*-pentyl-4-*epi*-isofagomine **163**.
An improved synthesis of **161** and related analogues was recently published by the same authors following the azido route. [171] Compound **161** was found to be a much more potent inhibitor of β-galactosidase (IC_{50} = 8 nM) than epimer **163** (IC_{50} = 13 μM). [170] Moreover, **161** behaved as a remarkable PC when evaluated on cell lines from patients affected by GM1-gangliosidosis and Morquio disease type B, two lysosomal storage disorders caused by deficiency of the human lysosomal enzyme β-galactosidase. In addition, **161** showed the capacity to dissociate readily from the enzyme in an acidic environment indicating that **161** is a promising drug candidate for the treatment of these two severe lysosomal storage disorders.

Conclusion

The RA, despite being a reaction known since a long time, it still represents one of the most versatile and useful tool to form new C-N bonds, thereby introducing an amine in a chemical structure. The intramolecular variant of this reaction has recently gained a renewed attention due to its efficient application to the synthesis of naturally occurring polyhydroxypiperidines and their synthetically functionalized analogues as potential therapeutic agents.
Among the reducing agents, $NaBH_3CN$ and H_2 in the presence of catalysts are the most frequently employed. The former is more selective towards imine reduction and it is often the method of choice on a laboratory scale. However, its involvement in industrial processes is limited by the toxic nature of cyanide by-products which increases the risk of HCN release in acidic medium.
From the green chemistry viewpoint, RA reactions involving H_2 in the presence of solid catalysts are definitely more appealing. First, H_2 has a relative low cost and produces nearly zero-waste. Second, the reaction can be automatized using flow systems in which a continuous flow of hydrogen and solvents are passed through a packed column containing solid catalysts. We can envisage that in the

next future the research will take advantage of such novel technologies to further improve the overall method performance. Moreover, the hydrogenation procedures allow to employ several nitrogen containing moieties (amines, imines, nitrone, azide, nitro) as substrates for the RA enabling highly efficient tandem one-pot processes. These aspects are particularly important in the development of industrial processes for the more therapeutically appealing compounds. The collection of the reported examples, which does not pretend to be exhaustive, seeks to put forward useful information for the further exploitation of RA methodology in the synthesis of new iminosugars or, more generally, as an intermediate step in the total synthesis of natural compounds.

Chapter 3: Synthesis of alkylated Azasugars: potential Pharmacological Chaperones for Gaucher Disease

Introduction

Following the Lab longstanding interest in the total synthesis of polyhydroxylated nitrogen heterocycles and their non-natural analogues as glycosidases inhibitors [151] [154] [156] [172] [173], the research group found that the peculiar configuration of trihydroxypiperidine **165** (Scheme 3.1) [120] [121] [123], the enantiomer of a natural product, imparted 50% of inhibition towards human GCase enzyme in leukocytes isolated from healthy donors at 1 mM. [159]

The compound **165** was obtained through the double reductive amination reaction (DRA) on a key masked dialdehyde intermediate **135** using $BnNH_2$ and H_2 in the presence of catalyst $Pd(OH)_2/C$, with excellent yield on 4 steps (debenzylation, imine formation, reduction of imine and RA on the anomeric carbon), followed by deprotection (Scheme 3.1). Aldehyde **135** was easily synthesized from an inexpensive sugar (D-mannose) in four steps with a high overall yield (85%), without the need for any chromatographic purification. [174]

Recently, the research group reported the synthesis of trihydroxypiperidines with an eight carbon atom chain at either the endocyclic (**169**) or an exocyclic nitrogen (**167**). The synthesis of compound **169** involved a double reductive amination on deprotected aldehyde **164**, with octylamine and $NaBH_3CN$ as the reducing agent (in MeOH and in the presence of 3Å MS and CH_3COOH), followed by acetonide deprotection in acidic conditions (Scheme 3.1). [175] The compound **167** was synthesized starting from the ketone key intermediate **166** obtained through protection of the endocyclic nitrogen atom of compound **62** with a *tert*-butyloxycarbonyl (Boc) group followed by oxidation with Dess Martin periodinane (DMP) (Scheme 3.1). Compounds **169** and **167** were able to strongly inhibit GCase on a pool of leukocytes from healthy donors with percentages of inhibition higher than 90% at 1 mM concentration resulting in an interesting IC_{50} = 30 µM and 40 µM, respectively. Compounds **169** and **167** showed measurable chaperoning activity with human fibroblasts derived from Gaucher patients bearing the N370/RecNcil mutation (up to 1.25-fold or 1.50-fold increase of mutant GCase activity at 100 µM concentration, respectively). [159] Therefore, once again the presence of a lipophilic chain played a pivotal role for inhibition.

Based on the observation of the subtle role played by the alkyl chain in the biological activity, the position of the alkyl chain seems to be crucial for the activity. Indeed, while for iminosugar analogues the N-alkylation gave good PCs for GCase, in the case of azasugars the alkylation of the carbon adjacent to nitrogen furnished better PCs for GD as shown by the previously mentioned examples on IFG and DIX derivatives (see *Chapter 1*).

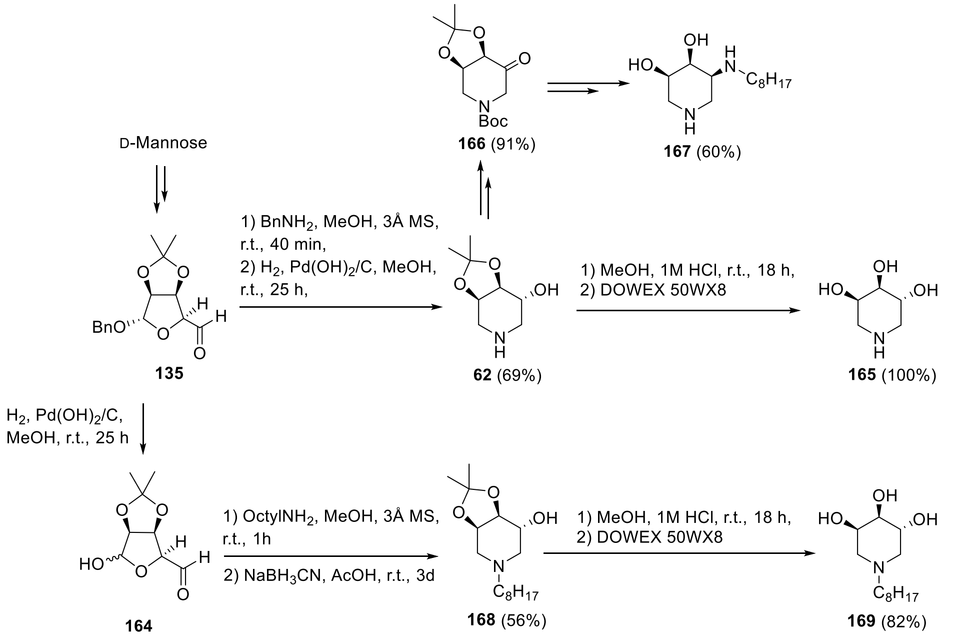

Scheme 3.1: State of the art.

The aim of the work was to synthesize trihydroxypiperidine azasugars alkylated in different positions (and with different configurations).

- synthesis of trihydroxypiperidines **147** and **151** alkylated at C-2 with chains of different lengths, in order to investigate the role of the length, position and configuration of the alkyl chain on this differently configured piperidine skeleton.

The adopted synthetic strategy to access C-2 substituted trihydroxypiperidines relies on a stereodivergent approach that employs a carbohydrate-derived nitrone **140**, readily derived from aldehyde **135** in 85% yield by reaction with *N*-benzyl hydroxylamine in dry CH_2Cl_2, as the key intermediate (Scheme 3.2). [165] The research group recently observed that the stereoselectivity of the addition of MeMgBr to nitrone **140** can be controlled by the presence or absence of Lewis acids, affording two diastereoisomeric hydroxylamines in diastereomeric ratio up to 7:1 when a suitable Lewis acid was added. [149] We exploited this strategy employing Grignard reagents generated from primary alkyl halides with long chains to access hydroxylamines **144** and **148** with opposite configuration at C-2. Since the nitrogen atom is already installed on the molecules, the hydroxylamines can be directly employed for the final cyclizations reactions. The reductive amination (RA), followed by deprotection of acetonide group, afforded compounds **147** and **151** (Scheme 3.2). This synthetic approach was exploited in this thesis, opening the possibility of investigating the effect on pharmacological activity of varying the configuration of the newly created C-2 stereogenic center, as well as the effect of the chain length introduced in the addition step. First structural modifications on the lead compound are also reported.

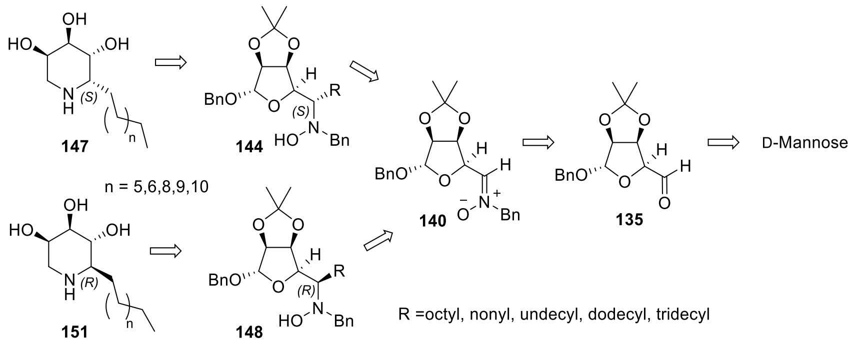

Scheme 3.2: Retrosynthetic stereodivergent strategy to yield trihydroxypiperidines **147** and **151** from D-mannose.

- synthesis of trihydroxypiperidines 1,2-disubstituted with octyl alkyl chains **170** and **171**, that should better mimic the structure of glucosylceramide.

The synthetic strategy based on the addition of octylMgBr to the new nitrone **174a** followed by reductive amination. The key intermediate **174a** was obtained throught the one-pot condensation/oxidation of octylamine and aldehyde **135** with urea–hydrogen peroxide (UHP) as the stoichiometric oxidant in the presence of catalytic methyltrioxorhenium (MTO). Access to both epimers of trihydroxypiperidines 1,2-disubstituted at the newly created stereocenter was guaranteed by carrying out the addition in the absence or presence of a Lewis acid (Scheme 3.3).

The potential of this one-pot reaction in the synthesis of new carbohydrate-derivative nitrones starting from the aldehyde **135** with different amines has been investigated in this work.

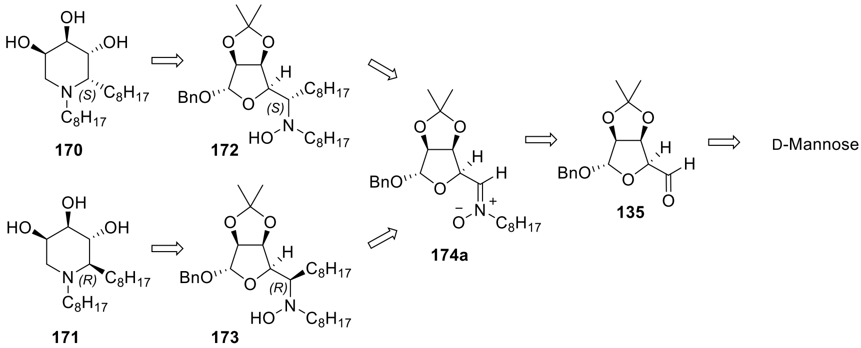

Scheme 3.3: Retrosynthetic stereodivergent strategy to yield trihydroxypiperidines **171** and **172** from D-mannose.

- synthesis of "all-cis" trihydroxypiperidines

the synthesis is based on the known ketone intermediate **166**. [174] Ketone **166** was functionalized through three different synthetic strategies: i) reduction to the "all-cis" alcohol followed by Williamson reaction afforded the ether **175**; ii) reductive amination of **166** with dodecyl amine provided the new amino azasugar **176**; iii) addition of organolithium derivatives followed by proper manipulation allowed access to diversely C-3 functionalized compounds **177** and **178** (Scheme 3.4).

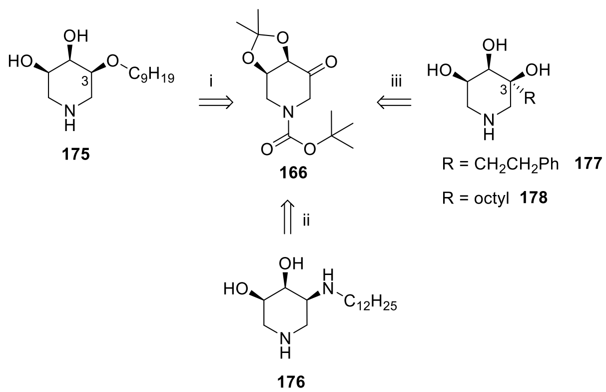

Scheme 3.4: Compounds synthesized through the functionalization of ketone **166**.

The aim was to investigate the role of the alkyl chain at the C-3 position either maintaining the three hydroxyl groups (as in compound **178**), or via alkylation of the hydroxy group at C-3 (as in ether **175**) on the GCase inhibitory and PC activity. Moreover, the new compound **178** was compared with its analogue bearing an eight-carbon atom chain on the exocyclic nitrogen (**167**) in order to investigate the effect of the chain's length on the biological properties.

The biological evaluation of the alkylated trihydroxypiperidines towards human lysosomal enzymes and the *ex vivo* activity on fibroblasts derived from Gaucher patients bearing the N370/RecNcil and L444P/L444P mutations was also investigated by candidate. Furthermore, at the end of *Chapter 3*, the synthetic approaches undertaken to obtain 2,2-dioctyl trihydroxypiperidine are reported.

3.1 Synthesis of 2-alkyl trihydroxypiperidines

3.1.1 Results and discussions

3.1.1.1 Chemistry: synthesis and structural assignment

The retrosynthetic strategy employed for the preparation of the compounds assayed in this work is shown in Scheme 3.2. We previously observed that the addition of MeMgBr and EtMgBr to the carbohydrate-derived aldehyde **135**, obtained from D-mannose, and to nitrone **140** derived thereof [165] proceeded with opposite diastereofacial preference. However, the addition of a suitable Lewis Acid, while having little effect with aldehyde **135** resulting in only a slight decrease in diastereoselectivity, was able to afford a complete reversal of the diastereofacial preference when nitrone **140** was used as the electrophile. [149] The effect of Lewis acids in the reaction of organometallic reagents with several α-alkoxy and *N*-benzyl glycosyl nitrones has been previously and extensively investigated by Merino, Dondoni and co-workers. [176]-[179]

We envisaged that exploitation of this strategy with the carbohydrate-derived nitrone **140** would lead to the stereoselective synthesis of two series of epimeric hydroxylamines **144** and **148**, depending on the presence of Lewis acids, bearing alkyl chains of different length at the carbon atom adjacent to nitrogen. This would open the way to the preparation of trihydroxypiperidines **147** and **151** with the same configuration of compound **8** at C-3, C-4 and C-5 and bearing alkyl chains at C-2 with either configuration, *via* intramolecular reductive amination/ring closure/deprotection of **144** and **148** (Scheme 3.2). Structural diversity could be achieved using the wide library of Grignard reagents. The described synthetic approach required an efficient and easy access to gram quantities of nitrone **140**, which was prepared from commercially available D-mannose *via* aldehyde intermediate **135** [180] in five steps and with an overall yield of 80%. [165] [178] The reaction conditions employed and the results obtained in the addition of several Grignard reagents to the carbohydrate-derived nitrone **140** are shown in Table 3.1.

Table 3.1: Additions of Grignard reagents to nitrone **140** performed in THF, in the presence or absence of Lewis acids.

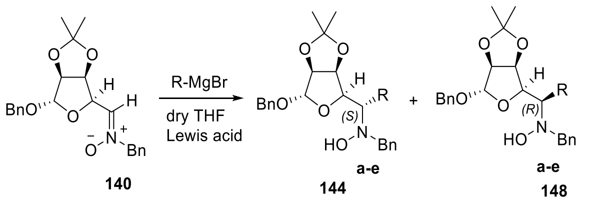

R = octyl (**a**)
R = nonyl (**b**)
R = undecyl (**c**)
R = dodecyl (**d**)
R = tridecyl (**e**)

Reagent RMgBr	**Entry**	Grignard reagent equiv.	Lewis acid (1 equiv.)	Temp (°C)	Time (h)	**144 : 148 ratio**[a]		**Yield (144+148)**[b]
R= octyl (**a**)	**1**	1.8	none	-78	2	**144a:148a**	5.6 : 1	57%
	2	1.8	none	-30	2		4.7 : 1	83%
	3	1.8	$BF_3{\cdot}Et_2O$	-30	2		1 : 5.6	85%
R= nonyl (**b**)	**4**	2.3	none	-78	3	**144b:148b**	3.3 : 1	52%
	5	1.8	$BF_3{\cdot}Et_2O$	-30	2		1 : 3.0	78%
R= undecyl (**c**)	**6**	4	none	-78	4	**144c:148c**	4.2 : 1	70%
	7	4	$BF_3{\cdot}Et_2O$	-30	4		1 : 3.0	75%
R= dodecyl (**d**)	**8**	4.5	none	-78	4	**144d:148d**	4.5 : 1	70%
	9	1.1	none	-78	5		2.5 : 1	20% [c]
	10	2.8	none	-78 → -30	4		3.3 : 1	65%
	11	2.3	none	-30	2		3.4 : 1	76%
	12	2.3	$BF_3{\cdot}Et_2O$	-30	2		1 : 9.0	70%
	13	2.3	$MgCl_2$	-30	4		1 : 1.3	50%
	14	2.3	$InCl_3$	-30 → r.t.	27		1 : 1.1	10% [c]
	15	2.3	Et_2AlCl	-30	2		1 : 1.5	75%
R= tridecyl (e)	**16**	3	none	-78	3.5	**144e:148e**	4.2 : 1	60%
	17	2	$BF_3{\cdot}Et_2O$	-30	2		1 : 6.0	87%

a Determined by integration of signals in the 1H-NMR spectra of the crude reaction mixture. b Determined on the basis of the total amount of R and S adducts recovered after purification by column chromatography. c Conversion was ca. 50%.

The addition of different Grignard reagents RMgBr (R = octyl, nonyl, undecyl, dodecyl, tridecyl) to nitrone **140** was initially performed in THF at -78 °C for 2 hours without the addition of Lewis acid. The corresponding hydroxylamines were obtained as a mixture of two diastereoisomers **144** and **148** with good isolated yields (from 52% to 70%). Hydroxylamines **144** with the *S* absolute configuration at the newly formed stereocenter were obtained in all cases as the major diastereoisomers with *dr* ranging from 3.3:1 (Entry 4, Table 3.1) to 5.6:1 (Entry 1, Table 3.1). Screening for assessing optimal reaction conditions was carried out using dodecyl magnesium bromide ($nC_{12}H_{25}MgBr$) in THF (Entries 8-15; Table 3.1). An excess of the Grignard reagent was employed (2.3 - 4.5 equivalents) to allow complete conversions of nitrone. The use of stoichiometric amounts of dodecyl magnesium bromide (1.1 equivalents) resulted in only 50% conversion of **140** even upon prolonging the reaction time to 5 h, and hydroxylamines were recovered in low yields (20%) (Entry 9, Table 3.1). In the absence of Lewis Acid, the temperature was kept at -78 °C to reach optimal diastereomeric ratios. Indeed, by increasing the reaction temperature from -78 °C to -30 °C the selectivity slightly decreased (Entry 10 and 11 *vs* 8, Entry 2 *vs* 1). The configuration of the newly created stereocenter was unambiguously established by the ^{1}H-NMR spectra and 1D-NOESY and X-ray study at a later stage of the synthetic strategy, i.e. after ring closure to the piperidine compound. Indeed, although in all cases the two diastereoisomers **144** and **148** were readily separable through flash column chromatography (FCC), they suffered from low stability and a tendency to oxidize to the corresponding nitrones **145** and **149** in air (Scheme 3.5). The stereochemical outcome of the addition reaction of the organometallic species RMgBr in the absence of Lewis acid is in agreement with a preferred attack to the *Si* face of nitrone **140**. This mode is favoured as the result of the formation of a six-membered Cram-chelate transition state, which involves coordination of the *N*-oxide oxygen and the ring oxygen to magnesium, as depicted in Figure 3.1. On the basis of our previous results with MeMgBr, [149] $BF_3{\cdot}Et_2O$ was initially chosen as the Lewis acid for inverting the stereoselectivity: the addition of $BF_3{\cdot}Et_2O$ (1.0 equiv.) to the reaction mixture at – 30 °C resulted in the formation of hydroxylamines **144** and **148** with excellent overall yields (from 70% to 87%, Table 3.1, Entries 3, 5, 7, 12 and 17). More importantly, addition of BF_3 allowed complete reversal of the selectivity in favour of the epimeric hydroxylamines **148** with an *R*-configuration of the newly formed stereocenter, obtained as the major diastereoisomers (3-9:1 *dr*). In particular, a remarkable 9:1

dr in favour of the hydroxylamine **148d** was attained in the case of dodecyl magnesium bromide addition to **140** (Table 3.1, Entry 12). Other Lewis acids tested in the reaction ($MgCl_2$, $InCl_3$ and Et_2AlCl, Table 3.1, Entries 13-15), showed lower selectivities, as well as less efficiency in most cases.

The stereochemical outcome of the reaction catalysed by BF_3 is in agreement with a preferred attack of the Grignard to the *Re* face of the nitrone, which can be explained by invoking a strong preference for a TS in the conformation shown in Figure 3.2, analogous to that proposed by Merino and co-workers for the allylation of a related nitrone. [164] Upon considering this conformation, the highly coordinating *N*-oxide oxygen lies in a relatively uncrowded region where it can accommodate the bulky Lewis acid, leaving the *Re* face of the nitrone more accessible for the attack. With less encumbering Lewis acids such as $MgCl_2$ and $InCl_3$ (Table 3.1, Entries 13 and 14), other possible conformations compete to attack the opposite *Si* diastereoface. Conversely, Et_2AlCl, that had shown a diastereoselectivity comparable to $BF_3.Et_2O$ with MeMgBr as the Grignard reagent, [149] gave a modest 1.5 *dr* in favour of the *R*-epimer **148d** with dodecylmagnesium bromide. The unique behaviour of $BF_3.Et_2O$ may also be related to the ability of the other Lewis acids to expand coordination, thus stabilizing possible chelate conformations.

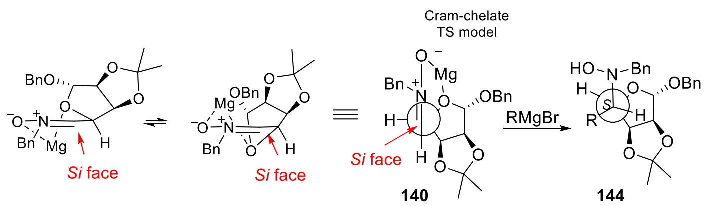

Figure 3.1: Postulated Cram-chelate transition state for the preferred nucleophilic attack to the *Si* face of nitrone **140** in the absence of Lewis acid leading to hydroxylamines **144**, *S*-configured at the newly formed stereocenter.

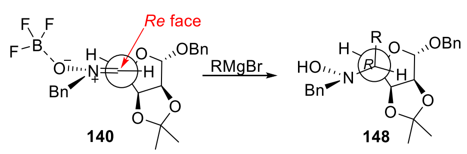

Figure 3.2: Postulated transition state for the preferred nucleophilic attack to the *Re* face of nitrone **140** in the presence of $BF_3{\cdot}Et_2O$ leading to hydroxylamines **148**, *R*-configured at the newly formed stereocenter.

As stated above, all of the hydroxylamines **144** and **148** were efficiently separated by flash column chromatography and their structural assignment was unambiguously accomplished after transformation to the corresponding target piperidines **147** and **151**.

Due to the low stability of hydroxylamines **144** and **148**, which showed a tendency to spontaneously partially oxidize to the corresponding nitrones **145** and **149** (50% conversion as evaluated by ^{1}H-NMR upon standing in air at room temperature for 30 minutes, that does not proceed further), their characterization was only based on ^{1}H-NMR and MS analysis immediately after purification by column chromatography. Therefore, the complete characterization of pure nitrones **145** and **149** was carried out after oxidation of the hydroxylamines **144** and **148** with the hypervalent iodine reagent IBX [181] [182] in dry CH_2Cl_2, which provided the corresponding nitrones in excellent yields (Scheme 3.5).

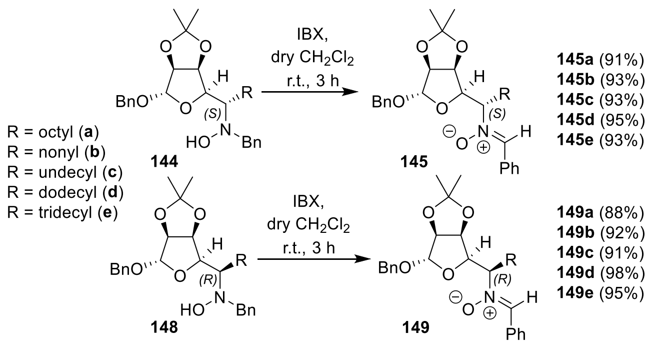

Scheme 3.5: Oxidation of hydroxylamines **144** and **148** with IBX: synthesis of nitrones **145** and **149**.

To our delight, the subsequent reductive amination/ring closure occurred without any problems using the hydroxylamine/nitrone mixtures as a substrate, since both compounds were reduced to the same *N*,*N*-secondary amines under the reaction conditions. The experimental conditions were optimized using the mixtures hydroxylamines **144d**/**145d** and **148d**/**149d** bearing a dodecyl chain as model substrates. Protected piperidines **146d** and **150d**, respectively, were obtained in low yields (20-21%) after 4 days by employing H_2 as a reducing agent (balloon) in the presence of Pd/C catalyst in MeOH (0.015 M) followed by treatment with a strongly basic resin. Addition of 2 equivalents of acetic acid was highly beneficial, enhancing the yields of **146d** and **150d** to 93% and 88%, respectively, with no deprotection of the acetonide groups being observed (Scheme 3.6).

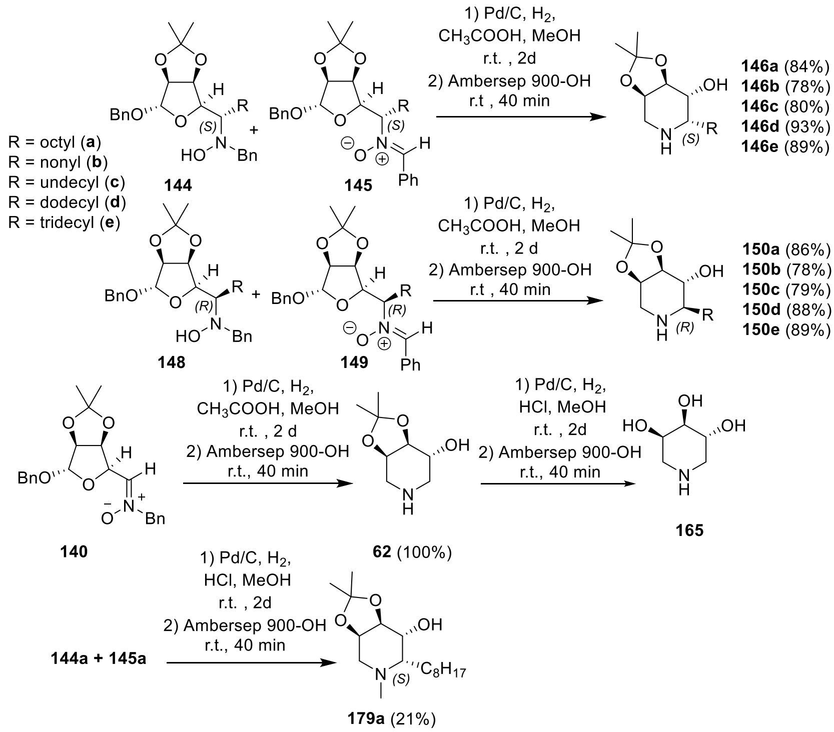

Scheme 3.6: The ring-closure reductive amination sequence.

Further purification by FCC was not always necessary. These reaction conditions were then employed to obtain all the other piperidines **146** and **150** shown in Scheme 3 (78-93% overall yields). The yields are remarkable considering that the products derive from at least five distinguished reaction steps (*N*- and *O*-debenzylation, hydroxylamine/nitrone reduction, condensation and C=N reduction). The same reaction conditions were also applied to nitrone **140** to afford quantitatively after 2 days the piperidine **62**, previously obtained by a different strategy. [174] [175] Compound **62** is an important intermediate in the synthesis of piperidines **165**, this latter possessing PC properties towards GCase enzyme. [159] Conversely, when the reaction was performed on the **144a/145a** mixture in the presence of HCl (instead of CH_3COOH), the *N*-methylpiperidine

179a was obtained with a low 21% yield, probably due to concomitant acetonide deprotection (Scheme 3.6).

At this stage of the synthesis, it was possible to establish unambiguously the stereochemical outcome of the Grignard addition described in Table 3.1, thanks to a careful analysis of the ^{1}H-NMR, 2D-NMR and 1D-NOESY spectra carried out on piperidines **146** and **150**. The ^{1}H-NMR signals of the azasugar portion, together with their coupling constants, are shown in Tables 3.2 and 3.3 for piperidines **146** and **150**, respectively. The two chair conformations for each compound series are depicted in Figure 3.3. For derivatives **146**, 1D-NOESY spectra did not help to elucidate the structural assignment. However, their ^{1}H-NMR spectra showed small couplings constants for $^{3}J_{2-3}$, $^{3}J_{3-4}$ and $^{3}J_{4-5}$ in the range of 2.1-2.8 Hz, 2.6-3.4 Hz and 5.0-5.4 Hz, respectively. This pattern is in agreement with an *S* absolute configuration at C-2, with the piperidine displaying a preferred $^{1}C_{4}$ conformation in which the bulky R chain lies in the equatorial position and 3-H and 4-H are in a (pseudo)equatorial orientation (Figure 3.3).
In the 1D-NOESY spectra of compounds **150**, strong NOE correlation peaks were observed between 2-H and 4-H, 4-H and 6-H_b and 2-H and 6-H_b, which confirmed the *R*-configuration at C-2. Indeed, the axial orientation of 2-H derives from a preferred $^{4}C_{1}$ conformation which accommodates the bulky R chain again in an (pseudo)equatorial position (Figure 3.3). The higher coupling constant observed for the signals of 4-H of compounds **150a-e** compared to **146a-e** further confirmed a (pseudo)axial orientation of this proton with a (pseudo) *ax-ax* relationship with 3-H (J = 7.0-7.3 Hz). As expected, the more deshielded 6-H_a protons are in a (pseudo)equatorial position in both preferred conformations of derivatives **146** and **150**. Finally, the absolute configuration at C-2 of piperidines **150** and their preferred conformation in the solid state was unambiguously ascertained by X-ray crystallography performed on a single crystal of **150e** (Figure 3.4). A small distortion from a typical chair conformation, due to the presence of the dioxolane moiety, is indicated by the observed coupling constants between 3-H, 4-H and 5-H and confirmed by the X-ray structure of compound **150e** (Figure 3.4). This distortion was further confirmed by DFT studies using ORCA software performed on an X-ray structure of **150e** (see the

Experimental Section). A dihedral angle of around 158° (compared to 180° of a typical *axial-axial* in a chair conformation) was measured for 3-H/C-3/C-4/H-4 and a dihedral angle of around 35° (compared to 60° of the chair conformation) was found for H-4/C-4/C-5/H-5. These data are in agreement with the ^{1}H NMR signal of H-4, which showed a J = 7.0 Hz with H-3 and a J = 5.3 Hz with H-5.

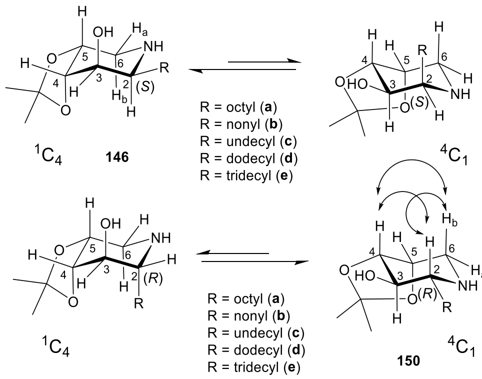

Figure 3.3: The two possible chair conformations of piperidines **146** and **150**. Double-ended arrows show the observed diagnostic NOE correlation peaks in the 1D-NMR spectra.

Table 3.2: ^{1}H-NMR chemical shifts (δ) and coupling constants (J) of the protons in the azasugar portion of compounds **146**.

	2-H		3-H		4-H		5-H		6-H$_a$		6-H$_b$	
Comp	δ (ppm)	^3J, ^3J (Hz)	δ (ppm)	^3J, ^3J (Hz)	δ (ppm)	^3J, ^3J (Hz)	δ (ppm)	^3J (Hz)	δ (ppm)	^2J, ^3J (Hz)	δ (ppm)	^2J, ^3J (Hz)
146a	2.72 (td)	7.0 2.3	3.80 (t)	2.8	4.14 (dd)	5.4 3.4	4.19 (q)	5.6	3.05 (dd)	13.4 5.5	2.66 (dd)	13.6 7.6
146b	2.72 (td)	7.0 2.1	3.80 (t)	2.8	4.14 (dd)	5.4 3.4	4.19 (q)	5.6	3.05 (dd)	13.3 5.8	2.66 (dd)	13.5 7.5
146c	2.72 (td)	8.2 2.3	3.80 (t)	2.6	4.14 (dd)	5.0 3.4	4.19 (q)	5.3	3.04 (dd)	13.4 5.4	2.67 (dd)	13.4 7.4
146d	2.72 (td)	7.0 2.1	3.80 (t)	2.8	4.14 (dd)	5.2 3.2	4.19 (q)	5.8	3.04 (dd)	13.2 5.8	2.67 (dd)	13.2 7.2
146e	2.72 (td)	8.0 2.2	3.80 (t)	2.6	4.14 (dd)	5.0 3.2	4.19 (q)	6.3	3.04 (dd)	13.2 5.6	2.67 (dd)	13.2 7.2

Table 3.3: ^{1}H-NMR chemical shifts (δ) and coupling constants (*J*) of the protons in the azasugar portion of compounds **150**.

	2-H	3-H	4-H		5-H	6-H$_a$	6-H$_b$	
Comp	δ (ppm)	δ (ppm)	δ (ppm)	^3J, ^3J (Hz)	δ (ppm)	δ (ppm)	δ (ppm)	^2J, ^3J (Hz)
150a	2.25-2.19 (m)	3.28-3.23 (m)	3.84 (dd)	7.3 5.4	4.21-4.19 (m)	3.28-3.23 (m)	2.91 (dd)	14.8 3.0
150b	2.26-2.19 (m)	3.31-3.23 (m)	3.84 (dd)	7.2 5.5	4.21-4.19 (m)	3.31-3.23 (m)	2.92 (dd)	14.8 3.0
150c	2.24-2.19 (m)	3.30-3.23 (m)	3.84 (dd)	7.2 5.5	4.20-4.19 (m)	3.30-3.23 (m)	2.90 (dd)	14.8 3.8
150d	2.26-2.20 (m)	3.28-3.22 (m)	3.83 (dd)	7.2 5.4	4.20-4.18 (m)	3.28-3.22 (m)	2.90 (dd)	14.8 3.4
150e	2.27-2.20 (m)	3.27-3.22 (m)	3.85 (dd)	7.0 5.3	4.20-4.19 (m)	3.27-3.22 (m)	2.90 (dd)	15.0 3.2

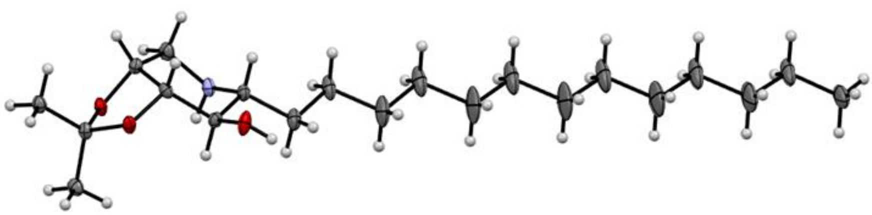

Figure 3.4: X-ray crystal structure of compound **150e**. Data can be obtained free of charge from the Cambridge Crystallographic Data Centre at the following link: http://www.ccdc.cam.ac.uk/services/structures?access=referee&searchdepnums=1909512&searchauthor=faggi

Final deprotection of the acetonide protecting groups under acidic conditions (aqueous HCl in MeOH) followed by basic treatment as above led to the final trihydroxypiperidines **147** and **151** with good yields and to compound **180a** (Scheme 3.7).

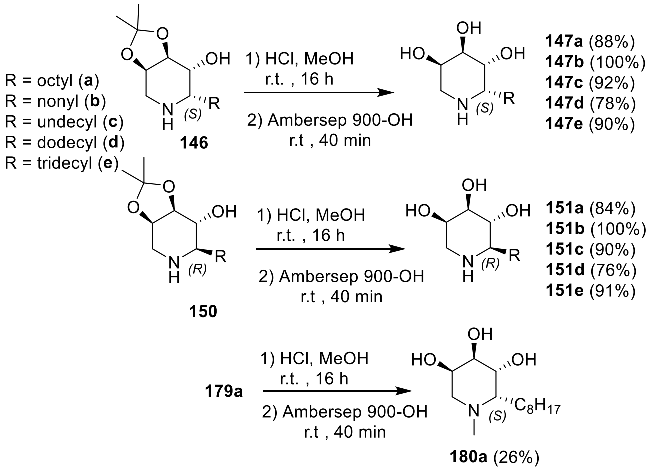

Scheme 3.7: The final deprotection step: synthesis of trihydroxypiperidines **147a-e**, **151a-e** and **180a**.

3.1.1.2 Preliminary biological screening towards commercial glycosidases

A preliminary biological screening of the whole set of compounds **147a-e** and **151a-e** (at 100 µM inhibitor concentration) was performed was performed thanks to the collaboration with Prof. Antonio Moreno-Vargas and Macarena Martínez-Bailéne (Departamento de Química Orgánica, Facultad de Química, Universidad de Sevilla) towards a panel of 12 commercial glycosidases (α-L-fucosidase EC 3.2.1.51 from Homo sapiens, α-galactosidase EC 3.2.1.22 from coffee beans, β-galactosidases EC 3.2.1.23 from *Escherichia coli* and *Aspergillus oryzae,* α-glucosidases EC 3.2.1.20 from yeast and rice, amyloglucosidase EC 3.2.1.3 from *Aspergillus niger,* β-glucosidase EC 3.2.1.21 from almonds, α-mannosidase EC 3.2.1.24 from Jack beans, β-mannosidase EC 3.2.1.25 from snail, β-*N*-acetylglucosaminidases EC 3.2.1.30 from Jack beans and bovine kidney). No inhibition was found except for compound **151d**, able to impart 20% inhibition to β-glucosidase from almonds at this concentration.

Even though this value did not reveal strong inhibition, in our experience the inhibition data towards commercial and human glycosidases do not always match. [159] [183] For instance, compound **170** gave only 50% inhibition of β-glucosidase from almonds at 1 mM, [175] but resulted a strong inhibitor of human lysosomal GCase (98% inhibition at 1 mM, IC_{50} = 30 µM). [159] Therefore, we carried out further biological screening towards human lysosomal glycosidases.

3.1.1.3 Preliminary biological screening towards human lysosomal glycosidases

A preliminary biological screening of the whole set of compounds **147a-e** and **151a-e** at 1 mM inhibitor concentration towards a panel of 7 human lysosomal enzymes, namely α-fucosidase (α-Fuc), β-galactosidase (β-Gal), α-galactosidase (α-Gal), α-mannosidase (α-Man), β-mannosidase (β-Man), α-glucosidase (α-Glu) and β-glucosidase (β-Glu or GCase) and the results are shown in Figure 3.5.

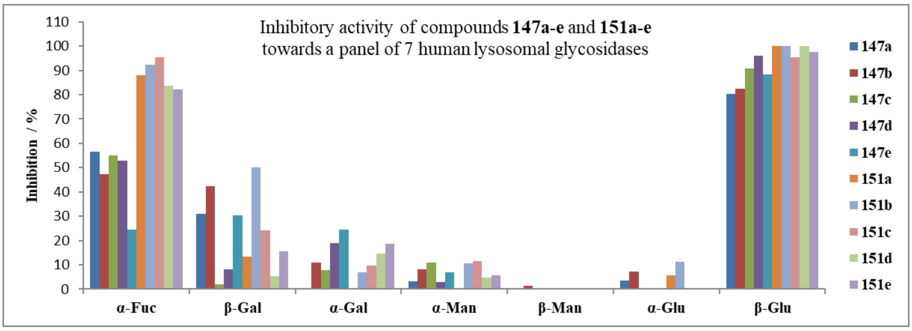

Figure 3.5: Inhibition percentage of lysosomal α-fucosidase (α-Fuc), β-galactosidase (β-Gal), α-galactosidase (α-Gal), α-mannosidase (α-Man), β-mannosidase (β-Man), α-glucosidase (α-Glu) and β-glucosidase (β-Glu or GCase) in an extract from human leukocytes isolated from healthy donors, incubated with 1 mM concentration of compounds **147a-e** and **151a-e**.

We tested the inhibitors at a higher concentration than in the previous screening on commercial glycosidases (1 mM *vs* 100 µM) in order not to discard potential pharmacological chaperones, which in our experience can be identified also among modest inhibitors. [159] Moreover, the screening aimed to highlight selectivity with respect to other lysosomal enzymes. Our data clearly showed that our compounds are selective inhibitors of the GCase enzyme, with percentage of inhibition ranging from 80% for compound **147a** to 100% for compounds **151a, 151b** and **151d**. Therefore, the first requirement for an effective PC for GD, which is to have an affinity towards the target protein (GCase), was demonstrated (see Section 3.1.1.4). [184] A remarkable inhibitory activity was also found towards human α-fucosidase (α-Fuc), but only for piperidines **151a-e** with the *R* configuration at C-2 (82-96% inhibition), while piperidines **147a-e** with the *S* configuration at C-2 showed only moderate inhibition of α-Fuc (24-57% inhibition). The stereochemical pattern of the carbinol stereocentres of piperidines **147** and **151** reflects that of L-fucose. For this reason, the detected activity towards α-fucosidase (α-Fuc) is not surprising, also considering that trihydroxypiperidine **165** is a known inhibitor of commercial α-L-fucosidase with an IC_{50} = 90.3 μM, and its *N*-octyl derivative **169** maintained a 77% inhibition (at 1mM) towards this enzyme. [175]

3.1.1.4 Inhibitory activity of GCase and enzyme kinetics

The whole set of compounds **147a-e** and **151a-e**, together with compound **180a** was compared to that of compound **169**, whose activity was previously reported. [159] For each compound, the IC_{50} was determined, and the results are reported in Table 4. These experiments were performed at Molecular and Cell Biology Laboratory of Neurometabolic Diseases (Meyer Children's Hospital and Department of Neurosciences, Pharmacology and Child Health of University of Florence) under the supervision of Prof. Amelia Morrone.

Table 3.4: GCase inhibition in human leukocytes from healthy donors.

Entry	Compound	GCase inhibition [%][a]	IC_{50} [μM][b]
1	**169**	98	30.0 ± 1.0
2	**147a**	80	93.5 ± 5.3
3	**147b**	83	143 ± 20
4	**147c**	91	100.0 ± 40.0
5	**147d**	96	23.3 ± 4.0
6	**147e**	88	160.0 ± 30.0
7	**151a**	100	29.3 ± 1.8
8	**151b**	100	8 ± 1.0
9	**151c**	95	7.0 ± 1.0
10	**151d**	100	1.5 ± 0.1
11	**151e**	98	9.0 ± 2.0
12	**181a**	50	>1000

[a] Percentage inhibition of GCase in human leukocytes extracts incubated with azasugars (1 mM). [b] IC_{50} values were determined by measuring GCase activity at different concentrations of each inhibitor.

Our results clearly show that all the newly synthesized trihydroxypiperidines, apart from *N*-methylated compound **180a** (for which a moderate 50% inhibition was detected), are able to strongly inhibit GCase with percentages of inhibition higher than 80% (Table 3.4 and Figure 3.5). The IC_{50} values obtained, fell into the micromolar range for **147a-e** and **151a-e**, and allowed to show the effect of shifting the alkyl chain from the nitrogen atom (as in compound **169**) to C-2 on activity. Indeed, while this shift provoked a slight decrease in activity for the *S*-configured trihydroxypiperidine **147a** (Table 3.4 , Entry 2 *vs* 1), the inhibitory activity was maintained for compound **151a** with the *R* configuration (Table 3.4 , Entry 7 *vs* 1). Upon IC_{50} calculation, an interesting trend also emerged. The trihydroxypiperidines **151** with the *R* configuration at C-2 (Table 3.4 , Entries 7-11) were more active than corresponding epimeric trihydroxypiperidines **147** with the *S* configuration (Table 3.4 , Entries 2-6). Comparison of the activity of compounds bearing the same alkyl chain length (Table 3.4 , Entry 7 *vs* 2, Entry 8 *vs* 3, Entry 9 *vs* 4, Entry 10 *vs* 5 and Entry 11 *vs* 6) showed, in particular, that the trihydroxypiperidines **151** *R*-configured at C-2 were 3- to 18-fold more active than the corresponding trihydroxypiperidines **147** *S*-configured at C-2 (see also Figure 3.6). For each series, the best inhibitors were the compounds bearing the dodecyl alkyl chain (IC_{50} = 1.5 μM for compound **151d** and IC_{50} = 23.3 μM for compound **147d**), respectively (Table 3.4 , Entries 10 and 5).

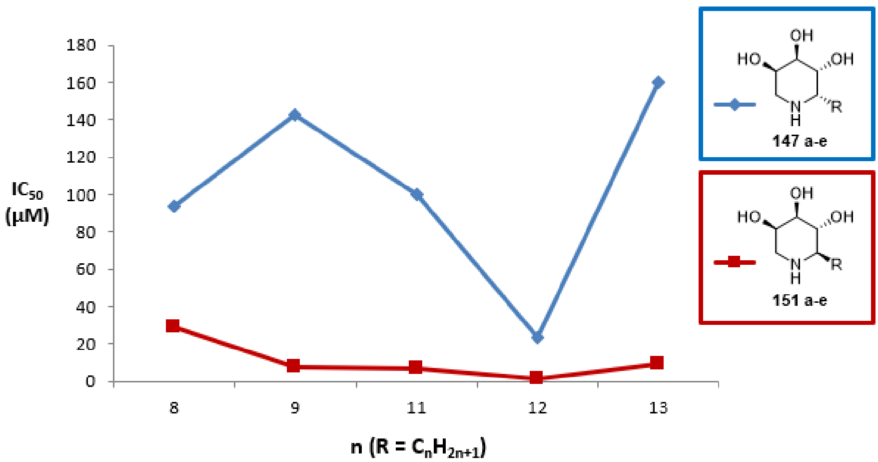

Figure 3.6: The IC_{50} trend for trihydroxypiperidines **151** (with the *R* configuration at C-2) and trihydroxypiperidines **147** (with the *S* configuration at C-2).

Kinetic analyses were performed to determine the mechanism of action of the best inhibitor **151d**, in collaboration with Dr. Paolo Paoli (Department of Experimental and Clinical Biomedical Sciences, University of Florence). In particular, the dependence of the main kinetic parameters (K_m and V_{max}) from the inhibitor concentration were analyzed and the results are reported in Figure 3.7. It was found that compound **151d** acts as a competitive GCase inhibitor, with a K_i value of 3.6 µM. The same competitive behavior was observed also for the less potent inhibitor of the compounds with the *R* configuration at C-2 **151a**, for which a K_i value of 18.5 µM was calculated in Figure 3.8. We therefore assume that all compounds with the *R* configuration at C-2 are competitive GCase inhibitors. Unfortunately, despite our efforts, we were not able to determine the K_i value and to highlight the action mechanism of the compounds with the *S* configuration at C-2 because of the incoherent results obtained during the tests performed. In particular, no significant variation in either Km or Vmax was observed upon increasing inhibitor concentration. We do not know why these compounds show such as unusual behavior.

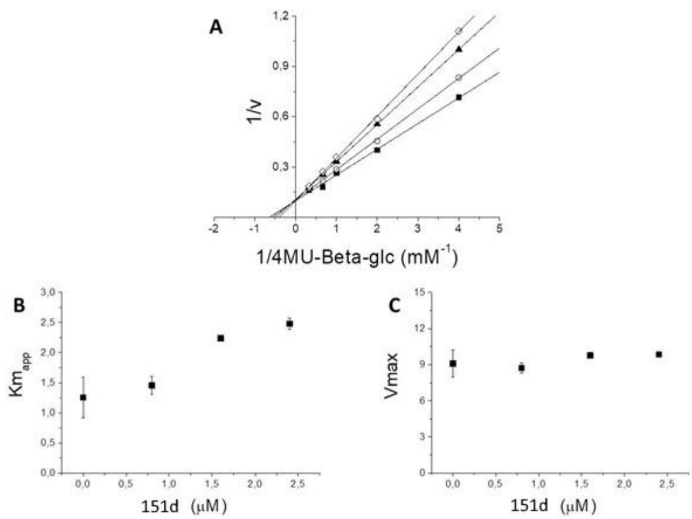

Figure 3.7: Kinetic analysis of compound **151d** (A) Double reciprocal plots. 4-Methylumbelliferyl-β-D-glucoside was employed as a substrate. The concentrations of compound **151d** are: ■, 0 µM; ○, 0.8 µM; ▲, 1.6 µM; ◇, 2.4 µM. Data reported in the figures represent the mean values ± S.E.M. (n = 3). (B, C) Behaviour of K_m and V_{max} at different concentrations of compound **151d**.

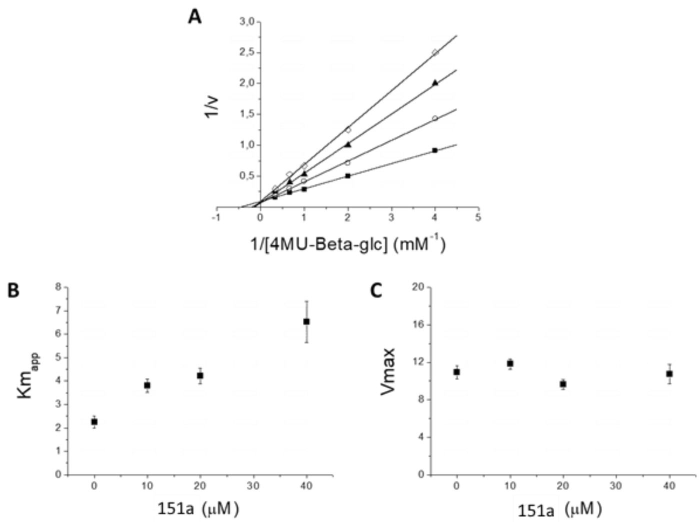

Figures 3.8: Kinetic analysis of compound **151a**. (A) Double reciprocal plots. 4-Methylumbelliferyl-β-D-glucoside is employed as a substrate. The concentrations of compound **151a** are: ■, 0 μM; ○, 10 μM; ▲, 20 μM; ◇, 40 μM. Data reported in the figures represent the mean values ± S.E.M. (n = 3). (B, C) Behaviour of K_m and V_{max} at different concentrations of compound **151a**.

3.1.1.5 Pharmacological chaperoning activity

The second requirement for an effective PC is smooth dissociation from the target enzyme when the active site is replaced by its natural substrate in the lysosome, which reflects in rescue of enzymatic activity. Therefore, once verified the ability of the synthesized piperidines to interact with glucocerebrosidase, their properties as GCase enhancers were assayed at different concentrations in fibroblasts derived from Gaucher patients bearing the N370/RecNcil mutation (Table 3.5 and Figure 3.9). All new compounds showed GCase activity rescue of 1.2- to 1.9-fold except for derivatives **147b**, **147e** and **151b**, for which no rescue was observed at the tested concentrations, after incubation (4 days) with mutated fibroblasts (see the Experimental Section). Very similar enhancements at similar concentrations were found for couples of compounds with the same alkyl chain independently to the configuration of the substituents (Table 3.5, 1.35-1.39 at 1 μM for compounds **151d** and **147d**, 1.22-1.30 at 50 nM for **151c** and **147c**). The only exception was compound **151a** bearing the octyl chain, which gave a remarkable enhancement compared to its epimer **147a**, although at a higher concentration (Table 3.5, 1.86 at 50 µM for compound **151a** *vs* 1.33 at 10 nM for **147a**), thus representing our best chaperone to date. It is also worth noting that the best inhibitory activity does not correspond to the best GCase rescue on cell lines, as already observed for other series of compounds. [185] While the best inhibitory activity was found for compounds bearing the dodecyl alkyl chain, in each series, the best pharmacological chaperoning properties were obtained with the octyl trihydroxypiperidines **147a** and **151a**. A balance between pharmacological chaperoning ability and inhibitory activity at a given compound concentration must be pursued to obtain the desired effect on cell lines.

Comparing these new data with those previously reported for *N*-octyl trihydroxypiperidine **169**, we may deduce that best enhancements are afforded by moving the alkyl chain from the nitrogen atom to the C-2 position. Indeed, a comparable enzymatic rescue but at a much lower concentration was found for **147a** compared to **169** (1.33 at 10 nM *vs* 1.25 at 100 µM, Table 3.5), and a remarkable 1.86-fold maximal increase at 50 µM was found for our best chaperone **151a**. The third requirement for an effective PC depends not only on affinity for the target enzyme, but also on bioavailability in terms of membrane permeability, subcellular distribution and metabolism. [27] [186] Thus, the actual intracellular concentration of an imino- or azasugar after treatment is likely much lower than its extracellular localization. Interestingly, **151a** was effective as PC at concentrations in the same range as its IC_{50} (29.3 µM, Table 4), while IFG rescued GCase only at a concentration (10-100 µM) significantly higher than its IC_{50} (30 nM), [82] indicating a better membrane permeability than IFG. The chaperoning activity of **151a** compares well with that of *N*-octyl-deoxynojirimycin (*N*-octyl-DNJ, 1.7-fold at 20 µM) reported by Asano et al. [187] Similar enhancement values were previously observed for C-6 propyl IFG [84] and α-C-nonyl DIX (**8**), [85] although at a lower concentration.

To endorse the chaperoning effect of compound **151a** on cell lines bearing a neuronopathic *GBA* mutation, fibroblasts carrying the L444P/L444P mutation were also assayed. A remarkable rescue of 1.8-fold in GCase activity was observed at 100 µM for compound **151a** (Table 3.5). This result is particularly outstanding, since L444P is the most common mutation leading to a severe Gaucher Disease phenotype with central nervous system involvement, [188] but is refractory to most pharmacological chaperone candidates. For instance, IFG and some DIX derivatives, that gave a high rescue on N370S mutated fibroblasts, were not able to increase GCase activity in human L444P fibroblasts more than 1.2-1.4-fold at any concentration. [189]-[191] Conversely, the 1.35-fold enhancement found at 1 µM for compound **151d** towards the N370S/RecNcil cell lines was not observed on L444P *GBA* fibroblasts (see the Experimental Section). These experiments also suggest that cell viability remarkably decreased with compounds bearing the longer alkyl chains (undecyl, dodecyl, tridecyl). For instance, at 100 µM concentration, only compounds bearing the octyl chain (in different position and with different configuration, namely **170**, **147a** and **151a,** see Table 3.5 and Figure 3.9) were not toxic after 4 days incubation (see also *3.1.1.6 Effect of compound 151a on cell viability*).

Table 3.5: GCase rescue on mutated fibroblasts bearing the N370S/RecNcil. The GCase activity was determined in lysates from mutated fibroblasts incubated for 4 days with different concentrations of compounds **169**, **147a-147e** and **151a-151e** or without (control). The values reported in the table give the activity ratio for each compound at a given concentration *vs* the control.

	Compound										
Concentration	**169**	**147a**	**147b**	**147c**	**147d**	**147e**	**151a**	**151b**	**151c**	**151d**	**151e**
10 nM	0.95	**1.33**	0.95	0.70	0.78	0.93	0.99	0.80	0.30	0.72	1.25
50 nM	nd[c]	nd[c]	nd[c]	**1.30**	nd[c]	0.88	nd[c]	nd[c]	**1.22**	nd[c]	**1.29**
100 nM	0.74	0.97	0.92	0.77	1.18	0.88	1.16	1.01	0.57	1.07	1.26
1 µM	1.01	0.93	0.87	0.72	**1.39**	0.30	1.18	0.92	0.38	**1.35**	0.56
10 µM	1.10	0.97	0.69	_[b]	0.37	_[b]	1.63	0.93	_[b	1.06	_[b]
50 µM	1.18[a]	0.38	0.50	_[b]	_[b]	_[b]	**1.86**	0.88	_[b]	_[b]	_[b]
100 µM	**1.25**	0.36	_[b]	_[b	_[b]	nd[b]	**1.76 (1.80)**[d]	_[b]	_[b]	_[b]	nd[c]

[a] This value corresponds to a 20 µM compound concentration instead of 50 µM. [b] The flasks containing cells incubated with this concentration of compound showed low cell viability that hampered the assay. [c] Not determined. [d] GCase rescue on mutated fibroblasts bearing the homozygous L444P mutation.

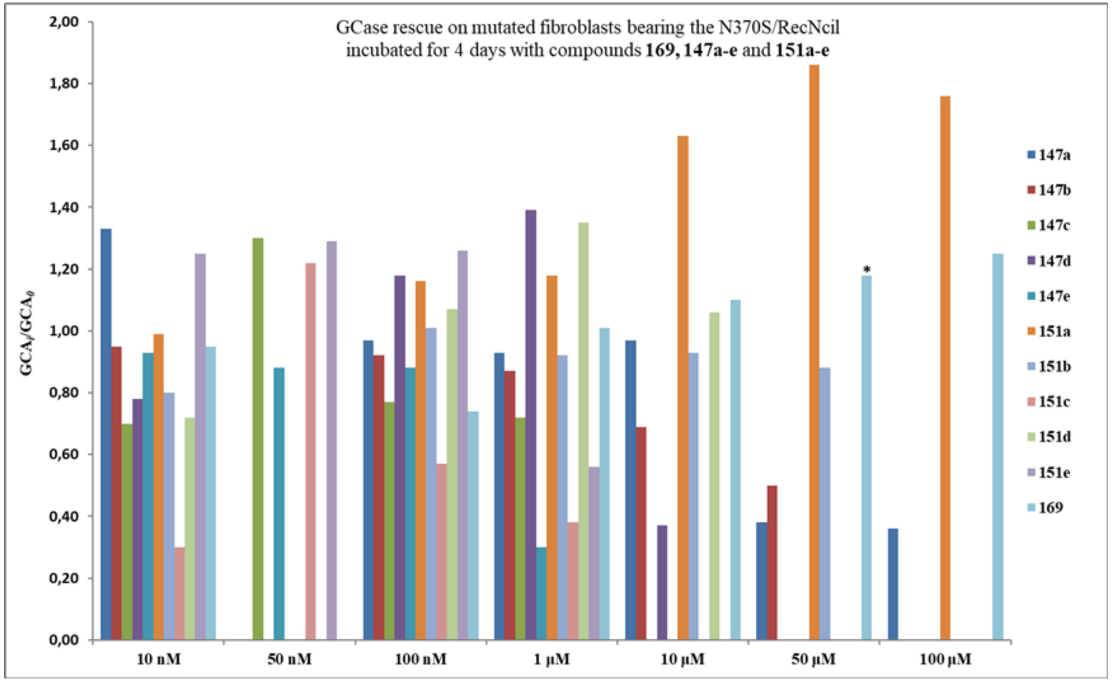

Figure 3.9: GCase activity rescue is reported as the ratio between the GCase activity measured in human fibroblasts derived from GD patients bearing N370S/RecNcil mutations measured after 4 days of incubation with compounds **169**, **147a-147e**, **151a-151e** (GCA_i) and the GCase activity of the corresponding control (GCA_0, namely the GCase activity measured in human fibroblasts derived from GD patients bearing N370S/RecNcil mutations measured after 4 days of incubation without any compound). * This value corresponds to a 20 µM compound concentration instead of 50 µM. See Table 4 for the explanation of missing values at certain concentrations (low cell viability or n.d.).

3.1.1.6 Effect of compound 151a on cell viability

In order to evaluate the impact of our best chaperone **151a** on cell viability, an MTT test was carried out using fibroblasts bearing the N370/RecNcil mutations, and fibroblasts bearing the homozygous L444P mutation, in collaboration with Dr. Paolo Paoli, Department of Experimental and Clinical Biomedical Sciences, University of Florence; the results are shown in Figure 3.10. The assays highlight negligible toxicity even at the highest concentration (100 µM) and for prolonged time towards cells bearing the N370/RecNcil mutations (Figure 3.10-A). Towards cells bearing the homozygous L444P mutations, a considerable reduction of cell viability was found only for longer times (48 h) and for the highest concentrations, while cell viability remained good after 24 h at a 100 µM concentration (Figure 3.10-B). Overall, these results suggest low toxicity for compound **151a** on different cell lines.

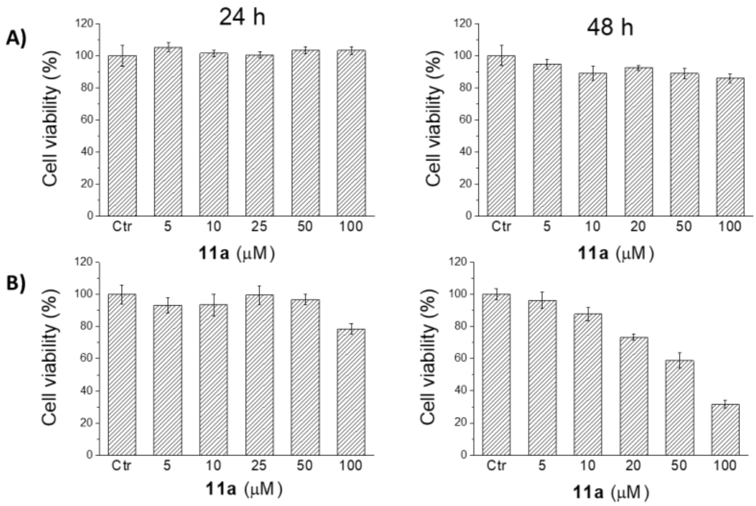

Figure 3.10: Viability assay. Fibroblasts from patients bearing N370S/RecNcil mutations (A) and the homozygous L444P mutations (B) were incubated for 24 and 48 hours in the presence of compound **151a** at different concentrations. After this time, the viability of cells was evaluated using MMT assay. Obtained values were normalized with respect to control experiments. Data reported represent the mean value ± S.E.M. (n = 8).

3.1.1.7 Docking studies

In order to investigate the different behavior of the synthesized compounds **147** and **151** a molecular docking study with Autodock 4.2 [192] was performed, in collaboration with Dr. Sara Giachetti of the Department of Chemistry, University of Florence. To validate our approach we carried out a preliminary redocking study with the human protein β-glucocebrosidase (PDB code 2NSX) with the crystallized molecule isofagomine (IFG (**2**)). The redocking experiment proved the reliability of our methodology, since we found for IFG the same orientation in the active site of the complex determined by X-ray (see the Experimental Section). [193] To compare the orientation of our alkylated piperidines in the GCase active site with a similar alkylated iminosugar, we docked the α-1-C-tridecyl-DAB in the GCase active site, which had been previously investigated by Kato, Hirono and co-workers with a different docking protocol. The docking method employed showed interactions of both the pyrrolidine portion and the long alkyl chain similar to the reported study (see the Experimental Section). [194] [195] After validation of the protocol, we applied the docking procedure to compounds **147** and **151**. As representative examples, trihydroxy piperidines **151a** and **151d** (with the *R* configuration at C-2), and **147d** (with the *S* configuration at C-2) were compared to isofagomine (IFG, **2**) (Figure3.11).

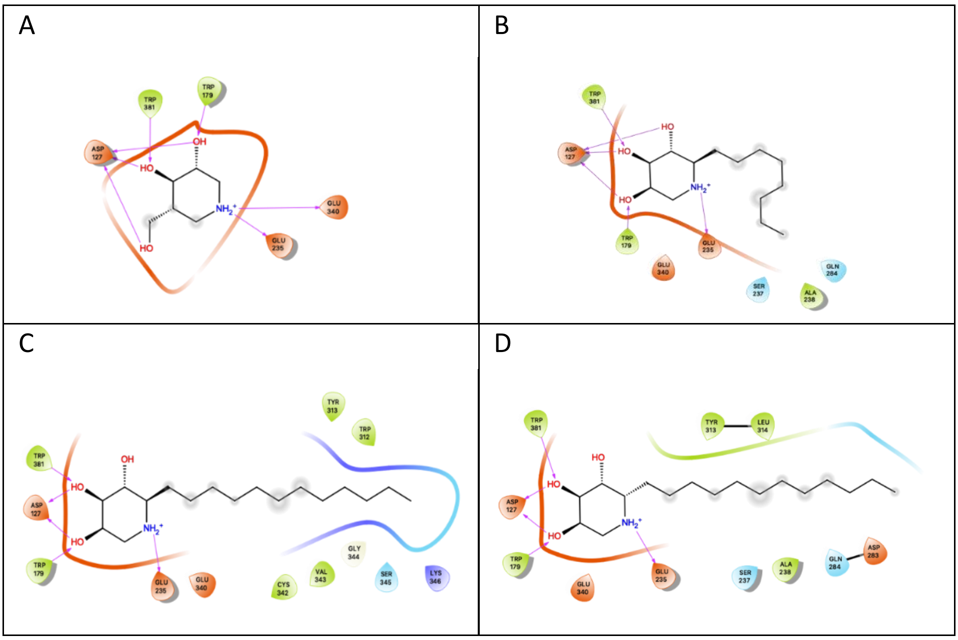

Figure 3.11: Binding modes of IFG (**3**) (pdb code 2NSX) (A), and **151a** (B), **151d** (C) and the most probable orientation for **147d** (D) within the GCase active site by docking procedures.

We found that piperidines **151** (*R* configuration at C-2) bind the same pocket as IFG in the binding active site of 2NSX (Figure 3.11, A-C). In particular, the hydroxyl groups and positive nitrogen of **151** had favorable hydrogen bonds with TRP381, GLU235, TRP179 and non-ionic hydrogen bond to ASP127. Therefore, differences in configuration and substitution at C-5 with respect to IFG do not affect the key hydrogen bonds essential for the ligand binding with GCase.
In addition, the docking analysis revealed a different orientation depending on the side chain's length. For the octyl and the nonyl derivatives, the chain interacts with SER237, ALA238, GLN284, thus provoking a chain folding (Figure 3.12). For the undecyl, dodecyl and tridecyl derivatives, the analysis revealed key favorable hydrophobic van der Waals interactions with TRP312, TYR313, LYS346, SER345, CYS342 residues, which placed the side chain in an extended conformation (Figure 3.12), occupying the same hydrophobic pocket reported by Kato, Hirono and co-workers for the α-1-C-tridecyl-DAB derivative. [195]

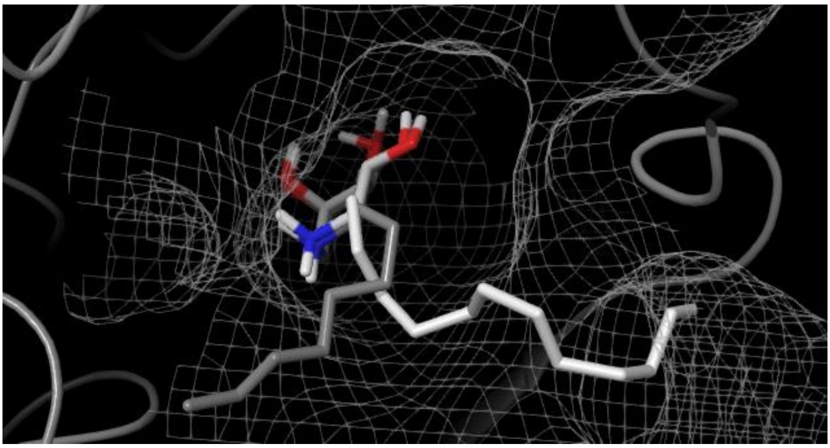

Figure 3.12: Binding modes of **151d** (light grey) and **151a** (dark grey) within the GCase active site by docking procedures.

Conversely, docking analyses for compounds **147** indicate that their piperidine portion do not bind the active site of GCase with a unique orientation. This result may at least partially explain the inhibitory data, which showed an average lower inhibitory potency for the compounds whit *S* configuration at C-2.

3.1.2 Structural modifications of compound 151a

We started to study the structure-activity relationships (SAR) of compound **151a**, which showed the best biological properties, to identify those positions on the molecule that can be modified to improve some properties, including: solubility, potency, selectivity, permeability, toxicity, pharmacokinetics and distinguish these positions from others, where such changes cannot be undertaken.

The inversion of configuration at C-3 in compound **184** was achieved through a protection-oxidation–reduction-deprotection sequence (Schemes 3.8).

Protection of alcohol **150a** with the *tert*-butyloxycarbonyl group followed by oxidation with Dess Martin provided the key ketone intermediate **182** with good yield on two steps with 72% (Scheme 3.8). The ketone intermediate underwent reduction in the presence of sodium boron hydride with good yield (Scheme 3.8).

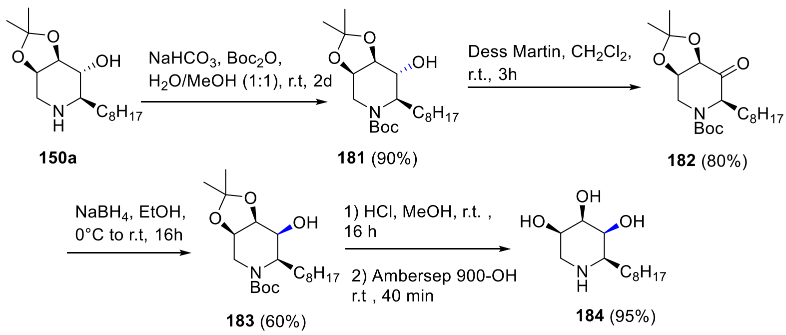

Scheme 3.8: Synthesis of compound **184**.

The high stereoselectivity observed in the reduction of **182** to **183** by the hydride anion, derived from a favoured axial attack on the C-3 carbonyl group *anti* to the vicinal C=O bond, according to the Felkin–Anh model (Figure 3.13). [196] [197]

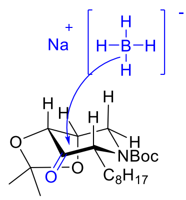

182

Figure 3.13: Favoured axial attack of the hydride anion on C=O bond.

Final deprotection of the acetonide protecting group in alcohol **183** under acidic conditions (aqueous HCl in MeOH), followed by basic treatment with excellent yield (95%), afforded the final trihydroxypiperidine **184** as free amine with good yield (Scheme 3.8).

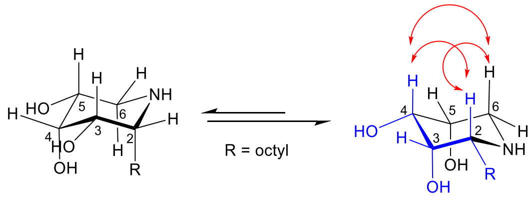

Figure 3.14. The two possible chair conformations of piperidine **184**. Dihedral angles between bonds analysed for the determination of the preferred conformation are shown in blue. Red double-ended arrows show the observed diagnostic NOE correlation peaks in the 1D-NOESY NMR spectra.

The inversion of configuration at C-3 in compound **184** and its preferred conformation was established on the basis of careful analysis of their ^{1}H-NMR and 1D-NOESY spectra. 1D-NOESY studies for compound **184** showed a strong NOE peak between proton 2-H and 6-Hb and 4-H (Figure 3.14). Moreover the ^{1}H-NMR spectrum showed a large singlet for the proton 3-H, which is consistent with two *eq-ax* relationships with both 2-H and 4-H (Table 3.6). These evidences confirm the S stereochemistry at C-3 and a conformation in which the chain bulky is in equatorial position.

Table 3.6: ^{1}H-NMR chemical shifts (δ) and coupling constants (J) of the protons in the azasugar portion of compound **184**.

Comp. 184	**2H**		**3-H**	**4H**	**5H**	**6Ha**		**6H$_b$**	
	δ (ppm)	^2J (Hz)	δ (ppm)	δ (ppm)	δ (ppm)	δ (ppm)	^2J (Hz)	δ (ppm)	^2J (Hz)
	2.44 (t)	6.5	3.73 (brs)	3.46 (brs)	3.79 (brs)	3.02 (d)	13.4	2.69	13.8

The new synthesized trihydroxypiperidine **184** exhibited 77% GCase inhibitory activity at 1 mM in human leukocyte homogenates with IC_{50}= 28.0 + 0.5 µM.
This data shows how the inversion of configuration at C-3 does not affect the inhibitory activity compared with the epimer **151a**. Further investigations on

fibroblasts from GD patients are ongoing.

We then synthesized a potential prodrug (compound **187**) of the **151a** compound with the aim of increasing its solubility and cellular permeability on cell lines. A prodrug is an inactive form of the drug; however, its chemistry helps to overcome certain inherent hurdles of the parent therapeutic agent, and could significantly contribute to optimal pharmacokinetics. The compound **187** is converted into the active form through the esterase enzymes in *ex vivo*. The **187** compound was synthesized starting from the compound **151a** through a selective protection-acetylation–deprotection sequence. Protection of the piperidine nitrogen of **151a** with benzylbromide, followed by peracetylation of the free hydroxyl groups in **185** afforded compound **186** in good yield on two steps (63%). Final deprotection of the benzyl protecting group in compound **186** by hydrogenation afforded the prodrug compound **187** in excellent yield (90%) (Scheme 3.9).

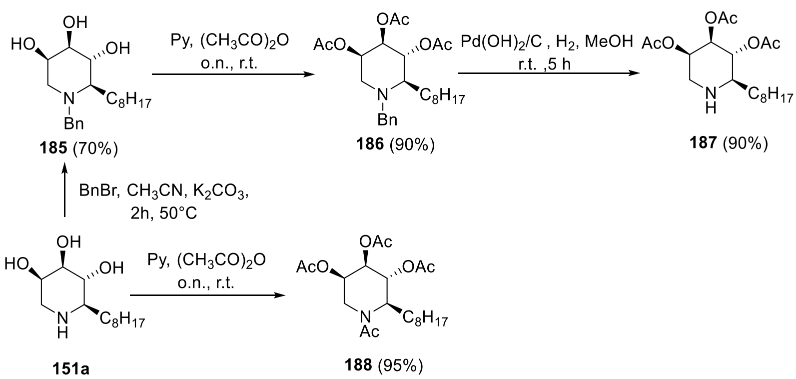

Scheme XX: Synthesis of acetylated derivatives of compounds **151a**.

Cell studies will be conduced to verify the effect of the acetyl groups on the ability of facilitate crossing of biological barriers. Moreover, we also synthesized the completely acetylated compound **188** (Scheme 3.9) to verify how the loss of basicity on nitrogen can affect the PC activity.

3.1.3 Experimental Section

General Experimental Procedures for the syntheses:

Commercial reagents were used as received. All reactions were carried out under magnetic stirring and monitored by TLC on 0.25 mm silica gel plates (Merck F254). Column chromatographies were carried out on Silica Gel 60 (32–63 µm) or on silica gel (230–400 mesh, Merck). Yields refer to spectroscopically and analytically pure compounds unless otherwise stated. ^{1}H-NMR spectra were recorded on a Varian Gemini 200 MHz, a Varian Mercury 400 MHz or on a Varian INOVA 400 MHz instruments at 25 °C. ^{13}C-NMR spectra were recorded on a Varian Gemini 50 MHz or on a Varian Mercury 100 MHz instruments. Chemical shifts are reported relative to $CDCl_3$ (^{1}H: δ = 7.27 ppm, ^{13}C: δ = 77.0 ppm). Integrals are in accordance with assignments, coupling constants are given in Hz. For detailed peak assignments 2D spectra were measured (g-COSY, g-HSQC) and 1D-NOESY. IR spectra were recorded with a IRAffinity-1S Shimadzu spectrophotometer. ESI-MS spectra were recorded with a Thermo Scientific™ LCQ fleet ion trap mass spectrometer. ICP analyses were performed with a Thermo Finnigan FLASH EA 1112 CHN/S analyser. Optical rotation measurements were performed on a JASCO DIP-370 polarimeter.

Synthesis of hydroxylamines 144a-e and 148a-e

- Method A: general procedure without Lewis acid

A solution of nitrone **140** in dry THF (0.03 M) was stirred at a given temperature under nitrogen atmosphere and the appropriate solution of Grignard reagent was slowly added. The reaction mixture was stirred until a TLC control (PEt/AcOEt 1:1) attested the disappearance of the starting material. A 1M NaOH solution (10 mL) and Et_2O (10 mL) were added to the mixture at 0 °C and left stirring for 20 minutes. The two layers were separated and the aqueous layer was extracted with Et_2O (2x10 mL). The combined organic layers were washed with brine (2x30 mL), dried with Na_2SO_4 and concentrated under reduced pressure to give a mixture of hydroxylamines **144** and **148** (the **144**:**148** ratio was determined by integration of ^{1}H-NMR signals of the crude reaction mixtures). The crude mixture was purified by silica gel column chromatography (gradient eluent from PEt/AcOEt 13:1 to 10:1) to give **144** (R_f = 0.48, PEt/AcOEt 10:1) and **148** (R_f = 0.33, PEt/AcOEt 10:1).

The secondary hydroxylamines **144** and **148** spontaneously oxidize to the corresponding nitrones **145** and **149**, so we could only perform ^{1}H-NMR and MS-

ESI spectra immediately after their purification by column chromatography.

Synthesis of benzyl-2,3-*O*-(1-methylethylidene)-β-L-gulofuranoside-5-(octyl)-5-(*N*-benzyl-hydroxylamine) (144a) and **benzyl-2,3-*O*-(1-methylethylidene)-α-D-mannofuranoside-5-(octyl)-5-(*N*-benzyl- hydroxylamine) (148a):** Application of the general procedure A to 225 mg (0.59 mmol) of **140** with 2.0 M solution of octylmagnesium bromide in diethyl ether (1.06 mmol, 0.53 mL) at –30 °C for 2 h furnished a mixture of **144a** and **148a** (**144a**:**148a** ratio 4.7:1). Purification by column chromatography (gradient eluent from PEt/AcOEt 13:1 to 10:1) afforded 200 mg (0.4 mmol) of **144a** and 40 mg (0.08 mmol) of **148a** corresponding to 83% total yield.

144a: colorless oil. ^{1}H-NMR (200 MHz, $CDCl_3$) δ = 7.44-7.28 (m, 10H, Ar), 5.16 (s, 1H, 1-H), 4.92 (bs, OH), 4.78 (d, J=12.0 Hz, 1H, H_a-OBn), 4.73 (dd, J=5.8, 3.0 Hz, 1H, 3-H), 4.63 (d, J=6.0 Hz,1H, 2-H), 4.57 (d, J=12.0 Hz, 1H, H_b-OBn), 4.42 (dd, J=9.5, 3.3 Hz, 1H, 4-H), 4.29 (d, J=14.0 Hz, 1H, H_a-NBn), 4.00 (d, J=14.0 Hz, 1H, H_b-NBn), 3.35-3.28 (m, 1H, 5-H), 1.54-1.50 (m, 4H, 1'H and 2'H) 1.45 (s, 3H, Me), 1.32-1.23 (m, 13H, Me, 3'H-7'H), 0.89 (t, J = 6.0 Hz, 3H, 8'$H_{a\text{-}b\text{-}c}$) ppm. $C_{30}H_{43}NO_5$: mass required m/z = 497.31; mass found - MS (ESI) m/z (%) = 498.40 (100) $[M+H]^+$.

148a: colorless oil. ^{1}H-NMR (200 MHz, $CDCl_3$) δ = 7.36-7.30 (m, 10H, Ar), 5.08 (s, 1H, 1-H), 4.82 (dd, J=5.8, 3.5 Hz, 1H, 3-H), 4.72-4.62 (m, 2H, 2-H and H_a-OBn), 4.49 (d, J=12.0 Hz, 1H, H_b-OBn), 4.32 (dd, J=6.8, 3.5 Hz, 1H, 4-H), 3.93 (s, 2H, $H_{a\text{-}b}$-NBn), 3.33 (q, J=6.2 Hz, 1H, 5-H), 1.78-1.71 (m, 2H, 1'H), 1.60-1.54 (m, 2H, 2'H), 1.44 (s, 3H, Me), 1.33-1.29 (m, 13H, Me , 3'H-7'H), 0.89 (t, J = 6.0 Hz, 3H, 8'$H_{a\text{-}b\text{-}c}$) ppm. $C_{30}H_{43}NO_5$: mass required m/z = 497.31; mass found - MS (ESI) m/z (%) = 498.40 (100) $[M+H]^+$.

Synthesis of benzyl-2,3-*O*-(1-methylethylidene)-β-L-gulofuranoside-5-(nonyl)-5-(*N*-benzyl-hydroxylamine) (144b) and benzyl-2,3-*O*-(1-methylethylidene)-α-D-mannofuranoside-5-(nonyl)-5-(*N*-benzyl-hydroxylamine) (148b): Application of the general procedure A to 400 mg (1.04 mmol) of **140** with 1.2 M solution of nonylmagnesium bromide in THF (2.3 mmol, 2.05 mL) at –78 °C for 3 h furnished a mixture of **144b** and **148b** (**144b**:**148b** ratio 3.3:1). Purification by column chromatography (gradient eluent from PEt/AcOEt 13:1 to 10:1) afforded 250 mg (0.48 mmol) of **144b** and 30 mg (0.06 mmol) of **148b** corresponding to 52% total yield.

144b: colorless oil. ^{1}H-NMR (400 MHz, $CDCl_3$) δ = 7.42-7.25 (m, 10H, Ar), 5.16 (s, 1H, 1-H), 4.90 (bs, OH), 4.78 (d, J=12.0 Hz, 1H, H_a-OBn), 4.73 (dd, J=5.3, 3.5 Hz, 1H, 3-H), 4.63 (d, J= 8.0 Hz, 1H, 2-H), 4.57 (d, J=12.0 Hz, 1H, H_b-OBn), 4.42 (dd, J= 9.5, 3.2 Hz, 1H, 4-H), 4.29 (d, J=14.0 Hz, 1H, H_a-NBn), 4.00 (d, J=14.0 Hz, 1H, H_b-NBn), 3.31-3.29 (m, 1H, 5-H), 1.63-1.61 (m, 1H, 1'H_a), 1.55-1.50 (m, 2H, 1'H_b and 2'H_a) 1.45 (s, 3H, Me), 1.32-1.25 (m, 16H, Me, 2'H_b, 3'H-8'H), 0.89 (t, J = 6.0 Hz, 3H, 9'$H_{a\text{-}b\text{-}c}$) ppm. $C_{31}H_{45}NO_5$: mass required m/z = 511.70; mass found - MS (ESI) m/z (%) = 534.39 (100) $[M+Na]^+$, 512.40 (95) $[M+H]^+$.

148b: colorless oil. ^{1}H-NMR (400 MHz, $CDCl_3$) δ = 7.37-7.24 (m, 10H, Ar), 5.07 (s, 1H, 1-H), 4.94 (bs, 1H, OH), 4.82 (dd, J= 8.0, 4.0 Hz, 1H, 3-H), 4.69 (d, J=12 Hz, 1H, H_a-OBn), 4.63 (d, J=8.0 Hz, 1H, 2-H), 4.49 (d, J=12.0 Hz, 1H, H_b-OBn), 4.32 (dd, J= 6.7, 3.7 Hz, 1H, 4-H), 3.93 (s, 2H, $H_{a\text{-}b}$-NBn), 3.33 (q, J= 6.2 Hz, 1H, 5-H), 1.78-1.72 (m, 2H, 1'H), 1.58-1.48 (m, 2H, 2'H), 1.43 (s, 3H, Me), 1.32-1.20 (m, 15H, Me , 3'H-8'H), 0.89 (t, J = 6.0 Hz, 3H, 9'$H_{a\text{-}b\text{-}c}$) ppm. $C_{31}H_{45}NO_5$: mass required m/z = 511.70; mass found - MS (ESI) m/z (%) = 534.39 (100) $[M+Na]^+$.

Synthesis of benzyl-2,3-*O*-(1-methylethylidene)-β-L-gulofuranoside-5-(undecyl)-5-(*N*-benzyl-hydroxylamine) (144c) and benzyl-2,3-*O*-(1-methylethylidene)-α-D-mannofuranoside-5-(undecyl)-5-(*N*-benzyl-hydroxylamine) (148c): Application of the general procedure A to 200 mg (0.52 mmol) of **140** with 0.6 M solution of undecylmagnesium bromide in THF (2.08 mmol, 3.6 mL) at –78 °C for 4 h furnished a mixture of **144c** and **148c** (**144c**:**148c** ratio 4.2:1). Purification by column chromatography (gradient eluent from PEt/AcOEt 13:1 to 10:1) afforded 166 mg (0.30 mmol) of **144c** and 30 mg (0.06 mmol) of **148c** corresponding to 70% total yield.

144c: colorless oil. ^{1}H-NMR (200 MHz, $CDCl_3$) δ = 7.43-7.29 (m, 10H, Ar), 5.17 (s, 1H, 1-H), 4.92 (bs, OH), 4.78 (d, J=12.4 Hz, 1H, H_a-OBn), 4.76 (dd, J=6.0, 3.0 Hz, 1H, 3-H), 4.64 (d, J=8.0 Hz, 1H, 2-H), 4.58 (d, J=12.0 Hz, 1H, H_b-OBn), 4.42 (dd, J=9.0, 3.0 Hz, 1H, 4-H), 4.29 (d, J=14.0 Hz, 1H, H_a-NBn), 4.01 (d, J=14.0 Hz, 1H, H_b-NBn), 3.32-3.28 (m, 1H, 5-H), 1.54-1.20 (m, 26H, Me, Me, 1'H-10'H), 0.89 (t, J

= 6.0 Hz, 3H, 11'$H_{a\text{-}b\text{-}c}$) ppm. $C_{33}H_{49}NO_5$: mass required m/z = 539.36; mass found - MS (ESI) m/z (%) = 540.69 (100) $[M+H]^+$.

148c: colorless oil. ^{1}H-NMR (200 MHz, $CDCl_3$) δ = 7.36-7.29 (m, 10H, Ar), 5.08 (s, 1H, 1-H), 5.00 (bs, OH), 4.82 (dd, J=6.0, 3.0 Hz, 1H, 3-H), 4.70 (d, J=12.0 Hz, 1H, H_a-OBn), 4. 63 (d, J=6.0 Hz,1H, 2-H), 4.50 (d, J=12.0 Hz, 1H, H_b-OBn), 4.38 (dd, J=6.8, 3.4 Hz, 1H, 4-H), 3.92 (s, 2H, $H_{a\text{-}b}$-NBn), 3.33 (q, J=6.0 Hz, 1H, 5-H), 1.78-1.23 (m, 26H, Me, Me, 1'H-10'H), 0.90 (t, J = 6.0 Hz, 3H, 11'$H_{a\text{-}b\text{-}c}$) ppm. $C_{33}H_{49}NO_5$: mass required m/z = 539.36; mass found - MS (ESI) m/z (%) = 562.66 (100) $[M+Na]^+$, 540.69 (79) $[M+H]^+$.

Synthesis of benzyl-2,3-*O*-(1-methylethylidene)-β-L-gulofuranoside-5-(dodecyl)-5-(*N*-benzyl-hydroxylamine) (144d) and benzyl-2,3-*O*-(1-methylethylidene)-α-D-mannofuranoside-5-(dodecyl)-5-(*N*-benzyl-hydroxylamine) (148d): Application of the general procedure A to 261 mg (0.68 mmol) of **140** with 1.0 M solution of dodecylmagnesium bromide in diethyl ether (1.56 mmol, 1.6 mL) at –30 °C for 2 h furnished a mixture of **144d** and **148d** (**144d**:**148d** ratio 3.4:1). Purification by column chromatography (gradient eluent from PEt/AcOEt 13:1 to 10:1) afforded 236 mg (0.43 mmol) of **144d** and 42 mg (0.08 mmol) of **148d** corresponding to 70% total yield.

144d: colorless oil. ^{1}H-NMR (200 MHz, $CDCl_3$) δ = 7.38-7.31 (m, 10H, Ar), 5.15 (s, 1H, 1-H), 4.77 (d, J=12.0 Hz, 1H, H_a-OBn), 4.71 (dd, J=6.0, 3.5 Hz, 1H, 3-H), 4.63 (d, J= 6.0 Hz, 1H, 2-H), 4.57 (d, J=12.0 Hz, 1H, H_b-OBn), 4.41 (dd, J=9.0, 3.0 Hz, 1H, 4-H), 4.28 (d, J=14.0 Hz, 1H, H_a-NBn), 3.97 (d, J=14.0 Hz, 1H, H_b-NBn), 3.31-3.27 (m, 1H, 5-H), 1.55-1.26 (m, 28H, Me, Me, 1'H-11'H), 0.88 (t, J = 6.8 Hz, 3H, 12'$H_{a\text{-}b\text{-}c}$) ppm. $C_{34}H_{51}NO_5$: mass required m/z = 553.38; mass found - MS (ESI) m/z (%) = 554.67 (57) $[M+H]^+$.

148d: colorless oil. ^{1}H-NMR (200 MHz, $CDCl_3$) δ = 7.45-7.28 (m, 10H, Ar), 5.07 (s, 1H, 1-H), 4.83 (dd, J=6.0, 2.0 Hz, 1H, 3-H), 4.68 (d, J=12.0 Hz, 1H, H_a-OBn), 4.63 (d, J= 6.0 Hz,1H, 2-H), 4.49 (d, J=12.0 Hz, 1H, H_b-OBn), 4.33 (dd, J= 6.0, 2.0 Hz, 1H, 4-H), 3.93 (s, 2H, $H_{a\text{-}b}$-NBn), 3.32 (q, J= 6.2 Hz, 1H, 5-H), 1.78-1.72 (m, 1H, 1'H_a), 1.60-1.52 (m, 2H, 1'H_b and 2'H_a), 1.43 (s, 3H, Me), 1.31-1.22 (m, 22H, Me, 2'H_b and 3'H-11'H), 0.88 (t, J = 6.7 Hz, 3H, 12'$H_{a\text{-}b\text{-}c}$) ppm. $C_{34}H_{51}NO_5$: mass required m/z = 553.38; mass found - MS (ESI) m/z (%) = 554.67 (50) $[M+H]^+$.

Synthesis of benzyl-2,3-*O*-(1-methylethylidene)-β-L-gulofuranoside-5-(tridecyl)-5-(*N*-benzyl-hydroxylamine) (144e) and benzyl-2,3-*O*-(1-methylethylidene)-α-D-mannofuranoside-5-(tridecyl)-5-(*N*-benzyl-hydroxylamine) (148e): Application of the general procedure A to 200 mg (0.52 mmol) of **140** with 0.4 M solution of tridecylmagnesium bromide in THF (1.56 mmol, 3.8 mL) at –78 °C for 3.5 h furnished a mixture of **144e** and **148e** (**144e**:**148e** ratio 4.2:1). Purification by column chromatography (gradient eluent from PEt/AcOEt 13:1 to 10:1) afforded 125 mg (0.22 mmol) of **144e** and 50 mg (0.09 mmol) of **148e** corresponding to 60% total yield.

144e: colorless oil. ^{1}H-NMR (400 MHz, $CDCl_3$) δ = 7.42-7.25 (m, 10H, Ar), 5.17 (s, 1H, 1-H), 4.88 (bs, OH), 4.78 (d, J=12.0 Hz, 1H, H_a-OBn), 4.72 (dd, J= 6.0, 3.6 Hz, 1H, 3-H), 4.63 (d, J= 6.0 Hz, 1H, 2-H), 4.58 (d, J=12.0 Hz, 1H, H_b-OBn), 4.42 (dd, J=9.2, 3.2 Hz, 1H, 4-H), 4.28 (d, J=14.0 Hz, 1H, H_a-NBn), 3.99 (d, J=14.0 Hz, 1H, H_b-NBn), 3.32-3.27 (m, 1H, 5-H), 1.62-1.61 (m, 1H, 1'H_a), 1.55-1.51 (m, 2H, 1'H_b and 2'H_a), 1.45 (s, 3H, Me), 1.32-1.28 (m, 24H, Me , 2'H_b and 3'H-12'H), 0.89 (t, J = 6.0 Hz, 3H, 13'$H_{a\text{-}b\text{-}c}$) ppm. $C_{35}H_{53}NO_5$: mass required m/z = 567.39; mass found - MS (ESI) m/z (%) = 568.33 (86) $[M+H]^+$, 590.37 (47) $[M+Na]^+$, 1155.71 (100) $[2M+Na]^+$.

148e: colorless oil. ^{1}H-NMR (400 MHz, $CDCl_3$) δ = 7.38-7.25 (m, 10H, Ar), 5.07 (s, 1H, 1-H), 4.83 (dd, J=6.0, 3.5 Hz, 1H, 3-H), 4.69 (d, J=12.0 Hz, 1H, H_a-OBn), 4.63 (d, J=5.6 Hz, 1H, 2-H), 4.60 (bs, OH), 4.50 (d, J=12.0 Hz, 1H, H_b-OBn), 4.32 (dd, J=6.8, 3.2 Hz, 1H, 4-H), 3.93 (s, 2H, $H_{a\text{-}b}$-NBn), 3.32 (q, J=6.3 Hz, 1H, 5-H), 1.79-1.73 (m, 1H, 1'H_a), 1.60-1.54 (m, 2H, 1'H_b and 2'H_a), 1.44 (s, 3H, Me), 1.33-1.24 (m, 24H, Me , 2'H_b and 3'H-12'H), 0.88 (t, J = 6.8 Hz, 3H, 13'$H_{a\text{-}b\text{-}c}$) ppm. $C_{35}H_{53}NO_5$: mass required m/z = 567.39; mass found - MS (ESI) m/z (%) = 568.31 (100) $[M+H]^+$, 590.30 (34) $[M+Na]^+$.

Synthesis of hydroxylamines 144a-e and 148a-e

- Method B: general procedure with Lewis acid

To a stirred solution of nitrone **140** in dry THF (0.03 M) at room temperature, Lewis acid was added and the resulting mixture was stirred at room temperature under nitrogen atmosphere for 15 minutes. The reaction mixture was cooled at -30 °C and treated with the appropriate solution of the Grignard reagent. The

reaction mixture was stirred at -30 °C until a TLC control (PEt/AcOEt 1:1) attested the disappearance of the starting material. A 1M NaOH solution (10 mL) and Et_2O (10 mL) were added to the mixture at 0 °C and left stirring for 20 minutes. The two layers were separated and the aqueous layer was extracted with Et_2O (2x10 mL). The combined organic layers were washed with brine (2x30 mL) and dried with Na_2SO_4 and concentrated under reduced pressure to give a mixture of hydroxylamines **144** and **148** (the **144**:**148** ratio was as determined by integration of ^{1}H-NMR signals of the crude reaction mixture). The crude was purified by silica gel column chromatography (gradient eluent from PEt/AcOEt 13:1 to 10:1) to give **144** (R_f = 0.48, PEt/AcOEt 10:1) and **148** (R_f = 0.33, PEt/AcOEt 10:1).
The secondary hydroxylamines **144** and **148** spontaneously oxidize to the corresponding nitrones **145** and **149**, so we could only perform the ^{1}H-NMR and MS-ESI spectra immediately after their purification by column chromatography.

Synthesis of benzyl-2,3-*O*-(1-methylethylidene)-β-L-gulofuranoside-5-(octyl)-5-(*N*-benzyl- hydroxylamine) (144a) and benzyl-2,3-*O*-(1-methylethylidene)-α-D-mannofuranoside-5-(octyl)-5-(*N*-benzyl- hydroxylamine) (148a): Application of the general procedure B to 202 mg (0.53 mmol) of **140** with boron trifluoride diethyl etherate (0.53 mmol, 65 μL) as Lewis acid and 2.0 M solution of octylmagnesium bromide in diethyl ether (0.95 mmol, 0.48 mL) for 2 h furnished a mixture of **144a** and **148a** (**144a**:**148a** ratio 1:5.6). Purification by column chromatography (gradient eluent from PEt/AcOEt 13:1 to 10:1) afforded 24 mg (0.05 mmol) of **144a** and 200 mg (0.40 mmol) of **148a** corresponding to 85% total yield.

Synthesis of benzyl-2,3-*O*-(1-methylethylidene)-β-L-gulofuranoside-5-(nonyl)-5-(*N*-benzyl-hydroxylamine) (144b) and benzyl-2,3-*O*-(1-methylethylidene)-α-D-mannofuranoside-5-(nonyl)-5-(*N*-benzyl- hydroxylamine) (148b): Application of the general procedure B to 400 mg (1.04 mmol) of **140** with boron trifluoride diethyl etherate (1.04 mmol, 129 μL) as Lewis acid and 1.2 M solution of nonylmagnesium bromide in THF (1.87 mmol, 1.65 mL) for 2 h furnished a mixture of **144b** and **148b** (**144b**:**148b** ratio 1:3). Purification by column chromatography (gradient eluent from PEt/AcOEt 13:1 to 10:1) afforded 50 mg

(0.10 mmol) of **144b** and 320 mg (0.63 mmol) of **148b** corresponding to 78% total yield.

Synthesis of benzyl-2,3-*O*-(1-methylethylidene)-β-L-gulofuranoside-5-(undecyl)-5-(*N*-benzyl-hydroxylamine) (144c) and benzyl-2,3-*O*-(1-methylethylidene)-α-D-mannofuranoside-5-(undecyl)-5-(*N*-benzyl-hydroxylamine) (148c): Application of the general procedure B to 200 mg (0.52 mmol) of **140** with boron trifluoride diethyl etherate (0.52 mmol, 64 μL) as Lewis acid and 0.6 M solution of undecylmagnesium bromide in THF (2.08 mmol, 3.8 mL) for 4 h furnished a mixture of **144c** and **148c** (**144c**:**148c** ratio 1:3). Purification by column chromatography (gradient eluent from PEt/AcOEt 13:1 to 10:1) afforded 35 mg (0.06 mmol) of **144c** and 160 mg (0.30 mmol) of **148c** corresponding to 75% total yield.

Synthesis of benzyl-2,3-*O*-(1-methylethylidene)-β-L-gulofuranoside-5-(dodecyl)-5-(*N*-benzyl-hydroxylamine) (144d) and benzyl-2,3-*O*-(1-methylethylidene)-α-D-mannofuranoside-5-(dodecyl)-5-(*N*-benzyl-hydroxylamine) (148d): Application of the general procedure B to 200 mg (0.52 mmol) of **140** with boron trifluoride diethyl etherate (0.52 mmol, 64 μL) as Lewis acid and 1.0 M solution of dodecylmagnesium bromide in diethyl ether (1.2 mmol, 1.2 mL) for 2h furnished a mixture of **144d** and **148d** (**144d**:**148d** ratio 1:9). Purification by column chromatography (gradient eluent from PEt/AcOEt 13:1 to 10:1) afforded 18 mg (0.03 mmol) of **144d** and 193 mg (0.35 mmol) of **148d** corresponding to 70% total yield.

Synthesis of benzyl-2,3-*O*-(1-methylethylidene)-β-L-gulofuranoside-5-(dodecyl)-5-(*N*-benzyl-hydroxylamine) (144d) and benzyl-2,3-*O*-(1-methylethylidene)-α-D-mannofuranoside-5-(dodecyl)-5-(*N*-benzyl-hydroxylamine) (148d): Application of the general procedure B to 100 mg (0.26 mmol) of **140** with diethylaluminum chloride solution (0.26 mmol, 67 μL) as Lewis acid and 1.0 M solution of dodecylmagnesium bromide in diethyl ether (0.6 mmol, 600 μL) for 2 h furnished a mixture of **144d** and **148d** (**144d**:**148d** ratio 1:1.5). Purification by column chromatography (gradient eluent from PEt/AcOEt

13:1 to 10:1) afforded 45 mg (0.08 mmol) of **144d** and 64 mg (0.12 mmol) of **148d** corresponding to 75% total yield.

Synthesis of benzyl-2,3-*O*-(1-methylethylidene)-β-L-gulofuranoside-5-(dodecyl)-5-(*N*-benzyl-hydroxylamine) (144d) and benzyl-2,3-*O*-(1-methylethylidene)-α-D-mannofuranoside-5-(dodecyl)-5-(*N*-benzyl-hydroxylamine) (148d): Application of the general procedure B to 100 mg (0.26 mmol) of **140** with $MgCl_2$ (0.26 mmol, 25 mg) as Lewis acid and 1.0 M solution of dodecylmagnesium bromide in diethyl ether (0.6 mmol, 0.6 mL) for 4 h furnished a mixture of **144d** and **148d** (**144d**:**148d** ratio 1:1.3). Purification by column chromatography (gradient eluent from PEt/AcOEt 13:1 to 10:1) afforded 30 mg (0.05 mmol) of **144d** and 42 mg (0.08 mmol) of **148d** corresponding to 50% total yield.

Synthesis of benzyl-2,3-*O*-(1-methylethylidene)-β-L-gulofuranoside-5-(tridecyl)-5-(*N*-benzyl-hydroxylamine) (144e) and benzyl-2,3-*O*-(1-methylethylidene)-α-D-mannofuranoside-5-(tridecyl)-5-(*N*-benzyl-hydroxylamine) (148e): Application of the general procedure B to 200 mg (0.52 mmol) of **140** with boron trifluoride diethyl etherate (0.52 mmol, 64 µL) as Lewis acid and 0.4 M solution of tridecylmagnesium bromide in THF (1.04 mmol, 2.5 mL) for 2 h furnished a mixture of **144e** and **148e** (**144e**:**148e** ratio 1:6). Purification by column chromatography (gradient eluent from PEt/AcOEt 13:1 to 10:1) afforded 36 mg (0.06 mmol) of **144e** and 222 mg (0.39 mmol) of **148e** corresponding to 87% total yield.

Synthesis of nitrones 145a-e and 149a-e

To a stirred solution of hydroxylamine **144** (or **148**) (0.072 mmol) in dry CH_2Cl_2 (1.5 mL), IBX (2-Iodoxybenzoic acid contains stabilizer (45 wt. %)-Sigma-Aldrich) (0.11 mmol) was added and the resulting mixture was stirred under nitrogen atmosphere at room temperature for 3 h, when a TLC check (PEt/AcOEt 10:1) attested the disappearance of the starting material. Saturated solution of $NaHCO_3$ (4 mL) was added and the two layers were separated and the aqueous layer was extracted with CH_2Cl_2 (3x5 mL). The combined organic layers were washed with brine (2x6 mL) and concentrated after drying with Na_2SO_4. The residue was purified by silica gel flash column chromatography (PEt/AcOEt from 10:1.2) to give nitrone **145** (or **149**) (R_f =0.34).

Synthesis of benzyl-2,3-*O*-(1-methylethylidene)-β-L-gulofuranoside-5-(octyl)-5-(phenylmethanimine oxide) (145a): Application of this procedure to 45 mg (0.09 mmol) of **144a** with 87 mg (0.14 mmol) of IBX furnished after purification by column chromatography 41 mg (0.08 mmol, 91% yield) of **145a** as a straw yellow oil.

145a: straw yellow oil. $[\alpha]_D^{25}$ = + 66 (c =0.63, $CHCl_3$). ^{1}H-NMR (400 MHz, $CDCl_3$) δ = 8.35-8.33 (m, 2H, HC=N and Ar), 7.45-7.39 (m, 4H, Ar), 7.31-7.23 (m, 5H, Ar), 5.01 (s, 1H, 1-H), 4.78-4.75 (m, 1H, 3-H), 4.67 (d, J=6.0 Hz,1H, 2-H), 4.61-4.58 (m, 2H, H_a-Bn and 4-H), 4.33 (d, J=12.0 Hz, 1H, H_b-Bn), 4.09-4.04 (m, 1H, 5-H), 2.17-2.14 (m, 1H, 1’H_a), 1.70-1.67 (m, 1H, 1’H_b), 1.50 (s, 3H, Me), 1.34-1.24 (m, 15H, Me and 2’H-7’H), 0.86 (t, J =7.0 Hz, 3H, 8’$H_{a\text{-}b\text{-}c}$) ppm. ^{13}C-NMR (50 MHz, $CDCl_3$) δ = 137.3 (s, 1C, Ar), 134.8 (d, 1C, Ar), 130.9 (s, 1C, Ar),130.1-127.8 (d, 10C, Ar and *C*=N), 112.6 (s, acetal), 104.6 (d, C-1), 85.5 (d, C-2), 79.8 (d, C-3), 79.2 (d, C-4), 76.8 (d, C-5), 68.8 (t, Bn), 31.9-22.7 (t, 9C, C-1’- C-7’and q, Me and q, Me), 14.2 (q, C-8’) ppm. MS (ESI): m/z (%) = 496.50 (4) $[M+H]^+$, 518.61 (10) $[M+Na]^+$, 1013.32 (100) $[2M+Na]^+$. IR ($CDCl_3$): ν = 957, 1080, 1114, 1209, 1456, 1582, 2245, 2857, 2930, 3032, 3065 cm^{-1}. $C_{30}H_{41}NO_5$ (495.30): calcd. C, 72.70; H, 8.34; N, 2.83; found C, 72.60; H, 8.50; N, 2.49.

Synthesis of benzyl-2,3-*O*-(1-methylethylidene)-α-D-mannofuranoside-5-(octyl)-5-(phenylmethanimine oxide) (149a): Application of this procedure to 50 mg (0.10 mmol) of **148a** with 94 mg (0.15 mmol) of IBX furnished after purification by column chromatography 44 mg (0.09 mmol, 88%) of **149a** as a straw yellow oil.

149a: straw yellow oil. $[\alpha]_D^{24}$ = + 71 (c =0.75, $CHCl_3$). ^{1}H-NMR (400 MHz, $CDCl_3$) δ = 8.30-8.27 (m, 2H, HC=N and Ar), 7.47-7.44 (m, 4H, Ar), 7.38-7.28 (m, 5H, Ar), 5.08 (s, 1H, 1-H), 4.71 (dd, J=5.8, 3.1 Hz, 1H, 3-H), 4.67 (d, J=12.0 Hz, 1H, H_a-Bn), 4.62 (d, J= 4.0 Hz,1H, 2-H), 4.52 (d, J=12 Hz, 1H, H_b-Bn), 4.50 (dd, J=8.0, 3.0 Hz, 1H, 4-H), 4.21-4.16 (m, 1H, 5-H), 2.16-2.13 (m, 1H, 1’H_a), 1.86-1.83 (m, 1H, 1’H_b), 1.49 (s, 3H, Me), 1.28-1.23 (m, 15H, 2’H-7’H and Me), 0.86 (t, J= 6.8 Hz, 3H, 8’$H_{a\text{-}}$

$_{b-c}$) ppm. ^{13}C-NMR (50 MHz, $CDCl_3$) δ = 137.5 (s, 1C, Ar), 136.1 (d, 1C, Ar), 130.7 (s, 1C, Ar),130.4-127.9 (d, 10C, Ar and *C*=N), 112.6 (s, acetal), 105.6 (d, C-1), 85.4 (d, C-2), 80.1 (d, C-4), 79.4 (d, C-3), 74.7 (d, C-5), 69.3 (t, Bn), 31.9-29.3 (t, 5C, C-1'- C-5'), 26.3 (q, Me), 26.1-22.7 (t, 3C, C-6'- C-7'and q, Me), 14.2 (q, C-8') ppm. MS (ESI): m/z (%) = 518.61 (7) $[M+Na]^+$, 1013.32 (100) $[2M+Na]^+$. IR ($CDCl_3$): ν = 957, 1080, 1148, 1209, 1454, 1582, 2245, 2857, 2928, 3032, 3065 cm^{-1}. $C_{30}H_{41}NO_5$ (495.30): calcd. C, 72.70; H, 8.34; N, 2.83; found C, 73.00; H, 8.67; N, 2.54.

Synthesis of benzyl-2,3-*O*-(1-methylethylidene)-β-L-gulofuranoside-5-(nonyl)-5-(phenylmethanimine oxide) (145b): Application of this procedure to 48 mg (0.09 mmol) of **144b** with 87.6 mg (0.14 mmol) of IBX furnished after purification by column chromatography 98.4 mg (0.19 mmol, 93%) of **145b** as a straw yellow oil.

145b: straw yellow oil. $[\alpha]_D^{26}$= + 61 (c =1.23, $CHCl_3$). ^{1}H-NMR (400 MHz, $CDCl_3$) δ = 8.34-8.32 (m, 2H, HC=N and Ar), 7.46-7.39 (m, 4H, Ar), 7.31-7.23 (m, 5H, Ar), 5.01 (s, 1H, 1-H), 4.77-4.75 (m, 1H, 3-H), 4.67 (d, J= 8.0 Hz,1H, 2-H), 4.61-4.58 (m, 2H, H_a-Bn and 4-H), 4.33 (d, J=12.0 Hz, 1H, H_b-Bn), 4.09-4.03 (m, 1H, 5-H), 2.17-2.14 (m, 1H, 1'H_a), 1.70-1.68 (m, 1H, 1'H_b), 1.50 (s, 3H, Me), 1.34-1.24 (m, 17H, Me and 2'H-8'H), 0.87 (t, J =7.0 Hz, 3H, 9'H_{a-b-c}) ppm. ^{13}C-NMR (100 MHz, $CDCl_3$) δ = 137.2 (s, 1C, Ar), 134.9 (d, 1C, Ar), 130.8 (s, 1C, Ar),130.1-127.9 (d, 10C, Ar and *C*=N), 112.6 (s, acetal), 104.5 (d, C-1), 85.4 (d, C-2), 79.8 (d, C-3), 79.1 (d, C-4), 76.8 (d, C-5), 68.8 (t, Bn), 32.0-22.8 (t, 10C, C-1'- C-8' and q, Me and q, Me), 14.2 (q, C-9') ppm. MS (ESI): m/z (%) = 1041.10 (100) $[2M+Na]^+$. IR (CDCl3): ν = 962, 1105, 1209, 1458, 1577, 2239, 2855, 2927, 3030, 3066 cm-1. $C_{31}H_{43}NO_5$ (509.31): calcd. C, 73.05; H, 8.50; N, 2.75; found C, 73.30; H, 8.40; N, 2.54.

Synthesis of benzyl-2,3-*O*-(1-methylethylidene)-α-D-mannofuranoside-5-(nonyl)-5-(phenylmethanimine oxide) (149b): Application of this procedure to 106 mg (0.21 mmol) of **148b** with 196 mg (0.32 mmol) of IBX furnished after purification by column chromatography 44.5 mg (0.09 mmol, 92%) of **149b** as a straw yellow oil.

149b: straw yellow oil. $[\alpha]_D^{26}$= + 76 (c =0.90, $CHCl_3$). ^{1}H-NMR (400 MHz, $CDCl_3$) δ = 8.29-8.27 (m, 2H, HC=N and Ar), 7.47-7.43 (m, 4H, Ar), 7.38-7.26 (m, 5H, Ar), 5.08 (s, 1H, 1-H), 4.72-4.70 (m, 1H, 3H), 4.67 (d, J=12.0 Hz, 1H, H_a-Bn), 4.62 (d, J= 4.0 Hz,1H, 2-H), 4.53-4.48 (m, 2H, 4-H and H_b-OBn), 4.20-4.15 (m, 1H, 5-H), 2.16-2.13 (m, 1H, 1'H_a), 1.86-1.83 (m, 1H, 1'H_b), 1.49 (s, 3H, Me), 1.34-1.23 (m, 17H, 2'H-8'H and Me), 0.87 (t, J= 5.0 Hz, 3H, 9'H_{a-b-c}) ppm. ^{13}C-NMR (100 MHz, $CDCl_3$) δ = 137.4 (s, 1C, Ar), 136.2 (d, 1C, Ar), 130.6 (s, 1C, Ar),130.4-127.9 (d, 10C, Ar and *C*=N), 112.5 (s, acetal), 105.5 (d, C-1), 85.3 (d, C-2), 80.0 (d, C-4), 79.3 (d, C-3), 74.6 (d, C-5), 69.2 (t, Bn), 32.0-22.8 (t, 10C, C-1'- C-8' and q, Me and q, Me), 14.2 (q, C-9') ppm. MS (ESI): m/z (%) = 1041.10 (100) $[2M+Na]^+$. IR ($CDCl_3$): ν = 972, 1082, 1145, 1211, 1456, 1581, 2241, 2857, 2928, 3030, 3066 cm^{-1}. $C_{31}H_{43}NO_5$ (509.31): calcd. C, 73.05; H, 8.50; N, 2.75; found C, 73.40; H, 8.25; N, 2.46.

Synthesis of benzyl-2,3-*O*-(1-methylethylidene)-β-L-gulofuranoside-5-(undecyl)-5-(phenylmethanimine oxide) (145c): Application of this procedure to 35 mg (0.07 mmol) of **144c** with 61 mg (0.10 mmol) of IBX furnished after purification by column chromatography 33 mg (0.06 mmol, 93%) of **145c** as a straw yellow oil.

145c: straw yellow oil. $[\alpha]_D^{25}$ = + 33 (c =10.6, $CHCl_3$). ^{1}H-NMR (400 MHz, $CDCl_3$) δ = 8.34-8.32 (m, 2H, HC=N and Ar), 7.46-7.41 (m, 4H, Ar), 7.31-7.23 (m, 5H, Ar), 5.00 (s, 1H, 1-H), 4.77-4.75 (m, 1H, 3-H), 4.66 (dd, J=5.8, 1.8 Hz,1H, 2-H), 4.60-4.57 (m, 2H, H_a-Bn and 4-H), 4.32 (d, J=12.0 Hz, 1H, H_b-Bn), 4.08-4.03 (m, 1H, 5-H), 2.16-2.10 (m, 1H, 1'H_a), 1.69-1.61 (m, 1H, 1'H_b), 1.50 (s, 3H, Me), 1.32-1.23 (m, 18H, 2'H-10'H), 1.32 (s, 3H, Me), 0.87 (t, J=6.0 Hz, 3H, 11'H_{a-b-c}) ppm. ^{13}C-NMR (50 MHz, $CDCl_3$) δ = 137.3 (s, 1C, Ar), 134.8 (d, 1C, Ar), 130.9 (s, 1C, Ar),129.7-127.9 (d, 10C, Ar and *C*=N), 112.6 (s, acetal), 104.6 (d, C-1), 85.5 (d, C-2), 79.8 (d, C-3), 79.5 (d, C-4), 76.8 (d, C-5), 68.8 (t, Bn), 32.1-27.7 (t, 8C, C-1'- C-8'), 26.3 (q, Me), 25.9 (t, C-9'), 24.9 (q, Me), 22.8 (t, C-10'), 14.2 (q, C-11') ppm. MS (ESI): m/z (%) = 538.64 (15) $[M+H]^+$, 560.65 (100) $[M+Na]^+$, 1097.21 (40) $[2M+Na]^+$. IR ($CDCl_3$): ν = 950, 1016, 1080, 1107, 1209, 1456, 1580, 2243, 2855, 2928, 3032, 3065 cm^{-1}. $C_{33}H_{47}NO_5$ (537.35): calcd. C, 73.71; H, 8.81; N, 2.6; found C, 73.79; H, 9.05; N, 2.40.

Synthesis of benzyl-2,3-*O*-(1-methylethylidene)-α-D-mannofuranoside-5-(undecyl)-5-(phenylmethanimine oxide) (149c): Application of this procedure to

43 mg (0.08 mmol) of **148c** with 75 mg (0.12 mmol) of IBX furnished after purification by column chromatography 39 mg (0.07 mmol, 91%) of **149c** as a straw yellow oil.

149c: straw yellow oil. $[\alpha]_D^{25}$ = + 46 (c =0.73, $CHCl_3$). ^{1}H-NMR (400 MHz, $CDCl_3$) δ = 8.29-8.27 (m, 2H, HC=N and Ar), 7.47-7.43 (m, 4H, Ar), 7.38-7.26 (m, 5H, Ar), 5.08 (s, 1H, 1-H), 4.72-4.70 (m, 1H, 3-H), 4.68 (d, J=12.0 Hz, 1H, H_a-Bn), 4.61 (dd, J=6.0, 1.6 Hz,1H, 2-H), 4.52 (d, J=12.0 Hz, 1H, H_b-Bn), 4.48 (dd, J=9.4, 3.0 Hz, 1H, 4-H), 4.19-4.15 (m, 1H, 5-H), 2.15-2.10 (m, 1H, 1'H_a), 1.85-1.82 (m, 1H, 1'H_b), 1.48 (s, 3H, Me), 1.33-1.23 (m, 21H, 2'H-10'H and Me), 0.86 (t, J= 6.0 Hz, 3H, 11'H_{a-b-c}) ppm. ^{13}C-NMR (100 MHz, $CDCl_3$) δ = 137.5 (s, 1C, Ar), 136.2 (d, 1C, Ar), 130.6 (s, 1C, Ar),130.5-128.0 (d, 10C, Ar and *C*=N), 112.6 (s, acetal), 105.6 (d, C-1), 85.3 (d, C-2), 80.0 (d, C-4), 79.4 (d, C-3), 74.7 (d, C-5), 69.2 (t, Bn), 32.0-22.8 (t, 12C, C-1'-C-10', q, Me and q, Me), 14.3 (q, C-11') ppm. MS (ESI): m/z (%) = 538.58 (12) $[M+H]^+$,560.65 (100) $[M+Na]^+$, 1097.16 (65) $[2M+Na]^+$. IR (CDCl3): ν = 972, 1022, 1080.14, 1126, 1211, 1454, 1582, 2243, 2857, 2928, 3032, 3065 cm^{-1}. $C_{33}H_{47}NO_5$ (537.35): calcd. C, 73.71; H, 8.81; N, 2.6; found C, 73.70; H, 9.01; N, 2.40.

Synthesis of benzyl-2,3-*O*-(1-methylethylidene)-β-L-gulofuranoside-5-(dodecyl)-5-(phenylmethanimine oxide) (145d): Application of this procedure to 15 mg (0.03 mmol) of **144d** with 29 mg (0.05 mmol) of IBX furnished after purification by column chromatography 14 mg (0.03 mmol, 95%) of **145d** as a straw yellow oil.

145d: straw yellow oil. $[\alpha]_D^{22}$ = + 28 (c =0.75, $CHCl_3$). ^{1}H-NMR (400 MHz, $CDCl_3$) δ = 8.34-8.32 (m, 2H, HC=N and Ar), 7.47-7.39 (m, 4H, Ar), 7.31-7.22 (m, 5H, Ar), 5.00 (s, 1H, 1-H), 4.76 (dd, J=8.0, 4.0 Hz, 1H, 3-H), 4.67 (d, J=4.0 Hz,1H, 2-H), 4.59 (d, J=12.0 Hz, 1H, H_a-Bn), 4.58 (d, J=12.0 Hz, 1H, 4-H), 4.33 (d, J=12.0 Hz, 1H, H_b-Bn), 4.08-4.02 (m, 1H, 5-H), 2.18 (s, acetone), 2.17-2.10 (m, 1H, 1'H_a), 1.69-1.64 (m, 1H, 1'H_b), 1.50 (s, 3H, Me), 1.33-1.16 (m, 20H, 2'H-11'H), 1.30 (s, 3H, Me), 0.87 (t, J= 7.0 Hz, 3H, 12'H_{a-b-c}) ppm. ^{13}C-NMR (50 MHz, $CDCl_3$) δ = 137.3 (s, 1C, Ar), 134.8 (d, 1C, Ar), 130.9 (s, 1C, Ar),130.1-127.9 (d, 10C, Ar and *C*=N), 112.6 (s, acetal), 104.6 (d, C-1), 85.5 (d, C-2), 79.8 (d, C-3), 79.2 (d, C-4), 76.8 (d, C-5), 68.8 (t, Bn), 32.1-27.7 (t, 9C, C-1'- C-9'), 26.3 (q, Me), 25.9 (t, C-10'), 24.9 (q, Me), 22.8 (t, C-11'), 14.2 (q, C-12') ppm. MS (ESI): m/z (%) = 552.62 (3) $[M+H]^+$,574.63 (10)

[M+Na]$^+$, 1125.32 (100) [2M+Na]$^+$. IR ($CDCl_3$): ν = 976, 1016, 1080, 1107, 1209, 1456, 1582, 2245, 2855, 2930, 3032, 3065 cm^{-1}. $C_{34}H_{49}NO_5$ (551.36): calcd. C, 74.01; H, 8.95; N, 2.54; found C, 74.28; H, 9.07; N, 2.20.

Synthesis of benzyl-2,3-*O*-(1-methylethylidene)-α-D-mannofuranoside-5-(dodecyl)-5-(phenylmethanimine oxide) (149d): Application of this procedure to 50 mg (0.09 mmol) of **148d** with 84 mg (0.14 mmol) of IBX furnished after purification by column chromatography 49 mg (0.09 mmol, 98%) of **149d** as a straw yellow oil.

149d: straw yellow oil. $[\alpha]_D^{23}$ = + 47 (c =0.65, $CHCl_3$). ^{1}H-NMR (400 MHz, $CDCl_3$) δ = 8.30-8.28 (m, 2H, HC=N and Ar), 7.45-7.41 (m, 4H, Ar), 7.38-7.26 (m, 5H, Ar), 5.08 (s, 1H, 1-H), 4.71 (dd, J=5.6, 3.2 Hz, 1H, 3-H), 4.66 (d, J=12.0 Hz, 1H, H_a-Bn), 4.61 (d, J=5.8 Hz,1H, 2-H), 4.51 (d, J=12.0 Hz, 1H, H_b-Bn), 4.49 (dd, J=9.3, 3.0 Hz, 1H, 4-H), 4.21-4.16 (m, 1H, 5-H), 2.17-2.11 (m, 1H, 1'H_a), 1.86-1.83 (m, 1H, 1'H_b), 1.49 (s, 3H, Me), 1.34-1.24 (m, 23H, 2'H-11'H and Me), 0.88 (t, J =8.0 Hz, 3H, 12'$H_{a\text{-}b\text{-}c}$) ppm. ^{13}C-NMR (50 MHz, $CDCl_3$) δ = 137.5 (s, 1C, Ar), 136.1 (d, 1C, Ar), 130.7 (s, 1C, Ar),130.4-127.9 (d, 10C, Ar and *C*=N), 112.6 (s, acetal), 105.6 (d, C-1), 85.4 (d, C-2), 80.1 (d, C-4), 79.4 (d, C-3), 74.7 (d, C-5), 69.3 (t, Bn), 32.0-29.5 (t, 9C, C-1'- C-9'), 26.3 (q, Me), 26.1-22.8 (t, 3C, C-10'- C-11'and q, Me), 14.2 (q, C-12') ppm. MS (ESI): m/z (%) = 574.63 (7) [M+Na]$^+$, 1125.32 (100) [2M+Na]$^+$. IR ($CDCl_3$): ν = 953, 1022, 1146, 1209, 1454, 1580, 2247, 2855, 3032.10, 3065 cm^{-1}. $C_{34}H_{49}NO_5$ (551.36): calcd. C, 74.01; H, 8.95; N, 2.54; found C, 74.39; H, 9.30; N, 2.20.

Synthesis of benzyl-2,3-*O*-(1-methylethylidene)-β-L-gulofuranoside-5-(tridecyl) -5-(phenylmethanimine oxide) (145e): Application of this procedure to 42 mg (0.07 mmol) of **144e** with 70 mg (0.11 mmol) of IBX furnished after purification by column chromatography 39 mg (0.07 mmol, 93%) of **145e** as a straw yellow oil.

145e: straw yellow oil. $[\alpha]_D^{25}$ = + 39 (c =0.80, $CHCl_3$). ^{1}H-NMR (400 MHz, $CDCl_3$) δ = 8.34-8.32 (m, 2H, HC=N and Ar), 7.46-7.39 (m, 4H, Ar), 7.37-7.23 (m, 5H, Ar), 5.01 (s, 1H, 1-H), 4.76 (dd, J= 5.8, 3.4 Hz, 1H, 3-H), 4.66 (d, J=6.0 Hz,1H, 2-H), 4.58 (d, J=11.2 Hz, 1H, H_a-Bn), 4.59 (d, J=8.0 Hz, 1H, 4-H), 4.33 (d, J=12.0 Hz, 1H, H_b-Bn), 4.09-4.03 (m, 1H, 5-H), 2.17-2.11 (m, 1H, 1'H_a), 1.69-1.62 (m, 1H, 1'H_b),1.50

(s, 3H, Me), 1.39-1.23 (m, 22H, 2'H-12'H), 1.33 (s, 3H, Me), 0.86 (t, J = 6.8 Hz, 3H, 13'$H_{a\text{-}b\text{-}c}$) ppm. ^{13}C-NMR (100 MHz, $CDCl_3$) δ = 137.2 (s, 1C, Ar), 134.8 (d, 1C, Ar), 130.9 (s, 1C, Ar),130.1-127.9 (d, 10C, Ar and *C*=N), 112.6 (s, acetal), 104.5 (d, C-1), 85.4 (d, C-2), 79.8 (d, C-3), 79.2 (d, C-4), 76.7 (d, C-5), 68.8 (t, Bn), 32.1-22.8 (t, 14C, C-1'- C-12', q, Me and q, Me), 14.3 (q, C-13') ppm. MS (ESI): m/z (%) = 588.30 (19) $[M+Na]^+$, 1152.82 (100) $[2M+Na]^+$. IR ($CDCl_3$): ν = 957, 1016, 1080, 1209, 1458, 1581, 2239, 2855, 2928, 303, 3067, cm^{-1}. $C_{35}H_{51}NO_5$ (565.38): calcd. C, 74.30; H, 9.09; N, 2.48; found C, 74.30; H, 9.15; N, 2.47.

Synthesis of benzyl-2,3-*O*-(1-methylethylidene)-α-D-mannofuranoside-5-(tridecyl)-5-(phenylmethanimine oxide) (149e): Application of this procedure to 41 mg (0.07 mmol) of **148e** with 68 mg (0.11 mmol) of IBX furnished after purification by column chromatography 39 mg (0.07 mmol, 95%) of **149e** as a straw yellow oil.

149e: straw yellow oil. $[\alpha]_D^{25}$ = + 49 (c =1.20, $CHCl_3$). ^{1}H-NMR (400 MHz, $CDCl_3$) δ = 8.29-8.27 (m, 2H, HC=N and Ar), 7.47-7.43 (m, 4H, Ar), 7.38-7.26 (m, 5H, Ar), 5.08 (s, 1H, 1-H), 4.71 (dd, J=5.2, 3.2 Hz, 1H, 3-H), 4.66 (d, J=11.6 Hz, 1H, H_a-Bn), 4.61 (d, J= 6.0 Hz,1H, 2-H), 4.51 (d, J=12.0 Hz, 1H, H_b-Bn),4.49 (dd, J=9.3, 3.8 Hz, 1H, 4-H), 4.20-4.15 (m, 1H, 5-H), 2.16-2.11 (m, 1H, 1'H_a), 1.85-1.83 (m, 1H, 1'H_b), 1.49 (s, 3H, Me), 1.34-1.24 (m, 25H, 2'H-12'H and Me), 0.88 (t, J= 6.6 Hz, 3H, 13'$H_{a\text{-}b\text{-}c}$) ppm.^{13}C-NMR (100 MHz, $CDCl_3$) δ = 137.5 (s, 1C, Ar), 136.2 (d, 1C, Ar), 130.6 (s, 1C, Ar),130.5-128.0 (d, 10C, Ar and *C*=N), 112.6 (s, acetal), 105.6 (d, C-1), 85.3 (d, C-2), 80.1 (d, C-4), 79.4 (d, C-3), 74.7 (d, C-5), 69.2 (t, Bn), 32.1-22.8 (t, 14C, C-1'- C-12',q, Me and q, Me), 14.3 (q, C-13') ppm.MS (ESI): m/z (%) = 588.34 (32) $[M+Na]^+$, 1152.67 (100) $[2M+Na]^+$. IR ($CDCl_3$): ν = 973, 1022, 1082, 1209, 1456, 1582, 2239, 2853, 2930, 3030, 3067 cm^{-1}. $C_{35}H_{51}NO_5$ (565.38): calcd. C, 74.30; H, 9.09; N, 2.48; found C, 74.49; H, 8.98; N, 2.35.

Synthesis of 3-hydroxy-4,5-*O*-(1-methylethylidene)-2-substituted piperidine 146a-e and 150a-e

To a mixture of nitrone **145** (or **149**) and hydroxylamine **144** (or **148**) in dry MeOH (0.015 M), acid acetic (2 equivalents) and Pd/C were added under nitrogen atmosphere. The mixture was stirred at room temperature under hydrogen atmosphere (balloon) for 2 days, until a control by ^{1}H-NMR spectroscopy attested the presence of acetate salt of 3-hydroxy-4,5-*O*-(1-methylethylidene)-2-substituted piperidine **146** (or **150**). The mixture was filtered through Celite® and the solvent was removed under reduced pressure. The corresponding free amine was obtained by dissolving the residue in MeOH, then the strongly basic resin Ambersep 900-OH was added, and the mixture was stirred for 40 minutes. The resin was removed by filtration and the crude product was purified, if necessary, on silica gel by flash column chromatography (CH_2Cl_2/MeOH/ NH_4OH (6%) 15:1:0.1) to afford 3-hydroxy-4,5-*O*-(1-methylethylidene)-2-substituted piperidines **146** (or **150**) (R_f = 0.57).

Synthesis of (2*S*,3*R*,4*S*,5*R*)-3-hydroxy-4,5-*O*-(1-methylethylidene)-2-octylpiperidine (146a): Application of the general procedure to 200 mg (0.40 mmol) of **144a** with 100 mg of Pd/C and 45 µL of acid acetic furnished, after Ambersep 900-OH and purification by column chromatography, 96 mg (0.34 mmol, 84%) of **146a** as a white solid.

146a: white solid m.p. 117-119 °C. $[\alpha]_D^{23}$ = + 28 (c =2.0, $CHCl_3$). ^{1}H-NMR (400 MHz, CD_3OD) δ = 4.19 (q, J = 5.6 Hz, 1H, 5-H), 4.14 (dd, J = 5.4, 3.4 Hz, 1H, 4-H), 3.80 (t, J = 2.8 Hz, 1H, 3-H), 3.05 (dd, *J* = 13.4, 5.5 Hz, 1H, 6-H_a), 2.72 (td, J=7.0, 2.3 Hz, 1H, 2-H), 2.66 (dd, J = 13.6, 7.6 Hz, 1H, 6-H_b), 1.51 (quint, J=7.1 Hz, 1H, 1'H_a), 1.47 (s, 3H, Me), 1.43-1.31 (m, 16H, 1'H_b, Me and 2'H-7'H), 0.91 (t, J = 6.8 Hz, 3H, 8'H_{a-b-c}) ppm. ^{13}C-NMR (50 MHz, CD_3OD) = 110.0 (s, acetal), 78.0 (d, C-4), 72.3 (d, C-5), 68.6 (d, C-3), 55.5 (d, C-2), 47.7 (t, C-6), 33.0-23.7 (t, 9C, C-1'- C-7', q, Me, q, Me), 14.4 (q, C-8') ppm. MS (ESI): m/z (%) = 286.31 (100) $[M+H]^+$. IR (CD_3OD): ν = 1153, 1171, 1219, 1246, 1287, 1379, 1462, 2247, 2301, 2641, 2859, 2931, 3341 cm^{-1}. $C_{16}H_{31}NO_3$ (285.23): calcd. C, 67.33; H, 10.95; N, 4.91; found C, 67.14; H, 10.86; N, 4.60.

Synthesis of (2*R*,3*R*,4*S*,5*R*)-3-hydroxy-4,5-*O*-(1-methylethylidene)-2-octylpiperidine (150a): Application of the general procedure to 50 mg (0.10 mmol) of **148a** with 25 mg of Pd/C and 11 µL of acid acetic furnished, after Ambersep 900-OH and purification by column chromatography, 25 mg (0.09 mmol, 86%) of **150a** as a white solid.

150a: white solid m.p. 39-41 °C. $[\alpha]_D^{25}$ = – 57 (c =0.75, $CHCl_3$). ^{1}H-NMR (400 MHz, CD_3OD) δ = 4.21-4.19 (m, 1H, 5-H), 3.84 (dd, J=7.3, 5.4 Hz, 1H, 4-H), 3.28-3.23 (m, 2H, 6-H_a and 3-H), 2.91 (dd, J=14.8, 3.0 Hz, 1H, 6-H_b), 2.25-2.19 (m, 1H, 2-H), 1.84-1.78 (m, 1H, 1'H_a), 1.50 (s, 3H, Me), 1.34 (s, 3H, Me), 1.33-1.30 (m, 13H, 1'-H_b and 2'H-7'H), 0.90 (t, J = 7.0 Hz, 3H, 8'$H_{a,b,c}$) ppm. ^{13}C-NMR (50 MHz, CD3OD) = 110.1 (s, acetal), 81.8 (d, C-4), 75.8 (d, C-3), 75.3 (d, C-5), 60.2 (d, C-2), 46.8 (t, C-6), 33.0-30.4 (t, 6C, C-1'- C-6'), 28.5 (q, Me), 26.6 (q, Me), 23.7 (t, C-7'), 14.4 (q, C-8') ppm. 1D-NOESY: Irradiation of 2-H gave a NOE at 4-H and 6-H_b, and irradiation of 4-H gave a NOE at 2-H and 6-H_b. MS (ESI): m/z (%) = 286.31 (100) $[M+H]^+$. IR (CD_3OD): ν = 1161, 1221, 1244, 1381, 2295, 2423, 2642, 2859, 2930, 3335 cm^{-1}. $C_{16}H_{31}NO_3$ (285.23): calcd. C, 67.33; H, 10.95; N, 4.91; found C, 67.53; H, 10.85; N, 4.75.

Synthesis of (2*S*,3*R*,4*S*,5*R*)-3-hydroxy-4,5-O-(1-methylethylidene)-2-nonylpiperidine (146b): Application of the general procedure to 202 mg (0.39 mmol) of **144b** with 101 mg of Pd/C and 45 µL of acid acetic furnished, after Ambersep 900-OH and purification by column chromatography, 91 mg (0.31 mmol, 78%) of **146b** as a white solid.

146b: white solid m.p. 107-109 °C. $[\alpha]_D^{26}$= + 50 (c =1.02, $CHCl_3$). ^{1}H-NMR (400 MHz, CD_3OD) δ = 4.19 (q, J = 5.6 Hz, 1H, 5-H), 4.14 (dd, J = 5.4, 3.4 Hz, 1H, 4-H), 3.80 (t, J = 2.8 Hz, 1H, 3-H), 3.05 (dd, J = 13.3, 5.8 Hz, 1H, 6-H_a), 2.72 (td, J=7.0, 2.1 Hz, 1H, 2-H), 2.66 (dd, J = 13.5, 7.5 Hz, 1H, 6-H_b), 1.54-1.50 (m, 1H, 1'H_a), 1.47 (s, 3H, Me), 1.43-1.30 (m, 18H, 1'H_b, Me and 2'H-8'H), 0.90 (t, J = 6.0 Hz, 3H, 9'H_{a-b-c}) ppm. ^{13}C-NMR (100 MHz, CD_3OD) = 109.9 (s, acetal), 77.9 (d, C-4), 72.2 (d, C-5), 68.4 (d, C-3), 55.4 (d, C-2), 47.3 (t, C-6), 33.1-23.2 (t, 10C, C-1'- C-8', q, Me, q, Me), 14.5 (q, C-9') ppm. MS (ESI): m/z (%) = 300.18 (100) $[M+H]^+$. IR (CD_3OD): ν = 1155, 1221, 1244, 1379, 1460, 2247, 2634, 2859, 2929, 3343 cm^{-1}. $C_{17}H_{33}NO_3$ (299.45): calcd. C, 68.19; H, 11.11; N, 4.68; found C, 68.35; H, 11.03; N,4.40.

Synthesis of (2*R*,3*R*,4*S*,5*R*)-3-hydroxy-4,5-O-(1-methylethylidene)-2-nonylpiperidine (150b): Application of the general procedure to 275 mg (0.54 mmol) of **148b** with 138 mg of Pd/C and 68 µL of acid acetic furnished, after Ambersep 900-OH and purification by column chromatography, 125 mg (0.42

mmol, 78%) of **150b** as a colorless oil.

150b: colorless oil. $[\alpha]_D^{26}$ = – 23 (c =2.60, $CHCl_3$). ^{1}H-NMR (400 MHz, CD_3OD) δ = 4.21-4.19 (m, 1H, 5-H), 3.84 (dd, J=7.2, 5.5 Hz, 1H, 4-H), 3.31-3.23 (m, 2H, 6-H_a and 3-H), 2.92 (dd, J=14.8, 3.0 Hz, 1H, 6-H_b), 2.26-2.19 (m, 1H, 2-H), 1.83-1.78 (m, 1H, 1'H_a), 1.50 (s, 3H, Me), 1.34-1.30 (m, 18H, 1'-H_b, 2'H-8'H and Me), 0.90 (t, J = 6.8 Hz, 3H, 9'$H_{a,b,c}$) ppm. ^{13}C-NMR (100 MHz, CD_3OD) = 110.1 (s, acetal), 81.8 (d, C-4), 75.8 (d, C-3), 75.3 (d, C-5), 60.2 (d, C-2), 48.6 (t, C-6), 31.1-23.7 (t, 10C, C-1'-C-8, q, Me and q, Me), 14.4 (q, C-9') ppm. 1D-NOESY: Irradiation of 2-H gave a NOE at 4-H and 6-H_b, and irradiation of 4-H gave a NOE at 2-H and 6-H_b. MS (ESI): m/z (%) = 300.32 (100) $[M+H]^+$. IR (CD_3OD): ν = 1167, 1219, 1246, 1379, 2639, 2859, 2930, 3346 cm^{-1}. $C_{17}H_{33}NO_3$ (299.45): calcd. C, 68.19; H, 11.11; N, 4.68; found C, 68.54; H, 10.93; N,4.32.

Synthesis of (2*S*,3*R*,4*S*,5*R*)-3-hydroxy-4,5-*O*-(1-methylethylidene)-2-undecylpiperidine (146c): Application of the general procedure to 134 mg (0.25 mmol) of **144c** with 67 mg of Pd/C and 29 µL of acid acetic furnished, after Ambersep 900-OH and purification by column chromatography, 66 mg (0.20 mmol, 80%) of **146c** as a white solid.

146c: white solid m.p. 102-103 °C. $[\alpha]_D^{23}$ **=** + 14 (c =0.45, $CHCl_3$). ^{1}H-NMR (400 MHz, CD_3OD) δ = 4.19 (q, J = 5.3 Hz, 1H, 5-H), 4.14 (dd, J = 5.0, 3.4 Hz, 1H, 4-H), 3.80 (t, J = 2.6 Hz, 1H, 3-H), 3.04 (dd, *J* = 13.4, 5.4 Hz, 1H, 6-H_a), 2.72 (td, J=8.2 , 2.3 Hz, 1H, 2-H), 2.67 (dd, J = 13.4, 7.4 Hz, 1H, 6-H_b), 1.52 (quint, J=7.0 Hz, 1H, 1'H_a), 1.47 (s, 3H, Me), 1.33 (s, 3H, Me), 1.44-1.30 (m, 19H, 1'H_b and 2'H-10'H), 0.90 (t, J = 7.0 Hz, 3H, 11'$H_{a\text{-}b\text{-}c}$) ppm. ^{13}C-NMR (50 MHz, CD_3OD) = 109.9 (s, acetal), 78.8 (d, C-4), 72.2 (d, C-5), 68.5 (d, C-3), 55.5 (d, C-2), 47.3 (t, C-6), 33.1-30.5 (t, 8C, C-1'- C-8'), 28.5 (q, Me), 27.2 (t, C-9'), 26.3 (q, Me), 23.7 (t, C-10'), 14.4 (q, C-11') ppm. MS (ESI): m/z (%) =328.44 (100) $[M+H]^+$. IR (CD_3OD): ν = 1159, 1219, 1244, 1379, 1464, 2262, 2299, 2641, 2857, 2930, 3345 cm^{-1}. $C_{19}H_{37}NO_3$ (327.28): calcd. C, 69.68; H, 11.39; N, 4.28; found C, 69.55; H, 11.05; N, 3.96.

Synthesis of (2*R*,3*R*,4*S*,5*R*)-3-hydroxy-4,5-*O*-(1-methylethylidene)-2-undecylpiperidine (150c): Application of the general procedure to 50 mg (0.10 mmol) of **148c** with 25 mg of Pd/C and 20 µL of acid acetic furnished, after treatment with Ambersep 900-OH and purification by column chromatography, 25 mg (0.08 mmol, 79%) of **150c** as a white solid.

150c: white solid m.p. 50-52 °C. $[\alpha]_D^{23}$ = – 11 (c =0.22, $CHCl_3$). ^{1}H-NMR (400 MHz, CD_3OD) δ = 4.20-4.19 (m, 1H, 5-H), 3.84 (dd, J=7.2, 5.5 Hz, 1H, 4-H), 3.30-3.23 (m, 2H, 6-H_a and 3-H), 2.90 (dd, J=14.8, 3.8 Hz, 1H, 6-H_b), 2.24-2.19 (m, 1H, 2-H), 1.81-1.79 (m, 1H, 1'H_a), 1.50 (s, 3H, Me), 1.34 (s, 3H, Me), 1.34-1.29 (m, 19H, 1'-H_b and 2'H-10'H), 0.90 (t, J = 6.8 Hz, 3H, 11'H) ppm. ^{13}C-NMR (100 MHz, CD_3OD) = 110.1 (s, acetal), 81.8 (d, C-4), 75.8 (d, C-3), 75.3 (d, C-5), 60.2 (d, C-2), 48.6 (t, C-6), 33.1-30.5 (t, 9C, C-1'- C-9'), 28.5 (q, Me), 26.6 (q, Me), 23.7 (t, C-10'), 14.4 (q, C-11') ppm. 1D-NOESY: Irradiation of 2-H gave a NOE at 4-H and 6-H_b, and irradiation of 4-H gave a NOE at 2-H and 6-H_b. MS (ESI): m/z (%) =328.44 (100) $[M+H]^+$. IR (CD_3OD): ν = 1116, 1221, 1381, 1462, 2312, 2642, 2856, 2928, 3354 cm^{-1}. $C_{19}H_{37}NO_3$ (327.28): calcd. C, 69.68; H, 11.39; N, 4.28; found C, 69.42; H, 11.70; N, 3.95.

Synthesis of (2*S*,3*R*,4*S*,5*R*)-3-hydroxy-4,5-*O*-(1-methylethylidene)-2-dodecylpiperidine (146d): Application of the general procedure to 230 mg (0.42 mmol) of **144d** with 115 mg of Pd/C and 48 µL of acid acetic furnished, after treatment with Ambersep 900-OH, 136 mg (0.04 mmol, 93%) of **146d** as a white solid.

146d: white solid m.p. 101-103 °C. $[\alpha]_D^{23}$ = + 43 (c =0.96, $CHCl_3$). ^{1}H-NMR (400 MHz, CD_3OD) δ = 4.19 (q, J = 5.8 Hz, 1H, 5-H), 4.14 (dd, J = 5.2, 3.2 Hz, 1H, 4-H), 3.80 (t, J = 2.8 Hz, 1H, 3-H), 3.04 (dd, *J* = 13.2, 5.8 Hz, 1H, 6-H_a), 2.72 (td, J=7.0, 2.1 Hz, 1H, 2-H), 2.67 (dd, J = 13.2, 7.2 Hz, 1H, 6-H_b), 1.52 (quint, J=7.2 Hz, 1H, 1'H_a), 1.47 (s, 3H, Me), 1.33 (s, 3H, Me), 1.44-1.29 (m, 21H, 1'H_b and 2'H-11'H), 0.90 (t, J= 6.8 Hz, 3H, 12'$H_{a\text{-}b\text{-}c}$) ppm. ^{13}C-NMR (50 MHz, CD_3OD) = 110.1 (s, acetal), 77.9 (d, C-4), 77.2 (d, C-5), 68.5 (d, C-3), 55.4 (d, C-2), 47.7 (t, C-6), 33.0-30.4 (t, 9C, C-1'- C-9'), 28.4 (q, Me), 27.2 (t, C-10'), 26.2 (q, Me), 23.7 (t, C-11'), 14.4 (q, C-12') ppm. MS (ESI): m/z (%) =342.27 (100) $[M+H]^+$. IR (CD_3OD): ν = 1167, 1219, 1381, 1460, 2228, 2266, 2438, 2642, 2857, 2928, 3345, cm^{-1}. $C_{20}H_{39}NO_3$ (341.54): calcd. C, 70.34; H, 11.51; N, 4.10; found C, 70.22; H, 11.43; N, 4.06.

Synthesis of (2*R*,3*R*,4*S*,5*R*)-3-hydroxy-4,5-*O*-(1-methylethylidene)-2-

dodecylpiperidine (150d): Application of the general procedure to 42 mg (0.08 mmol) of **148d** with 21 mg of Pd/C and 9 µL of acid acetic furnished, after Ambersep 900-OH, 23 mg (0.07mmol, 88%) of **150d** as a white solid.

150d: white solid m.p. 57-58 °C. $[\alpha]_D^{22}$ = – 12 (c =1.07, $CHCl_3$). ^{1}H-NMR (400 MHz, CD_3OD) δ = 4.20-4.18 (m, 1H, 5-H), 3.83 (dd, J=7.2, 5.4 Hz, 1H, 4-H), 3.28-3.22 (m, 2H, 6-H_a and 3-H), 2.90 (dd, J=14.8, 3.4 Hz, 1H, 6-H_b), 2.26-2.20 (m, 1H, 2-H), 1.83-1.78 (m, 1H, 1'H_a), 1.50 (s, 3H, Me), 1.34 (s, 3H, Me), 1.34-1.29 (m, 21H, 1'H_b and 2'H-11'H), 0.90 (t, J= 7.0 Hz, 3H, 12'$H_{a-b-c)}$ ppm. ^{13}C-NMR (50 MHz, CD_3OD) = 110.1 (s, acetal), 81.8 (d, C-4), 75.8 (d, C-3), 75.3 (d, C-5), 60.2 (d, C-2), 46.8 (t, C-6), 32.7-30.4 (t, 10C, C-1'- C-10'), 28.5 (q, Me), 26.6 (q, Me), 23.7 (t, C-11'), 14.4 (q, C-12') ppm. 1D-NOESY: Irradiation of 2-H gave a NOE at 4-H and 6-H_b, and irradiation of 4-H gave a NOE at 2-H and 6-H_b. MS (ESI): m/z (%) =342.19 (100) $[M+H]^+$. IR (CD_3OD): ν = 1221, 1381, 1466, 2263, 2442, 2641, 2857, 2928, 3354 cm^{-1}. $C_{20}H_{39}NO_3$ (341.54): calcd. C, 70.34; H, 11.51; N, 4.10; found C, 70.05; H, 11.73; N, 3.86.

Synthesis of (2*S*,3*R*,4*S*,5*R*)-3-hydroxy-4,5-*O*-(1-methylethylidene)-2-tridecylpiperidine (146e): Application of the general procedure to 107 mg (0.19 mmol) of **144e** with 54 mg of Pd/C and 22 µL of acid acetic furnished, after Ambersep 900-OH, 60 mg (0.17 mmol, 89%) of **146e** as a white solid.

146e: white solid m.p. 95-97 °C. $[\alpha]_D^{25}$ **=** + 6.5 (c = 0.40, $CHCl_3$). ^{1}H-NMR (400 MHz, CD_3OD) δ = 4.19 (q, J=6.3 Hz,1H, 5-H), 4.14 (dd, J = 5.0, 3.2 Hz, 1H, 4-H), 3.80 (t, J = 2.6 Hz, 1H, 3-H), 3.04 (dd, *J* = 13.2, 5.6 Hz, 1H, 6-H_a), 2.72 (td, J=8.0, 2.2 Hz, 1H, 2-H), 2.67 (dd, J = 13.2, 7.2 Hz, 1H, 6-H_b),1.52 (quint, J=8.4 Hz, 2H, 1'H_a), 1.47 (s, 3H, Me), 1.33 (s, 3H, Me), 1.36-1.28 (m, 23H, 1'H_b and 2'H-12'H), 0.90 (t, J = 7.0 Hz, 3H, 13'H_{a-b-c}) ppm. ^{13}C-NMR (100 MHz, CD_3OD) = 109.9 (s, acetal), 78.0 (d, C-4), 72.3 (d, C-5), 68.5 (d, C-3), 55.5 (d, C-2), 48.4 (t, C-6), 33.1-30.5 (t, 10C, C-1'-C-10'), 28.5 (q, Me), 27.3 (t, C-11'), 26.3 (q, Me), 23.7 (t, C-12'), 14.4 (q, C-13') ppm. MS (ESI): m/z (%) =356.17 (100) $[M+H]^+$. IR (CD_3OD): ν = 1146, 1219, 1379, 1462, 2247, 2288, 2641, 2857, 2930, 3354 cm^{-1}. $C_{21}H_{41}NO_3$ (355.31): calcd. C, 70.94; H, 11.62; N, 3.94; found C, 71.23; H, 10.40; N, 3.57.

Synthesis of (2*R*,3*R*,4*S*,5*R*)-3-hydroxy-4,5-*O*-(1-methylethylidene)-2-

tridecylpiperidine (150e): Application of the general procedure to 192 mg (0.34 mmol) of **148e** with 96 mg of Pd/C and 60 µL of acid acetic furnished, after Ambersep 900-OH, 108 mg (0.30 mmol, 89%) of **150e** as a white solid.

150e: white solid m.p. 54-56 °C. $[\alpha]_D^{25}$ = – 12 (c =0.71, $CHCl_3$). ^{1}H-NMR (400 MHz, CD_3OD) δ = 4.20-4.19 (m, 1H, 5-H), 3.85 (dd, J=7.0, 5.3 Hz, 1H, 4-H), 3.27-3.22 (m, 2H, 6-H_a and 3-H), 2.90 (dd, J=15.0, 3.2 Hz, 1H, 6-H_b), 2.27-2.20 (m, 1H, 2-H), 1.84-1.79 (m, 1H, 1'H_a), 1.50 (s, 3H, Me), 1.34 (s, 3H, Me), 1.33-1.28 (m, 23H, 1'H_b and 2'H-12'H), 0.90 (t, J = 6.8 Hz, 3H, 13'H_{a-b-c}) ppm. ^{13}C-NMR (100 MHz, CD_3OD) = 110.0 (s, acetal), 81.8 (d, C-4), 75.8 (d, C-3), 75.3 (d, C-5), 60.1 (d, C-2), 48.6 (t, C-6), 33.1-23.7 (t, 14C, C-1'- C-12', q, Me and q, Me), 14.5 (q, C-13') ppm. 1D-NOESY: Irradiation of 2-H gave a NOE at 4-H and 6-H_b, and irradiation of 4-H gave a NOE at 2-H and 6-H_b. MS (ESI): m/z (%) = 356.07 (100) $[M+H]^+$. IR (CD_3OD): ν = 1146, 1219, 1379, 2226, 2288, 2641, 2857, 2930, 3354 cm^{-1}. $C_{21}H_{41}NO_3$ (355.31): calcd. C, 70.94; H, 11.62; N, 3.94; found C, 71.30; H, 11.30; N, 3.66.

Compound **150e** was crystallized from MeOH to give crystals for X-ray analysis.

Synthesis of (3*R*,4*S*,5*R*)-5-hydroxy-3,4-*O*-(1-methylethylidene)-piperidine (62):

To a solution of nitrone **14** (915 mg, 2.39 mmol) in dry MeOH (150 mL), acid acetic (2 equivalents) and Pd/C (458 mg) were added under nitrogen atmosphere. The mixture was stirred at room temperature under hydrogen atmosphere (balloon) for 2 days, until a control by ^{1}H-NMR spectroscopy attested the presence of acetate salt of (3*R*,4*S*,5*R*)-5-hydroxy-3,4-*O*-(1-methylethylidene)-piperidine (**20**). The mixture was filtered through Celite® and the solvent was removed under reduced pressure. The corresponding free amine was obtained by dissolving the residue in MeOH, then the strongly basic resin Ambersep 900-OH was added, and the mixture was stirred for 40 minutes. The resin was removed by filtration to afford (3*R*,4*S*,5*R*)-5-hydroxy-3,4-*O*-(1-methylethylidene)-piperidine (414 mg, 2.39 mmol) in 100% yield.

62: ^{1}H-NMR (400 MHz, CD_3OD) δ ppm: 4.26-4.16 (m, 1H,), 3.91 (t, J= 6.1 Hz, 1H), 3.75-3.62 (m, 1H), 3.13 (dd, J= 14.5, 2.5 Hz, 1H), 3.01-2.94 (m, 1H), 2.94-2.86 (m, 1H), 2.38 (dd, J= 13.1, 9.2 Hz, 1H), 1.50 (s, 3H, Me), 1.35 (s, 3H, Me).

Synthesis of 2-substituted trihydroxypiperidines 147a-e and 151a-e

A solution of 3-hydroxy-4,5-*O*-(1-methylethylidene)-2-substituted piperidine **146** (or **150**) in MeOH (0.01 M) was left stirring with 12 M HCl (600 µL) at room temperature for 16 h. The crude mixture was concentrated to yield the hydrochloride salt of 2-substituted trihydroxy piperidine **147** (or **151**). The corresponding free amine was obtained by dissolving the residue in MeOH, then the strongly basic resin Ambersep 900-OH was added, and the mixture was stirred for 40 minutes. The resin was removed by filtration and the crude product, if necessary, was purified on silica gel by flash column chromatography (CH_2Cl_2/MeOH/ NH_4OH (6%) 2:1:0.05) to afford 2-substituted trihydroxypiperidine as free base **147** (or **151**) (R_f = 0.50).

Synthesis of (2*S*,3*R*,4*R*,5*R*)-2-octylpiperidine-3,4,5-triol (147a): Following the general procedure 12 M HCl (918 µL) was added to a solution of **146a** (74 mg, 0.26 mmol) and furnished, after treatment with Ambersep 900-OH and purification by column chromatography, 54 mg (0.22 mmol, 88%) of **147a** as a white solid.

147a: white solid m.p. 121-123 °C. $[\alpha]_D^{23}$ = + 22 (c =0.61, CH_3OH). ^{1}H-NMR (400 MHz, CD_3OD) δ = 3.86 (t, J=3.5 Hz, 1H, 4-H), 3.82 (td, J=8.1, 3.1 Hz, 1H, 5-H), 3.66 (dd, J=4.1, 1.7 Hz, 1H, 3-H), 2.80-2.77 (m, 1H, 2-H), 2.75 (d, J=8.2 Hz, 2H, 6-H_{a-b}), 1.49-1.30 (m, 14H, 1'H-7'H), 0.90 (t, J= 6.0 Hz, 3H, 8'H_{a-b-c}) ppm. ^{13}C-NMR (50 MHz, CD_3OD) = 72.6 (d, C-4), 71.7 (d, C-3), 67.2 (d, C-5), 54.1 (d, C-2), 47.0 (t, C-6), 33.0-23.6 (t, 7C, C-1' C-7'), 14.4 (q, C-8') ppm. MS (ESI): m/z (%) =246.37 (100) $[M+H]^+$. $C_{13}H_{27}NO_3$ (245.20): calcd. C, 63.64; H, 11.09; N, 5.71; found C, 63.96; H, 10.78; N, 5.91.

Synthesis of (2*R*,3*R*,4*R*,5*R*)-2-octylpiperidine-3,4,5-triol (151a): Following the general procedure 12 M HCl (318 µL) was added to a solution of **150a** (25 mg, 0.09 mmol) and furnished, after treatment with Ambersep 900-OH and purification purification by column chromatography, 20 mg (0.08 mmol, 84%) of **151a** as a white solid.

151a: white solid m.p. 68-70 °C. $[\alpha]_D^{24}$ = − 4.3 (c =0.63, CH_3OH). ^{1}H-NMR (400 MHz, CD_3OD) δ = 3.86-3.84 (m, 1H, 5-H), 3.35-3.31 (m, 2H, 4-H and 3-H), 2.94 (dd, J=14.0, 2.8 Hz, 1H, 6-H_a), 2.67 (d, J=15.6 Hz, 1H, 6-H_b), 2.30-2.22 (m, 1H, 2-H), 1.88-1.79 (m, 1H, 1'H_a), 1.56-1.52 (m, 1H, 2'H_a), 1.41-1.30 (m, 12H, 1'H_b, 2'H_b, 3'H-7'H), 0.90 (t, J = 6.9 Hz, 3H, 8'H_{a-b-c}) ppm. ^{13}C-NMR (50 MHz, CD_3OD) = 76.7 (d, C-4), 73.9 (d, C-3), 70.7 (d, C-5), 61.7 (d, C-2), 50.8 (t, C-6), 33.0-23.6 (t, 7C, C-1'and C-7'), 14.4 (q, C-8') ppm. MS (ESI): m/z (%) =246.35 (100) $[M+H]^+$. $C_{13}H_{27}NO_3$ (245.20): calcd. C, 63.64; H, 11.09; N, 5.71; found C, 63.97; H, 10.80; N, 5.34.

Synthesis of (2*S*,3*R*,4*R*,5*R*)-2-nonylpiperidine-3,4,5-triol (147b): Following the general procedure 12 M HCl (600 µL) was added to a solution of **146b (**68 mg, 0.23 mmol) and furnished, after treatment with Ambersep 900-OH, 58 mg (0.23 mmol, 100%) of **147b** as a white solid.

147b: white solid m.p. 135-136 °C. $[\alpha]_D^{26}$ = + 19 (c =0.38, CH_3OH). ^{1}H-NMR (400 MHz, CD_3OD) δ = 3.89 (t, J=3.4 Hz, 1H, 4-H), 3.84 (td, J= 8.1, 3.4 Hz, 1H, 5-H), 3.69 (d, J= 4.0 Hz, 1H, 3-H), 2.78-2.77 (m, 1H, 2-H), 2.75 (d, J= 7.9 Hz, 2H, 6-H_{a-b}), 1.48-1.30 (m, 16H, 1'H-8'H), 0.90 (t, J= 8.0 Hz, 3H, 9'H_{a-b-c}) ppm. ^{13}C-NMR (100 MHz, CD_3OD) = 72.6 (d, C-4), 71.7 (d, C-3), 67.2 (d, C-5), 54.1 (d, C-2), 47.0 (t, C-6), 33.1-23.7 (t, 8C, C-1' C-8'), 14.4 (q, C-9') ppm. MS (ESI): m/z (%) = 260.19 (100) $[M+H]^+$. $C_{14}H_{29}NO_3$ (259.38): calcd. C, 64.83; H, 11.27; N, 5.40; found C, 65.02; H, 11.10; N, 5.26.

Synthesis of (2*R*,3*R*,4*R*,5*R*)-2-nonylpiperidine-3,4,5-triol (151b): Following the general procedure 12 M HCl (600 µL) was added to a solution of **150b (**91 mg, 0.30 mmol) and furnished, after treatment with Ambersep 900-OH, 77 mg (0.30 mmol, 100%) of **151b** as a white solid.

151b: white solid m.p. 73-74 °C. $[\alpha]_D^{26}$ = – 22 (c =0.48, CH_3OH). ^{1}H-NMR (400 MHz, CD_3OD) δ = 3.84 (bs, 1H, 5-H), 3.31-3.19 (m, 2H, 4-H and 3-H), 2.90 (dd, J=14.0, 2.8 Hz, 1H, 6-H_a), 2.62 (d, J=14.0 Hz, 1H, 6-Hb), 2.22-2.17 (m, 1H, 2-H), 1.82-1.78 (m, 1H, 1'H_a), 1.49-1.47 (m, 1H, 2'H_a), 1.27-1.26 (m, 14H, 1'H_b, 2'H_b, 3'H-8'H), 0.86 (t, J = 6.9 Hz, 3H, 9'H_{a-b-c}) ppm. ^{13}C-NMR (100 MHz, CD_3OD) = 76.7 (d, C-4), 73.9 (d, C-3), 70.7 (d, C-5), 61.7 (d, C-2), 50.8 (t, C-6), 33.1-23.7 (t, 8C, C-1'and C-8'), 14.4 (q, C-9') ppm. MS (ESI): m/z (%) = 260.25 (100) $[M+H]^+$. $C_{14}H_{29}NO_3$ (259.38): C, 64.83; H, 11.27; N, 5.40; found C, 65.15; H, 11.00; N, 5.35.

Synthesis of (2*S*,3*R*,4*R*,5*R*)-2-undecylpiperidine-3,4,5-triol (147c): Following the general procedure 12 M HCl (635 µL) was added to a solution of **146c** (60 mg, 0.18 mmol) and furnished, after treatment with Ambersep 900-OH, 48 mg (0.17 mmol, 92%) of **147c** as a white solid.

147c: white solid, m.p. 130-132 °C. $[\alpha]_D^{26}$ = + 22 (c =0.21, CH_3OH). ^{1}H-NMR (400 MHz, CD_3OD) δ = 3.88-3.81 (m, 2H, 4-H and 5-H), 3.68 (d, J= 4.0, 1H, 3-H), 2.80-2.78 (m, 1H, 2-H), 2.75 (d, J=8.0 Hz, 2H, 6-$H_{a\text{-}b}$), 1.46-1.30 (m, 20H, 1'H-10'H), 0.91 (t, J = 6.2 Hz, 3H, 11'$H_{a\text{-}b\text{-}c}$) ppm. ^{13}C-NMR (50 MHz, CD_3OD) = 72.6 (d, C-4), 71.7 (d, C-3), 67.2 (d, C-5), 54.1 (d, C-2), 47.0 (t, C-6), 33.1-23.7 (t, 10C, C-1'- C-10'), 14.4 (q, C-11') ppm. MS (ESI): m/z (%) =288.21 (100) $[M+H]^+$. $C_{16}H_{33}NO_3$ (287.25): calcd. C, 66.86; H, 11.57; N, 4.87; found C, 66.54; H, 11.78; N, 4.86.

Synthesis of (2*R*,3*R*,4*R*,5*R*)-2-undecylpiperidine-3,4,5-triol (151c): Following the general procedure 12 M HCl (211 µL) was added to a solution of **150c** (20 mg, 0.06 mmol) and furnished, after Ambersep 900-OH, 15 mg (0.05 mmol, 90%) of **151c** as a white solid.

151c: white solid m.p. 70-72 °C. $[\alpha]_D^{25}$ = – 9.3 (c =0.15, CH_3OH). ^{1}H-NMR (400 MHz, CD_3OD) δ = 3.86-3.85 (m, 1H, 5-H), 3.36-3.29 (m, 2H, 4-H and 3-H), 2.95 (dd, J=14.2, 2.2 Hz, 1H, 6-H_a), 2.67 (d, J= 14.0 Hz, 1H, 6-H_b), 2.30-2.22 (m, 1H, 2-H), 1.87-1.83 (m, 1H, 1'H_a), 1.54-1.52 (m, 1H, 2'H_a), 1.32-1.30 (m, 18H, 1'H_b, 2'H_b, 3'H-10'H), 0.90 (t, J = 6.6 Hz, 3H, 11'$H_{a\text{-}b\text{-}c}$) ppm. ^{13}C-NMR (50 MHz, CD_3OD) = 76.6 (d, C-4), 73.7 (d, C-3), 70.7 (d, C-5), 61.7 (d, C-2), 50.8 (t, C-6), 33.1-23.7 (t, 10C, C-1'- C-10'), 14.44 (q, C-11') ppm. MS (ESI): m/z (%) =288.21 (100) $[M+H]^+$. $C_{16}H_{33}NO_3$ (287.25): calcd. C, 66.86; H, 11.57; N, 4.87; found C, 67.20; H, 11.52; N, 4.77.

Synthesis of (2*S*,3*R*,4*R*,5*R*)-2-dodecylpiperidine-3,4,5-triol (147d): Following the general procedure 12 M HCl (529 µL) was added to a solution of **146d** (46 mg, 0.13 mmol) and furnished, after Ambersep 900-OH, 35 mg (0.12 mmol, 78%) of **147d** as a white solid.

147d: white solid m.p. 141-143 °C. $[\alpha]_D^{21}$ = + 16 (c =1.00, CH_3OH). ^{1}H-NMR (400 MHz, CD_3OD) δ = 3.86 (t, J=3.4 Hz, 1H, 4-H), 3.82 (td, J= 8.2, 3 Hz, 1H, 5-H), 3.66 (dd, J = 4.0, 1.6 Hz, 1H, 3-H), 2.81-2.77 (m, 1H, 2-H), 2.75 (d, J=8.0 Hz, 2H, 6-$H_{a\text{-}b}$), 1.49-1.29 (m, 22H, 1'H-11'H), 0.90 (t, J = 6.8 Hz, 3H, 12'$H_{a\text{-}b\text{-}c}$) ppm. ^{13}C-NMR (50

MHz, CD_3OD) = 72.6 (d, C-4), 71.7 (d, C-3), 67.3 (d, C-5), 54.2 (d, C-2), 47.1 (t, C-6), 33.0-23.7 (t, 11C, C-1'- C-11'), 14.4 (q, C-12') ppm. MS (ESI): m/z (%) =302.33 (100) $[M+H]^+$. C17H35NO3 (301.47): calcd. C, 67.73; H, 11.70; N, 4.65; found C, 67.34; H, 11.57; N, 4.37.

Synthesis of (2*R*,3*R*,4*R*,5*R*)-2-dodecylpiperidine-3,4,5-triol (151d): Following the general procedure 12 M HCl (247 µL) was added to a solution of **150d** (23 mg, 0.07 mmol) and furnished, after treatment with Ambersep 900-OH and purification by column chromatography, 16 mg (0.05mmol, 76%) of **151d** as a white solid.

151d: white solid m.p. 79-81 °C. $[\alpha]_D^{23}$ = –12 (c =0.80, CH_3OH). ^{1}H-NMR (400 MHz, CD_3OD) δ = 3.86-3.85 (m, 1H, 5-H), 3.36-3.30 (m, 2H, 4-H and 3-H), 2.96 (dd, J=13.6, 2.8 Hz, 1H, 6-H_a), 2.69 (d, J=16.0 Hz, 1H, 6-H_b), 2.33-2.31 (m, 1H, 2-H), 1.88-1.83 (m, 1H, 1'H_a), 1.53-1.51 (m, 1H, 2'H_a), 1.32-1.29 (m, 20H, 1'H_b, 2'H_b, 3'H-11'H), 0.90 (t, J = 6.8 Hz, 3H, 12'$H_{a\text{-}b\text{-}c}$) ppm. ^{13}C-NMR (50 MHz, CD_3OD) = 76.7 (d, C-4), 74.0 (d, C-3), 70.8 (d, C-5), 61.7 (d, C-2), 50. 8 (t, C-6), 33.0-26.6 (t, 11C, C-1'- C-11'), 14.4 (q, C-12') ppm. MS (ESI): m/z (%) =302.33 (100) $[M+H]^+$. $C_{17}H_{35}NO_3$ (301.47): calcd. C, 67.73; H, 11.70; N, 4.65; found C, 67.35; H, 11.48; N, 4.60.

Synthesis of (2*S*,3*R*,4*R*,5*R*)-2-tridecylpiperidine-3,4,5-triol (147e): Following the general procedure 12 M HCl (600 µL) was added to a solution of **146e** (60 mg, 0.17 mmol) furnished, after Ambersep 900-OH, 49 mg (0.16 mmol, 90%) of **147e** as a white solid.

147e: white solid m.p. 129-131 °C. $[\alpha]_D^{26}$ = + 18 (c =0.24, CH_3OH). ^{1}H-NMR (400 MHz, CD3OD) δ = 3.86 (t, J=3.4 Hz, 1H, 4-H), 3.82 (td, J=8.4, 3.2 Hz, 1H, 5-H), 3.67-3.66 (m, 1H, 3-H), 2.79-2.77 (m, 1H, 2-H), 2.74 (d, J=8.4 Hz, 2H, 6-Ha-b), 1.47-1.29 (m, 1'H -12'H), 0.90 (t, J = 6.8 Hz, 3H, 13'$H_{a\text{-}b\text{-}c}$) ppm. ^{13}C-NMR (100 MHz, CD_3OD) = 72.6 (d, C-4), 71.7 (d, C-3), 67.3 (d, C-5), 54.1 (d, C-2), 47.0 (t, C-6), 33.1-23.7 (t, 12C, C-1'- C-12'), 14.4 (q, C-13') ppm. MS (ESI): m/z (%) = 316.23 (100) $[M+H]^+$. $C_{18}H_{37}NO_3$ (315.50): calcd. C, 68.53; H, 11.82; N, 4.44; found C, 68.80; H, 11.64; N, 4.34.

Synthesis of (2*R*,3*R*,4*R*,5*R*)-2-tridecylpiperidine-3,4,5-triol (151e): Following the general procedure 12 M HCl (1.13 mL) was added to a solution of **150e** (108 mg, 0.30 mmol) furnished, after Ambersep 900-OH, 86 mg (0.27 mmol, 91%) of **151e** as a white solid.

151e: white solid m.p. 80-82 °C. $[\alpha]_D^{26} = -11$ (c =0.22, CH_3OH). ^{1}H-NMR (400 MHz, CD_3OD) δ = 3.86-3.85 (m, 1H, 5-H), 3.38-3.35 (m, 2H, 4-H and 3-H), 2.97 (dd, J=13.6, 2.8 Hz, 1H, 6-H_a), 2.73 (d, J=12.0 Hz, 1H, 6-H_b), 2.37-2.33 (m, 1H, 2-H), 1.90-1.84 (m, 1H, 1'H_a), 1.54-1.51 (m, 1H, 2'H_a), 1.33-1.29 (m, 22 H, 1'Hb, 2'Hb, 3'H-12'H), 0.90 (t, J = 7.0 Hz, 3H, 13'H_{a-b-c}) ppm. ^{13}C-NMR (100 MHz, CD_3OD) = 76.4 (d, C-4), 73.5 (d, C-3), 70.3 (d, C-5), 61.7 (d, C-2), 49.6 (t, C-6), 31.1- 23.7 (t, 12C, C-1'- C-12'), 14.4 (q, C-13') ppm. MS (ESI): m/z (%) = 316.21 (100) $[M+H]^+$. $C_{18}H_{37}NO_3$ (315.50): calcd. C, 68.53; H, 11.82; N, 4.44; found C, 68.25; H, 12.09; N, 4.19.

Synthesis of (2*S*,3*R*,4*S*,5*R*)-3-hydroxy-4,5-*O*-(1-methylethylidene)-1-methyl-2-octylpiperidine (179a): To a mixture **144a** and **145a** (220 mg, 0.44 mmol as if it was only **144a**) in dry MeOH (27.8 mL), 1M HCl (880 µL), Pd/C (110 mg) was added under nitrogen atmosphere. The mixture was stirred at room temperature under hydrogen atmosphere (balloon) for 3 days, until a control by ^{1}H-NMR spectroscopy attested the presence of hydrochloride salt of **179a**. The mixture was filtered through Celite® and the solvent was removed under reduced pressure. The corresponding free amine was obtained by dissolving the residue in MeOH, then the strongly basic resin Ambersep 900-OH was added, and the mixture was stirred for 40 minutes. The resin was removed by filtration and the crude product was purified on silica gel by flash column chromatography (CH_2Cl_2/MeOH/ NH_4OH (6%) 15:1:0.1) to afford 27.7 mg (0.09 mmol) of **179a** (R_f = 0.47, 21%).

179a: white solid m.p. 112.8-115.3 °C. $[\alpha]_D^{20}$ = + 112 (c =0.60, $CHCl_3$). ^{1}H-NMR (400 MHz, CD_3OD) δ = 4.30 (q, J= 5.5 Hz, 1H, 5-H), 4.10 (t, J= 5.0 Hz, 1H, 4-H) , 3.87 (dd, J= 4.4, 3.2 Hz, 1H, 3-H), 2.93 (dd, J= 13.0, 5.0 Hz, 1H, 6-H_a), 2.50 (dd, J= 13.0, 6.2 Hz, 1H, 6-H_b), 2.43-2.39 (m, 1H, 2-H), 2.35 (s, 3H, *N*-Me), 1.51 (quint, J=7.1 Hz, 2H, 1'H_{a-b}), 1.48 (s, 3H, Me), 1.44-1.31 (m, 15H, Me and 2'H-7'H), 0.90 (t, J = 6.0 Hz, 3H, 8'H_{a-b-c}) ppm. ^{13}C-NMR (50 MHz, CD_3OD) = 109.9 (s, acetal), 77.8

(d, C-4), 73.4 (d, C-5), 69.3 (d, C-3), 63.5 (d, C-2), 55.1 (t, C-6), 43.6 (q, N-Me), 31.0-26.1 (t, 9C, C-1'- C-7', q, Me, q, Me), 14.4 (q, C-8') ppm. MS (ESI): m/z (%) = 300.46 (100) $[M+H]^+$. IR (CD_3OD): ν = 1150, 1219, 1246, 1381, 1422, 1464, 2297, 2455, 2858, 2930, 3339 cm^{-1}. $C_{17}H_{33}NO_3$ (299.25): calcd. C, 68.19; H, 11.11; N, 4.68; found C, 68.47; H, 10.85 N, 4.45.

Synthesis of (2*S*, 3*R*, 4*R*, 5*R*)-1-methyl-2-octylpiperidine-3,4,5-triol (180a): A solution of **179a** (27 mg, 0.09 mmol) in MeOH (6 mL) was left stirring with 12 M HCl (300 µL) at room temperature for 16 h. The crude mixture was concentrated to yield the hydrochloride salt of **180a**. The corresponding free amine was obtained by dissolving the residue in MeOH, then the strongly basic resin Ambersep 900-OH was added, and the mixture was stirred for 40 minutes. The resin was removed by filtration and the crude product was purified on silica gel by flash column chromatography (CH_2Cl_2/MeOH/ NH_4OH (6%) 2:1:0.05) to afford 6 mg (0.02 mmol) (yield 26%) of **180a** (R_f = 0.50).

180a: yellow oil. $[\alpha]_D^{23}$ = + 27 (c =0.20, CH_3OH). ^{1}H-NMR (400 MHz, CD_3OD) δ = 4.03-3.99 (m, 1H, 5-H), 3.82 (t, J= 3.5 Hz, 1H, 4-H) , 3.72 (dd, J= 4.1, 2.0 Hz, 1H, 3-H), 2.61 (dd, J= 11.0, 4.6 Hz, 1H, 6-H_a), 2.42 (t, J= 11.0 Hz, 1H, 6-H_b), 2.30-2.29 (m, 1H, 2-H), 2.27 (s, 3H, N-Me), 1.63-1.50 (m, 2H, 1'H_{a-b}), 1.48-1.27 (m, 12H, 2'H-7'H), 0.90 (t, J = 6.0 Hz, 3H, 8'H_{a-b-c}) ppm.^{13}C-NMR (50 MHz, CD_3OD) = 72.3 (d, C-4), 71.3 (d, C-5), 66.5 (d, C-3), 62.2 (d, C-2), 57.6 (t, C-6), 43.0 (q, N-Me), 33.0-23.7 (t, 7C, C-1'- C-7'), 14.5 (q, C-8') ppm. MS (ESI): m/z (%) = 282 (100) $[M+Na]^+$. $C_{14}H_{29}NO_3$ (259.39): calcd. C, 64.83; H, 11.27; N, 5.40; found C, 65.19; H, 11.30; N, 5.25.

Synthesis of (2*R*,3*R*,4*S*,5*R*)-3-hydroxy-4,5-*O*-(1-methylethylidene)-*N*-Boc-2-octylpiperidine (181): To a stirred solution of **150a** (0.371 g, 1.3 mmol) and $NaHCO_3$ (0.164 g, 1.95 mmol) in H_2O (5 mL), MeOH (5 mL), Boc_2O (0.419 g, 1.95 mmol) was added. The mixture was stirred at room temperature for 48 hours until a TLC control (CH_2Cl_2/MeOH/ NH_4OH (6%) 15:1:0.1) attested the disappearance of the starting material. The mixture was concentrated and extracted with AcOEt (3x20 mL). The combined organic layers were washed with brine, dried over Na_2SO_4 and the crude product was purified on silica gel by flash column chromatography (CH_2Cl_2/MeOH/ NH_4OH (6%) 20:1:0.1) to afford 426 mg (1.10 mmol, 85%, R_f = 0.36) of as a white solid.

181: white solid. m.p**.** 52-54 °C. $[\alpha]_D^{23} = -5.9$ (c =0.40 , $CHCl_3$). ^{1}H-NMR (400 MHz, $CDCl_3$) δ= 4.38-4.28 (m, 1H, 5-H), 4.02-3.94 (m, 2H, 4-H and 6-H_a), 3.79-3.64 (m, 2H, 2-H and 3-H), 3.00 (brs, 1H, OH), 2.71-2.65 (m, 1H, 6-H_b), 1.66 (brs, 2H, 1'H), 1.45 (s, 3H, Me),1.41 (s, 9H, *t*Bu), 1.30 (s, 3H, Me), 1.30-1.22 (m, 12H, 2'H-7'H), 0.83 (t, J= 5.3 Hz, 3H, 8'H) ppm. ^{13}C-NMR (100 MHz, $CDCl_3$) δ = 155.4 (s, N<u>C</u>OO), 109.6 (s, acetal), 80.3 (s, O<u>C</u>*t*Bu), 78.4 (d, C-4), 72.4 (d, C-3), 70.9 (d, C-5), 56.4, 55.8 (d, C-2 two rotamers), 41.4, 40.7 (t, C-6, two rotamers), 28.4 (q, 3C, *t*Bu), 31.9-22.7 (t, 7C, C-1'- C-7'and q, Me, q, Me), 14.2 (q, C-8') ppm. MS (ESI): m/z (%) = 408.21 (40) $[M+Na]^+$, 792.88 (100) $[2M+Na]^+$. IR ($CDCl_3$): ν = 957, 1070, 1163, 1215, 1250, 1412, 14.62, 16.84, 29.28, 3599 cm^{-1}. $C_{21}H_{39}NO_5$ (385.54). calcd. C, 65.42; H, 10.20; N, 3.63; found C, 65.50; H, 10.00; N, 3.72.

Synthesis of (2*R*,4*S*,5*R*)-3-oxo-4,5-*O*-(1-methylethylidene)-*N*-Boc-2-octylpiperidine (**182**): Dess-Martin periodinane (218 mg, 0.51 mmol) was added to a solution of **181** (131 mg, 0.34 mmol) in dry CH_2Cl_2 (15 mL) at room temperature. The reaction mixture was stirred for 3 hours until a TLC control (CH_2Cl_2/MeOH/ NH_4OH (6%) 15:1:0.1) attested the disappearance of the starting material. The mixture was extracted with $NaHCO_3$ saturated solution, dried over Na_2SO_4 and concentrated. The residue was purified by silica gel flash chromatography (Hex/AcOEt 4:1) to give **182** (78 mg, 0.20 mmol, 60%, R_f = 0.23) as a colorless oil.

182: colorless oil. $[\alpha]_D^{23}$ = + 20 (c =0.20, $CHCl_3$). ^{1}H-NMR (400 MHz, $CDCl_3$) δ = 4.85-4.74 (m, 1H, 5-H), 4.63-4.52 (m, 2H, 4-H and 6-H_a), 4.36-4.32 (m, 1H, 2-H), 2.63-2.57 (m, 1H, 6-H_b), 1.96 (brs, 1H, 1'H_a), 1.61-1.40 (m, 13H, 1'H_b, *t*Bu and Me), 1.35 (s, 3H, Me), 1.35-1.26 (m, 12H, 2'H-7'H), 0.83 (t, J= 4.6 Hz, 3H, 8'H_{a-b-c}) ppm. ^{13}C-NMR (100 MHz, $CDCl_3$) δ = 206.5 (s, C=O), 154.6 (s, N<u>C</u>OO), 112.2 (s, acetal), 81.2 (s, O<u>C</u>*t*Bu), 79.1 (d, C-4), 74.3 (d, C-5), 62.8, 62.0 (d, C-2, two rotamers), 44.9, 34.3 (t, C-6, two rotamers), 28.3 (q, 3C, *t*Bu), 31.9-22.7 (t, 7C, C-1'- C-7'and q, Me, q, Me), 14.2 (q, C-8') ppm. MS (ESI): m/z (%) = 422.18 (44) $[M+K]^+$, 807.20 (25) $[2M+K]^+$. IR ($CDCl_3$): ν = 422, 455, 677, 708, 721, 945, 1080, 1126, 1161, 1219, 1254, 1375, 1408, 1460, 1692, 1742, 2255, 2859, 2928 cm^{-1}.

$C_{21}H_{37}NO_5$ (383.53). calcd. C, 65.77; H, 9.72; N, 3.65; found C, 65.50; H, 9.83; N, 3.62.

Synthesis of (2*R*,3*S*,4*S*,5*R*)-3-hydroxy-4,5-*O*-(1-methylethylidene)-*N*-Boc-2-pentylpiperidine (183): A solution of **182** (0.078 g, 0.2 mmol) in EtOH (1.8 mL) was cooled to 0°C and $NaBH_4$ (20 mg, 0.50 mmol) was added. The reaction mixture was allowed to warm to room temperature and stirred for 18 hours until a TLC control (Hex/EtOAc 4:1). Then, water (0.4 mL) and MeOH (1.4 mL) were added and mixture was stirred for 10 hours at room temperature and concentrated under reduced pressure. The crude product was purified by silica gel flash chromatography (CH_2Cl_2/MeOH 10:1) to give **183** (45 mg, 0.10 mmol, 75%, R_f = 0.20) as a colourless oil.

183: colourless oil. $[\alpha]_D^{23}$ = – 66 (c =0.30, $CHCl_3$). ^{1}H-NMR (400 MHz, $CDCl_3$) δ = 4.28 (brs, 1H, 6-Ha), 4.13-4.12 (m, 1H, 5-H), 4.07-4.05 (m, 2H, 4-H and 3-H), 3.85-3.81 (m, 1H, 2-H), 3.09-2.98 (m, 1H, 6-Hb), 2.40 (brs, 1H, OH), 1.77-1.75 (m, 2H, 1'H), 1.52 (s, 3H, Me), 1.44 (s, 9H, tBu), 1.36 (s, 3H, Me), 1.28-1.25 (m, 12H, 2'H-7'H), 0.86 (t, J= 6.0 Hz, 3H, 8'H) ppm. ^{13}C-NMR (100 MHz, $CDCl_3$) *δ*= 154.9(s, N<u>C</u>OO), 109.8 (s, acetal), 80.1 (s, O<u>C</u>*t*Bu), 75.3 (d, C-4 or C-3), 71.6 (d, C-5), 66.3 (d, C-4 or C-3), 54.1, 53.6 (d, C-2, two rotamers), 41.6, 40.1 (t, C-6, two rotamers), 28.0 (q, 3C, *t*Bu), 32.0-22.8 (t,7C, C-1'- C-7'and q, Me, q, Me), 14.3 (q, C-8') ppm. MS (ESI): m/z (%) = 408.13 (100) $[M+Na]^+$, 792.80 (47) $[2M+Na]^+$. IR ($CDCl_3$): ν = 411, 440, 473, 569, 619, 650, 683, 768, 876, 961, 1159, 1213, 1240, 1288, 1377, 1414, 1460, 1682, 2247, 2857, 2926, 3580 cm^{-1}. $C_{21}H_{39}NO_5$ (385.54). calcd. C, 65.42; H, 10.20; N, 3.63; found C, 65.45; H, 9.99; N, 3.51.

Synthesis of (2*R*, 3*S*, 4*R*, 5*R*)-2-pentylpiperidine-3,4,5-triol (184): A solution of **183** (30 mg, 0.08 mmol) in MeOH (4 mL) was left stirring with 12 M HCl (15 µL) at room temperature for 16 h. The crude mixture was concentrated to yield the hydrochloride salt of **184**. The corresponding free amine was obtained by dissolving the residue in MeOH, then the strongly basic resin Ambersep 900-OH was added, and the mixture was stirred for 40 minutes. The resin was removed by filtration to afford 20 mg (0.08 mmol, 100%) of **184** as free base, as colorless oil.

184: colorless oil. $[\alpha]_D^{23}$ = – 20 (c =0.50, MeOH). ^{1}H-NMR (400 MHz, CD_3OD) δ= 3.79 (brs, 1H, 5-H), 3.72 (brs, 1H, 3-H), 3.46 (brs, 1H, 4-H), 3.02 (d, J= 13.4 Hz, 1H, 6-H_a), 2.69 (d, J=13.8 Hz, 1H, 6-H_b), 2.44 (t, J= 6.5 Hz, 1H, 2-H), 1.56-1.54 (m, 1H, 1'Ha), 1.49-1.44 (m, 1H, 2'Ha), 1.43-1.32 (m, 12H, 1'Hb, 2'Hb, 3'H-7'H), 0.90 (t, J = 6.0 Hz, 3H, 8'H) ppm. ^{13}C-NMR (100 MHz, CD_3OD) δ= 111.4 (radio interference), 72.6 (d, 1C, C-3), 71.4 (d, 1C, C-4), 71.0 (d, 1C, C-5), 60.0 (d, 1C, C-2), 51.6 (t, 1C, C-6), 33.1-23.7 (t, 7C, C-1'- C-7'), 14.5 (s, 1C, C-8') ppm. MS (ESI): m/z (%) = 246.20 (100) [M], 268.2 (7) $[M+Na]^+$, 537.20 (13) $[2M+Na]^+$. $C_{13}H_{27}NO_3$ (245.36). calcd. C, 63.64; H, 11.09; N, 5.71; found C, 63.55; H, 11.00; N, 5.83.

Sinthesis of (2R,3R,4R,5R)-1-benzyl-2-octylpiperidine-3,4,5-triol (185): To a stirred solution of compound **151a** (130 mg, 0.53 mmol) in acetonitrile (6 mL), K_2CO_3 (111 mg, 0.80 mmol) and benzylbromide were added. The resulting mixture was stirred at 50 °C for 3 hours until a TLC control (CH_2Cl_2/MeOH/ NH_4OH (6%) 1:1:0.1) attested the disappearance of the starting material. The solvent was evaporated under vacuum and the crude mixture was purified by silica gel column chromatography (eluent Hex/AcOEt 8:1) to give 124 mg (0.37 mmol, 70%) of **185** (R_f = 0.30) as a colorless oil.

185: a colorless oil. $[\alpha]_D^{25}$ = – 23 (c =0.63, MeOH). ^{1}H-NMR (400 MHz, CD_3OD) δ = 7.35-7.18 (m, 5H, Ar), 4.07 (d, J= 12.0, 1H, H_a-NBn), 3.74 (brs, 1H, 3-H), 3.64 (t, J= 8.0 Hz, 1H, 5-H), 3.32- 3.29 (m, 1H, 4-H), 3.12 (d, J= 12.0, 1H, H_b-NBn), 2.85 (d, J= 12.0, 1H, 6-H_a), 2.14-2.12 (m, 1H, 2-H), 2.08 (d, J= 12.0, 1H, 6-H_b), 1.89-1.81 (m, 2H, 1'H), 1.54-1.45 (m, 2H, 2'H), 1.30-1.26 (m, 10H, 3'H -7'H), 0.86 (t, J=6.0 Hz, 8'$H_{a,b,c}$) ppm. ^{13}C-NMR (100 MHz, CD_3OD) = 140.0 (s, 1C, Ar), 129.0-127.9 (d, 5C, Ar), 76.5 (d, C-4), 71.2 (d, C-5), 69.3 (d, C-3), 67.0 (d, C-2), 57.9 (t, 1C, Bn), 56.2 (t, C-6), 33.0-23.7 (t, 7C, C-1'- C-7'), 14.5 (q, 1C, C-8') ppm. MS (ESI): m/z (%) = 336.28 (100) $[M+H]^+$. $C_{20}H_{33}NO_3$ (335.25): calcd. C, 71.60; H, 9.92; N, 4.18; found C, 71.54; H, 10.00; N, 4.25.

Sinthesis of (2R,3R,4R,5R)-1-benzyl-2-octylpiperidine-3,4,5-triyl triacetate (186): A solution of **185** (108 mg, 0.32 mmol) in dry pyridine (4.2 mL) was stirred with acetic anhydride (768 µl, 8.05 mmol) at room temperature for 18 h. The crude mixture was diluted with toluene and then concentrated under vacuum.

The crude was purified by gradient silica gel column chromatography (Hex/AcOEt 15:1) to give 133 mg of the acetylated compound **186** (R_f =0.30, 0.29 mmol, 90 %) as a colorless oil.

186: a colorless oil. $[\alpha]_D^{25}$ = – 17 (c =1.00, $CHCl_3$). ^{1}H-NMR (400 MHz, $CDCl_3$) δ = 7.30-7.23 (m, 5H, Ar), 5.30 (t, J= 8.0 Hz, 1H, 3-H), 5.00 (brs, 1H, 5-H), 4.96- 4.92 (m, 1H, 4-H), 4.05 (d, J= 16.0, 1H, H_a-NBn), 3.31 (d, J= 16.0, 1H, H_b-NBn), 2.95 (d, J= 12.0, 1H, 6-H_a), 2.58-2.56 (m, 1H, 2-H), 4.05 (d, J= 16.0, 1H, 6-H_b),2.09 (s, 3H, Me), 2.07 (s, 3H, Me), 1.98 (s, 3H, Me), 1.73-1.67 (m, 1H, 1'H_a), 1.54-1.45 (m, 3H, 1'H_b and 2'H), 1.22-1.24 (m, 10H, 3'H -7'H), 0.85 (t, J=6.0 Hz, 8'$H_{a,b,c}$) ppm. ^{13}C-NMR (50 MHz, $CDCl_3$) = 170.2, 170.0, 169.0 (s, 3C, O*C*=O), 138.8 (s, 1C, Ar), 128.0-127.2 (d, 5C, Ar), 72.5 (d, C-4), 69.6 (d, C-3), 67.8 (d, C-5), 62.6 (d, C-2),55.5 (t, 1C, Bn), 50.8 (t, C-6), 31.9-20.8 (t, 7C, C-1'- C-7', q, 3C, Me), 14.2 (q, 1C, C-8') ppm. MS (ESI): m/z (%) = 462.0 (100) $[M+H]^+$. $C_{26}H_{39}NO_6$ (461.60): calcd. C, 67.65; H, 8.52; N, 3.03; found C, 67.70; H, 8.71; N, 2.98.

Sinthesis of (2R,3R,4R,5R)-2-octylpiperidine-3,4,5-triyl triacetate (187): To a solution of **186** (30 mg, 0.06 mmol) in MeOH (10 mL), $Pd(OH)_2$/C (15 mg) was added under nitrogen atmosphere. The mixture was stirred at room temperature under hydrogen atmosphere (balloon) for 5 hours, until a control by 1H-NMR spectroscopy attested the disappearance of benzyl group. The mixture was filtered through Celite® and the solvent was removed under reduced pressure to afford 22 mg of (2R,3R,4R,5R)-2-octylpiperidine-3,4,5-triyl triacetate **187** (0.06 mmol, 90 %) as a waxy solid.

187: waxy solid. $[\alpha]_D^{25}$ = – 15 (c =1.00, $CHCl_3$). ^{1}H-NMR (400 MHz, $CDCl_3$) δ = 5.84-5.83 (m, 1H, 5-H), 5.16- 5.26 (m, 2H, 4-H and 3-H), 3.11-2.80 (m, 2H, 6-H), 2.02 (s, 3H, Me), 2.00 (s, 3H, Me), 1.98 (s, 3H, Me), 1.22-1.24 (m, 1'H -7'H), 0.90 (t, J= 6.0 Hz, 8'$H_{a,b,c}$) ppm. ^{13}C-NMR (50 MHz, $CDCl_3$) = 170.2, 169.9, 169.0 (s, 3C, O*C*=O), 74.7 (d, C-4), 75.9 (d, C-3), 71.7 (d, C-5), 56.6(d, C-2), 45.0 (t, C-6), 33.0-30.4 (t, 7C, C-1'- C-7', q, 3C, Me), 14.3 (q, 1C, C-8') ppm. MS (ESI): m/z (%) = 372.90 (100) $[M+H]^+$. $C_{19}H_{33}NO_6$ (371.46): calcd. C, 61.43; H, 8.95; N, 3.77; found C, 61.21; H, 8.77; N, 3.80.

Sinthesis of (2R,3R,4R,5R)-1-acetyl-2-octylpiperidine-3,4,5-triyl triacetate

(188): A solution of **151a** (36 mg, 0.14 mmol) in dry pyridine (2.0 mL) was stirred with acetic anhydride (343 µl, 3.67 mmol) at room temperature for 18 h. The crude mixture was diluted with toluene and then concentrated under vacuum. The crude was purified by gradient silica gel column chromatography (Hex/AcOEt 15:1) to give 54 mg of the acetylated compound **188** (R_f = 0.3, 0.13 mmol, 95%) as white solid.

188: white solid. m.p.=120-122 °C. $[\alpha]_D^{25}$ = – 44 (c =1.00, $CHCl_3$). ^{1}H-NMR (400 MHz, $CDCl_3$) δ = 5.27-5.22(m, 1H, 5-H), 5.00-4.96 (m, 1H, 4-H), 4.93-4.89 (m, 1H, 3-H), 3.85-3.82 (m, 1H, 2-H), 3.73-3.70 (m, 1H, 6-H_a), 3.41-3.30 (m, 1H, 6-H_b), 2.12 (s, 3H, Me), 2.02 (s, 3H, Me), 2.00 (s, 3H, Me), 1.98 (s, 3H, Me), 1.74-1.67 (m, 2H, 1'H), 1.22-1.24 (m, 12H, 2'H-7'H), 0.86-0.84 (m, 3H, 8'$H_{a,b,c}$) ppm. ^{13}C-NMR (100 MHz, $CDCl_3$) = 171.0, 169.0, 169.8 (s, 1C, N*C*=O), 170.0 (s, 3C, O*C*=O), 71.0 (d, C-4), 67.1 (d, C-5), 65.82 (d, C-3), 51.0 (d, C-2), 40.0 (t, C-6), 32.0-21.0 (t, 6C, C-1'-C-7', q, 3C, Me), 14.4 (q, C-8') ppm. MS (ESI): m/z (%) = 414.70 (100) $[M+H]^+$. $C_{21}H_{35}NO_7$ (413.51): calcd. C, 61.00; H, 8.53; N, 3.39; found C, 61.21; H, 8.77; N, 3.40.

Preliminary biological screening towards commercial glycosidases

The percentage (%) of inhibition towards the corresponding glycosidase was determined by quadruplicate in the presence of 100 µM of the inhibitor on the well. Each enzymatic assay (final volume 0.12 mL) contains 0.01-0.5 units/mL of the enzyme (with previous calibration) and 4.2 mM aqueous solution of the appropriate *p*-nitrophenyl glycopyranoside (substrate) buffered to the optimal pH of the enzyme. Enzyme and inhibitor were pre-incubated for 5 min at r.t., and the reaction started by addition of the substrate. After 20 min of incubation at 37 °C, the reaction was stopped by addition of 0.1 mL of sodium borate solution (pH 9.8). The *p*-nitrophenolate formed was measured by visible absorption spectroscopy at 405 nm (Asys Expert 96 spectrophotometer). Under these conditions, the *p*-nitrophenolate released led to optical densities linear with both reaction time and concentration of the enzyme.

Preliminary biological screening towards human lysosomal glycosidases

The effect of 1mM concentration of **147a-e** and **151a-e** was assayed towards six lysosomal glycosidases other than GCase, namely: α-mannosidase, β-mannosidase, α-galactosidase, β-galactosidase, α-fucosidase from leukocytes isolated from healthy donors (controls) and α-glucosidase from lymphocytes isolated from healthy donors' flesh blood (controls). Isolated leukocytes or lymphocytes were disrupted by sonication, and a micro BCA protein assay kit (Sigma–Aldrich) was used to determine the total protein amount for the enzymatic assay, according to the manufacturer instructions.

α-Mannosidase activity was measured in a flat-bottomed 96-well plate. Azasugar solution (3 μL), 4.29 μg/μL leukocytes homogenate 1:10 (7 μL), and substrate 4-methylumbelliferyl-α-D-mannopyranoside (2.67 mM, 20 μL, Sigma–Aldrich) in Na phosphate/citrate buffer (0.2:0.1, M/M, pH 4.0) containing sodium azide (0.02%) were incubated at 37 °C for 1 h. The reaction was stopped by addition of sodium carbonate (200 μL; 0.5M, pH 10.7) containing Triton X-100 (0.0025 %), and the fluorescence 4-methylumbelliferone released by α-mannosidase activity was measured in SpectraMax M2 microplate reader (λex=365 nm, λem=435 nm; Molecular Devices). Inhibition is given with respect to the control (without azasugar). Data are mean SD (n=3).

β-Mannosidase activity was measured in a flat-bottomed 96-well plate. Azasugar solution (3 μL), 4.29 μg/μL leukocytes homogenate 1:10 (7 μL), and substrate 4-methylumbelliferyl-β-D-mannopyranoside (1.33 mM, 20 μL, Sigma–Aldrich) in Na phosphate/citrate buffer (0.2:0.1, M/M, pH 4.0) containing sodium azide (0.02%) were incubated at 37 °C for 1h. The reaction was stopped by addition of sodium carbonate (200 μL; 0.5M, pH 10.7) containing Triton X-100 (0.0025 %), and the fluorescence of 4-methylumbelliferone released by β-mannosidase activity was measured in SpectraMax M2 microplate reader (λex=365 nm, λem=435 nm; Molecular Devices). Inhibition is given with respect to the control (without azasugar). Data are mean SD (n=3).

α-Galactosidase activity was measured in a flat-bottomed 96-well plate. Azasugar solution (3 μL), 4.29 μg/μL leukocytes homogenate 1:3 (7 μL), and substrate 4-methylumbelliferyl α-D-galactopyranoside (1.47 mM, 20 μL, Sigma–Aldrich) in acetate buffer (0.1 M, pH 4.5) containing sodium azide (0.02%) were incubated at 37 °C for 1 h. The reaction was stopped by addition of sodium carbonate (200 μL; 0.5M, pH 10.7) containing Triton X-100 (0.0025 %), and the fluorescence 4-methylumbelliferone released by α-galactosidase activity was measured in SpectraMax M2 microplate reader (λex=365 nm, λem=435 nm; Molecular Devices). Inhibition is given with respect to the control (without azasugar). Data are mean SD (n=3).

β- Galactosidase activity was measured in a flat-bottomed 96-well plate. Azasugar solution (3 µL), 4.29 µg/µL leukocytes homogenate 1:10 (7 µL), and substrate 4-methylumbelliferyl β-D-galactopyranoside (1.47 mM, 20 µL, Sigma–Aldrich) in acetate buffer (0.1M, pH 4.3) containing NaCl (0.1M) and sodium azide (0.02%) were incubated at 37 °C for 1 h. The reaction was stopped by addition of sodium carbonate (200 µL; 0.5M, pH 10.7) containing Triton X-100 (0.0025 %), and the fluorescence 4-methylumbelliferone released by β-galactosidase activity was measured in SpectraMax M2 microplate reader (λex=365 nm, λem=435 nm; Molecular Devices). Inhibition is given with respect to the control (without azasugar). Data are mean SD (n=3).

α-Fucosidase activity was measured in a flat-bottomed 96-well plate. Azasugar solution (3 µL), 4.29 µg/µL leukocytes homogenate 1:3 (7 µL), and substrate 4-methylumbelliferyl α-L-fucopyranoside (1.51 mM, 20 µL, Sigma–Aldrich) in Na phosphate/citrate buffer (0.2:0.1, M/M, pH 5.5) were incubated at 37 °C for 1 h. The reaction was stopped by addition of sodium carbonate (200 µL; 0.5M, pH 10.7) containing Triton X-100 (0.0025 %), and the fluorescence 4-methylumbelliferone released by α- fucosidase activity was measured in SpectraMax M2 microplate reader (λex=365 nm, λem=435 nm; Molecular Devices). Inhibition is given with respect to the control (without azasugar). Data are mean SD (n=3).

α-Glucosidase activity was measured in a flat–bottomed 96 well plate. Azasugar solution (3 µL), 4.29 µg/µL lymphocytes homogenate (7µL) and 20 µL of substrate solution of 4-methylumbelliferyl-α-D-glucopyranoside (Sigma-Aldrich) in Na acetate buffer (0.2 M, pH 4.0) were incubated for 1 h at 37 °C. The reaction was stopped by the addition of a solution of sodium carbonate (200 µL; 0.5M, pH 10.7) containing Triton X-100 (0.0025 %), and the fluorescence of 4-methylumbelliferone released by α-glucosidase activity was measured in SpectraMax M2 microplate reader (λex=365 nm, λem=435 nm; Molecular Devices). Inhibition is given with respect to the control (without azasugar). Data are means of 3 values.

Biochemical characterization with human GCase:

The azasugars **147a-e**, **151a-e**, **180a** and **184** were screened towards GCase in leukocytes isolated from healthy donors (controls) at 1 mM concentrations. Isolated leukocytes were disrupted by sonication, and a micro BCA protein assay kit (Sigma–Aldrich) was used to determine the total protein amount for the enzymatic assay, according to the manufacturer instructions. Enzyme activity was measured in a flat-bottomed 96-well plate. Azasugar solution (3 µL), 4.29 µg/µL leukocytes homogenate (7 µL), and substrate 4-methylumbelliferyl-β-D-glucoside (3.33 mM, 20 µL, Sigma–Aldrich) in citrate/phosphate buffer (0.1:0.2, M/M, pH 5.8) containing sodium taurocholate (0.3%) and Triton X-100 (0.15%) at 37 °C were incubated for 1 h. The reaction was stopped by addition of sodium carbonate (200 µL; 0.5M, pH 10.7) containing Triton X-100 (0.0025 %), and the fluorescence of 4-methylumbelliferone released by β-glucosidase activity was measured in SpectraMax M2 microplate reader (λex=365 nm, λem=435 nm; Molecular Devices). Percentage GCase inhibition is given with respect to the control (without azasugar). Data are mean SD (n=3).

IC_{50} determination:

The IC_{50} values of inhibitors against GCase were determined by measuring the initial hydrolysis rate with 4-methylumbelliferyl-β-D-glucoside (3.33 mM). Data obtained were fitted to the following equation using the Origin Microcal program.

$$\frac{Vi}{Vo} = \frac{Max - Min}{1 + \left(\frac{x}{IC_{50}}\right)^{slope}} + Min$$

where V_i/V_o, represent the ratio between the activity measured in the presence of the inhibitor (V_i) and the activity of the control without the inhibitor (V_0), “x” the inhibitor concentration, Max and Min, the maximal and minimal enzymatic activity observed, respectively.

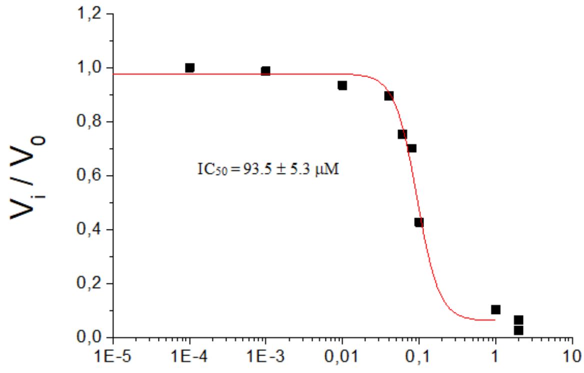

147a (mM)

IC$_{50}$ of compound **147a** towards GCase

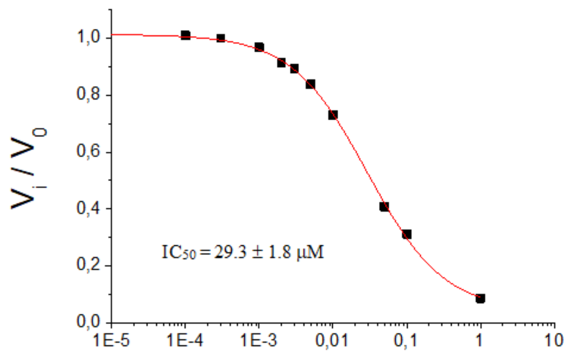

151a (mM)

IC$_{50}$ of compound **151a** towards GCase

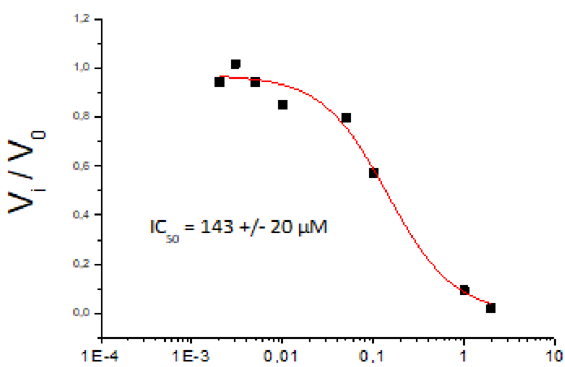

147b (mM)

IC$_{50}$ of compound **147b** towards GCase

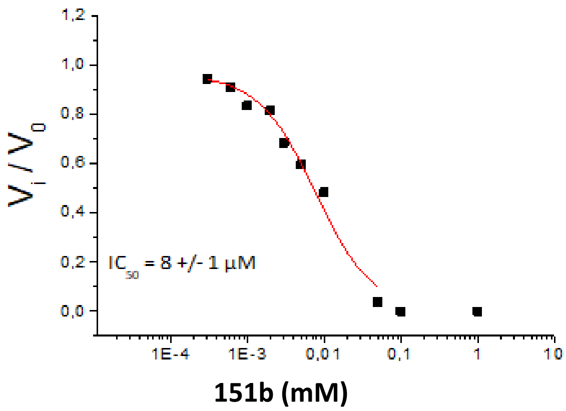

IC$_{50}$ of compound **151b** towards GCase

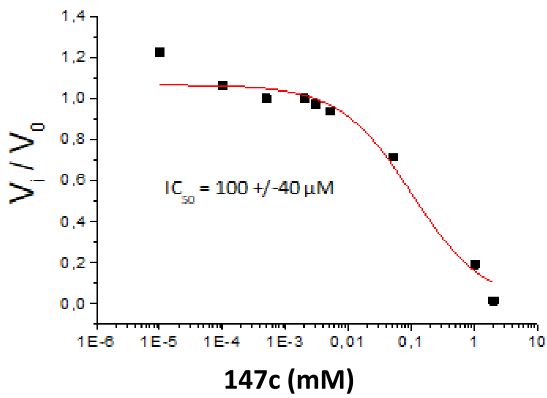

IC$_{50}$ of compound **147c** towards GCase

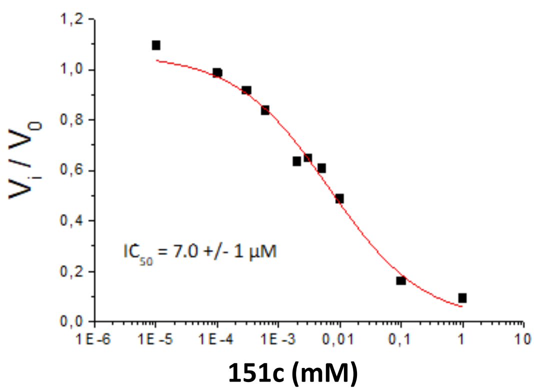

IC$_{50}$ of compound **151c** towards GCase

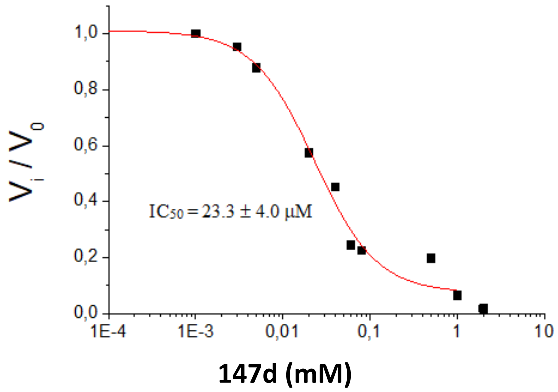

IC_{50} of compound **147d** towards GCase

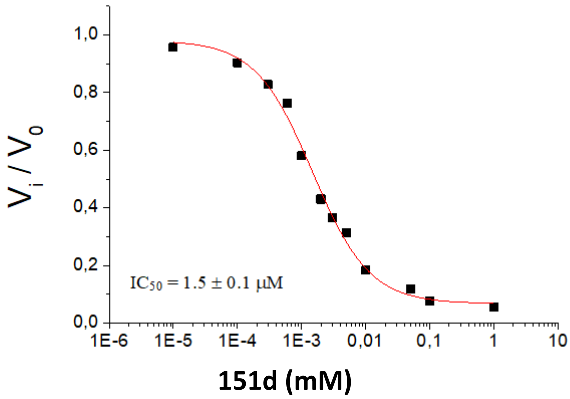

IC_{50} of compound **151d** towards GCase

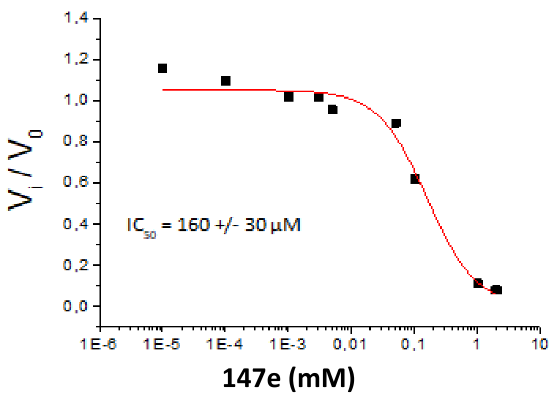

IC_{50} of compound **147e** towards GCase

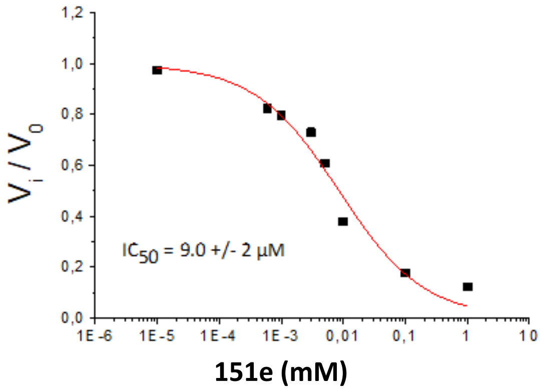

IC_{50} of compound **151e** towards GCase

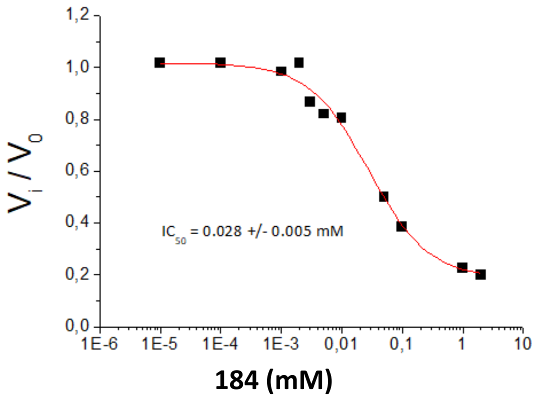

IC_{50} of compound **184** towards GCase

*Kinetic Analysis for compounds **151a** and **151d***

The action mechanism of both compounds **151a** and **151d** was determined studying the dependence of the main kinetic parameters (K_m and V_{max}) from the inhibitors concentration. The GCase activity was determined using the 4-methylumbelliferyl-β-D-glucoside as substrate. Kinetic data were analysed using the *Lineweaver-Burk* plot (double reciprocal plot). We found that experimental points described straight lines intersecting one each other in a point of *y* axis, suggesting that compounds **151a** and **151d** behave as competitive inhibitors.

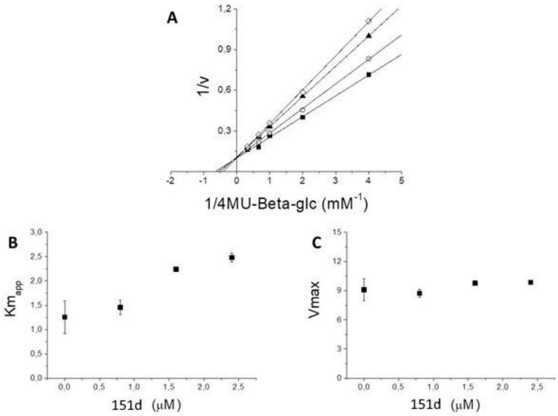

Kinetic analysis of compound **151d** (A) Double reciprocal plots. 4-Methylumbelliferyl-β-D-glucoside was employed as a substrate. The concentrations of compound **151d** are: ■, 0 µM; ○, 0.8 µM; ▲, 1.6 µM; ◇, 2.4 µM. Data reported in the figures represent the mean values ± S.E.M. (n = 3). (B, C) Behaviour of K_m and V_{max} at different concentrations of compound **151d**.

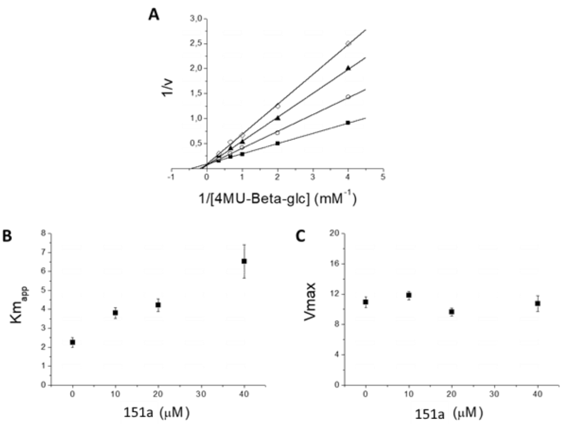

Kinetic analysis of compound 151a. (A) Double reciprocal plots. 4-Methylumbelliferyl-β-D-glucoside is employed as a substrate. The concentrations of compound **151a** are: ■, 0 μM; ○, 10 μM; ▲, 20 μM; ◇, 40 μM. Data reported in the figures represent the mean values ± S.E.M. (n = 3). (B, C) Behaviour of K_m and V_{max} at different concentrations of compound **151a**.

In agreement with this hypothesis, we observed that K_m value increase with increasing inhibitor concentrations, while the V_{max} value remained constant.

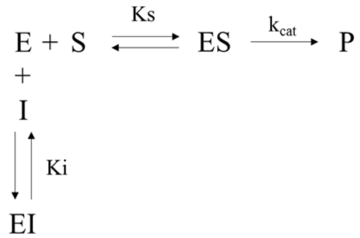

Competitive inhibition mechanism (E, free enzyme; S, substrate; P, reaction product; I, inhibitor; ES, enzyme-substrate complex; EI, enzyme-inhibitor complex; Ks, association constant of enzyme-substrate complex; Ki, dissociation constant of EI complex; Ks, association constant of E and S; k_{cat}, catalytic constant for the conversion of S into P).

Based on this evidence, the Ki value was determined using the following equation:

$$Slope = \frac{Km}{Vmax * Ki} * x + \frac{Km}{Vmax}$$

We calculated the Ki values for each compound, which resulted 18.5 ± 1.6 μM and 3.6 ± 0.1 μM for compounds **151a** and **151d**, respectively.

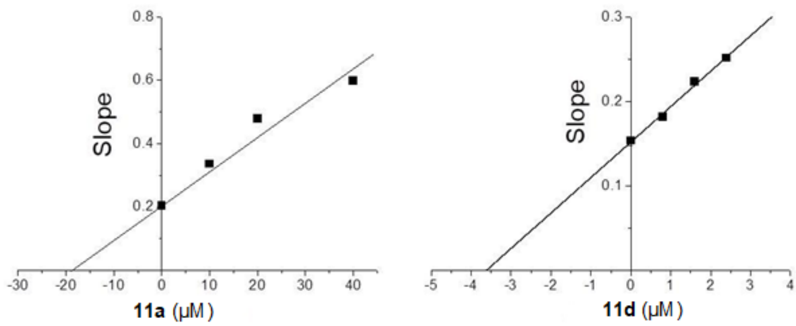

Plots for the determination of the Ki values of compounds **151a** and**151d**.

Pharmacological chaperoning activity

Fibroblasts with the N370S/RecNcil and L444P/L444P mutations from Gaucher disease patients were obtained from the "Cell line and DNA Biobank from patients affected by Genetic Diseases" (Gaslini Hospital, Genova, Italy).

Fibroblasts cells (13.5-15.0 x 10^4) were seeded in T25 flasks with DMEM supplemented with fetal bovine serum (10%), penicillin/streptomycin (1%), and glutamine (1%) and incubated at 37 °C with 5% CO_2 for 24 h. The medium was removed, and fresh medium containing the azasugars was added to the cells and left for 4 days. The medium was removed, and the cells were washed with PBS and detached with tripsin to obtain cell pellets, which were washed four times with PBS, frozen and lysed by sonication in water. Enzyme activity was measured as reported above. Reported data are mean S.D. (n=2).

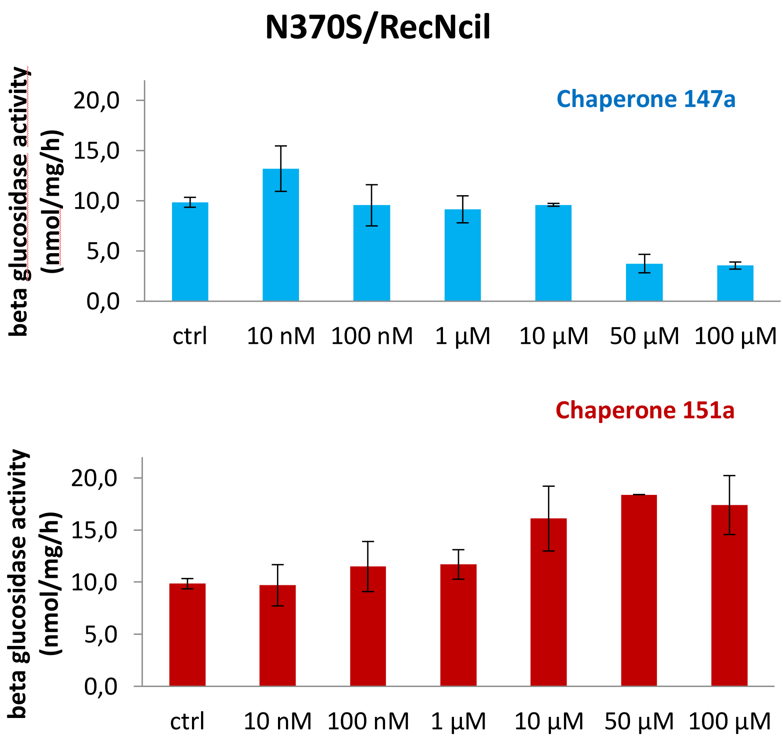

Fibroblasts derived from GD patients bearing N370/RecNcil mutations were incubated without (control, ctrl) or with 6 different concentrations (10 nM, 100 nM, 1 µM, 10 µM, 50 µM, 100 µM) of compounds **147a** and **151a**. After 4 days, the GCase activity was determined (as above described) in lysates from treated fibroblasts. Reported data are mean S.D. (n=2).

N370S/RecNil

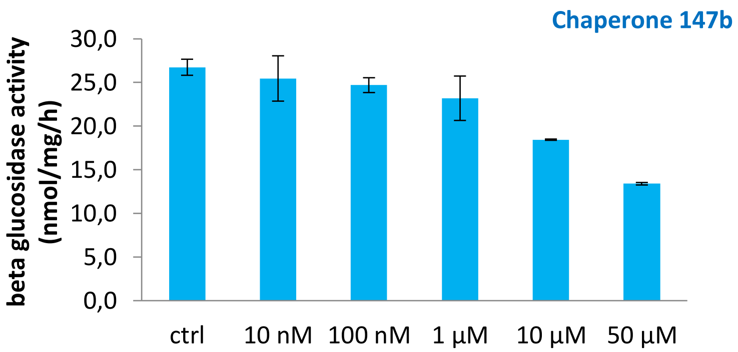

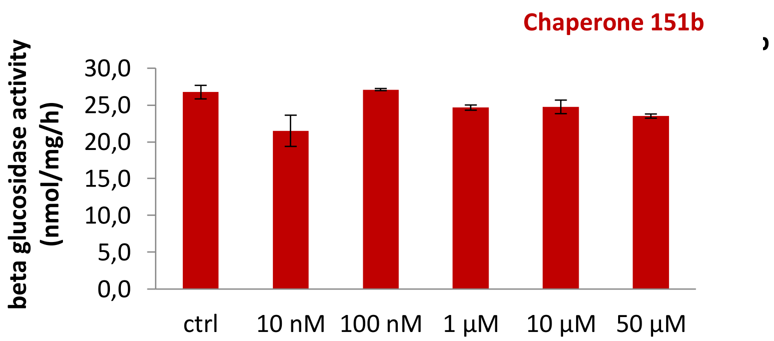

Fibroblasts derived from GD patients bearing N370/RecNcil mutations were incubated without (control, ctrl) or with 6 different concentrations (10 nM, 100 nM, 1 µM, 10 µM, 50 µM, 100 µM) of compounds **147b** and **151b**. After 4 days, the flasks containing cells incubated with 100 µM concentrations of **147b** and **151b** showed low cell viability that hampered to proceed with the assay. For the other concentrations, the GCase activity was determined (as above described) in lysates from treated fibroblasts. Reported data are mean S.D. (n=2).

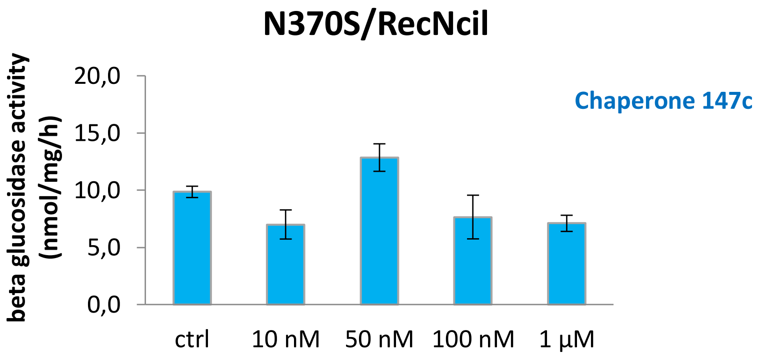

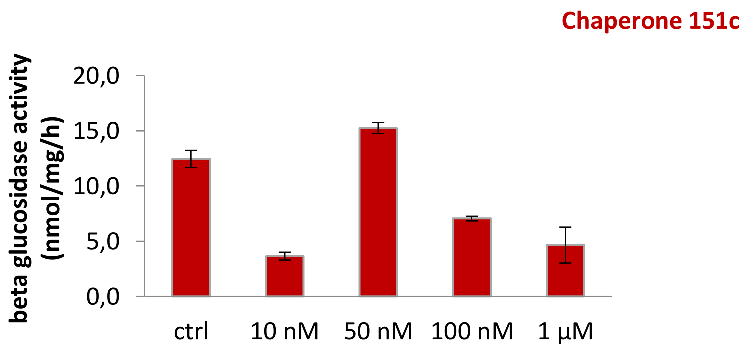

Fibroblasts derived from GD patients bearing N370/RecNcil mutations were incubated without (control, ctrl) or with 7 different concentrations (10 nM, 50 nM, 100 nM, 1 µM, 10 µM, 50 µM, 100 µM) of compounds **147c** and **151c**. After 4 days, the flasks containing cells incubated with 10 µM, 50 µM and 100 µM concentrations of **147c** and **151c** showed low cell viability that hampered to proceed with the assay. For the other concentrations, the GCase activity was determined (as above described) in lysates from treated fibroblasts. Reported data are mean S.D. (n=2).

N370S/RecNcil

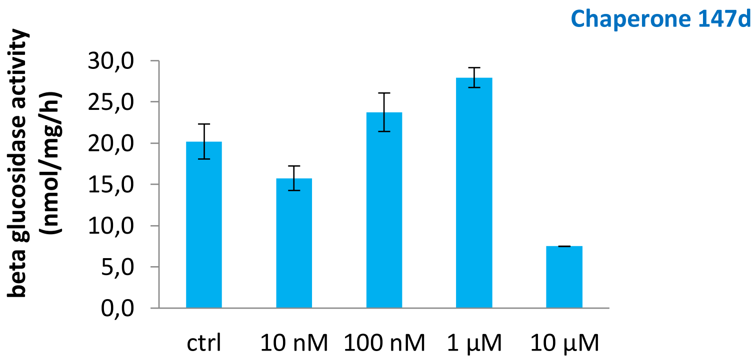

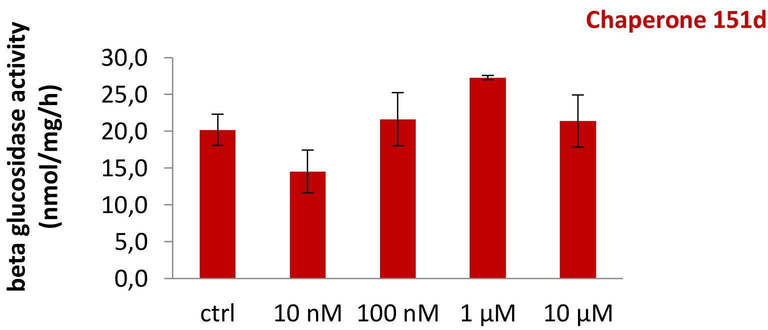

Fibroblasts derived from GD patients bearing N370/RecNcil mutations were incubated without (control, ctrl) or with 6 different concentrations (10 nM, 100 nM, 1 µM, 10 µM, 50 µM, 100 µM) of compounds **147d** and **151d**. After 4 days, the flasks containing cells incubated with 50 µM and 100 µM concentrations of **147d** and **151d** showed low cell viability that hampered to proceed with the assay. For the other concentrations, the GCase activity was determined (as above described) in lysates from treated fibroblasts. Reported data are mean S.D. (n=2).

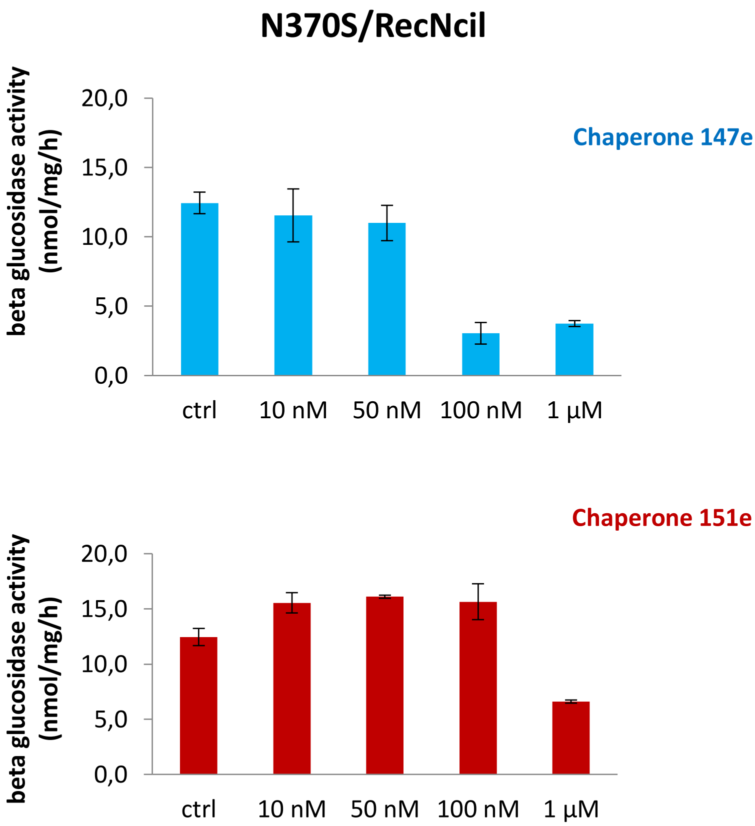

Fibroblasts derived from GD patients bearing N370/RecNcil mutations were incubated without (control, ctrl) or with 6 different concentrations (10 nM, 50 nM, 100 nM, 1 µM, 10 µM, 50 µM) of compounds **147e** and **151e**. After 4 days, the flasks containing cells incubated with 10 µM and 50 µM concentrations of **147e** and **151e** showed low cell viability that hampered to proceed with the assay. For the other concentrations, the GCase activity was determined (as above described) in lysates from treated fibroblasts. Reported data are mean S.D. (n=2).

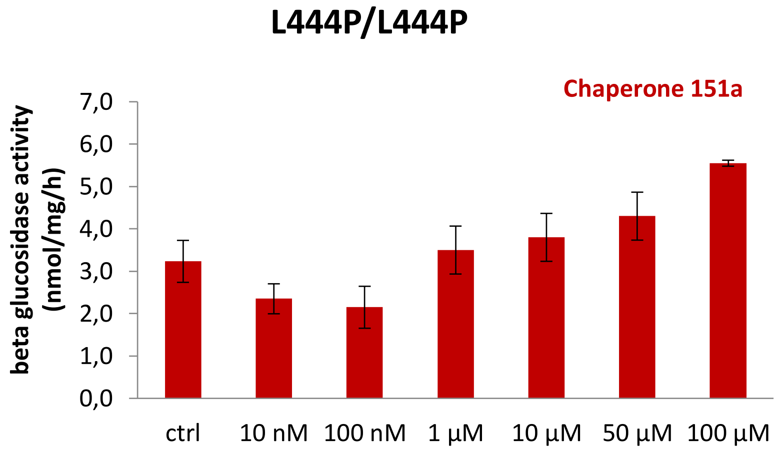

Fibroblasts derived from GD patients bearing L444P/L444P mutations were incubated without (control, ctrl) or with 6 different concentrations (10 nM, 100 nM, 1 µM, 10 µM, 50 µM, 100 µM) of compounds **151a**. After 4 days, the GCase activity was determined (as above described) in lysates from treated fibroblasts. Reported data are mean S.D. (n=2).

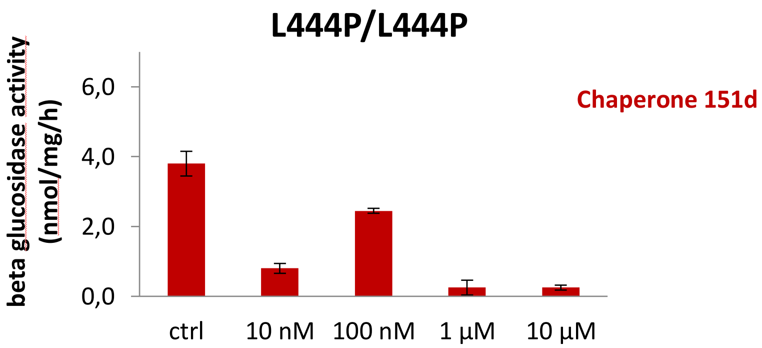

Fibroblasts derived from GD patients bearing L444P/L444P mutations were incubated without (control, ctrl) or with 6 different concentrations (10 nM, 100 nM, 1 µM, 10 µM, 50 µM, 100 µM) of compounds **151d**. After 4 days, the flasks containing cells incubated with 50 µM and 100 µM concentrations of **151d** showed low cell viability that hampered to proceed with the assay. For the other concentrations, the GCase activity was determined (as above described) in lysates from treated fibroblasts. Reported data are mean S.D. (n=2).

Cytotoxicity tests

MTT test was carried out using human fibroblasts bearing the N370/RecNcil mutations and L444P/L444P mutations at different concentrations. Fibroblasts were grown in the presence of Dulbecco's modified Eagle's medium supplemented with 10% fetal bovine serum (FBS), 1% glutamine, and 1% penicillin-streptomycin, at 37 °C in controlled atmosphere with 5% CO_2. For the experiments, cells were seeded at a density of 20000 cells per well in 24-well plates and grown for 24 h (or 48 h) before adding compounds. Compounds were dissolved in water; then aliquots of these were diluted in the growth medium. To preserve sterility of solutions, these were filtered with 0.22 µm filters before adding to the dishes containing fibroblasts. Then, cells were incubated at 37 °C in 5% CO_2 for 24 h (or 48 h). After this time, the media were replaced with medium containing 0.5 mg/mL of 3-(4,5-dimethylthiazol-2-yl)-2,5-diphenyltetrazolium bromide (MTT); the cells were incubated for an additional 1 h at 37 °C in 5% CO_2. Finally, the number of viable cells was quantified by the estimation of their dehydrogenase activity, which reduces MTT to water-insoluble formazan. Growth medium was removed and substituted with 300 µL of DMSO to dissolve the formazan produced. The quantitation was carried out measuring the absorbance of samples at 570 nm with the iMark microplate absorbance reader (BIO RAD) in a 96-well format.

Docking studies

Molecular docking was carried out using AutoDock 4.2 and MGL tools 1.5.6.56. The ligands structure was drawn and 3-D-optimized using Avogadro2. The crystal structure of human GCase complex with isofagomine (PDB code: 2NSX) was used for the docking analysis. The protein structure was prepared for docking by removal co-crystallized ligand and water molecules and by adding hydrogen atoms and Gasteiger charges to the protein. The active site for caring out molecular docking was defined by selectinga grid of 100 points per side and a grid spacing of 0.200 Å around the co-crystallized ligand isofagomine after it has been removed. Lamarkian generic algorithm was used for docking simulations. For each calculation, 27000 docking runs were performed using a population of 150 individuals and an energy evaluation of 2500000. Docked structures were rendered using Maestro.

3.2 Synthesis of 1,2-dioctyl trihydroxypiperidines

3.2.1 Results and discussions

3.2.1.1 Chemistry

The retrosynthetic strategy employed for the preparation of the compounds evaluated in this work is shown in Scheme 3.3. The synthetic strategy based on the addition of octylMgBr to the *N*-octyl nitrone **174a**, which derived from a one-pot condensation/oxidation of octylamine and aldehyde **135** with urea–hydrogen peroxide (UHP) as the stoichiometric oxidant in the presence of catalytic methyltrioxorhenium (MTO). [198] In this work we also show the potential and wide scope of this one-pot reaction in the synthesis of new carbohydrate-derivative nitrones starting from the aldehyde **135** with different amines. Access to both epimers of trihydroxypiperidines 1,2-disubstituted at the newly created stereocenter was guaranteed by carrying out the addition in the absence or presence of a suitable Lewis acid. This process provided the target trihydroxypiperidines with both configurations at C-2 after the final intramolecular reductive amination step.

3.2.1.1.1 One-pot synthesis of new carbohydrate-derivative nitrones from primary amines and a sugar-derived aldehyde catalysed by methyltrioxorhenium

The condensation / oxidation reaction with UHP in the presence of catalytic MTO, used to obtain our key intermediate nitrone **174a**, has been investigated starting from aldehyde **135** with different primary amines **189a-i**. Aldehyde **135** was synthesized in four steps from D-mannose on gram scale with an overall yield of 80%. [174] [180] This one-pot reaction proceed in one-pot to afford nitrones **174a-h** and **140**: condensation of **135** with primary amines **189a-i** followed by oxidation of the resulting imine intermediates. The results of the one-pot condensation / oxidation of primary amines and aldehyde **135** to nitrones are shown in Table 1. This reaction offers nitrones in a simple and regioselective way.

The reaction is operationally simple. To a stirred solution of aldehyde **135** and anhydrous Na_2SO_4 in MeOH at room temperature, the appropriate amine **189a-i** (1.2 equivalents) was added and the resulting mixture was stirred at room temperature under nitrogen atmosphere until a control by ^{1}H-NMR spectroscopy attested the formation of imine intermediates (for 3 hours). Anhydrous Na_2SO_4 was added to facilitate the condensation. The reaction mixture was cooled at 0 °C and UHP (3 equivalents) and MTO (4 mol%) were added sequentially. Upon addition of MTO, the mixture immediately became yellow as a result of the formation of catalytically active peroxorhenium species. [199]-[204] In case of cyclopropylamine **189e** and aldehyde **135,** the reaction mixture turned to blue after the addition of MTO due to the formation of nitrosocyclopropane. [205] The reaction mixture was stirred at room temperature for 16 h, when a TLC control (PEt/AcOEt 1:1) attested the disappearance of the starting material and the presence of a new spot UV visible, then the solvent was removed under reduced pressure. CH_2Cl_2 was added to the crude mixture, and the undissolved urea and Na_2SO_4 were removed by simple filtration. Removal of the solvent afforded the crude product, which was purified by flash column chromatography on silica gel. The addition of UHP from the beginning of the reaction, simultaneous to the addition of amines to **135**, did not lead to the formation of any nitrone probably due to premature oxidation of aldehyde or amine. Initially, this reaction was investigated with aliphatic amines (Table 3.7, Entries *1-5*). The amines with long chain **189a-b** provided the corresponding nitrones **174a-b** with completed conversions in good yields (80% and 70%, Table 3.7, Entries *1* and *2*) after purification on silica gel. The presence of bulky substituents on primary amines (**189c-d**) had low effects on the yield. Also in this case we obtained nitrones **174c-d** with good yields (65% and 60%, Table 3.7, Entries *3* and *4*). Unfortunately, we were not able to explain the low yield (45%) obtained with cyclopropylamine (**189e**) (Table 3.7, Entry *5*). As mentioned above, the addition of UHP and MTO, after condensation of cyclopropylamine **189e** and aldehyde **135**, afforded a blu mixture for the formation of nitrosocyclopropane. [205] We investigated the reaction with a defect of amine (0.8 equivalents). In a first step the mixture became yellow, but after 14 hours of reaction the mixture developed a blue colour and there was no product formation. Most likely, the intermediate imine was unstable and the equilibrium of formation was shifted towards the reagents. Reagents may have been subject to oxidation. In fact in this case formation of nitrone was not observed.

All the primary amines with aromatic substituents **189g-i** afforded nitrones **174g-h** and **140** after purification on silica gel in excellent yields (75–80%, Table 3.7, Entries 7-9). The one-pot condensation/oxidation of primary amines **189f-h-i** and aldehyde **135** with UHP and MTO in methanol afforded the corresponding nitrones with 80% yield *(*Entries *6*, *8* and *9*) instead the reaction conducted with the amine **189f** showed a slight reduction in yield (75%, Table 3.7, Entry *6* due to the bulkyness of the primary amine. Finally, the reaction carried out with aniline did not lead to the formation of the desired nitrone.

The nitrone **140** was obtained also from **135** in 85% yield by reaction with *N*-benzyl hydroxylamine in dry CH_2Cl_2. [178] The yields obtained with these two reactions are comparable. We would like to highlight that the one-pot reaction is an excellent tool to obtain new carbohydrate-derivative nitrones, but it cannot be carried out on a large scale (maximum 300 mg of **135**) as there was a strong decrease in yields, unlike the condensation reaction. The reaction with *N*-benzyl hydroxylamine in fact could be conducted on a gram-scale.

Table 3.7: Oxidative synthesis of nitrones **174a-h** and **140** from aldehyde **135** and primary amines **189a-i**.

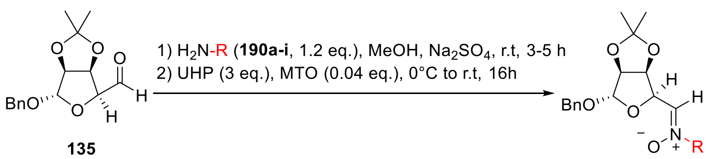

Entry	Amine 189a-i (1.2 eq.)	Nitrones	Yield
1	**189a** R= octyl	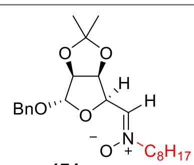 **174a**	80%

2	**189b** R= dodecyl	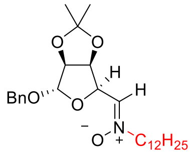 **174b**	70%
3	**189c** R= isopropyl	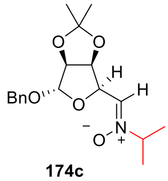 **174c**	65%
4	**189d** R= ciclohexyl	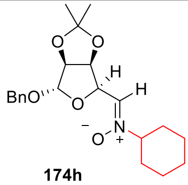 **174h**	60%
5	**189e** R= cyclopropyl	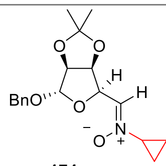 **174e**	45%
6	**189f** R= (*S*)-(-)-1-phenylethyl	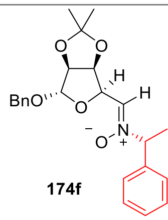 **174f**	75%
7	**189g** R= 2-(3-methoxyphenyl)ethyl	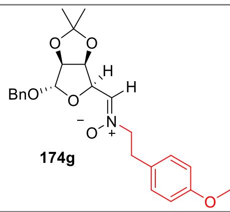 **174g**	80%
8	**189h** R= 2-methoxybenzyl	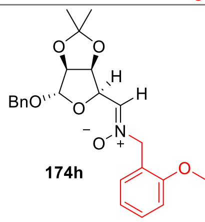 **174h**	80%

9	**189i** R= benzyl	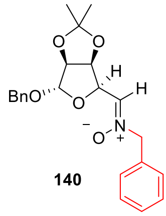 **140**	80%

These nitrones are excellent starting materials to obtain N-substituted piperidines. The nitrones **174a**, **174b** and **174d** were directly subjected to the reductive amination step, with H_2 as a reducing agent, Pd as catalyst and MeOH as solvent affording piperidines N-substituted **168**, **190** and **191** with excellent yields. Reductive amination starting from nitrone **140** provided piperidine **62** using H_2 as a reducing agent with quantitative yield (Scheme 3.10). The overall efficiency of this one-pot reaction is remarkable, considering that it results from a cascade of several synthetic steps (debenzylation, nitrone reduction, condensation with sugar aldehyde and C=N reduction).

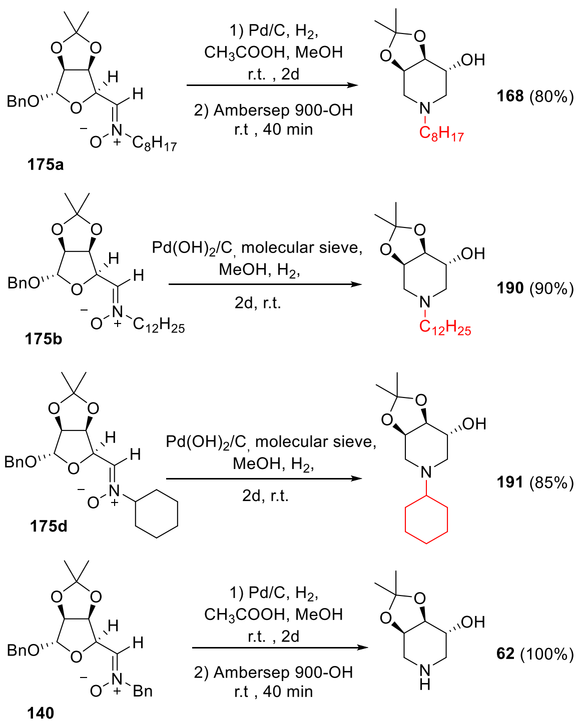

Scheme 3.10: The ring-closure reductive amination sequence starting from nitrones.

The piperidines **168** and **62** were previously obtained starting from the D-mannose derived aldehyde **135** through double reductive amination strategy (see Scheme 3.1). [174] [175] With the aim to investigate the chain length on the biological properties, starting from intermediate **190**, we synthetized the compound *N*-dodecyl piperidine **192** (Scheme 3.11) to compared with its analogue bearing an eight-carbon chain **169** on the nitrogen atom. Compound **190**, like its analogue, was also obtained through two synthetic strategies explored in our lab starting from D-mannose derived aldehyde **135**. The compound **190** was synthesized starting from nitrone **174b** through reductive amination, as described above, with an overall yield on two steps of 63% (Scheme 3.11-A) or starting from debenzylated aldehyde through double reductive amination (Scheme 3.11-B).

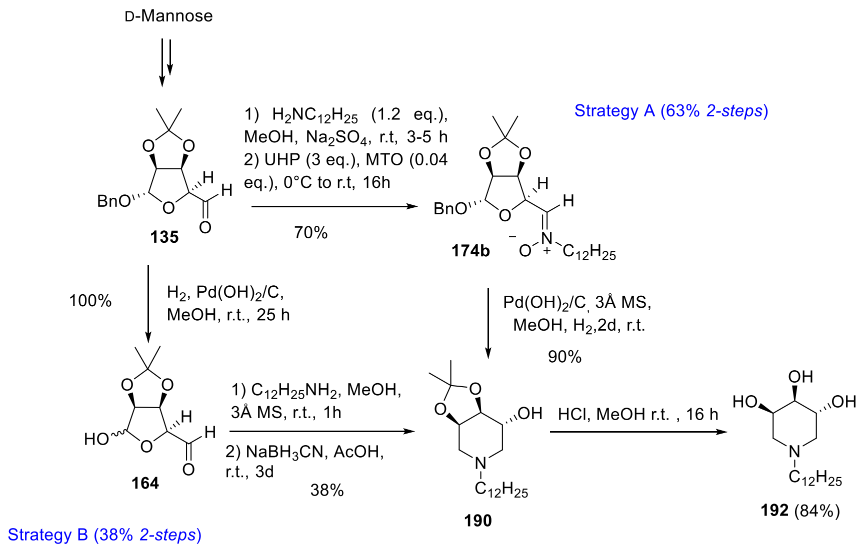

Scheme 3.11: Synthetic strategies for obtaining the **192** compound.

In particular, the "masked" dialdehyde **135** was subjected to catalytic hydrogenation in the presence of $Pd(OH)_2/C$ to remove the benzyl group at the anomeric position thus liberating the second aldehyde moiety. Dialdehyde **164** was thus employed as the substrate for the double reductive amination reaction with dodecylamine in the presence of $NaBH_3CN$ as the reducing agent, affording piperidine **190** with an overall yield on two steps of 38%. Comparing the two synthetic strategies it is clear that strategy A allows to obtain the compound **192** with a higher yield. The limitation of this synthetic strategy is represented by the reaction scale to obtain the key nitrone **174b**. in fact, as described above, the condensation/oxidation reaction with UHP in the presence of catalytic MTO cannot be carried out on a large scale (maximum 300 mg of **135**) as there was a strong decrease in yields.

The biological evaluation towards human lysosomal enzymes and the *ex vitro* activity on fibroblasts derived from Gaucher patients bearing the N370/RecNcil mutations of *N*-dodecyl trihydroxypiperidine was investigated and compared with its analogue bearing an eight-carbon chain on the nitrogen atom.

3.2.1.2 Synthesis of 1,2-dioctyl trihydroxypiperidines from a carbohydrate-derived nitrone

The synthetic strategy based on the addition of Grignard reagent onto nitrone **174a**, followed by intramolecular RA, provided access to trihydroxypiperidines 1,2-disubstituted (**170** and **171**). Lewis acid addition during the Grignard reaction allowed access to both epimers at the newly created stererocentre, providing the target trihydroxypiperidines with both configuration at C-2. We previously observed that the addition of Grignard reagents to the carbohydrate-derived nitrone **140** proceeded with opposite diastereofacial preference in the presence of absence of a suitable Lewis acid. The addition reaction, followed by reductive amination, allowed the introduction of different alkyl groups at C-2 position of the piperidine, obtaining 2-substituted piperidines with opposite configurations. [149] [157] [158] Based on our previous work, the addition of octylMgBr to nitrone **174a** was initially investigated in THF at -78 °C for 2 h without the addition of Lewis acid. This reaction proceeded readily to give the hydroxylamine **172**, with the *S* absolute configuration at the newly formed stereocenter, as the only diastereoisomer in good yield (75%) and excellent stereoselectivity (dr >98%) (Table 3.8, Entry *1*). The configuration of the newly created stereocenter was unambiguously established by the ^{1}H-NMR spectra and 1D-NOESY study at a later stage of the synthetic strategy. The diastereoselectivity of the Grignard addition did not change by increasing the reaction temperature from −78 to 0 °C (Table 3.8, Entry *2*). The addition of octylMgBr to nitrone **174a** showed a reversal of diastereoselectivity in the presence of $BF_3{\cdot}Et_2O$ in favour of the epimeric hydroxylamines **173** with the *R* configuration of the newly formed stereocenter with excellent stereoselectivity (dr >98%) and good yield (70%) (Table 3.8, Entry *3*).

Table 3.8: Additions of Grignard reagents to nitrone **175a** performed in THF, in the presence or absence of $BF_3{\cdot}Et_2O$.

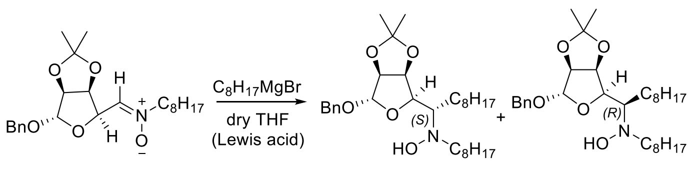

Reagent	Entry	Grignard reagent equiv.	Lewis acid (1 equiv.)	Temp (°C)	Time (h)	172 : 173 ratio	Yield
$C_8H_{17}MgBr$	**1**	1.8	none	-78	3	**172** > 98%	75%
	2	1.8	none	0	3	**172** > 98%	70%
	3	1.8	$BF_3{\cdot}Et_2O$	-30	2	**173** > 98%	70%

The stereochemical outcome of the addition reaction of octylMgBr to the nitrone **174a** in the presence or absence of Lewis acid is in agreement with the results obtained previously by our research group with the addition of several Grignard reagents onto nitrone **140**. [157] [158] The nucleophilic attack to the *Si* face of nitrone **174a** in the absence of Lewis acid led to hydroxylamine **172**, *S*-configured at the newly formed stereocenter due to the formation of a six-membered Cram-chelate transition state (Figure 3.14).

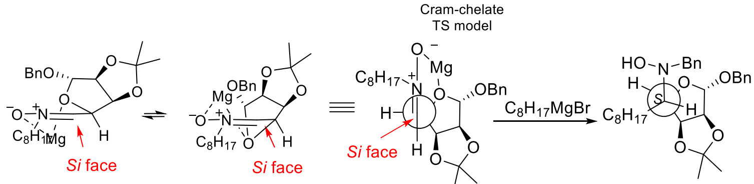

Figure 3.14: Postulated Cram-chelate transition state for the preferred nucleophilic attack to the *Si* face of nitrone **174a** in the absence of Lewis acid.

Instead, in the presence of $BF_3.Et_2O$, the nucleophilic attack to the *Re* face of the nitrone **174a** gave hydroxylamine **173**, *R*-configured at the newly formed stereocenter. We explain this result with the oxygen atom of the *N*-oxide being coordinated to the Lewis acid leaving the *Re* face of the nitrone more accessible for the attack (Figure 3.15).

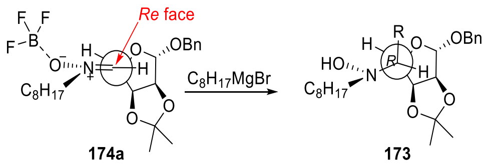

Figure 3.15: Postulated transition state for the preferred nucleophilic attack to the *Re* face of nitrone **174a** in the presence of $BF_3 \cdot Et_2O$.

The hydroxylamines **172** and **173**, derived from the addition of Grignard reagent onto **174a** nitrone, showed a spontaneous tendency to oxidize to the corresponding aldonitrones. The tendency to spontaneous oxidation was also observed previously with hydroxylamines **144** and **148** derived from the addition of Grignard reagents to nitrone **140**. [157] [158] Both hydroxylamines **172** and **173** showed a tendency to spontaneously partially oxidize to air to give the corresponding aldonitrones **193** and **194** (50% conversion as evaluated by ^{1}H-NMR upon standing in air at room temperature for 15 min, that does not proceed further). Due to the low stability of hydroxylamines **172** and **173** their characterization was only based on ^{1}H-NMR and ESI-MS analyses immediately after purification by column chromatography. Therefore, the complete characterization of pure nitrones **193** and **194** was carried out after regioselective oxidation of the hydroxylamines **172** and **173** with the hypervalent iodine reagent IBX [181] [182] in dry CH_2Cl_2, which provided the corresponding aldonitrones in excellent yields (Scheme 3.12). The reductive amination was performed on the hydroxylamine/nitrone mixtures by employing 2 equivalents of acetic acid and H_2 as a reducing agent (balloon) in the presence of Pd/C catalyst in MeOH (0.015 M), followed by treatment with a strongly basic resin to obtain **195** and **196** as free amines in excellent 90% and 80% yield, respectively, without deprotection of the acetonide groups (Scheme 3.13).

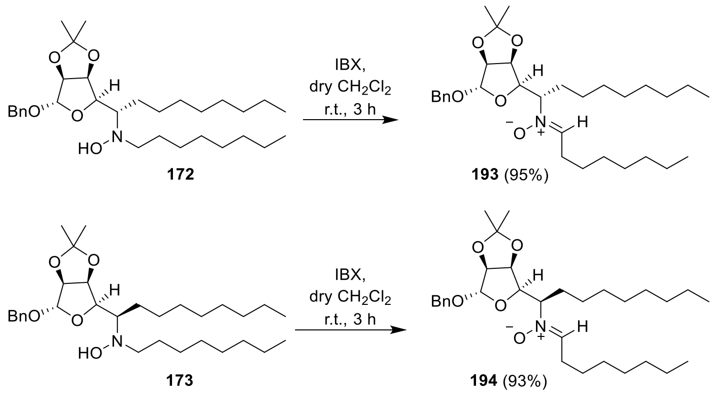

Scheme 3.12: Oxidation of hydroxylamines **172** and **173** with IBX: synthesis of nitrones **193** and **194**.

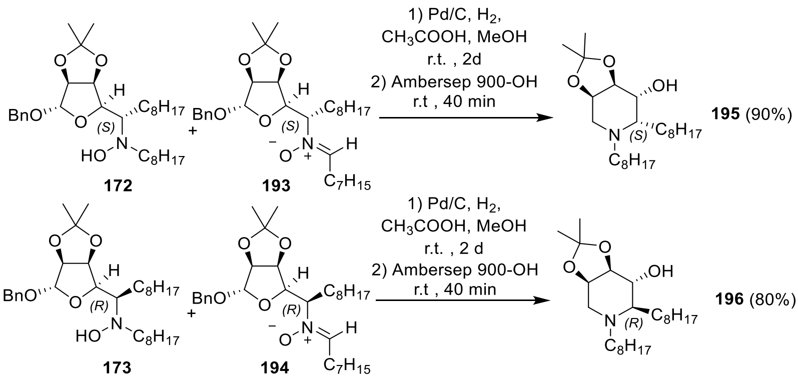

Scheme 3.13: The ring-closure reductive amination sequence.

At this stage of the synthesis, it was possible to establish unambiguously the stereochemical outcome of the Grignard addition described in Table 3.8, thanks to a careful analysis of the ^{1}H-NMR, 2D-NMR and 1D-NOESY spectra carried out on piperidines **195** and **196**. The 1H-NMR signals of the azasugar portion, together with their coupling constants, are shown in Tables 3.9 and 3.10 for piperidines **195** and **196**, respectively. The two chair conformations for each compound are reported in Figure 3.16. For derivatives **195**, 1D-NOESY did not show NOE correlation peaks between proton 2H and 4H. However, in the ^{1}H-NMR spectra the small couplings constants between 3H and 4H ($^3J_{3\text{-}4}$ = 4.0 Hz) are in agreement with the *S* absolute configuration at C-2, with the piperidine displaying a preferred $^{1}C_{4}$ conformation in which the octyl chain lies in the equatorial position and 3-H and 4-H are in a equatorial orientation (Figure3.16).

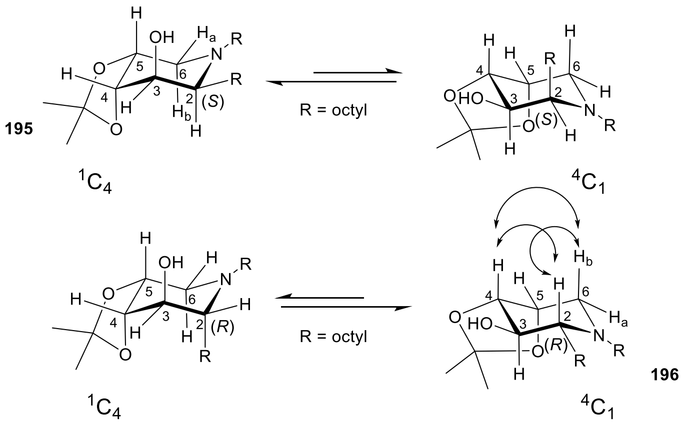

Figure 3.16: The two possible chair conformations of piperidines **195** and **196**. Double-ended arrows show the observed diagnostic NOE correlation peaks in the 1D-NOESY NMR spectra.

Table 3.9: ^{1}H-NMR chemical shifts (δ) and coupling constants (*J*) of the protons in the iminosugar portion of compound **195**.

	2H and 1'H$_a$	1'H$_b$	3H		4H		5H	6Ha		6Hb	
Comp	δ (ppm)	δ (ppm)	δ (ppm)	^{2}J ^{3}J (Hz)	δ (ppm)	^{3}J (Hz)	δ (ppm)	δ (ppm)	^{2}J ^{3}J (Hz)	δ (ppm)	^{2}J ^{3}J (Hz)
195	2.75 – 2.68 (m)	2.64 – 2.57 (m)	3.87 (dd)	6.4 4.0	4.04 (t)	6.0	4.26 –4.23 (m)	2.94 (dd)	14.0 4.0	2.82 (dd)	14.0 3.9

Table 3.10: ^{1}H-NMR chemical shifts (δ) and coupling constants (*J*) of the protons in the iminosugar portion of compound **196**.

	2H	3H		4H		5H		6H$_a$		6H$_b$ and 1'H$_a$	1'H$_b$
Comp	δ (ppm)	δ (ppm)	^{3}J (Hz)	δ (ppm)	^{3}J (Hz)	δ (ppm)	^{3}J (Hz)	δ (ppm)	^{2}J ^{3}J (Hz)	δ (ppm)	δ (ppm)
196	2.24–2.19 (m)	3.58 (t)	8.0	3.90 (t)	6.0	4.28 (q)	4.0	3.08 (dd)	13.6, 3.8	2.71–2.63 (m)	2.46 – 2.39 (m)

In the 1D-NOESY spectra of compounds **196**, strong NOE correlation peaks were observed between 2H and 4H, 4H and $6H_b$ and 2H and $6H_b$, which confirmed the *R* configuration at C-2. The axial orientation of 2H derives from a preferred $^4C1$ conformation which accommodates the octyl chain in an equatorial position (Figure3.16). The higher coupling constant observed for the signal of 4H of compound **196** was consistent with an *axial* orientation of this proton and an *ax-ax* relationship with 3-H (J = 8.0 Hz).

Final deprotection of the acetonide protecting groups under acidic conditions (aqueous HCl in MeOH) followed by basic treatment afforded the final trihydroxypiperidines **170** and **171** as free amines with good yields (Scheme 3.14).

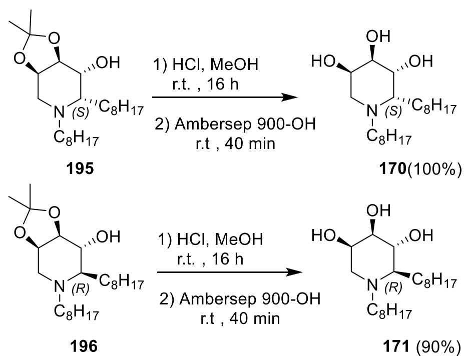

Scheme 3.14: The final deprotection step.

We then embarked with the synthesis of the trisubstituted trihydroxypiperidine **202**. We envisaged that the nitrone **194** could be a suitable intermediate to this aim. The Grignard addition to nitrone **194** proved difficult and sluggish, probably due to higher steric hindrance. The addition of heptylMgBr to nitrone **194** was initially investigated at different temperatures in dry THF without Lewis Acid but the hydroxylamine **197** was not obtained (Table 3.11, Entries 1 and 2). The addition of $BF_3{\cdot}Et_2O$ (1.0 equiv.) resulted in the formation of hydroxylamine **197** after 16 hours (Table 3.11, Entry 3). The hydroxylamine **197** was not stable and underwent rapid oxidation to the corresponding ketonitrones **198** and **199** (Scheme 3.15). In the ketonitrone **199**, the chirality center formed in the previous addition Grignard was lost. For this reason, **197** was identified only by

ESI-MS. The **198**:**199** ratio could not be determined by integration of signals into the ^{1}H-NMR spectra of the crude reaction mixture due to signals overlapping, complexity of crude and instability of ketones. The formation of ketonitrones **198** and **199** was attested through a single peak in the ESI-MS spectrum, but the two regioisomers had similar Rf with different eluents, so they were not separable by column chromatography.

Table 3.11: Additions of Grignard reagent to nitrone **194** performed in THF, in the presence or absence of Lewis acid.

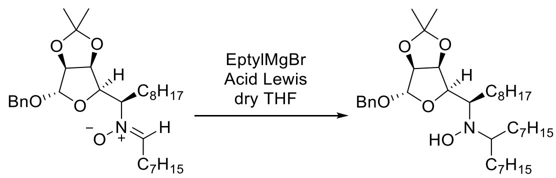

194 **197**

Reagent	Entry	Grignard reagent equiv.	Lewis acid (1 equiv.)	Temp (°C)	Time (h)	197
$C_7H_{15}MgBr$	**1**	2.5	none	-30 to r.t.	18	**n.o.**
	2	2.5	none	0 to r.t.	18	**n.o.**
	3	1.8	$BF_3 \cdot Et_2O$	-30	16	**n.s.**

not obtained (n.o.) not stable (n.s.)

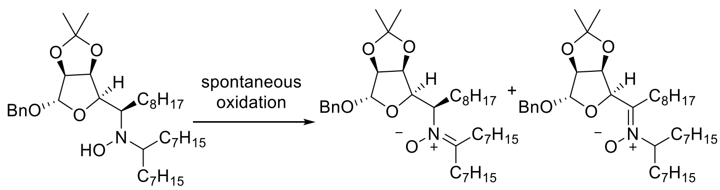

197 **198** **199**

Scheme 3.15: The hydroxylamine **197** is not stable and undergoes rapid oxidation to the corresponding ketonitrones **198** and **199**.

To overcome the rapid oxidation of the hydroxylamine **197** we employed successfully a one-pot procedure for the reduction of hydroxylamine in situ to the corresponding amine by means of indium powder in aqueous media. [206] [207] The one-pot Grignard addition-reduction allowed to obtain the corresponding amine **200** in 50% yield (Scheme 3.16). The reductive amination performed on the amine **200**, using 2 equivalents of acetic acid and H_2 as a reducing agent in the presence of Pd/C catalyst in MeOH, allowed to obtain **201** in 3 days with good 55% yield (Scheme 3.17). Final deprotection of the acetonide protecting groups performed under acidic conditions (aqueous HCl in MeOH) led to the hydrochloride salt of trihydroxypiperidines **202** (Scheme 3.17). The compound **202** will be investigated as potential inhibitor GCase and PC.

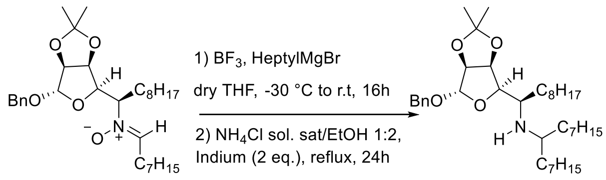

Scheme 3.16: One-Pot Grignard Additions-Reduction to Nitrone **194**.

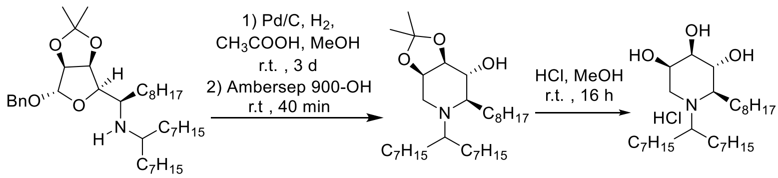

Scheme 3.17: The ring-closure reductive amination sequence and final deprotection step.

3.2.1.2 Preliminary biological screening towards commercial glycosidases

Preliminary biological screening of the whole set of compounds **170** and **171** (at 100 μM inhibitor concentration) was performed towards a panel of 12 commercial glycosidases (α-L-fucosidase EC 3.2.1.51 from Homo sapiens, α-galactosidase EC 3.2.1.22 from coffe beans, β-galactosidases EC 3.2.1.23 from Escherichia coli and Aspergillus oryzae, α-glucosidases EC 3.2.1.20 from yeast and rice, amyloglucosidase EC 3.2.1.3 from Aspergillus niger, β-glucosidase EC 3.2.1.21 from almonds, α-mannosidase EC 3.2.1.24 from Jack beans, β-mannosidase EC 3.2.1.25 from snail, β-*N*-acetylglucosaminidases EC 3.2.1.30 from Jack beans and bovine kidney). No inhibition was found except for compound **170** that showed 31% inhibition to β-glucosidase from almonds and about 40% for both compounds towards β-*N*-acetylglucosaminidase from bovine kidney at this concentration.

3.2.1.3. Inhibitory activity of GCase

The compounds **170**, **171** and **192** were tested at 1 mM for GCase inhibition in human leukocyte homogenates. The percentages of inhibition, together with the corresponding IC_{50} values, are shown in Table 6. The results obtained were compared with data of compound **169**, **147a, 151a** and **180a**. [159] [157] [158] Our results show that the newly synthesized trihydroxypiperidines were able to strongly inhibit GCase with 100% of inhibition at 1 mM with the IC_{50} values into the micromolar range (Table 3.12, Entries *8* and *9*). The trihydroxypiperidine 1,2-disubstituted **171** with the *R* configuration at C-2 (Table 3.12, Entry *9*) was more active than the corresponding epimeric trihydroxypiperidine 1,2-disubstituted **170** with the *S* configuration (Table 3.12, Entry *8*). This trend was also found in the trihydroxypiperidines alkylated at C-2 as shown in the Table 3.12 (Entries *3* and *4*). Regarding the 1,2-disubstituted trihydroxypiperidines, the presence of the additional octyl alkyl chain at the nitrogen atom did not have significant effects on the inhibitor activity. Indeed, if we compare the activity of the newly synthesized 1,2-disubstituted trihydroxypiperidines **170** and **171** with that of the trihydroxypiperidines alkylated at C-2 with the same configuration at C-2 (Table 3.12, Entry *3 vs 8 and* Entry *4 vs 9*), we can observe that the inhibitory activity was almost the same in case of **170** and slightly increased in the case of **171**. Comparing these new data with those previously reported for the *N*-octyl trihydroxypiperidine **169**, we deduce that the inhibitory activity of **170** decreased (Table 3.12, Entry *1 vs 8*), instead the inhibitory activity was slightly increased for compound **171** (Table 3.12, Entry *1 vs 9*).

The *N*-dodecyl compound **192** showed 99% inhibition when tested at 1 mM concentration, and a remarkable IC_{50} of 3.4 µM was measured (Table 3.12, Entry *2*). Compared to the inhibitory data previously found for the *N*-octyl derivative **169** (Table 3.12, Entry *1*), it clearly emerged that elongation of the chain of four carbon atoms resulted in a 10-fold increase of inhibitory activity (Table 3.12, Entry *1 vs 2*). This trend parallels what we recently observed with the analogue trihydroxypiperidines alkylated at C-2 (namely compounds **147a,b** and **151a,b**): the inhibitory activity of GCase increased in an alkyl-chain-dependent manner, with the C12 alkylated compounds being more active than the C8 alkylated. [159] [158]

Table 3.12: GCase inhibition and IC_{50} in human leukocytes from healthy donors.

Entry	Compound	GCase inhibition [%][a]	IC_{50} (μM)[b]
1	**169**	98	30.0 ± 1.0
2	**192**	99	3.4 ± 0.2
3	**147a**	80	93.5 ± 5.3
4	**151a**	100	29.3 ± 1.8
5	**180a**	50	>1000
6	**147d**	96	23.3 ± 4.0
7	**151d**	100	1.5± 0.1
8	**170**	100	100.0 ± 9.0
9	**171**	100	15.0 ± 4.0

[a] Percentage inhibition of GCase in human leukocytes extracts incubated with azasugars (1 mM). [b] IC_{50} values were determined by measuring GCase activity at different concentrations of each inhibitor.

3.2.1.4. Preliminary biological screening towards human lysosomal glycosidases

In order to investigate the selectivity of the new compounds towards GCase, **170** and **171** were tested at 1 mM towards five lysosomal glycosidases (α-mannosidase, β-mannosidase, α-galactosidase, β-galactosidase, α-fucosidase, α-glucosidase) from leukocytes isolated from healthy donors. The results are shown in the Figure 3.17.

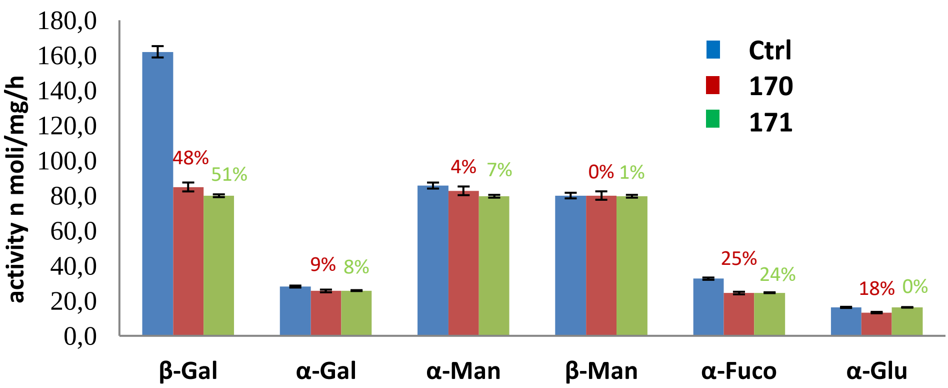

Figure 3.17: Biological screening towards six human lysosomal glycosidases.

Our data clearly showed that our compounds are selective inhibitors of the

GCase enzyme with respect to other lysosomal enzymes. Only moderate inhibitory activity was also found towards human inhibition of β-galactosidase for both compounds (~ 50%).

3.2.1.5 Pharmacological chaperoning activity

The ability of the new compounds **170** and **171** to enhance the activity of GCase was investigated in human fibroblasts derived from Gaucher patients bearing the N370/RecNcil and L444P/L444P mutations.

Unfortunately, no enzyme rescues for the new compounds were observed at the tested concentrations, after incubation (4 days), with both mutated fibroblasts. Comparing these new *in vitro* data with those previously reported for *N*-octyl trihydroxypiperidine **169** and C-2 octyl trihydroxypiperidine **147a** and **151a** [159] [157] [158], we may deduce that the simultaneous presence of two alkyl chains at the nitrogen atom and at C-2 did not lead to any pharmacological chaperoning activity towards the mutant enzyme. Rather, we highlighted higher toxicity for these compounds.

In fact, after 4 days, the flasks containing cells incubated with 100 µM and 50 µM concentrations of **170** and **171** exhibited low cell viability. We then assayed the ability of compound **192** to rescue the activity of mutant GCase in fibroblasts from Gaucher patients bearing the N370/RecNcil mutation.

Table 3.13: GCase activity rescue on N370/RecNcil mutated fibroblasts.

Entry	Compound	GCase activity rescue on N370/RecNcil mutated fibroblasts
1	**169**	1.25 fold at 100 µM
2	**192**	1.28 fold at 100 nM n.d. at 100 µM
3	**147a**	801.33 fold at 10 nM
4	**151a**	1.86 at 50 µM 1.76 fold at 100
5	**147d**	1.18 fold at 100 nM[c] n.d. at 100 µM[c]
6	**151d**	1.35 at 1 µM n.d. at 100 µM

7	**171**	no enhanchement
8	**172**	no enhanchement

n.d. = not determined

The GCase activity enhancements at different inhibitor concentrations are reported in Table 3.12 and were compared to those previously reported for C-alkylated piperidines **147a**, **151d**, **151a**, **151d** and *N*-octyl piperidine **169**.

Although a very similar enhancement in absolute value was obtained for the two N-alkylated compounds **169** and **192** (about 1.3-fold enzyme activity rescue, 30% recovery), compound **192** was active at a much lower concentration (Table 3.13, Entry 1 vs Entry 2, 100 µM vs 100 nM). This is a different trend from that observed with the C-alkylated azasugars; in that case the best GCase rescue was obtained with the C8-alkylated compound **151a**, our best PC to date (86% rescue at 50 µM), although the C12 alkylated **151b** was a better inhibitor (Table 3.13, Entry 4 vs 6). Indeed, the best inhibitors are not always the best pharmacological chaperones, since in *ex-vivo* assays other factors play a crucial role, such as cell permeability and cell viability. It is worth noting that it was not possible to evaluate the GCase rescue values at the highest concentration (50 µM and 100 µM) for the C- or *N*-dodecyl derivatives **147d**, **151d** and **192**, due to low cell viability.

Compound **192** was hypothesized to self-assemble in water due to its amphiphilic nature. With the aim of correlating the observed low cell viability in cells with the formation of micelles in aqueous dispersion, a physico-chemical characterization of compound **192** in water solution was carried out, thanks to the collaboration with Professor Pierandrea Lo Nostro at the Department of Chemistry of the University of Florence. The cmc (critical micellar concentration), the concentration above which the surfactant spontaneously produces self-assembled nanostructures in solution, was determined from surface tension measurements carried out with the Du Noüy ring method in pure water dispersions. The analysis showed a cmc value of 0.21 mM at 25° C. An MTT assay performed on N370/RecNcil mutated fibroblasts confirmed a remarkable decrease in cell viability (Figure 3.18) when compound **192** was tested at 50 µM concentration.

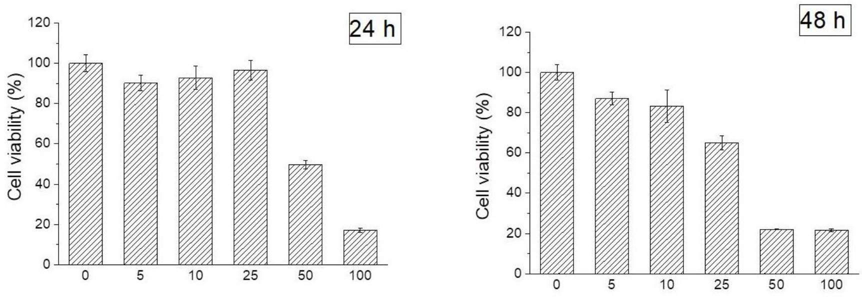

192 (μM) **192** (μM)

Figure 3.18: Fibroblasts from patients bearing N370S/RecNcil mutations on GCase enzyme were incubated for 24 and 48 h, in the presence of compound **192** at five different concentrations (5, 10, 25, 50 and 100 μM, respectively). After these times, viability of cells was evaluated using MMT assay. Value obtained were normalized with respect to control experiments. Data reported represent the mean value ± S.E.M. (n = 8).

Although the liquid medium used for the surface tension measurements is very different from the one used for the biological assessments, the concentration at which **192** is toxic to cells (50 μM) w lower than the cmc measured for this compound, and therefore its cytotoxicity can be considered independent of aggregation phenomena. This is consistent with previous reports on N-alkylated deoxynojirimycin derivatives, which showed a chain-dependent cytotoxicity for alkyl chains with above C8 carbon atoms. [208] [185]

3.2.2 Experimental Section

General Experimental Procedures for the syntheses:

Commercial reagents were used as received. All reactions were carried out under magnetic stirring and monitored by TLC on 0.25 mm silica gel plates (Merck F254). Column chromatographies were carried out on Silica Gel 60 (32–63 μm) or on silica gel (230–400 mesh, Merck). Yields refer to spectroscopically and analytically pure compounds unless otherwise stated. ^{1}H-NMR spectra were recorded on a Varian Gemini 200 MHz, a Varian Mercury 400 MHz or on a Varian INOVA 400 MHz instruments at 25 °C. ^{13}C-NMR spectra were recorded on a Varian Gemini 50 MHz or on a Varian Mercury 100 MHz instruments. Chemical shifts are reported relative to $CDCl_3$ (^{1}H: δ = 7.27 ppm, ^{13}C: δ = 77.0 ppm). Integrals are in accordance with assignments, coupling constants are given in Hz.

For detailed peak assignments 2D spectra were measured (g-COSY, g-HSQC) and 1D-NOESY. IR spectra were recorded with a IRAffinity-1S Shimadzu spectrophotometer. ESI-MS spectra were recorded with a Thermo Scientific™ LCQ fleet ion trap mass spectrometer. ICP analyses were performed with a Thermo Finnigan FLASH EA 1112 CHN/S analyser. Optical rotation measurements were performed on a JASCO DIP-370 polarimeter.

General Procedure for the Synthesis of Nitrones.

To a stirred solution of aldehyde **135** (200 mg, 0.72 mmol) and anhydrous Na_2SO_4 (380 mg) in MeOH (9 mL) at room temperature, the appropriate amine **189a-i** (1.2 equivalents) was added and the resulting mixture was stirred at room temperature under nitrogen atmosphere until a control by ^{1}H-NMR spectroscopy attested the formation of imine intermediates (for 3 hours). The reaction mixture was cooled at 0 °C and urea–hydrogen peroxide (UHP, 203 mg, 2.16 mmol), and methyltrioxorhenium (MTO, 7.2 mg, 0.29 mmol) were added sequentially. The reaction mixture was stirred at room temperature for 16 h, when a TLC check (PEt/AcOEt 1:1) attested the disappearance of the starting material and the presence of a new spot visible to the UV, then the solvent was removed under reduced pressure. CH_2Cl_2 was added to the crude mixture, and the undissolved urea was filtered off. Removal of the solvent afforded the crude product, which was purified by flash column chromatography on silica gel.

Synthesis of benzyl 2,3-*O*-(1-methylethylidene)-5-deoxy-*N*-octyl-D-lyxofuranosylamine *N*-oxide (174a): Application of the general procedure to 300 mg (1.08 mmol) of **135** with 215 µL (1.30 mmol) of octylamine furnished, after purification by column chromatography (Hex/AcOEt 2:1), 350 mg (0.86 mmol, 80%) of **174a** as a white solid (R_f = 0.34, Hex/AcOEt 2:1).

174a: white solid. m.p. 64-66 °C. $[\alpha]_D^{23}$ = – 8.2 (c =0.65, $CHCl_3$). ^{1}H NMR (400 MHz, $CDCl_3$) δ = 7.32 – 7.24 (m, 5H, Ar), 6.83 (d, J = 4.4 Hz, 1H, *H*C=N), 5.14 – 5.11 (m, 2H, 4-H and 3-H), 5.09 (s, 1H, 1-H), 4.65 (d, J = 12.0 Hz, 1H, H_a-OBn), 4.64 – 4.63 (m, 1H, 2-H), 4.43 (d, J = 12.0 Hz, 1H, H_b-OBn), 3.78 (t, J = 6.0 Hz, 2H, 1'-H), 1.95 – 1.91 (m, 1H, 2'-H_a), 1.85 – 1.83 (m, 1H, 2'-H_b), 1.38 (s, 3H, Me), 1.34 – 1.26 (m, 13H, 3'H – 7'H and Me), 0.85 (t, J = 6.0 Hz, 3H, 8'$H_{a\text{-}b\text{-}c}$) ppm. ^{13}C-NMR (100 MHz,

$CDCl_3$) δ = 137.0 (s, 1C, Ar), 135.1 (d, 1C, *C*=N), 128.5 – 127.9 (d, 5C, Ar), 112.6 (s, acetal), 105.0 (d, C-1), 85.4 (d, C-2), 79.7 (d, C-3), 76.4 (d, C-4), 69.0 (t, Bn), 65.3 (t, C-1'), 31.8 – 22.7 (t, 6C, C-2' – C-7'and q, 2C, Me), 14.1 (q, C-8') ppm. IR ($CDCl_3$): ν =970, 1028, 1101, 1161, 1209, 1267, 1356, 1456, 2232, 2928, 3034, 3066 cm^{-1}. MS (ESI): m/z (%) = 833.0 (100) $[2M+Na]^+$, 428.23 (20) $[M+Na]^+$. $C_{23}H_{35}NO_5$ (405.25): calcd. C, 68.12; H, 8.70; N, 3.45; found C,68.34; H,8.40; N,3.50.

Synthesis of benzyl 2,3-O-(1-methylethylidene)-5-deoxy-*N*-dodecyl-D-lyxofuranosylamine *N*-oxide (174b): Application of the general procedure to 200 mg (0.72 mmol) of **135** with 160 mg (0.86 mmol) of dodecylamine furnished, after purification by column chromatography (PEt /AcOEt 2:1), 233 mg (0.50 mmol, 70%) of **174b** as a white solid (R_f = 0.31, PEt /AcOEt 2:1).

174b: white solid. m.p. 95-97 °C. $[\alpha]_D^{20}$ = – 3.2 (c =0.81, $CHCl_3$). ^1H NMR (400 MHz, $CDCl_3$) δ = 7.34 – 7.26 (m, 5H, Ar), 6.86 (d, J = 4.8 Hz, 1H, *H*C=N), 5.18 – 5.14 (m, 2H, 4-H and 3-H), 5.13 (s, 1H, 1-H), 4.70 (d, J = 12.0 Hz, 1H, H_a-OBn), 4.69 – 4.66 (m, 1H, 2-H), 4.47 (d, J = 12.0 Hz, 1H, H_b-OBn), 3.82 (t, J = 7.0 Hz, 2H, 1'-H), 1.98 – 1.95 (m, 1H, 2'-H_a), 1.88 – 1.85 (m, 1H, 2'-H_b), 1.41 (s, 3H, Me), 1.32 – 1.26 (m, 21H, 3'H – 11'H and Me), 0.88 (t, J = 6.6 Hz, 3H, 12'H_{a-b-c}) ppm. ^{13}C-NMR (100 MHz, $CDCl_3$) δ = 137.1 (s, 1C, Ar), 135.2 (d, 1C, *C*=N), 128.6 – 128.0 (d, 5C, Ar), 112.7 (s, acetal), 105.1 (d, C-1), 84.7 (d, C-2), 79.8 (d, C-3), 76.5 (d, C-4), 69.1 (t, Bn), 65.5 (t, C-1'), 32.0 – 24.8 (t, 10C, C-2' – C-11'and q, 2C, Me), 14.2 (q, C-12') ppm. IR ($CDCl_3$): ν =972, 1026, 1087, 1161, 1211, 1263, 1356, 1456, 2232, 2928, 3034 cm^{-1}. MS (ESI): m/z (%) = 944.73 (100) $[2M+Na]^+$, 484.32 (30) $[M+Na]^+$. $C_{27}H_{43}NO_5$ (461.64): calcd. C, 70.25; H, 9.39; N, 3.03; found C,70.35; H,9.25; N,3.00.

Synthesis of benzyl 2,3-*O*-(1-methylethylidene)-5-deoxy-*N*-isopropyl-D-lyxofuranosylamine *N*-oxide (174c): Application of the general procedure to 200 mg (0.72 mmol) of **135** with 94 µL (0.86 mmol) of isopropylamine furnished, after purification by column chromatography (Hex /AcOEt 2:1), 157 mg (0.47 mmol, 65%) of **174c** as a colorless oil (R_f = 0.20, Hex /AcOEt 2:1).

174c: colorless oil. $[\alpha]_D^{24}$ = – 16 (c =1.00, $CHCl_3$). ^1H NMR (400 MHz, $CDCl_3$) δ = 7.36 – 7.26 (m, 5H, Ar), 6.93 (d, J = 6.8 Hz, 1H, *H*C=N), 5.20 – 5.13 (m, 2H, 4-H and

3-H), 5.12 (s, 1H, 1-H), 4.71 (d, J = 12.0 Hz, 1H, H_a-OBn), 4.70 – 4.67 (m, 1H, 2-H), 4.46 (d, J = 12.0 Hz, 1H, H_b-OBn), 4.13 (quint., J = 6.0 Hz, 1H, -CH(C*H*$_3$)$_2$), 1.47 – 1.43 (m, 6H, -CH(C*H*$_3$)$_2$), 1.41 (s, 3H, Me), 1.28 (s, 3H, Me) ppm. ^{13}C-NMR (50 MHz, $CDCl_3$) δ = 137.0 (s, 1C, Ar), 132.8 (d, 1C, *C*=N), 128.6 – 128.1 (d, 5C, Ar), 112.7 (s, acetal), 105.0 (d, C-1), 84.6 (d, C-2), 79.8 (d, C-3), 76.3 (d, C-4), 69.1 (t, Bn), 66.3 (d, -*C*H(CH$_3$)$_2$), 26.2 (q, Me), 24.8 (q, Me), 21.2 (q, -CH(*C*H$_3$)$_2$), 20.7 (q, -CH(*C*H$_3$)$_2$) ppm. IR ($CDCl_3$): ν =972, 1082, 1161, 1377, 1456, 1737, 2234, 2875, 2933, 2985, 3606, 3689 cm^{-1}. MS (ESI): m/z (%) = 358.12 (100) [M+Na]$^+$. $C_{18}H_{25}NO_5$ (335.17): calcd. C, 64.46; H, 7.51; N, 4.18; found C, 64.50; H, 7.71; N, 3.98.

Synthesis of benzyl 2,3-*O*-(1-methylethylidene)-5-deoxy-*N*-cyclohexyl-D-lyxofuranosylamine *N*-oxide (174d): Application of the general procedure to 200 mg (0.72 mmol) of **135** with 99 µL (0.86 mmol) of ciclohexylamine furnished, after purification by column chromatography (Hex/AcOEt 2:1), 162 mg (0.43 mmol, 60%) of **174d** as a white solid (R_f = 0.30, Hex/AcOEt 2:1).

174d: white solid. m.p.113-115 °C. $[\alpha]_D^{24}$ = – 11 (c =1.00, $CHCl_3$). ^{1}H NMR (400 MHz, $CDCl_3$) δ = 7.36 – 7.25 (m, 5H, Ar), 6.90 (d, J = 8.0 Hz, 1H, *H*C=N), 5.19 (t, J = 4.2 Hz, 1H, 4-H), 5.14 – 5.12 (m, 2H, 1-H and 3-H), 4.70 (d, J = 12.0 Hz, 1H, H_a-OBn), 4.67 (dd, J =6.0, 1.2 Hz, 1H, 2-H), 4.46 (d, J =12.0 Hz, 1H, H_b-OBn), 3.78 – 3.72 (m, 1H, 1’-H), 2.09 – 2.06 (m, 2H, 2’-H), 1.91 – 1.77 (m, 4H, 6’-H, 3’-H_a and 5’-H_a), 1.70 – 1.67 (m, 2H, 3’-H_b and 5’-H_b), 1.41 (s, 3H, Me), 1.36 – 1.20 (m, 5H, 4-H and Me) ppm. ^{13}C-NMR (50 MHz, $CDCl_3$) δ = 137.1 (s, 1C, Ar), 133.0 (d, 1C, *C*=N), 128.6 – 128.1 (d, 5C, Ar), 112.7 (s, acetal), 105.0 (d, C-1), 84.7 (d, C-2), 79.8 (d, C-3), 76.4 (d, C-4), 73.9 (d, C-1’), 69.0 (t, Bn), 31.4-31.0 (t, 2C, C-2’and C-6’), 26.2 – 24.8 (t, 3C, C-3’, C-4’ and C-5’and q, 2C, Me) ppm. IR ($CDCl_3$): ν = 968, 1026, 1088, 1161, 1211, 1359, 1382, 1454, 2231, 2939 cm^{-1}. MS (ESI): m/z (%) = 772.64 (100) [2M+Na]$^+$, 398.13 (98) [M+Na]$^+$. $C_{21}H_{29}NO_5$ (375.47): calcd. C, 67.18; H, 7.79; N, 3.73; found C, 67.00; H, 7.80; N, 3.75.

Synthesis of benzyl 2,3-O-(1-methylethylidene)-5-deoxy-*N*-cyclopropyl-D-lyxofuranosylamine *N*-oxide (174e): Application of the general procedure to 200 mg (0.72 mmol) of **135** with 60 µL (0.86 mmol) of cyclopropylamine furnished, after purification by column chromatography (PEt/AcOEt 2:1), 108 mg

(0.32 mmol, 45%) of **174e** as a colorless oil (R_f = 0.30, PEt/AcOEt 2:1).

174e: colorless oil. $[\alpha]_D^{25}$ = – 8.3 (c =1.00, $CHCl_3$). ^{1}H NMR (400 MHz, $CDCl_3$) δ = 7.35 – 7.26 (m, 5H, Ar), 7.08 (d, J = 8.0 Hz, 1H, HC=N), 5.26 – 5.23 (m, 1H, 4-H), 5.12 (s, 1H, 1-H), 5.07 – 5.04 (m, 1H, 3-H), 4.71 (d, J = 12.0 Hz, 1H, H_a-OBn), 4.67 – 4.68 (m, 1H, 2-H), 4.46 (d, J = 12.0 Hz, 1H, H_b-OBn), 3.59 – 3.57 (m, 1H, *c*-Pr-CH), 1.48 – 1.44 (m, 5H, *c*-Pr-CH_2 and Me), 1.28 (s, 3H, Me), 0.83 – 0.79 (m, 2H, *c*-Pr-CH_2) ppm. ^{13}C-NMR (50 MHz, $CDCl_3$) δ = 137.0 (s, 1C, Ar), 133.5 (d, 1C, *C*=N), 128.6 – 128.0 (d, 5C, Ar), 112.8 (s, acetal), 105.1 (d, C-1), 84.9 (d, C-2), 79.9 (d, C-3), 75.8 (d, C-4), 69.0 (t, Bn), 44.6 (d, c-Pr-*C*H), 26.2 (q, Me), 24.8 (q, Me), 5.6 (t, c-Pr-*C*H_2), 5.2 (t, c-Pr-*C*H_2) ppm. IR ($CDCl_3$): ν =968, 1026, 1103, 1209, 1269,1355, 1379, 1456, 2243, 2874, 2940 cm^{-1}. MS (ESI): m/z (%) = 688.55 (100) [2M+Na]$^+$, 356.14 (75) [M+Na]$^+$. $C_{18}H_{23}NO_5$ (333.38): calcd. C, 64.85; H, 6.95; N, 4.20; found C, 64.93; H, 7.03; N, 4.25.

Synthesis of benzyl 2,3-*O*-(1-methylethylidene)-5-deoxy-*N*-phenylethyl-D-lyxofuranosylamine *N*-oxide (174f): Application of the general procedure to 200 mg (0.72 mmol) of **135** with 110 µL (0.86 mmol) of (*S*)-(-)-1-phenylethylamine furnished, after purification by column chromatography (PEt/AcOEt 2:1), 214 mg (0.34 mmol, 75%) of **174f** as a white solid (R_f = 0.20, PEt/AcOEt 2:1).

174f: white solid. m.p. 97-99 °C. $[\alpha]_D^{25}$ = –5.4 (c =0.86, $CHCl_3$). ^{1}H NMR (400 MHz, $CDCl_3$) δ = 7. 50 (d, J = 8.0 Hz, 2H, Ar), 7.38 – 7.26 (m, 8H, Ar), 6.79 (d, J = 4.0 Hz, 1H, HC=N), 5.16 – 5.15 (m, 2H, 4-H and 3-H), 5.13 (s, 1H, 1-H), 5.10 (q, J = 8.0 Hz, 1H, (CH_3)C*H*Ar), 4.69 (d, J = 12.0 Hz, 1H, H_a-OBn), 4.66 – 4.65 (m, 1H, 2-H), 4.45 (d, J = 12.0 Hz, 1H, H_b-OBn), 1.84 (d, J = 6.8 Hz, 3H, (C*H_3*)CHAr), 1.35 (s, 3H, Me), 1.25 (s, 3H, Me) ppm. ^{13}C-NMR (100 MHz, $CDCl_3$) δ = 137.8 (s, 1C, Ar), 136.9 (s, 1C, Ar), 134.2 (d, 1C, C=N), 128.7 – 127.3 (d, 10C, Ar), 112.4 (s, acetal), 104.8 (d, C-1), 84.4 (d, C-2), 79.6 (d, C-3), 76.7 (d, C-4), 73.2, (d, (CH_3)CHAr), 68.9 (t, Bn), 26.0 (q, Me), 24.7 (q, Me), 18.7 (q, (CH_3)CHAr) ppm. IR ($CDCl_3$): ν = 970, 1382, 1456, 1496, 1608, 2249, 2873, 2938, 2983, 3034, 3406 cm^{-1}. MS (ESI): m/z (%) = 817.0 (100) [2M+Na]$^+$, 420.12 (61) [M+Na]$^+$. $C_{23}H_{27}NO_5$ (397.19): calcd. C, 69.50; H, 6.85; N, 3.52; found C, 69.45; H, 6.96; N, 3.65.

Synthesis of benzyl 2,3-*O*-(1-methylethylidene)-5-deoxy-*N*-(2-(3-

methoxyphenyl)ethyl)-D-lyxofuranosylamine *N*-oxide (174g): Application of the general procedure to 200 mg (0.72 mmol) of **135** with 120 µL (0.86 mmol) of 2-(3-methoxyphenyl)ethylamine furnished, after purification by column chromatography (PEt/AcOEt 2:1), 246 mg (0.58 mmol, 80%) of **174g** as a white solid (R_f = 0.20, PEt/AcOEt 2:1).

174g: white solid. m.p. 87-89 °C. $[\alpha]_D^{25}$ = – 18 (c =0.90, $CHCl_3$). ^{1}H NMR (400 MHz, $CDCl_3$) δ = 7.32 – 7.21 (m, 5H, Ar), 7.17 (t, J = 7.4 Hz, 1H, Ar-H_c), 6.76 (dd, J = 13.6, 7.6 Hz, 2H, Ar-H_b and Ar-H_d), 6.73 (s, 1H, Ar-H_a), 6.67 (d, J = 5.2 Hz, 1H, *H*C=N), 5.10 (t, J = 4.2 Hz, 1H, 4-H), 5.06 – 5.04 (m, 2H, 3-H and 1-H), 4.63 (d, J = 12.0 Hz, 1H, H_a-OBn), 4.62 – 4.60 (m, 1H, 2-H), 4.40 (d, J = 12.0 Hz, 1H, H_b-OBn), 3.98 (sext, J = 6.8 Hz, 2H, 1'-H), 3.73 (s, 3H, OCH_3), 3.18 (t, J = 7.2 Hz, 2H, 2'-H), 1.30 (s, 3H, Me), 1.23 (s, 3H, Me) ppm. ^{13}C-NMR (100 MHz, $CDCl_3$) δ = 159.9 (s, Ar-OCH_3), 139.0 (s, 1C, Ar), 137.0 (s, 1C, Ar), 135.5 (d, 1C, *C*=N), 129.8 (d, Ar-C_c), 128.5 – 128.0 (d, 5C, Ar), 121.0 (d, Ar-C_a), 114.4 (d, Ar-C_d), 112.7 (s, acetal), 112.5 (d, Ar-C_b), 105.1 (d, C-1), 84.7 (d, C-2), 79.8 (d, C-3), 76.3 (d, C-4), 68.9 (t, Bn), 66.1 (t, C-1'), 55.2 (q, OCH_3), 33.8(t, C-2'), 26.1 (q, Me), 24.7 (q, Me), ppm. IR ($CDCl_3$): ν = 976, 1078, 1159, 1211, 1379, 1460, 1490, 1604, 2241, 2839, 2876, 2941, 3032 cm^{-1}. MS (ESI): m/z (%) = 450.13 (100) $[M+Na]^+$. $C_{24}H_{29}NO_6$ (427.20): calcd. C, 67.43; H, 6.84; N, 3.28; found C,67.40; H,6.85; N, 3.22.

Synthesis of benzyl 2,3-*O*-(1-methylethylidene)-5-deoxy-*N*-(2-methoxybenzyl)-D-lyxofuranosylamine *N*-oxide (174h): Application of the general procedure to 200 mg (0.72 mmol) of **135** with 112 µL (0.86 mmol) of 2-methoxybenzylamine furnished, after purification by column chromatography (PEt/AcOEt 2:1), 238 mg (0.58 mmol, 80%) of **174h** as a white solid (R_f = 0.20, PEt/AcOEt 2:1).

174h: white solid. m.p. 118-120 °C. $[\alpha]_D^{25}$ = + 56 (c =0.65, $CHCl_3$). ^{1}H NMR (400 MHz, $CDCl_3$) δ = 7.42 – 7.26 (m, 7H, Ar, Ar-H_c and Ar-H_d), 6.99 (t, J = 6.6 Hz, 1H, Ar-H_b), 6.92 (d, J = 8.0 Hz, 1H, Ar-H_a), 6.79 (d, J = 4.0 Hz, 1H, *H*C=N), 5.17 – 5.10 (m, 2H, 4-H and 3-H), 5.09 (s, 1H, 1-H), 4.99 (q, J = 14.0 Hz, 2H, -CH_2Ar), 4.67 (d, J = 12.0 Hz, 1H, H_a-OBn), 4.66 – 4.65 (m, 1H, 2-H), 4.43 (d, J = 12.0 Hz, 1H, H_b-OBn), 3.85 (s, 3H, OCH_3), 1.35 (s, 3H, Me), 1.27 (s, 3H, Me) ppm. ^{13}C-NMR (100 MHz, $CDCl_3$) δ = 157.9 (s, Ar-OCH_3), 137.1 (s, 1C, Ar), 135.3 (d, 1C, *C*=N), 132.0 (d, Ar-C_d), 130.9 (d, Ar-C_c), 128.6 – 128.0 (d, 5C, Ar), 121.0 (d, Ar-C_b), 120.8 (s, 1C, Ar), 112.6 (s, acetal), 110.8 (d, Ar-C_a), 105.0 (d, C-1), 84.6 (d, C-2), 79.8 (d, C-3), 76.8 (d, C-4), 69.0 (t, Bn), 64.0 (t, -CH_2Ar), 55.2 (q, OCH_3), 26.2 (q, Me), 24.8 (q, Me), ppm. IR ($CDCl_3$): ν = 976, 1159, 1254, 1379, 1462, 1496, 1606, 2241, 2843, 2941, 3034 cm^{-1}. MS (ESI): m/z (%) = 849.0 (100) $[2M+Na]^+$, 436.1 (82) $[M+Na]^+$. $C_{23}H_{27}NO_6$ (413.47): calcd. C, 66.81; H, 6.58; N, 3.39; found C, 67.01; H, 6.50; N, 3.20.

Synthesis of benzyl 2,3-*O*-(1-methylethylidene)-5-deoxy-*N*-benzyl-D-lyxofuranosylamine *N*-oxide (140): Application of the general procedure to 200 mg (0.72 mmol) of **135** with 94 μL (0.86 mmol) of benzylamine furnished, after purification by column chromatography (PEt/AcOEt 3:1), 221 mg (0.56 mmol, 80%) of **140** as a white solid (R_f = 0.40, PEt/AcOEt 2:1).

140: ^{1}H-NMR (400 MHz,$CDCl_3$) δ ppm = 7.37 – 7.19 (m, 10 H,Ar), 6.75 (dd, J = 4.4, 2.4 Hz, 1H), 5.11 – 5.07 (m, 2H), 5.04 (s, 1H), 4.89 (s, 2H), 4.61 – 4.58 (m, 2H), 4.37 (d, J = 11.7 Hz, 1H), 1.30 (s, 3H), 1.21 (s, 3He) ppm. ^{13}C-NMR (50 MHz, $CDCl_3$) δ = 137.0 (q), 135.6 (s), 132.4 (d), 129.4 – 127.9 (d, 10 C), 112.6 (s, acetonide), 105.0 (d), 84.5 (d), 79.7 (d), 76.7 (d), 69.1 (t), 68.9 (t), 26.0 (q), 24.7 (q) ppm.

Synthesis of (2*S*, 3*R*, 4*S*, 5*R*)-3-hydroxy-4,5-*O*-(1-methylethylidene)- *N*-ciclohexyl-piperidine (191): To a solution of nitrone **174d** (117 mg, 0.31 mmol) in dry MeOH (30 mL), $Pd(OH)_2$/C (70 mg) was added under nitrogen atmosphere. The mixture was stirred at room temperature under hydrogen atmosphere (balloon) for 2 days, until a control by ^{1}H-NMR spectroscopy attested the presence of (3*R*,4*S*,5*R*)-5-hydroxy-3,4-*O*-(1-methylethylidene)- *N*- ciclohexyl-piperidine (**191**). The mixture was filtered through Celite® and the solvent was removed under reduced pressure to afford (2*S*, 3*R*, 4*S*, 5*R*)-3-hydroxy-4,5-*O*-(1-methylethylidene)- *N*- ciclohexyl-piperidine (67 mg, 0.26 mmol) as a colorless oil in 85% yield.

191: colorless oil. $[\alpha]_D^{24}$ = + 23 (c =1.00, $CHCl_3$). ^{1}H-NMR (400 MHz, CD_3OD) δ = 4.31 – 4.29 (m, 1H, 5-H), 3.87 – 3.84 (m, 1H, 4-H), 4.83 – 3.78 (m, 1H, 3-H), 3.04 (d, J = 12.0 Hz, 1H, 6-H_a), 2.83 (d, J = 12.0 Hz, 1H, 2-H_a), 2.76 (d, J = 15.0 Hz, 1H, 6-H_b), 2.52 – 2.41 (m, 1H, 1'H), 2.20 (t, J = 10.0 Hz, 1H, 2-H_b), 1.91– 1.89 (m, 2H, 2'H), 1.85 – 1.82 (m, 2H, 6'H), 1.68 – 1.65 (m, 1H, 4'H_a), 1.50 (s, 3H, Me), 1.45 (s, 3H, Me), 1.43– 1.22 (m, 4H, 3'H and 5'H), 1.18– 1.10 (m, 1H, 4'H_b) ppm. ^{13}C-NMR (100 MHz, CD_3OD) = 110.2 (s, acetal), 80.0 (d, C-4), 74.4 (d, C-5), 70.5 (d, C-3), 64.8 (d, C-1"), 53.3 (t, C-2), 50.7 (t, C-6), 29.6 – 26.5 (t, 5C, C-2' – C-6'and q, 2C, Me,) ppm. MS (ESI): m/z (%) = 256.16 (100) $[M+H]^+$, 278.11 (36) $[2M+Na]^+$. IR (CD_3OD): ν = 1073, 1110, 1220, 1380, 2065, 2640, 2858, 2930, 3340 cm^{-1}. $C_{14}H_{25}NO_3$ (255.36): calcd. C, 65.85; H, 9.87; N, 5.49; found C, 65.87; H, 9.77; N, 5.53.

Synthesis of (2*S*, 3*R*, 4*S*, 5*R*)-3-hydroxy-4,5-*O*-(1-methylethylidene) -*N*-octyl-piperidine (168): To a mixture nitrone **174a** (75 mg, 0.18 mmol) in dry MeOH (16 mL), acid acetic (2 equivalents) and Pd/C (40 mg) were added under nitrogen atmosphere. The mixture was stirred at room temperature under hydrogen atmosphere (balloon) for 2 days, until a control by ^{1}H-NMR spectroscopy attested the presence of acetate salt of (2*S*, 3*R*, 4*S*, 5*R*)-3-hydroxy-4,5-*O*-(1-methylethylidene) -*N*-octyl-piperidine (**168**). The mixture was filtered through Celite® and the solvent was removed under reduced pressure. The corresponding free amine was obtained by dissolving the residue in MeOH, then the strongly basic resin Ambersep 900-OH was added, and the mixture was stirred for 40 minutes. The resin was removed by filtration to afford (2*S*, 3*R*, 4*S*, 5*R*)-3-hydroxy-4,5-*O*-(1-methylethylidene) -*N*-octyl-piperidine (41 mg, 0.14 mmol) as a white solid in 80% yield.

168:^{1}H-NMR (400 MHz, $CDCl_3$) δ = 4.27 (dt, *J* = 7.6, 5.1 Hz, 1H), 4.08 (dd, *J* = 4.9, 3.9 Hz, 1H), 3.95 (dd, *J* = 7.6, 3.8 Hz, 1H), 2.82 (ddd, *J* = 7.7, 6.3, 1.5 Hz, 1H), 2.56 (d, *J* = 2.4 Hz, 2H), 2.43-2.34 (m, 3H), 1.50 (s, 3H), 1.48-1.41 (m, 4H) 1.35 (s, 3H), 1.33-1.20 (m, 8H), 0.88 (t, *J* = 6.8 Hz, 3H) ppm.

Synthesis of (2*S*, 3*R*, 4*S*, 5*R*)-3-hydroxy-4,5-*O*-(1-methylethylidene) -*N*-dodecyl-piperidine (190): To a solution of nitrone **174b** (65 mg, 0.14 mmol) in dry MeOH (15 mL), $Pd(OH)_2/C$ (40 mg) was added under nitrogen atmosphere. The mixture was stirred at room temperature under hydrogen atmosphere (balloon) for 2 days, until a control by ^{1}H-NMR spectroscopy attested the presence of (2*S*, 3*R*, 4*S*, 5*R*)-3-hydroxy-4,5-*O*-(1-methylethylidene)-*N*-dodecyl-piperidine (**190**). The mixture was filtered through Celite® and the solvent was removed under reduced pressure to afford (2*S*, 3*R*, 4*S*, 5*R*)-3-hydroxy-4,5-*O*-(1-methylethylidene) -*N*-dodecyl-piperidine (38 mg, 0.13 mmol) as a waxy solid in 90% yield.

190: colourless waxy solid. $[\alpha]_D^{22}$= + 12 (c =0.31 in $CHCl_3$); ^{1}H-NMR (400 MHz, $CDCl_3$): δ= 4.31 (pq, J = 6.2 Hz, 1H, 3-H), 4.08 (t, J = 4.4 Hz, 1H, 4-H), 3.97-3.94 (m, 1H, 5-H), 2.82 (dd, J = 12.0, 6.0 Hz, 1H, 2-H_a), 2.58 (d, J = 2.9 Hz, 2H, 6-H), 2.42-2.35 (m, 3H, 2-H_b and 1'H), 1.50-1.46 (m, 5H, Me and 2'H), 1.36 (s, 3H, Me), 1.31-1.25 (m, 18H, from 3'H to 11'H), 0.87 (t, J = 6.8 Hz, 3H, 12'H) ppm; ^{13}C-NMR (50 MHz, $CDCl_3$): δ= 109.5 (s, acetal), 77.3 (d, C-4), 72.4 (d, C-3), 67.8 (d, C-5), 58.1 (t, C-1'), 56.1 (t, C-2), 55.8 (t, C-6), 32.1-22.9(12C, t from C-2' to C-11'), 14.3 (q, C-12') ppm; IR ($CHCl_3$): ν = 3458, 2928, 2854, 1468, 1456, 1404, 1383, 1246, 1144 cm^{-1}. MS (ESI): *m/z* calcd (%) for $C_{20}H_{39}NO_3$ 341.29; found: 342.33 (100%, $[M+H]^+$). Elemental analysis**:** $C_{20}H_{39}NO_3$ (341.53) calcd. C, 70.33; H, 11.51; N, 4.10; found C, 70.51; H, 11.72, N, 4.22.

Synthesis of (3*R*,4*S*,5*R*)-5-hydroxy-3,4-*O*-(1-methylethylidene)-piperidine (62): To a solution of nitrone **140** (915 mg, 2.39 mmol) in dry MeOH (150 mL), acid acetic (2 equivalents) and Pd/C (458 mg) were added under nitrogen atmosphere. The mixture was stirred at room temperature under hydrogen atmosphere (balloon) for 2 days, until a control by ^{1}H-NMR spectroscopy attested the presence of acetate salt of (3*R*,4*S*,5*R*)-5-hydroxy-3,4-*O*-(1-methylethylidene)-piperidine (**62**). The mixture was filtered through Celite® and the solvent was removed under reduced pressure. The corresponding free amine was obtained by dissolving the residue in MeOH, then the strongly basic resin Ambersep 900-OH was added, and the mixture was stirred for 40 minutes. The resin was removed by filtration to afford (3*R*,4*S*,5*R*)-5-hydroxy-3,4-*O*-(1-methylethylidene)-piperidine (414 mg, 2.39 mmol) in 100% yield.

62: ^{1}H-NMR (400 MHz, CD_3OD) δ ppm: 4.26-4.16 (m, 1H,), 3.91 (t, J= 6.1 Hz, 1H), 3.75-3.62 (m, 1H), 3.13 (dd, J= 14.5, 2.5 Hz, 1H), 3.01-2.94 (m, 1H), 2.94-2.86 (m, 1H), 2.38 (dd, J= 13.1, 9.2 Hz, 1H), 1.50 (s, 3H, Me), 1.35 (s, 3H, Me).

Synthesis of (3*R*,5*R*)-1-dodecylpiperidine-3,4,5-triol (192): To a solution of **190** (563 mg, 1.65 mmol) in 55 mL of methanol, 1.38 ml of 37% HCl were added and the mixture was stirred at room temperature for 18 hours. After that an ^{1}H-NMR showed the disappearance of the methyl groups, the solvent was removed under reduced pressure. The crude was purified by FCC (CH_2Cl_2:MeOH:NH_3 10:1:0.1) affording pure **192** (R_f = 0.25, 419 mg, 1.39 mmol, 84% yield) as a white powder.

192: white powder. $[\alpha]_D^{22}$= – 20 (c =0.91 in MeOH); ^{1}H-NMR (400 MHz, CD_3OD): δ= 3.90 (dt, J = 5.7, 2.9 Hz, 1H, 3-H), 3.80 (td, J = 7.9, 4.0 Hz, 1H, 5-H), 3.42-3.39 (m, 1H, 4-H), 2.85-2.73 (m, 2H, 6-H_a and 2-H_a), 2.44-2.17 (m, 3H, 1'H and 2-H_b), 2.06-2.02 (m, 1H, 6-H_b), 1.54-1.45 (m, 2H, 2'H), 1.31-1.27 (m, 18H, from 3'H-11'H), 0.89 (t, J= 6.8 Hz, 3H, 12'H) ppm; ^{13}C-NMR (50 MHz, CD_3OD): δ= 75.1 (d, C-4), 69.5 (d, C-5), 68.9 (d, C-3), 59.2 (t, C-1'), 57.9 (t, C-2), 57.4 (t, C-6), 33.0-23.6 (10C, t, C-2' - C-11'), 14.3 (q, C-12') ppm; MS (ESI): *m/z* calcd (%) for $C_{17}H_{35}N_4O_3$ 301.26; found: 302.42 (100%, $[M+ H]^+$). Elemental analysis: $C_{17}H_{35}NO_3$ (301.53) calcd. C, 67.73; H, 11.70; N, 4.65; found C, 67.91; H, 11.53, N, 4.40.

Synthesis of hydroxylamines: benzyl-2,3-*O*-(1-methylethylidene)-β-L-gulofuranoside-5-(octyl)-5-(*N*-octyl-hydroxylamine) (173) and benzyl-2,3-*O*-(1-methylethylidene)-α-D-mannofuranoside-5-(octyl)-5-(*N*-octyl-hydroxylamine) (173).

- Procedure without Lewis acid.

A solution of nitrone **174a** in dry THF (0.03 M) was stirred at -78 °C under nitrogen atmosphere and 2.0 M solution of octylmagnesium bromide in diethyl ether (1.13 mmol, 600 µL) was slowly added. The reaction mixture was stirred at -78 °C under nitrogen atmosphere for 3 hours, when a TLC check (Hex/AcOEt 2:1) attested the disappearance of the starting material. A Saturated Ammonium Chloride Solution (10 mL) and Et_2O (10 mL) were added to the mixture at 0 °C and left stirring for 15 minutes. The two layers were separated and the aqueous layer was extracted with Et_2O (2x10 mL). The combined organic layers were washed with brine (2x30 mL), dried with Na_2SO_4 and concentrated under reduced pressure to give a mixture of hydroxylamines **172** and **173** (**172** > 98%). The crude mixture was purified by silica gel column chromatography (gradient eluent from Hex/AcOEt 12:1 to 10:1) to give 246 mg (0.47 mmol, 75%) of **172** (R_f = 0.36, Hex/AcOEt 12:1) as a colorless oil.

172: colorless oil. ^{1}H-NMR (400 MHz, $CDCl_3$) δ = 7.37 – 7.26 (m, 5H, Ar), 5.13 (s, 1H, 1-H), 5.11 (bs, OH), 4.69-4.66 (m, 2H, 3-H and H_a-OBn), 4.61 (d, J =4.0 Hz,1H, 2-H), 4.52 (d, J =12.0 Hz, 1H, H_b-OBn), 4.24 (dd, J =9.2, 3.0 Hz, 1H, 4-H), 3.31 – 3.26 (m, 1H, 5-H), 2.91 – 2.86 (m, 1H, 1'H_a), 2.77 – 2.72 (m, 1H, 1'H_b), 1.64 – 1.54 (m, 2H, 1"H), 1.45 – 1.27 (m, 30H, 2'H – 7'H, 1"H – 7"H, Me and Me), 0.88 (t, J = 8.0 Hz, 6H, 8'$H_{a\text{-}b\text{-}c}$ and 8"$H_{a\text{-}b\text{-}c}$) ppm. $C_{31}H_{53}NO_5$: mass required m/z = 519.77; mass found - MS (ESI) m/z (%) = 542.45 (100) $[M+Na]^+$, 520.37 (34) $[M+H]^+$.

The secondary hydroxylamine **172** spontaneously oxidize to the corresponding nitrone **193** so we could only perform ^{1}H-NMR and MS-ESI spectra immediately after their purification by column chromatography.

- Procedure with Lewis acid.

To a stirred solution of nitrone **174a** in dry THF (0.03 M) at room temperature, boron trifluoride diethyl etherate (0.82 mmol, 100 µL) was added and the resulting mixture was stirred at room temperature under nitrogen atmosphere for 15 minutes. The reaction mixture was cooled at -30 °C and 2.0 M solution of octylmagnesium bromide in diethyl ether (1.48 mmol, 800 µL) was slowly added. The reaction mixture was stirred at -30 °C under nitrogen atmosphere for 2 hours, when a TLC check (Hex/AcOEt 2:1) attested the disappearance of the starting material. A Saturated Ammonium Chloride Solution (10 mL) and Et_2O (10 mL) were added to the mixture at 0 °C and left stirring for 20 minutes. The two layers were separated and the aqueous layer was extracted with Et_2O (2x10 mL). The combined organic layers were washed with brine (2x30 mL), dried with Na_2SO_4 and concentrated under reduced pressure to give a mixture of hydroxylamines **172** and **173** (**173** > 98%). The crude mixture was purified by silica gel column chromatography (gradient eluent from Hex/AcOEt 12:1 to 10:1) to give 298 mg (0.57 mmol, 70%) of **173** (R_f = 0.20, Hex/AcOEt 12:1) as a colorless oil.

173: colorless oil. ^{1}H-NMR (400 MHz, $CDCl_3$) δ = 7.34 – 7.25 (m, 5H, Ar), 6.54 (bs, OH), 5.07 (s, 1H, 1-H), 4.77 – 4.76 (m, 1H, 3-H), 4.66 (d, J =12.0 Hz, 1H, H_a-OBn), 4.61 (d, J = 4.0 Hz, 1H, 2-H), 4.48 (d, J =12.0 Hz, 1H, H_b-OBn), 4.32 – 4.29 (m, 1H, 4-H), 3.30 (q, J =8.0 Hz, 1H, 5-H), 2.77 – 2.69 (m, 2H, 1'H), 1.65 – 1.58 (m, 2H, 1"H), 1.48 – 1.28 (m, 30H, 2'H – 7'H, 1"H – 7"H, Me and Me), 0.89 (t, J = 6.0 Hz, 6H, 8'$H_{a\text{-}b\text{-}c}$ and 8"$H_{a\text{-}b\text{-}c}$) ppm. $C_{31}H_{53}NO_5$: mass required m/z = 519.77; mass found - MS (ESI) m/z (%) = 520.36 (100) $[M+H]^+$, 542.31 (46) $[M+Na]^+$.

The secondary hydroxylamine **173** spontaneously oxidize to the corresponding nitrone **194**, so we could only perform the ^{1}H-NMR and MS-ESI spectra immediately after their purification by column chromatography.

Synthesis of benzyl-2,3-*O*-(1-methylethylidene)-β-L-gulofuranoside-5-(octyl)-5-(octyl oxide) (193): To a stirred solution of hydroxylamine **172** (213 mg, 0.41 mmol) in dry CH_2Cl_2 (6 mL), IBX (2-Iodoxybenzoic acid contains stabilizer (45 wt. %)-Sigma-Aldrich) (382 mg, 0.62 mmol) was added and the resulting mixture was stirred under nitrogen atmosphere at room temperature for 3 h, when a TLC check (Hex/AcOEt 12:1) attested the disappearance of the starting material. Saturated solution of $NaHCO_3$ (10 mL) was added and the two layers were separated and the aqueous layer was extracted with CH_2Cl_2 (3x10 mL). The combined organic layers were washed with brine (2x15 mL) and concentrated after drying with Na_2SO_4. The residue was purified by silica gel flash column chromatography (Hex/AcOEt from 2:1) to give 202 mg (0.39 mmol, 95%) of nitrone **193** (R_f =0.34, Hex/AcOEt from 2:1) as a straw yellow oil.
193: straw yellow oil. $[\alpha]_D^{24}$ = + 80 (c =0.80, $CHCl_3$). ^{1}H-NMR (400 MHz, $CDCl_3$) δ = 7.32 – 7.26 (m, 5H, Ar), 6.71 (t, J = 6.0 Hz, 1H, HC=N), 5.00 (s, 1H, 1-H), 4.71 – 4.70 (m, 1H, 3-H), 4.65 (s, 1H, H_a-OBn), 4.63 (d, J = 4.0 Hz, 1H, 2-H), 4.53 (dd, J = 8.0, 4.0 Hz, 1H, 4-H), 4.39 (d, J =12.0 Hz, 1H, H_b-OBn), 3.83 (t, J =10.0 Hz, 1H, 5-H), 2.55 (q, J = 6.7 Hz, 2H, 1'H), 2.06 (q, J = 10.7 Hz, 1H, 1"H_a), 1.60 – 1.54 (m, 3H, 2'H and 1"H_b), 1.45 (s, 3H, Me), 1.40 – 1.25 (m, 23H, Me, 3'H – 6'H, 2"H – 7"H), 0.89 – 0.84 (m, 6H, 8'H_{a-b-c} and 8"H_{a-b-c}) ppm. ^{13}C-NMR (50 MHz, $CDCl_3$) δ = 139.8 (d, 1C, *C*=N), 137.4 (s, 1C, Ar), 128.6 – 127.9 (d, 5C, Ar), 112.8 (s, acetal), 104.5 (d, C-1), 85.4 (d, C-2), 79.7 (d, C-3), 78.8 (d, C-4), 75.1 (d, C-5), 68.7 (t, Bn), 32.0 – 22.8 (t, 13C, C-1' – C-6'and C-1" – C-7"; q, 2C, Me,), 14.2 (q, 2C, C-7' and C-8") ppm. MS (ESI): m/z (%) = 1057.16 (100) $[2M+Na]^+$, 540.43 (23) $[M+Na]^+$. IR ($CDCl_3$): ν = 957, 1080, 1107, 1161, 1209, 1496, 1595, 2857, 2928, 3032, 3067 cm^{-1}. $C_{31}H_{51}NO_5$ (517.38): calcd. C, 71.92; H, 9.93; N, 2.71; found C, 71.90; H, 10.05; N, 3.01.

Synthesis of benzyl-2,3-*O*-(1-methylethylidene)-α-D-mannofuranoside-5-(octyl)-5-(octyl oxide) (194): To a stirred solution of hydroxylamine **173** (150 mg, 0.29 mmol) in dry CH_2Cl_2 (4.5 mL), IBX (2-Iodoxybenzoic acid contains stabilizer (45 wt. %)-Sigma-Aldrich) (273 mg, 0.44 mmol) was added and the resulting mixture was stirred under nitrogen atmosphere at room temperature for 3 h, when a TLC check (Hex/AcOEt 12:1) attested the disappearance of the starting material. Saturated solution of $NaHCO_3$ (8 mL) was added and the two layers were separated and the aqueous layer was extracted with CH_2Cl_2 (3x8 mL). The combined organic layers were washed with brine (2x13 mL) and concentrated after drying with Na_2SO_4. The residue was purified by silica gel flash column chromatography (Hex/AcOEt from 2:1) to give 140 mg (0.27 mmol, 93%) of nitrone **194** (R_f =0.35, Hex/AcOEt from 2:1) as a straw yellow oil.

194: straw yellow oil. $[\alpha]_D^{24}$ = – 48 (c =0.72, $CHCl_3$). ^{1}H-NMR (400 MHz, $CDCl_3$) δ = 7.35 – 7.26 (m, 5H, Ar), 6.71 (t, J = 6.0 Hz, 1H, HC=N), 5.03 (s, 1H, 1-H), 4.69 – 4.67 (m, 1H, 3-H), 4.64 (d, J =12.0 Hz, 1H, H_a-OBn), 4.60 (d, J = 8.0 Hz, 1H, 2-H), 4.48 (d, J =12.0 Hz, 1H, H_b-OBn), 4.40 (dd, J = 8.0, 4.0 Hz, 1H, 4-H), 3.93 (t, J =12.0 Hz, 1H, 5-H), 2.60 – 2.41 (m, 2H, 1'H), 2.10 – 2.01 (m, 1H, 1"H_a), 1.75 – 1.69 (m, 1H, 1"H_b), 1.59 – 1.49 (m, 2H, 2'H), 1.43 (s, 3H, Me), 1.39 – 1.24 (m, 23H, Me, 3'H_a-6'H and 2"H-7"H), 0.87 (t, J = 8 Hz, 6H, 8'H_{a-b-c} and 8"H_{a-b-c}) ppm. ^{13}C-NMR (100 MHz, $CDCl_3$) δ = 141.9 (d, 1C, *C*=N), 137.4 (s, 1C, Ar), 128.6 – 127.9 (d, 5C, Ar), 112.4 (s, acetal), 105.5 (d, C-1), 85.3 (d, C-2), 79.9 (d, C-4), 79.4 (d, C-3), 73.2 (d, C-5), 69.2 (t, Bn), 32.0 – 22.7 (t, 13C, C-1' – C-6'and C-1" – C-7"; q, 2C, Me,), 14.2 (q, 2C, C-7' and C-8") ppm. MS (ESI): m/z (%) = 1057.02 (100) $[2M+Na]^+$, 540.42 (32) $[M+Na]^+$. IR ($CDCl_3$): ν = 961, 1012, 1080, 1161, 1209, 1261, 1496, 1597, 2237, 2856, 2927, 3032, 3066 cm^{-1}. $C_{31}H_{51}NO_5$ (517.38): calcd. C, 71.92; H, 9.93; N, 2.71; found C, 71.80; H, 10.00; N, 2.63.

Synthesis of (2*S*, 3*R*, 4*S*, 5*R*)-3-hydroxy-4,5-*O*-(1-methylethylidene)-2-octyl-*N*-octyl-piperidine (195): To a mixture nitrone **193** and hydroxylamine **172** in dry MeOH (0.015 M), acid acetic (2 equivalents), Pd/C (107 mg) was added under nitrogen atmosphere. The mixture was stirred at room temperature under hydrogen atmosphere (balloon) for 2 days, until a control by ^{1}H-NMR spectroscopy attested the presence of acetate salt of (3a*R*,6*S*,7*R*,7a*S*)-2,2-dimethyl-5,6-dioctylhexahydro-[1,3]dioxolo[4,5-*c*]pyridin-7-ol. The mixture was filtered through Celite® and the solvent was removed under reduced pressure. The corresponding free amine was obtained by dissolving the residue in MeOH, then the strongly basic resin Ambersep 900-OH was added, and the mixture was stirred for 40 minutes. The resin was removed by filtration and the crude product was purified on silica gel by flash column chromatography (CH_2Cl_2/MeOH/ NH_4OH (6%) 10:1:0.1) to afford 150 mg (0.38 mmol, 90%) of **195** (R_f =0.50, CH_2Cl_2/MeOH/ NH_4OH (6%) 10:1:0.1) as a white solid.

195: white solid m.p. 50-52 °C. $[\alpha]_D^{25}$ = + 23 (c =0.77, $CHCl_3$). ^{1}H-NMR (400 MHz, CD_3OD) δ = 4.26 – 4.23 (m, 1H, 5-H), 4.04 (t, J = 6.0 Hz, 1H, 4-H), 3.87 (dd, J = 6.4, 4.0 Hz, 1H, 3-H), 2.94 (dd, J = 14.0, 4.0 Hz, 1H, 6-H_a), 2.82 (dd, J = 14.0, 3.9 Hz, 1H, 6-H_b), 2.75 – 2.68 (m, 2H, 2-H and 1'H_a), 2.64 – 2.57 (m, 1H, 1'H_b), 1.55 – 1.51 (m, 6H, Me, 1"H, 2'H_a), 1.48 – 1.32 (m, 26H, Me, 2'H_b, 3'H – 7'H and 2"H – 7"H), 0.91 (t, J = 6.0 Hz, 6H, 8'$H_{a\text{-}b\text{-}c}$ and 8"$H_{a\text{-}b\text{-}c}$) ppm. ^{13}C-NMR (50 MHz, CD_3OD) = 109.8 (s, acetal), 78.3 (d, C-4), 74.6 (d, C-5), 70.1 (d, C-3), 61.8 (d, C-2), 55.8 (t, C-1'), 49.2 (t, C-6), 30.7 – 23.7 (t, 13C, C-2' – C-7'and C-1" – C-7"; q, 2C, Me,), 14.4 (q, 2C, C-8' and C-8") ppm. MS (ESI): m/z (%) = 817.04 (100) $[2M+Na]^+$, 398.43 (75) $[M+H]^+$. IR (CD_3OD): ν = 1072, 1109, 1219, 1246, 1379, 1462, 2250, 2295, 2637, 2859, 2930, 3339 cm^{-1}. $C_{24}H_{47}NO_3$ (397.36): calcd. C, 72.49; H, 11.91; N, 3.52; found C, 72.50; H, 12.05; N, 3.85.

Synthesis (2*R*, 3*R*, 4*S*, 5*R*)-3-hydroxy-4,5-*O*-(1-methylethylidene)-2-octyl-*N*-octyl-piperidine (196): To a mixture nitrone **194** and hydroxylamine **173** in dry MeOH (0.015 M), acid acetic (2 equivalents), Pd/C (125 mg) was added under nitrogen atmosphere. The mixture was stirred at room temperature under hydrogen atmosphere (balloon) for 2 days, until a control by ^{1}H-NMR spectroscopy attested the presence of acetate salt of (3a*R*,6*R*,7*R*,7a*S*)-2,2-dimethyl-5,6-dioctylhexahydro-[1,3]dioxolo[4,5-*c*]pyridin-7-ol. The mixture was filtered through Celite® and the solvent was removed under reduced pressure. The corresponding free amine was obtained by dissolving the residue in MeOH, then the strongly basic resin Ambersep 900-OH was added, and the mixture was stirred for 40 minutes. The resin was removed by filtration and the crude product was purified on silica gel by flash column chromatography (CH_2Cl_2/MeOH/ NH_4OH (6%) 10:1:0.1) to afford 150 mg (0.38 mmol, 80%) of **196** (R_f =0.50, CH_2Cl_2/MeOH/ NH_4OH (6%) 10:1:0.1) as a straw yellow oil.

196: straw yellow oil. $[\alpha]_D^{25}$ = – 27 (c =0.92, $CHCl_3$). ^{1}H-NMR (400 MHz, CD_3OD) δ = 4.28 (q, J = 4.0 Hz, 1H, 5-H), 3.90 (t, J = 6.0 Hz, 1H, 4-H), 3.58 (t, J = 8.0 Hz, 1H, 3-H), 3.08 (dd, J = 13.6, 3.8 Hz, 1H, 6-H_a), 2.71 – 2.63 (m, 2H, 6-H_b and 1'H_a), 2.46 – 2.39 (m, 1H, 1'H_b), 2.24 – 2.19 (m, 1H, 2-H), 1.71 – 1.63 (m, 1H, 1"H_a), 1.60 – 1.53(m, 1H, 1"H_b), 1.47 (s, 3H, Me), 1.44 – 1.32 (m, 27H, Me, 2'H – 7'H and 2"H – 7"H), 0.91 (t, J = 6.0 Hz, 6H, 8'$H_{a\text{-}b\text{-}c}$ and 8"$H_{a\text{-}b\text{-}c}$) ppm. ^{13}C-NMR (100 MHz, CD_3OD) = 110.0 (s, acetal), 80.7 (d, C-4), 74.2 (d, C-5), 72.0 (d, C-3), 64.2 (d, C-2), 53.3 (t, C-1'), 51.3 (t, C-6), 33.1 – 23.7 (t, 13C, C-2' – C-7'and C-1" – C-7"; q, 2C, Me,), 14.4 (q, 2C, C-8' and C-8") ppm. 1D-NOESY: Irradiation of 2-H gave a NOE at 4-H and 6-H_b, and irradiation of 4-H gave a NOE at 2-H and 6-H_b. MS (ESI): m/z (%) = 398.40 (100) [M+H]$^+$. IR (CD_3OD): ν = 1084, 1117, 1219, 1246, 1379, 1464, 2293, 2640, 2857, 2930, 3343 cm^{-1}. $C_{24}H_{47}NO_3$ (397.36): calcd. C, 72.49; H, 11.91; N, 3.52; found C,72.40; H,11.89; N, 3.50.

Synthesis of (2*S*, 3*R*, 4*R* ,5*R*)-1,2-dioctylpiperidine-3,4,5-triol (170): A solution of **195** (150 mg, 0.38 mmol) in MeOH (24 mL) was left stirring with 12 M HCl (750 µL) at room temperature for 16 h. The crude mixture was concentrated to yield the hydrochloride salt of (2*S*,3*R*,4*R*,5*R*)-1,2-dioctylpiperidine-3,4,5-triol. The corresponding free amine was obtained by dissolving the residue in MeOH, then the strongly basic resin Ambersep 900-OH was added, and the mixture was stirred for 40 minutes. The resin was removed by filtration to afford 134 mg (0.38 mmol, 100%) of **170** as orange oil.

170: orange oil. $[\alpha]_{\mathrm{D}}^{25}$ = + 12 (c =0.91, CH_3OH). ^{1}H-NMR (400 MHz, CD_3OD) δ = 3.95 – 3.93 (m, 1H, 5-H), 3.77 – 3.74 (m, 2H, 4-H and 3-H), 2.67 – 2.53 (m, 5H, 2-H, 2-H, 6-H and 1'H), 1.55 – 1.51 (m, 2H, 1"H), 1.49 – 1.31 (m, 24H, 2'H – 7'H and 2"H – 7"H), 0.90 (t, J = 6.0 Hz, 6H, 8'$H_{a\text{-}b\text{-}c}$ and 8"$H_{a\text{-}b\text{-}c}$) ppm. ^{13}C-NMR (50 MHz, CD_3OD) = 72.5 (d, C-4), 71.3 (d, C-3), 67.4 (d, C-5), 59.4 (d, C-2), 54.2 (t, C-1'), 53.2 (t, C-6), 33.1 – 23.7 (t, 13C, C-2' – C-7'and C-1" – C-7"), 14.4 (q, 2C, C-8' and C-8") ppm. MS (ESI): m/z (%) =358.42 (100) [M+H]$^+$. $C_{21}H_{43}NO_3$ (357.58): calcd. C, 70.54; H, 12.12; N, 3.92; found C, 70.54; H, 12.15; N, 4.10.

Synthesis of (2*R*, 3*R*, 4*R*, 5*R*)-1,2-dioctylpiperidine-3,4,5-triol (171): A solution of **196** (131 mg, 0.32 mmol) in MeOH (20 mL) was left stirring with 12 M HCl (650 µL) at room temperature for 16 h. The crude mixture was concentrated to yield the hydrochloride salt of (2*R*,3*R*,4*R*,5*R*)-1,2-dioctylpiperidine-3,4,5-triol. The corresponding free amine was obtained by dissolving the residue in MeOH, then the strongly basic resin Ambersep 900-OH was added, and the mixture was stirred for 40 minutes. The resin was removed by filtration to afford 107 mg (0.30 mmol, 90%) of **171** as yellow oil.

171: yellow oil. $[\alpha]_D^{25}$ = –15 (c =0.84, CH_3OH). ^{1}H-NMR (400 MHz, CD_3OD) δ = 3.84 (bs, 1H, 5-H), 3.53 (t, J = 8.0 Hz, 1H, 3-H), 3.29 – 3.24 (m, 1H, 4-H), 2.98 (dd, J = 12.0, 4.0 Hz, 1H, 6-H_a), 2.71 – 2.65 (m, 1H, 1'H_a), 2.39 – 2.32 (m, 2H, 6-H_b and 1'H_b), 2.08 – 2.06 (m, 1H, 2-H),1.78 – 1.73 (m, 1H, 1"H_a), 1.69 – 1.62 (m, 1H, 1"H_b), 1.50 – 1.32 (m, 24H, 2'H – 7'H and 2"H – 7"H), 0.90 (t, J = 6.0 Hz, 6H, 8'$H_{a\text{-}b\text{-}c}$ and 8"$H_{a\text{-}b\text{-}c}$) ppm. ^{13}C-NMR (100 MHz, CD_3OD) = 76.6 (d, C-4), 71.5 (d, C-3), 69.5 (d, C-5), 66.0 (d, C-2), 54.2 (t, C-6), 53.2 (t, C-1'), 33.1 – 23.8 (t, 13C, C-2' – C-7'and C-1" – C-7"), 14.5 (q, 2C, C-8' and C-8") ppm.MS (ESI): m/z (%) =358.42 (100) $[M+H]^+$. $C_{21}H_{43}NO_3$ (357.58): calcd. C, 70.54; H, 12.12; N, 3.92; found C,70.35; H, 11.99; N, 4.02.

Synthesis of benzyl-2,3-*O*-(1-methylethylidene)-α-D-mannofuranoside-5-(octyl)-5-(*N*-pentadecan-8-amine) (200): To a stirred solution of nitrone **194** (190 mg, 0.37 mmol) in dry THF (7 mL) at room temperature, boron trifluoride diethyl etherate (0.37 mmol, 46 µL) was added and the resulting mixture was stirred at room temperature under nitrogen atmosphere for 15 minutes. The reaction mixture was cooled at -30 °C and a solution of heptylmagnesium bromide in THF (0.74 mmol, 1.00 mL) was slowly added. The reaction mixture was stirred at room temperature under nitrogen atmosphere for 16 hours, when a TLC check (Hex/AcOEt 2:1) attested the disappearance of the starting material. A 2:1 solution of EtOH and sat. aq. NH_4Cl (3mL) and indium powder (85 mg, 0.74 mmol) are added; this mixture is heated under reflux. After completion of the reaction (TLC control), the mixture is cooled, filtered over Celite and concentrated. Then, a sat. Na_2CO_3 solution (15 mL) is added and the product is extracted with ethyl acetate (3x15 mL). The organic phase is dried over anhydrous Na_2SO_4, then filtered and concentrated. The crude mixture was purified by silica gel column chromatography (gradient eluent CH_2Cl_2/MeOH/ NH_4OH (6%) 20:1:0.1)) to give 100 mg (0.17 mmol, 50%) of **200** (R_f = 0.50, CH_2Cl_2/MeOH/ NH_4OH (6%) 20:1:0.1)) as a colorless oil.

200: colorless oil. $[\alpha]_D^{24}$ = + 9.1 (c =1.20, $CHCl_3$). ^{1}H-NMR (400 MHz, $CDCl_3$) δ = 7.34 – 7.23 (m, 5H, Ar), 5.04 (s, 1H, 1-H), 4.77 – 4.75 (m, 1H, 3-H), 4.66 (d, *J* =12.0 Hz, 1H, H_a-OBn), 4.62 – 4.59 (m, 1H, 2-H), 4.46 (d, J =12.0 Hz, 1H, H_b-OBn), 3.83 – 3.81 (m, 1H, 4-H), 3.06 – 3.05 (m, 1H, 5-H), 2.65 (brs, 1H, 6-H), 1.62 – 1.27 (m, 44H, Me, 1'H – 6'H, 2"H – 7"H, 1'''H – 6'''H, Me and Me), 0.89 – 0.87 (m, 9H, 7'H_{a-b-c} , 8"H_{a-b-c} and 7"'H_{a-b-c}) ppm. ^{13}C-NMR (50 MHz, $CDCl_3$) δ = 137.8 (s, 1C, Ar), 128.5 – 127.8 (d, 5C, Ar), 112.2 (s, acetal), 105.3 (d, C-1), 85.3 (d, C-2), 82.4 (d, C-4), 80.1 (d, C-3), 69.8 (t, Bn), 54.8 (d, C-6), 52.9 (d, C-5), 32.1 – 22.8 (t, 19C, C-1' – C-6', C-1''' – C-6'''and C-1" – C-7"; q, 2C, Me,), 14.2 (q, 3C, C-7', C-7''' and C-8") ppm. MS (ESI): m/z (%) = 602.41 (100) [M+Na]$^+$. IR ($CDCl_3$): ν = 957, 1080, 1107, 1161, 1209, 1496, 1595, 2857, 2928, 3032, 3067 cm^{-1}. $C_{38}H_{67}NO_4$ (601.96): calcd. C, 75.82; H, 11.22; N, 2.33; found C, 76.01; H, 11.02; N, 2.02.

Synthesis of (2*R*, 3*R*, 4*S*, 5*R*)-3-hydroxy-4,5-*O*-(1-methylethylidene)-2-octyl-*N*-pentadecan-8-yl-piperidine (201): To a solution of amine **200** (50 mg, 0.08 mmol) in dry MeOH (10 mL), acid acetic (2 equivalents), Pd/C (25 mg) was added under nitrogen atmosphere. The mixture was stirred at room temperature under hydrogen atmosphere (balloon) for 2 days, until a control by ^{1}H-NMR spectroscopy attested the presence of acetate salt of (2*R*, 3*R*, 4*S*, 5*R*)-3-hydroxy-4,5-*O*-(1-methylethylidene)-2-octyl-*N*- pentadecan-8-yl-piperidine. The mixture was filtered through Celite® and the solvent was removed under reduced pressure. The corresponding free amine was obtained by dissolving the residue in MeOH, then the strongly basic resin Ambersep 900-OH was added, and the mixture was stirred for 40 minutes. The resin was removed by filtration to afford **201** (20 mg, 0.04 mmol) as a straw yellow oil in 50% yield.

201: straw yellow oil. $[\alpha]_D^{24}$ = – 16 (c =0.40, $CHCl_3$).^{1}H-NMR (400 MHz, CD_3OD) δ = 4.23 – 4.21 (m, 1H, 5-H), 3.91 (t, J = 8.0 Hz, 1H, 4-H), 3.62 (t, J = 8.0 Hz, 1H, 3-H), 3.08 (dd, J = 14, 4.0 Hz, 1H, 6-H_a), 2.62 – 2.59 (m, 2H, 6-H_b and 8'H), 2.37 (brs, 1H, 2-H), 1.66 – 1.59 (m, 4H, 1"H–2''H), 1.40 (s, 3H, Me), 1.32 – 1.20 (m, 37H, Me, 2'H – 7'H, 9'H – 14'H and 3"H – 7"H), 0.91 (t, J = 6.0 Hz, 9H, 1'H_{a-b-c} , 15'H_{a-b-c} and 8"H_{a-b-c}) ppm. ^{13}C-NMR (100 MHz, CD_3OD) = 110.0 (s, acetal), 80.8 (d, C-4), 74.8 (d, C-5), 72.7 (d, C-3), 64.4 (d, C-2), 58.4 (d, C-8'), 44.9 (t, C-6), 33.1 – 30.5 (t, 19C, C-2' – C-7', C-8' – C-14' and C-1" – C-7"; q, 2C, Me,), 14.4 (q, 3C, C-1', C-15' and

C-8”) ppm. MS (ESI): m/z (%) = 496.20 (100) [M+H]$^+$. IR (CD_3OD): ν = 1084, 1246, 1380, 1463, 2293, 2640, 2857, 2930, 3342 cm^{-1}. $C_{31}H_{61}NO_3$ (495.83): calcd. C, 75.09; H, 12.40; N, 2.82; found C, 75.03; H, 12.76; N, 2.53.

Synthesis of (2*R*,3*R*,4*R*,5*R*)-2-octyl-1-(pentadecan-8-yl)-piperidine-3,4,5-triol hydrochloride (202): A solution of **201** (60 mg, 0.12 mmol) in MeOH (10 mL) was left stirring with 12 M HCl (300 µL) at room temperature for 16 h. The crude mixture was concentrated to yield the hydrochloride salt of (2*R*,3*R*,4*R*,5*R*)-2-octyl-1-(pentadecan-8-yl)-piperidine-3,4,5-triol (53 mg, 0.11 mmol) **202** as yellow waxy solid in 90% yield.

202: yellow waxy solid. $[\alpha]_D^{23}$ = – 31 (c =0.50, MeOH). ^{1}H-NMR (400 MHz, CD_3OD) δ = 4.14 (brs, 1H, 5-H), 3.81 (t, J = 9.0 Hz, 1H, 3-H), 3.56 (t, J = 8.0, 4.0 Hz, 1H, 4-H), 3.42 – 3.38 (m, 2H, 6-H_a and 8’H), 3.23 (d, J = 12.0 Hz, 1H, 6-H_b), 3.18 – 3.16 (m, 1H, 2-H), 1.92 – 1.89 (m, 2H, 1’’H), 1.84 – 1.79 (m, 2H, 7’H), 1.75 – 1.70 (m, 2H, 9’H),1.61 – 1.29 (m, 32H, 2’H – 6’H, 10’H – 14’H and 2”H – 7”H), 0.91 – 0.89 (m, 9H, 1’$H_{a\text{-}b\text{-}c}$, 15’$H_{a\text{-}b\text{-}c}$ and 8”$H_{a\text{-}b\text{-}c}$) ppm. ^{13}C-NMR (100 MHz, CD_3OD) = 74.2 (d, C-4), 71.0 (d, C-3), 66.9 (d, C-5), 66.4 (d, C-2), 63.0 (d, C-8’), 51.6 (t, C-6), 33.2 – 23.7 (t, 19C, C-2’ – C-7’, C-9’ – C-14’and C-1” – C-7”), 14.4 (q, 3C, C-1’, C-15’ and C-8”) ppm. MS (ESI): m/z (%) = 456.35 (100) [M+H]$^+$. $C_{28}H_{58}ClNO_3$ (492.23): calcd. C, 68.32; H, 11.88; N, 2.85; found C, 68.30; H, 11.90 ; N, 2.93.

Preliminary biological screening towards commercial glycosidases

The percentage (%) of inhibition towards the corresponding glycosidase was determined by quadruplicate in the presence of 100 µM of the inhibitor on the well. Each enzymatic assay (final volume 0.12 mL) contains 0.01-0.5 units/mL of the enzyme (with previous calibration) and 4.2 mM aqueous solution of the appropriate *p*-nitrophenyl glycopyranoside (substrate) buffered to the optimal pH of the enzyme. Enzyme and inhibitor were pre-incubated for 5 min at r.t., and the reaction started by addition of the substrate. After 20 min of incubation at 37 °C, the reaction was stopped by addition of 0.1 mL of sodium borate solution (pH 9.8). The *p*-nitrophenolate formed was measured by visible absorption spectroscopy at 405 nm (Asys Expert 96 spectrophotometer). Under these conditions, the *p*-nitrophenolate released led to optical densities linear with both reaction time and concentration of the enzyme.

	% Inhibition at 0.1 mM	
	170	**171**
α-L-fucosidase EC 3.2.1.51 Homo sapiens	-	-
α-galactosidase EC 3.2.1.22 coffee beans	-	-
β-galactosidase EC 3.2.1.23 *Escherichia coli*	-	-
Aspergillus oryzae	-	-
α-glucosidase EC 3.2.1.20 yeast	-	-
rice	-	-
amyloglucosidase EC 3.2.1.3 *Aspergillus niger*	-	-
β-glucosidase EC 3.2.1.21 almonds	31	-
α-mannosidase EC 3.2.1.24 Jack beans	-	-
β-mannosidase EC 3.2.1.25 snail	-	-
β-*N*-acetylglucosaminidase EC 3.2.1.30 Jack beans	-	-
bovine kidney	44	43

"-": no inhibition (or less than 15%) detected.

*Percentage of GCase inhibition of compounds **192**, **170** and **171** towards human GCase*

The azasugars **192**, **170** and **171** were screened towards GCase in leukocytes isolated from healthy donors (controls). Isolated leukocytes were disrupted by sonication, and a micro BCA protein assay kit (Sigma–Aldrich) was used to determine the total protein amount for the enzymatic assay, according to the manufacturer instructions. Enzyme activity was measured in a flat-bottomed 96-well plate. Azasugar solution (3 µL), 4.29 µg/µL leukocytes homogenate (7 µL), and substrate 4-methylumbelliferyl-β-D-glucoside (3.33 mM, 20 µL, Sigma–Aldrich) in citrate/phosphate buffer (0.1:0.2, M/M, pH 5.8) containing sodium taurocholate (0.3%) and Triton X-100 (0.15%) at 37 °C were incubated for 1 h. The reaction was stopped by addition of sodium carbonate (200 µL; 0.5M, pH 10.7) containing Triton X-100 (0.0025 %), and the fluorescence of 4-methylumbelliferone released by β-glucosidase activity was measured in SpectraMax M2 microplate reader (λex=365 nm, λem=435 nm; Molecular Devices). Percentage GCase inhibition is given with respect to the control (without azasugar). Data are mean SD (n=3).

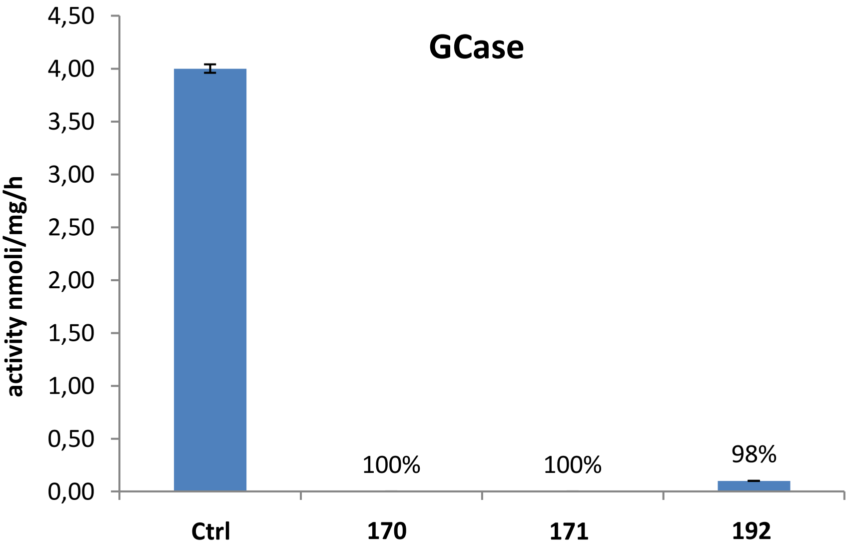

Percentage of GCase inhibition of the whole collection of compounds in human leukocytes extracts incubated with azasugars at 1 mM concentration.

IC_{50} determination: The IC_{50} values of inhibitors against GCase were determined by measuring the initial hydrolysis rate with 4-methylumbelliferyl-β-D-glucoside (3.33 mM). Data obtained were fitted to the following equation using the Origin Microcal program.

$$\frac{Vi}{Vo} = \frac{Max - Min}{1 + \left(\frac{x}{IC_{50}}\right)^{slope}} + Min$$

where V_i/V_o, represent the ratio between the activity measured in the presence of the inhibitor (V_i) and the activity of the control without the inhibitor (V_0), "x" the inhibitor concentration, Max and Min, the maximal and minimal enzymatic activity observed, respectively.

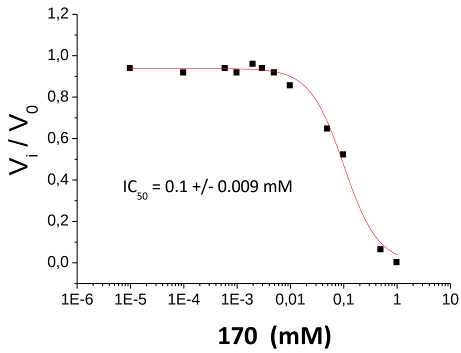

IC_{50} of compound **170** towards GCase

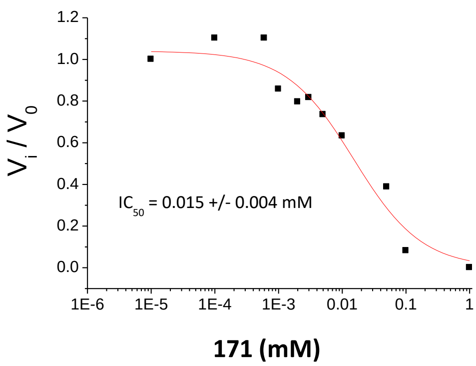

IC_{50} of compound **171** towards GCase

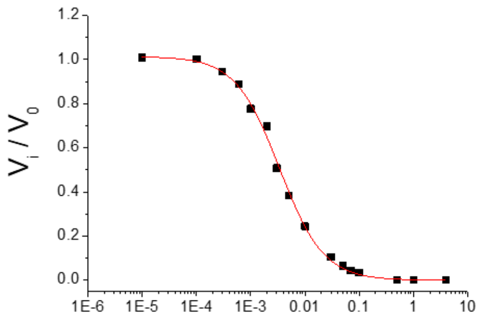

IC_{50} of compound **192** towards GCase

Preliminary biological screening towards human lysosomal glycosidases

The effect of 1mM concentration of **170** and **171** was assayed towards six lysosomal glycosidases other than GCase, namely: α-mannosidase, β-mannosidase, α-galactosidase, β-galactosidase, α-fucosidase from leukocytes isolated from healthy donors (controls) and α-glucosidase from lymphocytes isolated from healthy donors' flesh blood (controls). Isolated leukocytes or lymphocytes were disrupted by sonication, and a micro BCA protein assay kit (Sigma–Aldrich) was used to determine the total protein amount for the enzymatic assay, according to the manufacturer instructions.

α-Mannosidase activity was measured in a flat-bottomed 96-well plate. Azasugar solution (3 μL), 4.29 μg/μL leukocytes homogenate 1:10 (7 μL), and substrate 4-methylumbelliferyl-α-D-mannopyranoside (2.67 mM, 20 μL, Sigma–Aldrich) in Na phosphate/citrate buffer (0.2:0.1, M/M, pH 4.0) containing sodium azide (0.02%) were incubated at 37 °C for 1 h. The reaction was stopped by addition of sodium carbonate (200 μL; 0.5M, pH 10.7) containing Triton X-100 (0.0025 %), and the fluorescence 4-methylumbelliferone released by α-mannosidase activity was measured in SpectraMax M2 microplate reader (λex=365 nm, λem=435 nm; Molecular Devices). Inhibition is given with respect to the control (without azasugar). Data are mean SD (n=3).

β-Mannosidase activity was measured in a flat-bottomed 96-well plate. Azasugar solution (3 μL), 4.29 μg/μL leukocytes homogenate 1:10 (7 μL), and substrate 4-methylumbelliferyl-β-D-mannopyranoside (1.33 mM, 20 μL, Sigma–

Aldrich) in Na phosphate/citrate buffer (0.2:0.1, M/M, pH 4.0) containing sodium azide (0.02%) were incubated at 37 °C for 1h. The reaction was stopped by addition of sodium carbonate (200 μL; 0.5M, pH 10.7) containing Triton X-100 (0.0025 %), and the fluorescence of 4-methylumbelliferone released by β-mannosidase activity was measured in SpectraMax M2 microplate reader (λex=365 nm, λem=435 nm; Molecular Devices). Inhibition is given with respect to the control (without azasugar). Data are mean SD (n=3).

α-Galactosidase activity was measured in a flat-bottomed 96-well plate. Azasugar solution (3 μL), 4.29 μg/μL leukocytes homogenate 1:3 (7 μL), and substrate 4-methylumbelliferyl α-D-galactopyranoside (1.47 mM, 20 μL, Sigma–Aldrich) in acetate buffer (0.1 M, pH 4.5) containing sodium azide (0.02%) were incubated at 37 °C for 1 h. The reaction was stopped by addition of sodium carbonate (200 μL; 0.5M, pH 10.7) containing Triton X-100 (0.0025 %), and the fluorescence 4-methylumbelliferone released by α-galactosidase activity was measured in SpectraMax M2 microplate reader (λex=365 nm, λem=435 nm; Molecular Devices). Inhibition is given with respect to the control (without azasugar). Data are mean SD (n=3).

β- Galactosidase activity was measured in a flat-bottomed 96-well plate. Azasugar solution (3 μL), 4.29 μg/μL leukocytes homogenate 1:10 (7 μL), and substrate 4-methylumbelliferyl β-D-galactopyranoside (1.47 mM, 20 μL, Sigma–Aldrich) in acetate buffer (0.1M, pH 4.3) containing NaCl (0.1M) and sodium azide (0.02%) were incubated at 37 °C for 1 h. The reaction was stopped by addition of sodium carbonate (200 μL; 0.5M, pH 10.7) containing Triton X-100 (0.0025 %), and the fluorescence 4-methylumbelliferone released by β-galactosidase activity was measured in SpectraMax M2 microplate reader (λex=365 nm, λem=435 nm; Molecular Devices). Inhibition is given with respect to the control (without azasugar). Data are mean SD (n=3).

α-Fucosidase activity was measured in a flat-bottomed 96-well plate. Azasugar solution (3 μL), 4.29 μg/μL leukocytes homogenate 1:3 (7 μL), and substrate 4-methylumbelliferyl α-L-fucopyranoside (1.51 mM, 20 μL, Sigma–Aldrich) in Na phosphate/citrate buffer (0.2:0.1, M/M, pH 5.5) were incubated at 37 °C for 1 h. The reaction was stopped by addition of sodium carbonate (200 μL; 0.5M, pH 10.7) containing Triton X-100 (0.0025 %), and the fluorescence 4-

methylumbelliferone released by α- fucosidase activity was measured in SpectraMax M2 microplate reader (λex=365 nm, λem=435 nm; Molecular Devices). Inhibition is given with respect to the control (without azasugar). Data are mean SD (n=3).

α-Glucosidase activity was measured in a flat–bottomed 96 well plate. Azasugar solution (3 µL), 4.29 µg/µL lymphocytes homogenate (7µL) and 20 µL of substrate solution of 4-methylumbelliferyl-α-D-glucopyranoside (Sigma-Aldrich) in Na acetate buffer (0.2 M, pH 4.0) were incubated for 1 h at 37 °C. The reaction was stopped by the addition of a solution of sodium carbonate (200 µL; 0.5M, pH 10.7) containing Triton X-100 (0.0025 %), and the fluorescence of 4-methylumbelliferone released by α-glucosidase activity was measured in SpectraMax M2 microplate reader (λex=365 nm, λem=435 nm; Molecular Devices). Inhibition is given with respect to the control (without azasugar). Data are means of 3 values.

Pharmacological chaperoning activity

Fibroblasts with the N370S/RecNcil or L444P/L444P mutations from Gaucher disease patients were obtained from the “Cell line and DNA Biobank from patients affected by Genetic Diseases” (Gaslini Hospital, Genova, Italy). Fibroblasts cells (13.5-15.0 x 10^4) were seeded in T25 flasks with DMEM supplemented with fetal bovine serum (10%), penicillin/streptomycin (1%), and glutamine (1%) and incubated at 37 °C with 5% CO_2 for 24 h. The medium was removed, and fresh medium containing the azasugars was added to the cells and left for 4 days. The medium was removed, and the cells were washed with PBS and detached with tripsin to obtain cell pellets, which were washed four times with PBS, frozen and lysed by sonication in water. Enzyme activity was measured as reported above. Reported data are mean S.D. (n=2).

N370S/RecNil

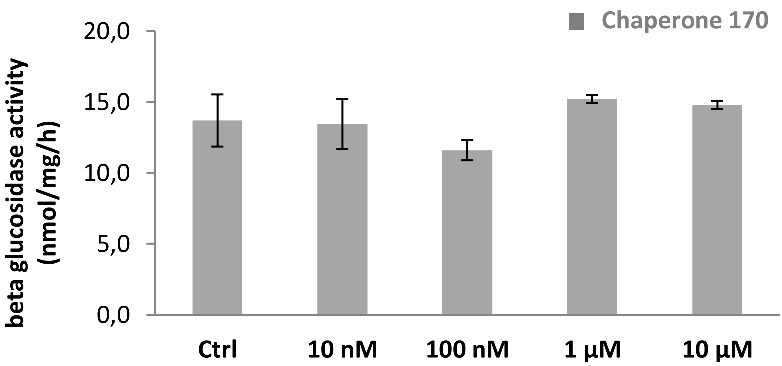

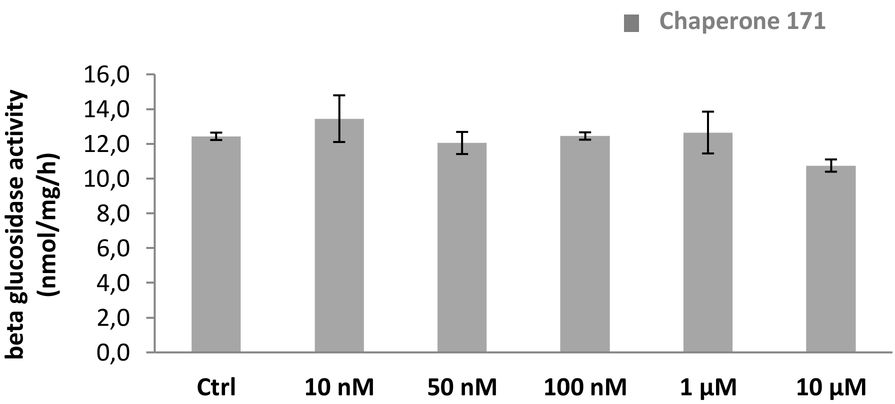

Fibroblasts derived from GD patients bearing N370/RecNcil mutations were incubated without (control, ctrl) or with different concentrations of compounds **170** or **171**. After 4 days, the flasks containing cells incubated with 50 µM and 100 µM concentrations of **170** or **171** showed low cell viability that hampered to proceed with the assay. For the other concentrations, the GCase activity was determined in lysates from treated fibroblasts. Reported data are mean S.D. (n=2).

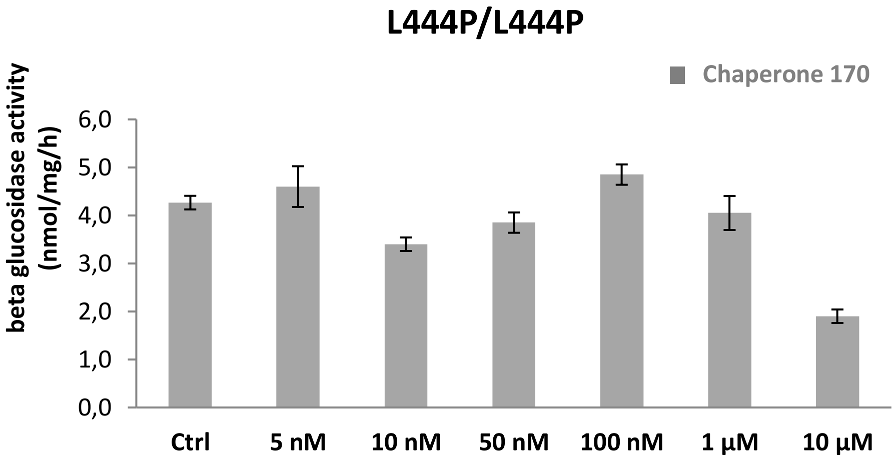

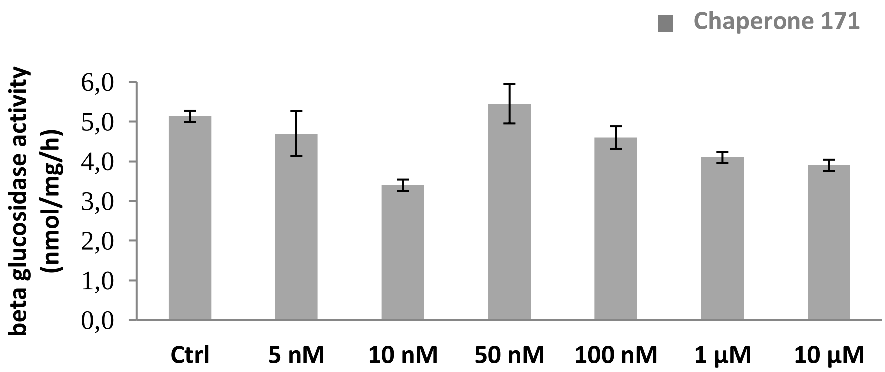

Fibroblasts derived from GD patients bearing L444P/L444P mutations were incubated without (control, ctrl) or with 7 different concentrations (5 nM, 10 nM, 50 nM, 100 nM, 1 µM, 10 µM, 50 µM) of compounds **170** or **171**. After 4 days, the flasks containing cells incubated with 50 µM concentrations of **170** or **171** showed low cell viability that hampered to proceed with the assay. For the other concentrations, the GCase activity was determined in lysates from treated fibroblasts. Reported data are mean S.D. (n=2).

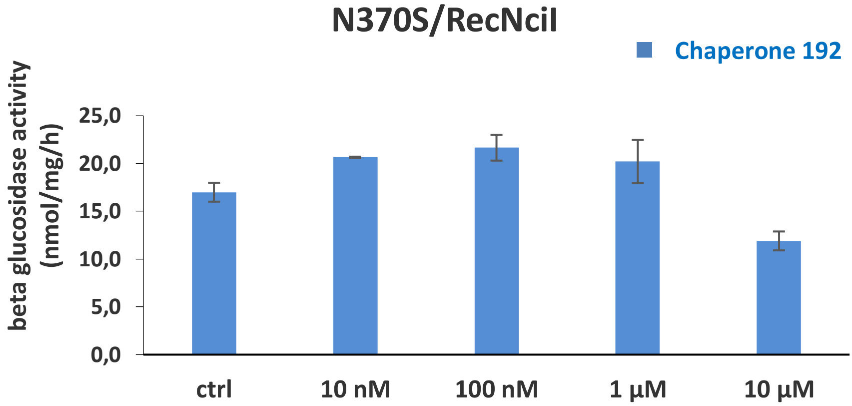

Fibroblasts derived from GD patients bearing N370/RecNcil mutations were incubated without (control, ctrl) or with 6 different concentrations (10 nM, 100 nM, 1 µM, 10 µM, 50 µM, 100 µM) of compound **192**. After 4 days, the flasks containing cells incubated with 100 µM and 50 µM concentrations of **192** showed low cell viability that hampered to proceed with the assay. For the other concentrations, the GCase activity was determined (as described) in lysates from treated fibroblasts. Reported data are mean S.D. (n=2).

Cytotoxicity tests

MTT test was carried out using human fibroblasts bearing the N370/RecNcil mutations at different concentrations. Fibroblasts were grown in the presence of Dulbecco's modified Eagle's medium supplemented with 10% fetal bovine serum (FBS), 1% glutamine, and 1% penicillin-streptomycin, at 37 °C in controlled atmosphere with 5% CO_2. For the experiments, cells were seeded at a density of 20000 cells per well in 24-well plates and grown for 24 h (or 48 h) before adding compounds. Compounds **192** was dissolved in water; then aliquots of these were diluted in the growth medium. To preserve sterility of solutions, these were filtered with 0.22 µm filters before adding to the dishes containing fibroblasts. Then, cells were incubated at 37 °C in 5% CO_2 for 24 h (or 48 h). After this time, the media were replaced with medium containing 0.5 mg/mL of 3-(4,5-dimethylthiazol-2-yl)-2,5-diphenyltetrazolium bromide (MTT); the cells were incubated for an additional 1 h at 37 °C in 5% CO_2. Finally, the number of viable cells was quantified by the estimation of their dehydrogenase activity, which reduces MTT to water-insoluble formazan. Growth medium was removed and substituted with 300 µL of DMSO to dissolve the formazan produced. The quantitation was carried out measuring the absorbance of samples at 570 nm with the iMark microplate absorbance reader (BIO RAD) in a 96-well format.

Determination of the critical micelle concentration (cmc)

The critical micellar concentration (cmc) of the sample was measured using the Du Noüy ring tensiometer (Krüss GmbH, Germany). 30 mL of a 6 mM water solution of the sample were used as starting solution and the sample was diluted directly in the measurement vessel through a microdispenser unit reaching the final concentration of $2{\cdot}10^{-6}$ M. The solution was magnetically stirred after each dilution for 30 seconds before the measurement to homogenize the sample. The immersion depth in the liquid was fixed at 0.5 mm and the return distance was set as 20% of the immersion depth to ensure the break of the meniscus on the immersed platinum-iridium ring. The radius of the ring and the wire diameter were given by the manufacturer as 9.545 mm and 0.37 mm, respectively. The measurement was performed at 25 °C and temperature was controlled using a Peltier temperature control unit with an accuracy of ±0.1 °C. Based on the input parameters (ring dimension, density and viscosity of the sample, temperature), the surface tension at each concentration was computed using Eq. X.

$$\gamma = \frac{F_{max}}{L{\cdot}cos\theta} \qquad \text{Eq. X}$$

where F_{max} is the force maximum occurring when the lamella is aligned vertically to the ring plane, γ is the interfacial tension of the liquid, θ is the contact angle between the ring and the liquid and L is the circumference of the ring.

3.3 Synthesis of "*all-cis*" trihydroxypiperidines

3.3.1 Results and discussions

3.3.1.1 Chemistry: synthesis from a carbohydrate derived ketone

The key ketone intermediate **166** offered the possibility to investigate the role of the stereochemistry and the presence of alkyl chains at C-3 on GCase inhibition, with respect to the compounds shown above in this *Chapter*.

The key ketone **166**, precursor of all the new compounds, was synthesized as previously reported from aldehyde **135**, derived in turn from inexpensive D-mannose in four steps with a high overall yield (85%). The piperidine **203** was obtained through a double reductive amination procedure [174] [209] followed by protection of the endocyclic nitrogen atom with a *tert*-butyloxycarbonyl (Boc) group. Oxidation of **203** with Dess Martin periodinane (DMP) gave ketone **166**, which was diastereoselectively reduced to the "*all-cis*" alcohol **204** with $NaBH_4$ in EtOH (Scheme 3.18). [174]

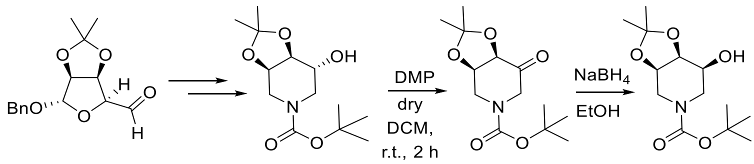

135 203 166 204

Scheme 3.18: Previous work to synthesize ketone **166** and the alcohols **203** and **204**.

The "*all-cis*" ether **205** was obtained through a Williamson synthesis following a recently reported procedure on a similar substrate. [210] Treatment of alcohol **204** with sodium hydride in dry DMF, alkylation with 1-nonyl bromide gave ether **205** with a 53% yield. Concomitant deprotection of acetonide and Boc groups under acidic conditions (aqueous HCl in MeOH), followed by treatment with the strongly basic resin Ambersep 900-OH, gave ether **175** with a 70% yield (Scheme 3.19). In order to investigate the role of different configurations at C-3 on biological activity, the diastereomeric alcohol **203** was treated similarly to give protected ether **206** with a 54% yield. Deprotection of **206** as above yielded ether **208** quantitatively (Scheme 3.19).

Ketone **166** was also converted to the amine **207** through a reductive amination employing dodecyl amine. The reaction was performed in dry MeOH under catalytic hydrogenation on $Pd(OH)_2/C$ and gave, after purification by FCC, the protected piperidine **207** with a 55% yield. Final deprotection under acidic conditions followed by treatment with Ambersep 900-OH resin gave the free amine **176** in 83% yield (Scheme 3.18). The "*all-cis*" configuration in compound **207** was established by comparison of its ^1H NMR spectrum with those of similar compounds with a different alkyl chain at the exocyclic nitrogen atom. [175] The broad singlet at 4.41 ppm observed for 4-H in the ^{1}H NMR spectrum of **207** is consistent with *eq*-*ax* relationships with both 3-H and 5-H occurring in its chair conformations.

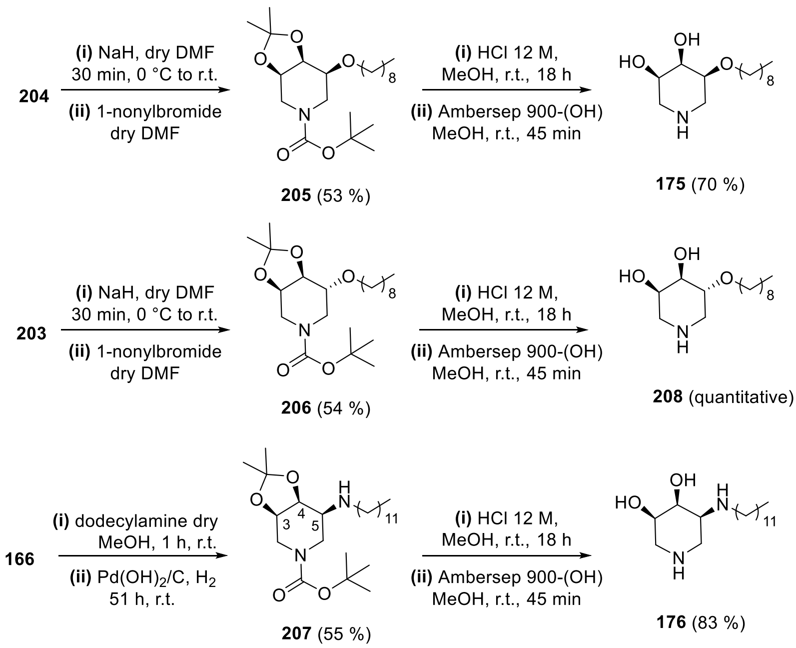

Scheme 3.19: Synthetic strategies to obtain ethers **175** and **208** and the amine **176**.

To obtain compound **177** and **178**, we turned our attention to the addition of alkynyl organometallic reagents, namely lithium acetylides generated in situ by treating terminal alkynes with butyl lithium. The results of the addition are reported in Table 3.14. The alkynes were treated with BuLi (1.5 equivalents) at -78 °C for 30 minutes, followed by the addition of ketone **166** at -78 °C. The reaction mixture was allowed to warm to room temperature and left to react for 2.5 – 3 hours, then worked-up. In both reported cases, FCC of the crude mixtures afforded good yields (77-78%) of adducts with both simple and functionalized alkenes (Table 3.14). A single diastereoisomer was obtained in all cases, which was ascribed the *S*-configuration at the newly formed C-3 stereocenter on the basis of the following considerations. Alkynyl lithium derivatives are small nucleophiles which typically prefer an axial rather than an equatorial attack on cyclohexanones [211]-[213] in order to avoid torsional strain. [214]

Table 3.14: Addition reactions of lithium acetylides to ketone **166**.

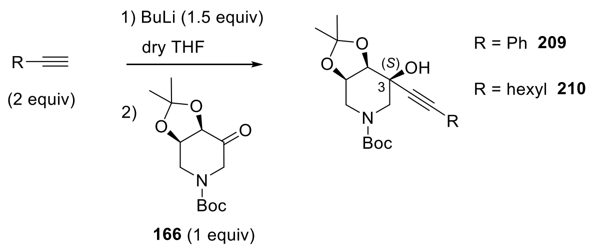

Entry[a]	Alkyne	Time (h)	Product	Yield (%)
1	phenylacetylene	2.5	**209**	77
2	1-octyne	3	**210**	78

[a]All the experiments were carried out in dry THF with temperatures ranging from -78 °C to room temperature, with ketone **166** (1.0 equiv.) and BuLi (1.5 equiv.).

In Figure 3.19 the two more stable chair conformations of ketone **166** are depicted. Only in the $^6C_3$ conformation nucleophilic axial attack at C-3 experiences a stabilizing interaction by the low lying energy σ* orbital of the antiperiplanar C-O bond at C-4, according to a favourable Felkin-Anh model. [196] [197] Thus, based on stereoelectronic and steric considerations, we assumed that nucleophilic attacks occurred selectively at the *Re* face of ketone **166**, giving the "*all-cis"* 3,4,5-trihydroxypiperidines (Figure 3.19). A careful analysis of the ^{1}H NMR spectra of derivatives and the products of their transformations supports this structural assignment (see below).

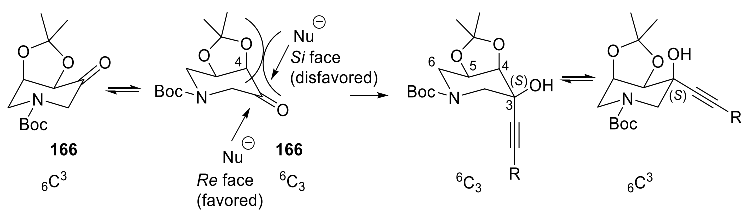

Figure 3.19: Stereochemical outcome of the addition of lithium acetylides to ketone **166**.

Compounds **209** and **210** were subjected to acidic treatment for the concomitant removal of acetonide and Boc protecting groups, leading to the "*all-cis*" trihydroxypiperidines **211** and **212** in good yields (54-71%) after treatment with the strongly basic resin Ambersep 900-OH. The triple bond was subsequently reduced by catalytic hydrogenation in the presence of $Pd(OH)_2/C$ in EtOH to give azasugars **177** and **178** (39-98%) (Scheme 3.20).

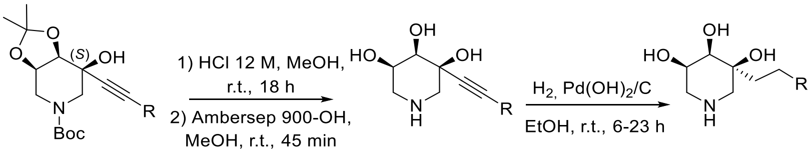

R = Ph, **209** **211** (54 %) **177** (39 %)

R = hexyl, **210** **212** (71 %) **178** (98 %)

Scheme 3.20: Synthesis of trihydroxypiperidines **177** and **178**.

Relevant chemical shifts and coupling constants are reported in Tables 3.15 and 3.16 for H-4, H-5 and H-6 in ^{1}H NMR spectra in selected compounds of the two series of protected (in $CDCl_3$) and deprotected (in CD_3OD) trihydroxypiperidines, respectively. These values show regularities (the same applies to H-2 signals) which allowed us to ascribe the same configuration at C-3 for all compounds. Moreover, the shape of the signals and their coupling constants, where detectable, are consistent with the *S* absolute configuration tentatively assigned on the basis of mechanistic considerations. Indeed, the signal of H-5 appears as a broad singlet (or as a narrow multiplet), which is in agreement with its equatorial position in a preferred chair conformation which places the R substituent equatorially, *ie*, in the (3*S*) configuration ($_6C^3$ alcohol in Figure 3.19). The lack of large *ax-ax* coupling constants is confirmed by signals of H-6. The observed upfield shift (0.3-0.5 ppm) of H-4 within the two series of compounds on turning from the alkynyl to the saturated substituents, consistent with H-4 falling in the deshielding cone of the triple bond in the former derivatives when in a *cis* relationship, further supports this assignment.

Table 3.15: Chemical shifts and coupling constants of H-4, H-5 and H-6 of protected compounds **211** and **212**, in $CDCl_3$.

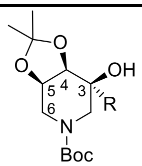	**H-4**	**H-5**	**H-6a**	**H-6b**
	δ (ppm)	δ (ppm)	δ (ppm)	δ (ppm)

R = 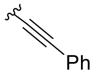, **211**	4.36 (d, J= 6.7 Hz)	4.52-4.40 (m)	3.92-3.70 (m)	3.67-3.55 (m)
R= 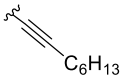, **212**	4.24 (d, J= 6.9 Hz)	4.47-4.34 (m)	3.74-3.54 (m)	

Table 3.16: Chemical shifts and coupling constants of H-4, H-5 and H-6 of protected compounds **211**, **212**, **177** and **178**, in CD_3OD.

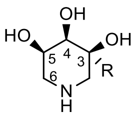	**H-4** δ (ppm)	**H-5** δ (ppm)	**H-6a** δ (ppm)	**H-6b** δ (ppm)
R = 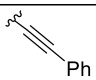, **211**	3.89 (brs)	3.98-3.91 (m)	2.86-2.76 (m)	
R = 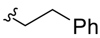, **177**	3.51 (brd, J= 2.2 Hz)	3.81 (brs)	2.96 (dd, J= 13.7, 4.0 Hz)	2.76-2.70 (m)
R= 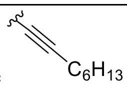, **212**	3.75 (brs)	3.90-3.84 (m)	2.78-2.70 (m)	
R = octyl, **177**	3.44 (brs)	3.77 (brs)	2.92 (d, J= 12.6 Hz)	2.68 (d, J= 12.6 Hz)

3.3.1.2 Preliminary biological screening towards commercial glycosidases

However, the screening on a panel of 12 commercial glycosidasesof compounds **176**, **178** and **208** (see Experimental section), showed that only trihydroxypiperidine **176** (bearing a dodecyl chain connected at C-3 through a nitrogen atom) was able to inhibit β-glucosidase from almonds. In particular, compound **176** showed an IC_{50} = 85 µM towards this enzyme, which prompted us to evaluate compounds all new compounds on human lysosomal β-glucosidase (GCase).

3.3.1.3 Preliminary biological screening towards β-Glucosidase

The best GCase inhibitor was compound **176**, bearing a dodecylamino substituent at C-3 (IC_{50} = 6.4 µM, Table 3, Entry 2). Regarding the newly synthesized ethers, the *"all-cis"* **175** showed an inhibitory activity towards GCase one order of magnitude greater than its epimer **208** (IC_{50} = 12 µM *vs* IC_{50} = 130 µM, Table 3, Entries 1 *vs* 5). Among the compounds derived from organometal addition reactions, the lowest inhibitory activities were observed for trihydroxypiperidines **177** and **211** bearing the phenylethyl or the phenylethynyl substituent, respectively (Table 3.17, Entries 3 and 6). Conversely compound **212**, bearing the triple bond and a longer aliphatic substituent, showed 65% inhibition, which increased considerably after hydrogenation to **178** (Table 3.17, Entries 7 *vs* 4). This latter compound showed a moderate IC_{50} = 60 µM, which is close to that observed for trihydroxypiperidines bearing an octyl chain at C-2, previously synthesized in our group (**151a** and **147a**, Table 3.17, Entries 9 and 11). [157] [158] These data overall show that GCase inhibition higher than 90% is guaranteed by the presence of a long alkyl chain (eight, nine or twelve carbon atoms, compounds **175**, **176**, **178** and **208**). This parallels previous studies which showed that alkylated imino- and azasugars are strong GCase inhibitors due to favorable interaction of the alkyl chain with the hydrophobic domain of the enzyme. [85] [195] However, in terms of IC_{50} values, a remarkable difference was found between compounds **175** and **208**, in agreement with previous observations by Martin, Compain and co-workers on differently configured ethers derived from 1,5-dideoxy, 1-5-imino-D-xylitol (DIX). [215] Moreover, good GCase inhibitors can be identified among piperidines with only two free hydroxy groups (e.g. **175**, **176** and **208**), as previously observed with different azasugars. [215]

Table 3.17: β-Galactosidase (β-Gal) and β-Glucosidase (GCase) inhibition in human leukocytes from healthy donors.

Entry	Compound	GCase	
		Inhibition (%) [a]	IC_{50} (µM) [b]
1	**175** 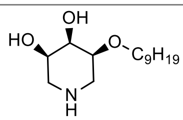	98	12 ± 6
2	**176** 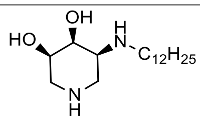	100	6.4 ± 0.7
3	**177** 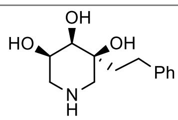	36	n.d.

4	**178**	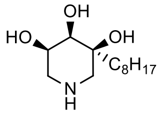	93	60 ± 23
5	**208**	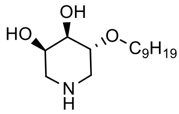	100	130 ± 13
6	**211**	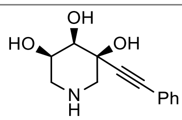	25	n.d.
7	**212**	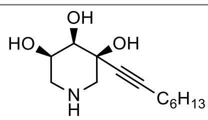	65	n.d.
8	**167**	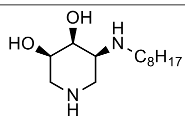	93	40 ± 3
9	**151a**	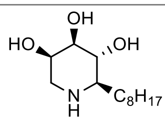	100	29 ± 2
10	**151d**	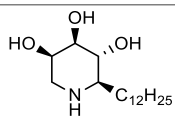	100	1.5 ± 0.1
11	**147a**	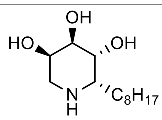	80	94 ± 5

[a] Percentage inhibition of β-glucosidase (GCase) in human leukocytes extracts incubated with compounds (1 mM).[b] IC_{50} values were determined by measuring GCase activity at different concentrations of each inhibitor for compounds (n.d.= not determined).

3.3.1.4 Pharmacological chaperoning activity

We then assayed the strongest GCase inhibitors **175**, **176** and **178** (IC_{50} lower than 100 μM) in human fibroblasts derived from Gaucher patients bearing the N370S mutation. None of the compounds gave enzyme rescue when tested at six different concentrations (10 nM, 100 nM, 1 μM, 10 μM, 50 μM, 100 μM) (see the Experimental section). In particular, compound **176** showed remarkable toxicity at the highest concentrations (50 μM, 100 μM). Notably, the stronger inhibitory activity of **176** with respect to **167** does not correspond to a higher chaperoning activity (indeed, compound **167** was able to rescue GCase activity of 1.5-fold at 100 µM). [159] The same behavior is evident by comparing the C-2 alkylated trihydroxypiperidines **151d** and 1**47a**. The best inhibitor was the dodecyl alkylated (compound **151d**) but the best chaperone was the octyl-derivative **151a**. The inefficacy of dodecyl alkylated compounds **176** and **151d** as PCs can be ascribed to the cytotoxicity imparted by the twelve-carbon atom alkyl chains. These data are also consistent with other reports on amphiphilic N-alkylated iminosugars, which suggest that cytotoxicity is strongly chain-length dependent and that potent inhibitors with chains longer than C_8 can be toxic when assayed in cell lines. [208] [216]

3.3.2 Experimental Section

General Experimental Procedures for the syntheses

Commercial reagents were used as received. All reactions were carried out under magnetic stirring and monitored by TLC on 0.25 mm silica gel plates (Merck F254). Column chromatographies were carried out on Silica Gel 60 (32–63 µm) or on silica gel (230–400 mesh, Merck). Yields refer to spectroscopically and analytically pure compounds unless otherwise stated. ^{1}H-NMR spectra were recorded on a Varian Gemini 200 MHz, a Varian Mercury 400 MHz or on a Varian INOVA 400 MHz instrument at 25 °C. ^{13}C-NMR spectra were recorded on a Varian Gemini 200 MHz or on a Varian Mercury 400 MHz instrument. Chemical shifts are reported relative to $CDCl_3$ (^{13}C: δ = 77.0 ppm), or to CD_3OD (^{13}C: δ = 49.0 ppm). Integrals are in accordance with assignments, coupling constants are given in Hz. For detailed peak assignments 2D spectra were measured (COSY, HSQC, NOESY, and NOE as necessary). IR spectra were recorded with a IRAffinity-1S SHIMADZU system spectrophotometer. ESI-MS spectra were recorded with a Thermo Scientific™ LCQ fleet ion trap mass spectrometer. Elemental analyses were performed with a Thermo Finnigan FLASH EA 1112 CHN/S analyzer. Optical rotation measurements were performed on a JASCO DIP-370 polarimeter.

Synthesis of (3*R*,4*S*,5*S*)-3,4-*O*-(1-methylethylidene)-5-nonyloxy-*N*-Boc-piperidine (205): NaH (7 mg, 0.3 mmol, 60% on mineral oil) was added to a solution of **204** (22 mg, 0.08 mmol) in dry DMF (1.2 mL) at 0 °C. The mixture was stirred at room temperature for 30 min then 1-bromononane (54 µL, 0.28 mmol) was added and the reaction mixture was stirred at room temperature for 72 h, until the disappearance of the starting material was observed *via* TLC (CH_2Cl_2/MeOH/NH_4OH (6%) 10:1:0.1). Then, water was slowly added and the reaction mixture was extracted with AcOEt (3×3 mL). The combined organic layer was washed with sat. $NaHCO_3$ and brine and concentrated after drying with Na_2SO_4. The crude residue was purified by flash column chromatography on silica gel (Hexane/AcOEt 8:1) to give 17 mg of **205** (R_f = 0.3, Hexane/AcOEt 8:1, 0.04 mmol, 53%) as a colourless oil.

205: colourless oil. $[\alpha]_D^{21}$ = + 18 (c =0.75, $CHCl_3$). ^{1}H-NMR (400 MHz, $CDCl_3$) δ ppm = 4.51-4.44 (m, 1H, 3-H), 4.28 (brs, 1H, 4-H), 3.85-3.07 (m, 7H, 2-H, 6-H, 5-H, 1'H), 1.66-1.56 (m, 2H, 2'H), 1.49 (s, 3H, Me), 1.45 (s, 9H, t-Bu), 1.36 (s, 3H, Me), 1.34-1.20 (m, 12H, 3'H- 8'H), 0.90-0.85 (m, 3H, 9'H). ^{13}C-NMR (50 MHz, $CDCl_3$) δ ppm = 155.3 (s, 1C, N$\underline{C}$OO), 109.8 (s, 1C, O$\underline{C}$(CH_3)$_2$), 80.0 (s, 1C, O$\underline{C}$(CH_3)$_3$), 73.4 (d, 1C, C-5), 72.7 (d, 2C, C-3, C-4), 70.4 (t, 1C, C-1'), 44.0, 42.8, 41.8, 41.5 (t, 2C, C-2, C-6), 32.0-22.8 (t, 7C, C-2'- C-8' and q, 2C, OC($\underline{C}H_3$)$_2$), 28.6 (q, 3C, OC($\underline{C}H_3$)$_3$), 14.2 (q, 1C, C-9'). MS-ESI (m/z, %) = 422.16 (100) $[M+Na]^+$, 820.89 (17) $[2M+Na]^+$. IR ($CDCl_3$): ν = 2959, 2928, 2857, 2249, 1686, 1375, 1261, 1165, 1101, 1172, 1008 cm^{-1}. $C_{22}H_{41}NO_5$ (399.56): calcd. C, 66.13; H, 10.34; N, 3.51; found C, 66.23; H, 10.32; N, 3.45.

Synthesis of (3*S*,4*R*,5*R*)-4,5-dihydroxy-3-(nonyloxy)piperidine (175): A solution of **205** (15 mg, 0.04 mmol) in MeOH (3 mL) was left stirring with 12 M HCl (60 µL) at room temperature for 18 h. The crude mixture was concentrated to yield **175** as the hydrochloride salt. The corresponding free amine was obtained by dissolving the residue in MeOH (4 mL), then the strongly basic resin Ambersep 900-OH was added and the mixture was stirred for 45 minutes. The resin was removed by filtration and the crude product was purified on silica gel by flash column chromatography (CH_2Cl_2/MeOH/ NH_4OH (6%) 10:1:0.1) to afford 7 mg of **175** (R_f= 0.2, CH_2Cl_2/MeOH/ NH_4OH (6%) 10:1:0.1, 0.03 mmol, 70 %) as a pale yellow oil.

175: pale yellow oil. $[\alpha]_D^{22}$ = – 4.6 (c =0.54, MeOH). ^{1}H-NMR (400 MHz, CD_3OD) δ ppm: 4.01 (brs, 1H, 4-H), 3.60-3.45 (m, 3H, 5-H, 1'-H), 3.38-3.32 (m, 1H, 3-H), 2.84-2.66 (m, 4H, 2-H, 6-H), 1.63-1.54 (m, 2H, 2'H), 1.40-1.25 (m, 12H, 3'H - 8'H-), 0.90 (t, J= 6.9 Hz, 3H, 9'H). ^{13}C-NMR (100 MHz, CD_3OD) δ ppm: 78.5 (d, 1C, C-3), 70.5 (d, 1C, C-5), 70.4 (t, 1C, C-1'), 70.3 (d, 1C, C-4), 47.5, 44.7 (t, 2C, C-2, C-6), 33.1-23.7 (t, 7C, C-2'-C-8'), 14.4 (q, 1C, C-9'). MS-ESI (m/z, %) = 260.12 (100) $[M+H]^+$, 282.29 (58) $[M+Na]^+$, 540.91 (25) $[2M+Na]^+$. $C_{14}H_{29}NO_3$ (259.38): calcd. C, 64.83; H, 11.27; N, 5.40; found C, 64.85; H, 11.13; N, 5.60.

Synthesis of (3*R*,4*S*,5*R*)-3,4-*O*-(1-methylethylidene)-5-nonyloxy-*N*-Boc-piperidine (206): NaH (11 mg, 0.46 mmol, 60% on mineral oil) was added to a solution of **203** (57 mg, 0.21 mmol) in dry DMF (3 mL) at 0 °C. The mixture was stirred at room temperature for 30 min then 1-bromononane (140 µL, 0.73 mmol) was added and the reaction mixture was stirred at room temperature for 40 h, until the disappearance of the starting material was observed *via* TLC (CH_2Cl_2/MeOH/NH_4OH (6%) 10:1:0.1). Then, water was slowly added and the reaction mixture was extracted with AcOEt (3×5 mL). The combined organic layer was washed with sat. $NaHCO_3$ and brine and concentrated after drying with Na_2SO_4. The crude residue was purified by flash column chromatography on silica gel (Hexane/AcOEt 10:1) to give 45 mg of **206** (R_f = 0.4, Hexane/AcOEt 7:1, 0.11 mmol, 54%) as a colourless oil.

206: a colourless oil. $[\alpha]_D^{27}$= + 1.8 (c =0.96, $CHCl_3$). ^{1}H-NMR (400 MHz, $CDCl_3$) δ ppm: 4.31-4.26 (m, 1H, 3-H), 4.13 (brs, 1H, 4-H), 3.92-3.82 (m, 1H, 2-H_a), 3.58-3.28 (m, 6H, 2-H_b, H-5, 6-H, 1'H), 1.59-1.48 (m, 2H, 2'H), 1.45 (s, 12H, Me, t-Bu), 1.33 (s, 3H, Me), 1.32-1.17 (m, 12H, 3'H - 8'H), 0.87 (t, J= 6.2 Hz, 3H, 9'H). ^{13}C-NMR (50 MHz, $CDCl_3$) δ ppm: 155.8 (s, 1C, N<u>C</u>OO), 109.1 (s, 1C, O<u>C</u>$(CH_3)_2$), 79.8 (s, 1C, O<u>C</u>$(CH_3)_3$), 74.8 (d, 1C, C-5), 74.5 (d, 1C, C-4), 72.6 (d, 1C, C-3), 69.6 (t, 1C, C-1'), 43.0, 42.0 (t, 1C, C-2), 42.0-40.8 (t, 1C, C-6), 32.0-22.8 (t, 7C, C-2'- C-8'), 28.6 (q, 3C, OC(<u>C</u>$H_3)_3$), 26.3, 25.0 (q, 2C, OC(<u>C</u>$H_3)_2$), 14.2 (q, 1C, C-9'). IR ($CDCl_3$): ν = 2930, 2859, 1686, 1416, 1375, 1260, 1165, 1101, 1063, 1016 cm^{-1}. MS-ESI (m/z, %) = 422.17 (100) $[M+Na]^+$, 821.05 (96) $[2M+Na]^+$. $C_{22}H_{41}NO_5$ (399.56): calcd. C, 66.13; H, 10.34; N, 3.51; found C, 66.15; H, 10.40; N, 3.60.

Synthesis of (3*R*,4*R*,5*R*)-4,5-dihydroxy-3-(nonyloxy)piperidine (208): A solution of **206** (54 mg, 0.14 mmol) in MeOH (6 mL) was left stirring with 12 M HCl (150 µL) at room temperature for 18 h. The crude mixture was concentrated to yield 21 as hydrochloride salt. The corresponding free amine was obtained by dissolving the residue in MeOH (5 mL), then the strongly basic resin Ambersep 900-OH was added, and the mixture was stirred for 45 minutes. The resin was removed by filtration to give 36 mg of **208** (0.14 mmol, 100% yield) as a pale yellow oil.

208: pale yellow oil. $[\alpha]_D^{25}$ = – 40 (c =0.48, MeOH). ^{1}H-NMR (400 MHz, CD_3OD) δ ppm: 3.84-3.77 (m, 1H, 5-H), 3.67-3.60 (m, 1H, 4-H), 3.60-3.52 (m, 2H, 1'H) 3.46-3.39 (m, 1H, 3-H), 3.02 (d, J= 13.4 Hz, 1H, 2-H_a), 2.82 (dd, J= 6.1, 13.2 Hz, 1H, 6-H_a), 2.65 (d, J= 13.3 Hz, 1H, 6-H_b), 2.48-2.38 (m, 1H, 2-H_b), 1.62-1.51 (m, 2H, 2'H), 1.41-1.20 (m, 12H, 3'H - 8'H), 0.90 (t, J= 5.9 Hz, 3H, 9'H). ^{13}C-NMR (50 MHz, CD_3OD) δ ppm: 78.6 (d, 1C, C-3), 73.2 (d, 1C, C-4), 71.2 (t, 1C, C-1'), 69.5 (d, 1C, C-5), 49.3 (t, 1C, C-6), 47.1 (t, 1C, C-2), 33.0-23.7 (t, 7C, C-2'-C-8'), 14.4 (q, 1C, C-9'). MS-ESI (m/z, %) = 260.18 (100) $[M+H]^+$. $C_{14}H_{29}NO_3$ (259.38): calcd. C, 64.83; H, 11.27; N, 5.40; found C, 64.50; H, 11.38; N, 5.30.

Synthesis of (3*R*,4*S*,5*S*)-5-dodecylamino-3,4-*O*-(1-methylethylidene)-*N*-Boc-piperidine (207): Ketone **166** (63 mg, 0.23 mmol) and dodecylamine (65 mg, 0.35 mmol) were dissolved in MeOH (3 mL), and molecular sieves (3 Å pellets; 25 mg) were added. The reaction mixture was stirred at room temperature for 1 h and then $Pd(OH)_2/C$ (30 mg) was added. The mixture was stirred at room temperature under hydrogen atmosphere for 51 h. The catalyst and the molecular sieves were removed by filtration, washed several times with MeOH and the solvent was evaporated under vacuum. The crude residue was purified by flash column chromatography on silica gel (gradient eluent from Hexane/AcOEt 5:1 to 2:1) to afford 56 mg of **207** (R_f = 0.4, Hexane/AcOEt 2:1, 0.13 mmol, 55%) as a colourless oil.

207: colourless oil. $[\alpha]_D^{27}$= + 1.9 (c =0.90, $CHCl_3$). ^{1}H-NMR (400 MHz, $CDCl_3$) δ ppm: 4.41 (brs, 1H, 4-H), 4.29 (brs, 1H, 3-H), 3.85-3.40 (m, 2H), 3.40-3.22 (m, 1H), 2.99-2.84 (m, 1H), 2.83-2.75 (m, 1H, 5-H), 2.74-2.54 (m, 2H, 1'H), 1.44 (s, 12H, Me, t-Bu), 1.33 (s, 3H, Me), 1.31-1.17 (m, 20H, 2'H - 11'H), 0.86 (t, J= 6.6 Hz, 3H, 12'H). ^{13}C-NMR (100 MHz, $CDCl_3$) δ ppm : 155.4 (s, 1C, N$\underline{C}$OO), 108.9 (s, 1C, O$\underline{C}(CH_3)_2$), 79.8 (s, 1C, O$\underline{C}(CH_3)_3$), 72.5 (d, 2C, C-3, C-4), 53.7 (d, 1C, C-5), 47.2 (t, 1C, C-1'), 43.6, 43.3, 42.4, 42.3 (t, 2C, C-2, C-6), 32.0-22.6 (t, 10C, C-2’- C-11’ and q, 2C, OC(C̲H3)2, 28.6 (q, 3C, OC(C̲H3)3), 14.2 (q, 1C, C-12’). IR ($CDCl_3$): ν = 3300, 2958, 2927, 2854, 1686, 1414, 1373, 1260, 1165,1098, 1007 cm^{-1}. MS-ESI (m/z, %) = 441.28 (100) $[M+H]^+$, 463.23 (91) $[M+Na]^+$, 903.11 (51) $[2M+Na]^+$. $C_{25}H_{48}N_2O_4$ (440.66): calcd. C, 68.14; H, 10.98; N, 6.36; found C, 68.30; H, 10.78; N, 6.33.

Synthesis of (3*R*,4*S*,5*S*)-3,4-dihydroxy-5-(dodecylamino)piperidine (176): A solution of **207** (45 mg, 0.10 mmol) in MeOH (6 mL) was left stirring with 12 M HCl (150 μL) at room temperature for 18 h. The crude mixture was concentrated to yield 10 as hydrochloride salt. The corresponding free amine was obtained by dissolving the residue in MeOH (5 mL), then the strongly basic resin Ambersep 900-OH was added and the mixture was stirred for 45 minutes. The resin was removed by filtration to give 25 mg of **176** (0.08 mmol, 83%) as a white solid.
176: white solid. m.p. = 92-94 °C. $[\alpha]_D^{24}$ = – 5.2 (c =0.85, MeOH). ^{1}H-NMR (400 MHz, CD_3OD) δ ppm: 4.00 (brs, 1H, 4-H), 3.58-3.51 (m, 1H, 3-H), 2.80-2.51 (m, 7H, 2-H, 6-H, 5-H, 1’H), 1.55-1.47 (m, 2H, 2’H), 1.37-1.26 (m, 18H, 3’H - 11’H), 0.90 (t, J= 6.0 Hz, 3H, 12’H). ^{13}C-NMR (50 MHz, CD_3OD) δ ppm: 70.9 (d, 1C, C-3), 69.8 (d, 1C, C-4), 58.7 (d, 1C, C-5), 47.4, 45.4 (t, 3C, C-1’, C-2, C-6), 33.1-23.7 (t, 10C, C-2’- C-11’) 14.4 (q, 1C, C-12’). MS-ESI (m/z, %) = 301.28 (100) $[M+H]^+$. $C_{17}H_{36}N_2O_2$ (300.48): calcd. C, 67.95; H, 12.08; N, 9.32; found C, 67.96; H, 12.03; N, 9.53.

General procedure for the addition of lithium acetylides to ketone 166

To a dry THF solution (0.24 M) of alkyne (2 eq.), *n*-BuLi (1.5 eq.) was added dropwise over 5 min at –78 °C under nitrogen atmosphere. The solution was allowed to warm to 0 °C over 1 h and held at 0 °C for an additional 30 min. The solution was then re-cooled to –78 °C and ketone 8 (1 eq.) was added in one portion. The solution was allowed to warm to room temperature and stirred at room temperature until the disappearance of ketone **166** was attested by a TLC control (PEt/AcOEt 2:1). A saturated aqueous solution of NH_4Cl was added and the reaction mixture was extracted with AcOEt (3x). The combined organic layer was washed with water, sat. $NaHCO_3$ and brine and concentrated after drying with Na_2SO_4. The crude compound was purified by flash column cromatograpy.

Synthesis of (3*S*,4*R*,5*R*)-3-hydroxy-4,5-*O*-(1-methylethylidene)-3-(phenylethynyl)-*N*-Boc-piperidine (209): Application of the general procedure to ketone **166** (60 mg, 0.24 mmol) with phenylacetylene (54 µL, 0.49 mmol) and *n*-BuLi (150 µL, 0.37 mmol, 2.5 M) gave, after purification by flash column chromatography on silica gel (Hexane/AcOEt 4:1), 69 mg of **209** (R_f = 0.2, 0.18 mmol, 77 %) as a pale yellow oil.

209: pale yellow oil. $[\alpha]_D^{27}$ = + 9.4 (c =1.05, $CHCl_3$). ^{1}H-NMR (400 MHz, $CDCl_3$) δ ppm: 7.40-7.34 (m, 2H, Ar), 7.30-7.21 (m, 3H, Ar), 4.52-4.40 (m, 1H, 5-H), 4.36 (d, J= 6.8 Hz, 1H, 4-H), 3.92-3.70 (m, 2H, 2-H_a, 6-H_a), 3.67-3.55 (m, 1H, 6-H_b), 3.37-3.28 (m, 1H, 2-H_b), 3.09-2.97 (m, 1H, OH), 1.50 (s, 3H, Me), 1.40 (s, 9H, t-Bu), 1.36 (s, 3H, Me). ^{13}C-NMR (50 MHz, $CDCl_3$) δ ppm: 155.2 (s, 1C, N<u>C</u>OO), 132.0, 129.0, 128.4 (d, 5C, Ar), 121.9 (s, 1C, Ar), 109.9 (s, 1C, O<u>C</u>(CH_3)$_2$), 88.1, 86.4 (s, 2C, C-1', C-2'), 80.2 (s, 1C, O<u>C</u>(CH_3)$_3$), 77.1 (d, 1C, C-4), 72.5 (d, 1C, C-5), 67.4 (s, 1C, C-3), 48.3, 47.5 (t, 1C, C-6), 42.7, 41.9 (t, 1C, C-2), 28.5 (q, 3C, OC(<u>C</u>H_3)$_3$), 27.0 (q, 1C, OC(<u>C</u>H_3)$_2$), 25.0 (q, 1C, OC(<u>C</u>H_3)$_2$). IR ($CDCl_3$) ν = 3541, 2982, 2934, 2251, 1688, 1600, 1260, 1215, 1163 cm^{-1}. MS-ESI (m/z, %) = 769.01 (100) $[2M+Na]^+$, 396.11 (21) $[M+Na]^+$. $C_{21}H_{27}NO_5$ (373.44): calcd. C, 67.54; H, 7.29; N, 3.75; found C, 67.40; H, 7.33; N, 3.76.

Synthesis of (3*S*,4*R*,5*R*)-3-hydroxy-4,5-*O*-(1-methylethylidene)-3-(oct-1-yn-1-yl)-*N*-Boc-piperidine (210): Application of the general procedure to ketone **166** (120 mg, 0.45 mmol) with 1-octyne (131 µL, 0.89 mmol) and *n*-BuLi (267 µL, 0.67 mmol, 2.5 M) gave, after purification by flash column chromatography on silica gel (Hexane/AcOEt 4:1), 134 mg of **210** (R_f = 0.2, 0.35 mmol, 78%) as a colourless oil.

210: colourless oil. $[\alpha]_D^{27}$ = + 5.5 (c =1.03, $CHCl_3$). ^{1}H-NMR (400 MHz, $CDCl_3$) δ ppm: 4.47-4.34 (m, 1H, 5-H), 4.24 (d, J= 6.9 Hz, 1H, 4-H), 3.74-3.54 (m, 3H, 2-H_a, 6-H), 3.22 (d, J= 12.3 Hz, 1H, 2-H_b), 2.87 (brs, 1H, OH), 2.19-2.12 (m, 2H, 3'H), 1.48 (s, 3H, Me), 1.43 (s, 9H, t-Bu), 1.35 (s, 3H, Me), 1.34-1.15 (m, 8H, 4'H - 7'H), 0.91-0.79 (m, 3H, 8'H). ^{13}C-NMR (100 MHz, $CDCl_3$) δ ppm: 155.2 (s, 1C, N<u>C</u>OO), 109.6 (s, 1C, O<u>C</u>(CH_3)$_2$), 87.5, 79.4 (s, 2C, C-1', C-2'), 80.0 (s, 1C, O<u>C</u>(CH_3)$_3$), 77.2 (d, 1C, C-4), 72.4 (d, 1C, C-5), 66.8 (s, 1C, C-3), 48.3, 47.5 (t, 1C, C-2), 42.5, 41.6 (t, 1C, C-6), 31.3 - 22.6 (t, 4C, C-4' - C-7') e 26.9 (q, 1C, OC(<u>C</u>H_3)$_2$), 24.9 (q, 1C, OC(<u>C</u>H_3)$_2$), 28.5 (q, 3C, OC($\underline{C}H_3$)$_3$), 18.8 (t, 1C, C-3'), 14.1 (q, 1C, C-8'). IR ($CDCl_3$) ν = 3543, 2961, 2932, 2862, 2249, 1730, 1458, 1412, 1375, 1215, 1167, 1142, 1045 cm^{-1}. MS-ESI (m/z, %) = 785.02 (100) $[2M+Na]^+$, 404.12 (32) $[M+Na]^+$. $C_{21}H_{35}NO_5$ (381.51): calcd. C, 66.11; H, 9.25; N, 3.67; found C, 66.34; H, 9.38; N, 3.73.

General procedure for the synthesis of trihydroxypiperidines 211 and 212

A solution of protected compound in MeOH was left stirring with 12 M HCl at room temperature for 18 h. The crude mixture was concentrated to yield the deprotected compound as hydrochloride salt. The corresponding free amine was obtained by dissolving the residue in MeOH, then the strongly basic resin Ambersep 900-OH was added, and the mixture was stirred for 45 minutes. The resin was removed by filtration and the crude product, if necessary, was purified on silica gel by flash column chromatography to afford the 3-substituted trihydroxypiperidine as free base.

Synthesis of (3*S*,4*R*,5*R*)-3,4,5-trihydroxy-3-(phenylethynyl)-piperidine (211): Application of the general procedure to **209** (48 mg, 0.13 mmol) with HCl (150 µL) in MeOH (7 mL) furnished, after treatment with Ambersep 900-OH and purification by column chromatography on silica gel (CH_2Cl_2/MeOH/NH_4OH (6%) 10:1:0.1), 16 mg of **211** (R_f = 0.2, 0.07 mmol, 53%) as waxy white solid.

211: waxy white solid. $[\alpha]_D^{24}$ = – 59 (c =0.65, MeOH). ^{1}H-NMR (400 MHz, CD_3OD) δ ppm: 7.51-7.43 (m, 2H, Ar), 7.38-7.27 (m, 3H, Ar), 3.98-3.91 (m, 1H, 5-H), 3.89 (brs, 1H, 4-H), 3.01 (d, J= 13.1 Hz, 1H, 2-H_a), 2.86-2.76 (m, 3H, 2-H_b, 6-H). ^{13}C-NMR (50 MHz, CD_3OD) δ ppm: 132.7-129.4 (d, 5C, Ar), 123.8 (s, 1C, Ar), 90.7, 87.0 (s, 2C, C-1', C-2'), 74.8 (d, 1C, C-4'), 71.1 (s, 1C, C-3), 69.9 (d, 1C, C-5), 52.7 (t, 1C, C-2), 48.0 (t, 1C, C-6). MS-ESI (m/z, %) = 234.00 (100) $[M+H]^+$. $C_{13}H_{15}NO_3$ (233.26): calcd. C, 66.94; H, 6.48; N, 6.00; found C, 66.80; H, 6.33; N, 6.07.

Synthesis of (3*S*,4*R*,5*R*)-3,4,5-trihydroxy-3-(oct-1-yn-1-yl)-piperidine (212): Application of the general procedure to **210** (120 mg, 0.30 mmol) with HCl (150 µL) in MeOH (7 mL) furnished, after treatment with Ambersep 900-OH and purification by column chromatography on silica gel (CH_2Cl_2/MeOH/NH_4OH (6%) 10:1:0.1), 51 mg of **212** (R_f = 0.2, 0.21 mmol, 71%) as a colourless oil.

212: olourless oil. $[\alpha]_D^{25}$ = – 24 (c =0.42, $CHCl_3$). ^{1}H-NMR (400 MHz, CD_3OD) δ ppm: 3.90-3.84 (m, 1H, 5-H), 3.75 (brs, 1H, 4-H), 2.87 (d, J= 13.0 Hz, 1H, 2-H_a), 2.78-2.70 (m, 2H, 6-H), 2.62 (d, J= 13.0 Hz, 1H, 2-H_b), 2.25 (t, J= 6.8 Hz, 2H, 3'H), 1.57-1.25 (m, 8H, 4'H-7'H), 0.92 (t, J= 6.8 Hz, 3H, 8'H). ^{13}C-NMR (50 MHz, CD_3OD) δ ppm: 88.0, 81.9 (s, 2C, C-1'and C-2'), 75.1 (d, 1C, C-4), 70.7 (s, 1C, C-3), 69.8 (d, 1C, C-5), 52.7 (t, 1C, C-2), 47.7 (t, 1C, C-6), 32.4, 29.6, 23.6 (t, 4C, C-4', C-5', C-6'-C-7'), 19.4 (t, 1C, C-3'), 14.4 (q, 1C, C-8'). MS-ESI (m/z, %) = 504.92 (100) $[2M+Na]^+$, 242.02 (94) $[M+H]^+$, 264.14 (47) $[M+Na]^+$. $C_{13}H_{23}NO_3$ (241.33): calcd. C, 64.70; H, 9.61; N, 5.80; found C, 64.94; H, 9.49; N, 5.50.

General procedure for the reduction of triple bond to piperidines 177 and 178. To a solution of the deprotected compound in EtOH, $Pd(OH)_2/C$ was added under nitrogen atmosphere. The mixture was stirred at room temperature under hydrogen atmosphere until a ^{1}H-NMR analysis attested the presence of aliphatic hydrogens at 1'C and 2'C (6-23 h). The catalyst was removed by filtration, washed several times with EtOH, and the solvent was evaporated under vacuum. The crude product, if necessary, was purified on silica gel by flash column chromatography to afford the corresponding completely reduced 3-substituted trihydroxypiperidine.

Synthesis of (3*S*,4*R*,5*R*)-3,4,5-trihydroxy-3-(2-phenylethyl)-piperidine (177): Application of the general procedure to **211** (13 mg, 0.05 mmol) with $Pd(OH)_2/C$ (7 mg) in EtOH (1 mL) furnished, after purification by column chromatography on silica gel (CH_2Cl_2/MeOH/NH_4OH (6%) 10:1:0.1), 5 mg of the corresponding reduced trihydroxypiperidine **177** (R_f = 0.2, 0.02 mmol, 39%) as orange oil.

177: orange oil. $[\alpha]_D^{24}$ = – 13 (c =0.36, MeOH). ^{1}H-NMR (400 MHz, CD_3OD) δ ppm: 7.27-7.19 (m, 4H, Ar), 7.18-7.10 (m, 1H, Ar), 3.81 (brs, 1H, 5-H), 3.51 (brd, J= 2.2 Hz, 1H, 4-H), 2.96 (dd, J= 4.0, 13.7 Hz, 1H, 6-H_a), 2.88 (d, J= 13.1 Hz, 1H, 2-H_a), 2.76-2.70 (m, 1H, 6-H_b), 2.70-2.62 (m, 2H, H-2'), 2.59 (d, J=13.1 Hz, 1H, 2-H_b), 1.97-1.88 (m, 1H, 1'H_a), 1.86-1.76 (m, 1H, 1'H_b). ^{13}C-NMR (100 MHz, CD_3OD) δ ppm: 143.9 (s, 1C, Ar), 129.4 - 126.7 (d, 5C, Ar), 74.8 (s, 1C, C-3), 72.7 (d, 1C, C-4), 70.8 (d, 1C, C-5), 54.8 (t, 1C, C-2), 53.5 (t, 1C, C-6), 39.6 (t, 1C, C-1'), 30.7 (t, 1C, C-2'). MS-ESI (m/z, %) = 238.09 (100) $[M+H]^+$, 260.14 (65) $[M+Na]^+$, 497.20

(16) [2M+Na] $^+$. $C_{13}H_{19}NO_3$ (237.29): calcd. C, 65.80; H, 8.07; N, 5.90; found C, 65.53; H, 8.25; N, 5.81.

Synthesis of (3*S*,4*R*,5*R*)-3,4,5-trihydroxy-3-octyl-piperidine (178): Application of the general procedure to **212** (40 mg, 0.17 mmol) with $Pd(OH)_2$/C (20 mg) in EtOH (2 mL) furnished 41 mg of the corresponding reduced trihydroxypiperidine **178** (0.17 mmol, 98%) as orange oil.

178: orange oil. $[\alpha]_D^{23}$ = – 9.0 (c =1.00, MeOH). ^{1}H-NMR (400 MHz, CD_3OD) δ ppm: 3.77 (brs, 1H, 5-H), 3.44 (brs, 1H, 4-H), 2.92 (d, J= 12.6 Hz, 1H, 6-H_a), 2.77 (d, J= 13.6, 1H, 2-H_a), 2.68 (d, J= 12.6 Hz, 1H, 6-H_b), 2.50 (d, J= 13.6 Hz, 1H, 2-H_b), 1.67-1.51 (m, 2H, 1'H), 1.36-1.25 (m, 12H, 2'H - 7'H), 0.90 (m, 3H, 8'H). ^{13}C-NMR (50 MHz, CD_3OD) δ ppm: 75.1 (s, 1C, C-3), 72.5 (d, 1C, C-4), 70.9 (d, 1C, C-5), 53.6 (t, 1C, C-2), 50.7 (t, 1C, C-6), 37.3 (t, 1C, C-1'), 33.1 - 23.7 (t, 6C, C-2'-C-7'), 14.4 (q, 1C, C-8'). MS-ESI (m/z, %) = 246.15 (100) [M+H] $^+$, 268.26 (22) [M+Na] $^+$, 513.00 (10) [2M+Na] $^+$. $C_{13}H_{27}NO_3$ (245.36): calcd. C, 63.64; H, 11.09; N, 5.71; found C, 63.78; H, 11.01; N, 5.92.

Preliminary biological screening towards commercial glycosidases

A panel of 12 commercial glycosidases (α-fucosidase EC 3.2.1.51 from Homo sapiens, α-galactosidase EC 3.2.1.22 from coffee beans, β-galactosidases EC 3.2.1.23 from *Escherichia coli* and *Aspergillus oryzae*, α-glucosidases EC 3.2.1.20 from yeast and rice, amyloglucosidase EC 3.2.1.3 from *Aspergillus niger*, β-glucosidase EC 3.2.1.21 from almonds, α-mannosidase EC 3.2.1.24 from Jack beans, β-mannosidase EC 3.2.1.25 from snail, β-*N*-acetylglucosaminidases EC 3.2.1.52 from Jack beans and bovine kidney) was screened.The percentage (%) of inhibition towards the corresponding glycosidase was determined in quadruplicate in the presence of 100 μM of the inhibitor on the well. Each enzymatic assay (final volume 0.12 mL) contains 0.01–0.5 units/mL of the enzyme (with previous calibration) and 4.2 mM aqueous solution of the appropriate *p*-nitrophenyl glycopyranoside (substrate) buffered to the optimal pH of the enzyme. Enzyme and inhibitor were pre-incubated for 5 min at r.t., and the reaction started by addition of the substrate. After 20 min of incubation at 37 °C, the reaction was stopped by the addition of 0.1 mL of sodium borate solution (pH 9.8). The *p*-nitrophenolate formed was measured by visible absorption spectroscopy at 405 nm (Asys Expert 96 spectrophotometer). Under these conditions, the *p*-nitrophenolate released led to optical densities linear with both reaction time and concentration of the enzyme (for more details, see the Supplementary Materials). The IC_{50} value (concentration of inhibitor required for 50% inhibition of enzyme activity) was determined from plots of % inhibition *versus* different inhibitor concentrations. Each point of the graph is the average of four measures. The standard deviation for each point has been also represented in the graph.

	% Inhibition at 0.1 mM		
	176	**178**	**208**
α-L-fucosidase EC 3.2.1.51			
Homo sapiens	-	-	-
α-galactosidase EC 3.2.1.22			
coffee beans	-	-	-
β-galactosidase EC 3.2.1.23			
Escherichia coli	-	-	-
Aspergillus oryzae	-	-	-
α-glucosidase EC 3.2.1.20			
yeast	-	-	-
rice	-	-	-
amyloglucosidase EC 3.2.1.3			
Aspergillus niger	-	-	-
β-glucosidase EC 3.2.1.21			
almonds	51±1	-	-
α-mannosidase EC 3.2.1.24			
Jack beans	-	-	-
β-mannosidase EC 3.2.1.25			
snail	-	-	-
β-*N*-acetylglucosaminidase EC 3.2.1.52			
Jack beans	-	-	-
bovine kidney	-	-	-

"-": no inhibition.

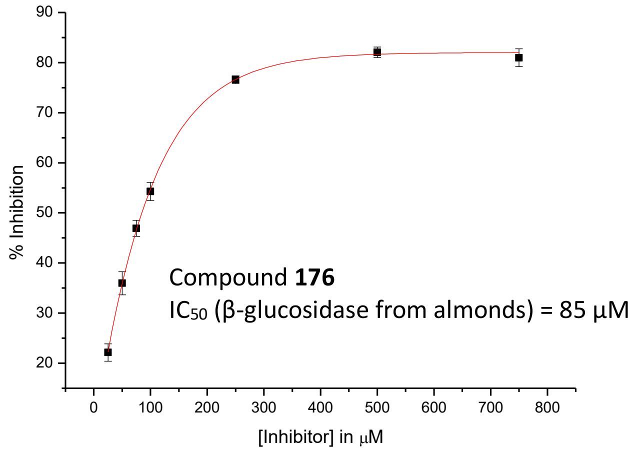

IC_{50} of compound 10 towards β-glucosidase from almonds

Biological screening towards human lysosomal β-glucosidase (GCase)

The new compounds were screened at 1 mM concentration towards β-galactosidase (β-Gal) and β-glucosidase (GCase) in leukocytes isolated from healthy donors (controls). Isolated leukocytes were disrupted by sonication, and a micro BCA protein assay kit (Sigma–Aldrich) was used to determine the total protein amount for the enzymatic assay, according to the manufacturer's instructions. GCase activity was measured in a flat-bottomed 96-well plate. Compound solution (3 μL), 4.29 μg/μL leukocytes homogenate (7 μL), and substrate 4-methylumbelliferyl-β-D-glucoside (3.33 mM, 20 μL, Sigma–Aldrich) in citrate/phosphate buffer (0.1:0.2, M/M, pH 5.8) containing sodium taurocholate (0.3%) and Triton X-100 (0.15%) at 37 °C were incubated for 1 h. The reaction was stopped by addition of sodium carbonate (200 μL; 0.5M, pH 10.7) containing Triton X-100 (0.0025 %), and the fluorescence of 4-methylumbelliferone released by β-glucosidase activity was measured in SpectraMax M2 microplate reader (λex=365 nm, λem=435 nm; Molecular Devices). Percentage GCase inhibition is given with respect to the control (without compound). Data are mean SD (n=3). For compounds showing GCase inhibitory activity higher than 80% at 1 mM concentration, the IC_{50} values were determined by measuring the initial hydrolysis rate with 4-methylumbelliferyl-β-D-glucoside (3.33 mM). Data obtained were fitted by using the appropriate Equation.

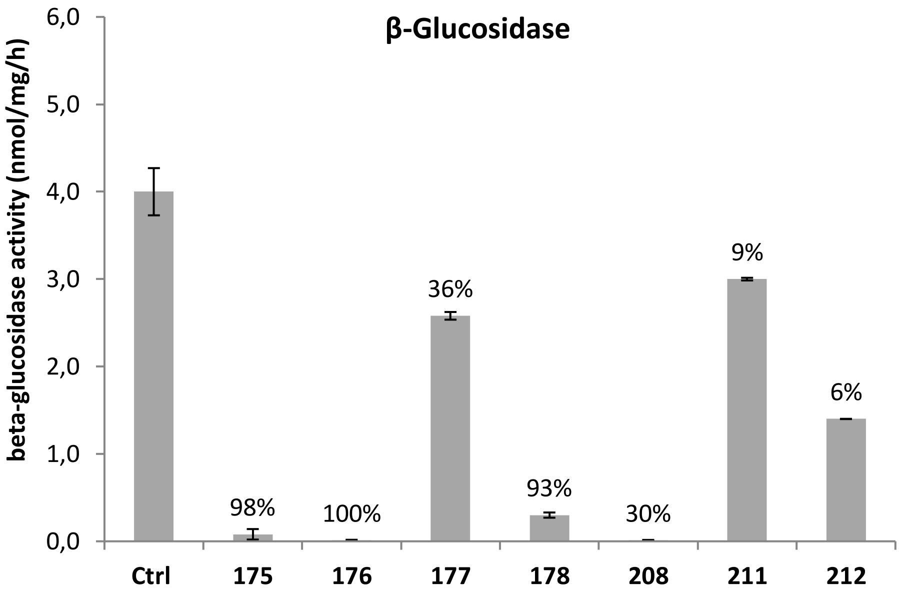

Percentage of GCase inhibition of the whole collection of compounds in human leukocytes extracts incubated with azasugars at 1 mM concentration.

*IC_{50} for compounds **175, 176, 178** and **208** towards human lysosomal β-glucosidase*

The IC_{50} values of inhibitors against β-glucosidase were determined by measuring the initial hydrolysis rate with 4-methylumbelliferyl-β-D-glucoside (3.33 mM). Data obtained were fitted to the following equation using the Origin Microcal program.

$$\frac{Vi}{Vo} = \frac{Max - Min}{1 + \left(\frac{x}{IC_{50}}\right)^{slope}} + Min$$

where V_i/V_o, represent the ratio between the activity measured in the presence of the inhibitor (V_i) and the activity of the control without the inhibitor (V_0), “x” the inhibitor concentration, Max and Min, the maximal and minimal enzymatic activity observed, respectively.

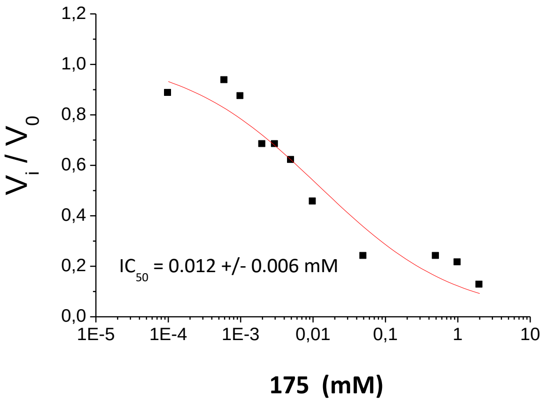

IC$_{50}$ of compound **175** towards GCase

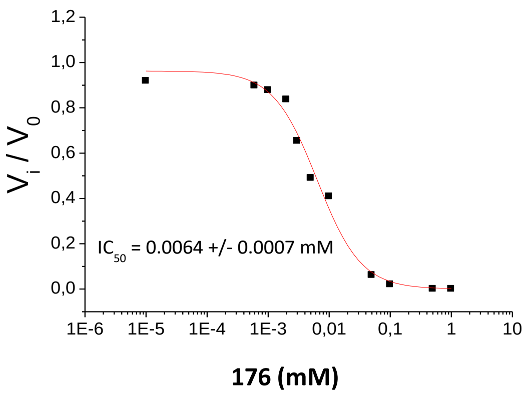

IC$_{50}$ of compound **176** towards GCase

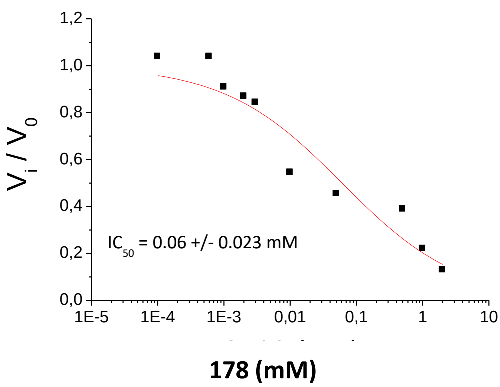

IC$_{50}$ of compound **178** towards GCase

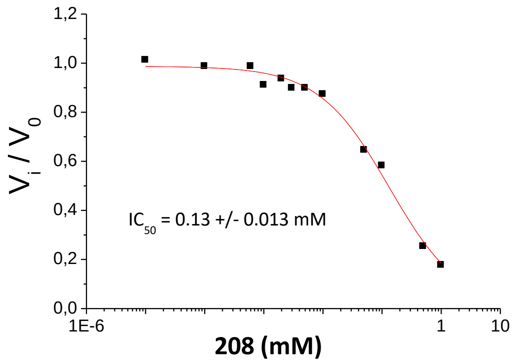

IC_{50} of compound **208** towards GCase

Pharmacological chaperoning activity

Fibroblasts with the N370S/RecNcil mutation from Gaucher disease patients were obtained from the "Cell line and DNA Biobank from patients affected by Genetic Diseases" (Gaslini Hospital, Genova, Italy). Fibroblasts cells (20.0 x 10^4) were seeded in T25 flasks with DMEM supplemented with fetal bovine serum (10%), penicillin/streptomycin (1%), and glutamine (1%) and incubated at 37 °C with 5% CO_2 for 24 h. The medium was removed, and fresh medium containing the compounds **175**, **176** or **178** at different concentrations (10 nM, 100 nM, 1 µM, 10 µM, 50 µM, 100 µM) was added to the cells and left for 4 days. The medium was removed, and the cells were washed with PBS and detached with trypsin to obtain cell pellets, which were washed four times with PBS, frozen and lysed by sonication in water. Enzyme activity was measured as reported above. Reported data are mean S.D. (n=2).

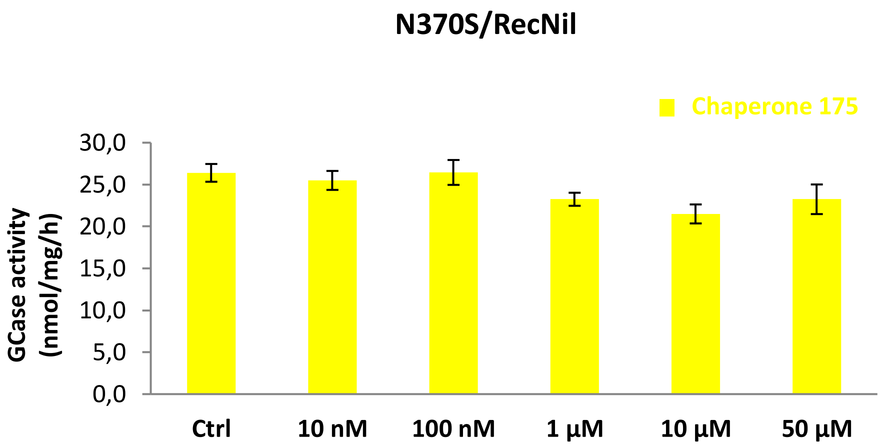

GCase activity in human fibroblasts derived from GD patients bearing N370/RecNcil mutations in the presence of compound **175**. The flasks containing cells incubated with 100 µM concentrations showed low cell viability that hampered to proceed with the assay.

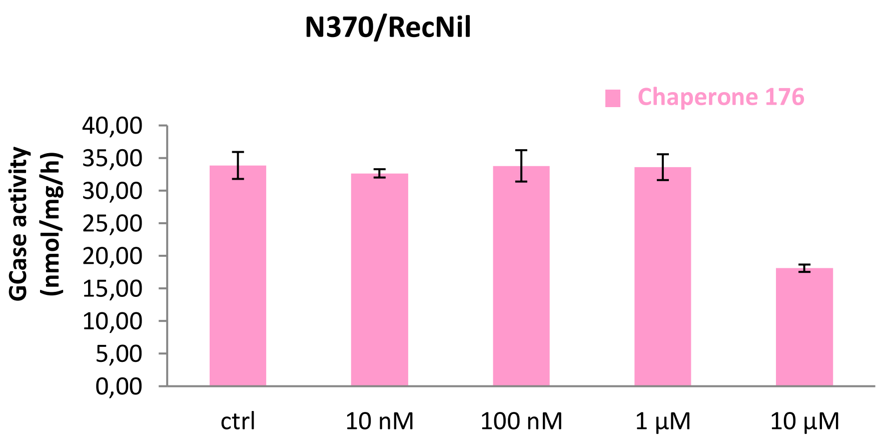

GCase activity in human fibroblasts derived from GD patients bearing N370/RecNcil mutations in the presence of compound **176**. The flasks containing cells incubated with 100 µM and 50 µM concentrations showed low cell viability that hampered to proceed with the assay.

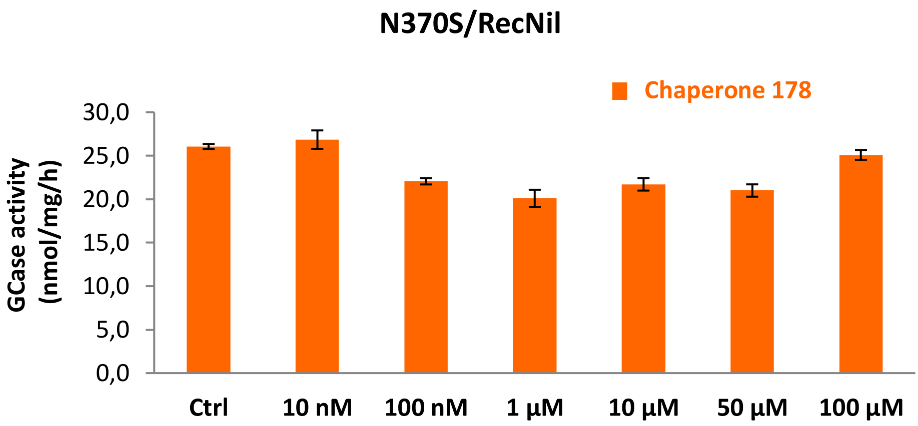

GCase activity in human fibroblasts derived from GD patients bearing N370/RecNcil mutations in the presence of compound **178**.

3.4 Exploring strategies to obtain 2,2-dioctyl trihydroxypiperidine

3.4.1 Results and discussions

Different synthetic approaches have been undertaken to introduce two octyl chains in C-2 position on the piperidine skeleton with the aim of investigating the biological activity of 2,2-dioctyl trihydroxypiperidine **213** as GCase inhibitor and PC. The retrosynthetic strategies to yield **213** from D-mannose are reported in Scheme 3.21.

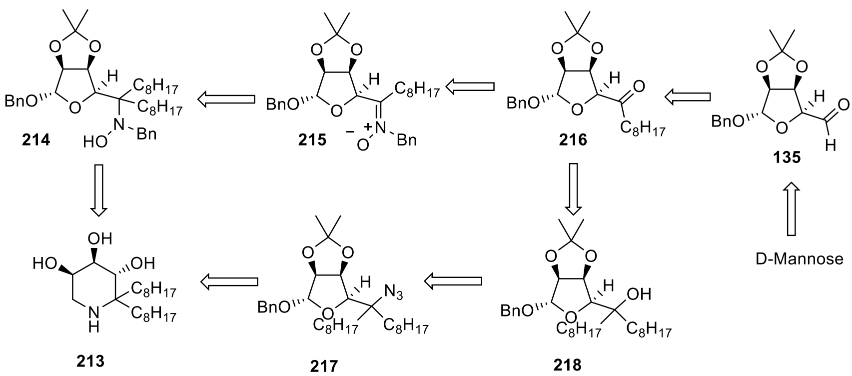

Scheme 3.21: The retrosynthetic strategies to yield 2,2-dioctyl trihydroxypiperidine from D-mannose.

The synthetic approaches is based on the ketone intermediate **216** obtained from the addition of Grignard reagent onto the aldehyde followed by oxidation of the resulting alcohol with good yield on two steps (80%, see Experimental section)**.** One synthetic approach involved the synthesis of the ketonitrone **215** derivative starting from the intermediate **216**, followed by addition of octylMgBr to introduced the second alkyl chain and subsequent reductive amination and deprotection. We tried to synthesize the corresponding ketonitrone under different reaction conditions using benzylhydroxylamine. Unfortunately there was no completely disappearance of the starting material **216** and the ketonitrone, highlighted in TLC as a new formed spot, were not stable and could not be isolated.

The second synthetic approach involved the synthesis of compound **218** as key intermediate (Scheme 3.21). The compound **218** was obtained by Grignard addition onto ketone **216** in good yield (see Experimental section). The Grignard addition allowed to introduce a second alkyl chain. Then, the scope was to introduce the nitrogen moiety such as an azido group. We initially tried to introduce the nitrogen atom by preparing the corresponding mesylate compound as substrate for the subsequent nucleophilic substitution with NaN_3. Unfortunately, the tertiary alcohol did not undergo mesylation most likely due to the high steric hindrance. We therefore attempted to introduce the azido group in a one-pot reaction which involved the use of trifluoromethanesulfonic anhydride and NaN_3. However, we did not observe any formation of the desired product and we therefore failed in the synthesis of compound **217** through this strategy.

The third strategy explored the method described by Kai-Jiong Xiao and co-workers based on the one-pot sequential reductive alkylation of amides with Grignard reagents through amide activation. This one-pot reaction allowed the transformation of amides into the corresponding tert-alkylamines by a one-pot reductive bisalkylation with different organometallic reagents in a simple and direct manner. [217] The key amide compound **220** was synthesized starting from the carboxylic acid **219** obtained by oxidation of our aldehyde **135** as reported in literature. [218] [219] The coupling reaction between compound **219** and dibenzyl amine was optimized using hydroxybenzotriazole and 1-ethyl-3-(3-dimethylaminopropyl)carbodiimide as acid activators (Schema 3.22). The one-pot reaction was examined on the amide derivative **220** with octylMgBr. To achieve the required one-pot reaction under milder conditions, triflic anhydride was selected as the amide activator and 2,6-di-*tert*-butyl-4-methylpyridine (DTBMP) as the base. To a cooled solution (-78 °C) of amide (1.0 equivalent) and 2,6-di-*tert*-butyl-4-methylpyridine (1.2 equiv) in CH_2Cl_2 (5 mL) Tf_2O (1.2 equivalents) was added in a dropwise manner and stirred at -78 °C for 45 min. A solution of octylMgBr (3.0 equivalents) was added dropwise to the resultant mixture. Then the reaction was warmed slowly to room temperature and stirred for 16 hours. The reaction was quenched with a saturated ammonium chloride solution and extracted with CH_2Cl_2. At the moment the amine of interest **221** has been identified by ESI-MS on the complex mixture of reaction crude. The one-pot reaction will be optimized and compound **221** purified and characterized. Then, the synthetic strategy will involve the reductive amination and subsequent deprotection of acetonide to obtain the target 2,2-dioctyl trihydroxypiperidine.

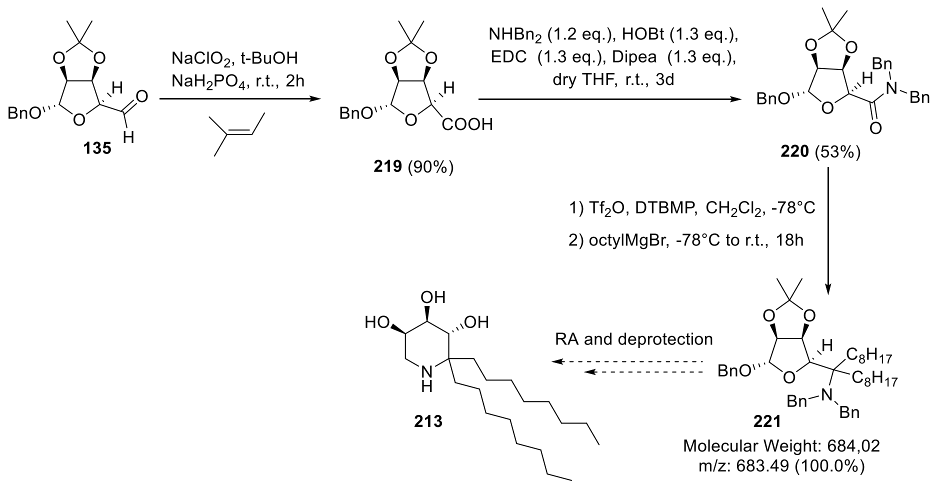

Scheme 3.22: The strategy explored the method described by Kai-Jiong Xiao to obtain 2,2-dioctyl trihydroxypiperidine.

3.4.2 Experimental Section

General Experimental Procedures for the syntheses:

Commercial reagents were used as received. All reactions were carried out under magnetic stirring and monitored by TLC on 0.25 mm silica gel plates (Merck F254). Column chromatographies were carried out on Silica Gel 60 (32–63 µm) or on silica gel (230–400 mesh, Merck). Yields refer to spectroscopically and analytically pure compounds unless otherwise stated. ^{1}H-NMR spectra were recorded on a Varian Gemini 200 MHz, a Varian Mercury 400 MHz or on a Varian INOVA 400 MHz instruments at 25 °C. ^{13}C-NMR spectra were recorded on a Varian Gemini 50 MHz or on a Varian Mercury 100 MHz instruments. Chemical shifts are reported relative to $CDCl_3$ (^{1}H: δ = 7.27 ppm, ^{13}C: δ = 77.0 ppm). Integrals are in accordance with assignments, coupling constants are given in Hz. For detailed peak assignments 2D spectra were measured (g-COSY, g-HSQC) and 1D-NOESY. IR spectra were recorded with a IRAffinity-1S Shimadzu spectrophotometer. ESI-MS spectra were recorded with a Thermo Scientific™ LCQ fleet ion trap mass spectrometer. ICP analyses were performed with a Thermo Finnigan FLASH EA 1112 CHN/S analyser. Optical rotation measurements were performed on a JASCO DIP-370 polarimeter.

Synthesis of benzyl 2,3-*O*-(1-methylethylidene)-D-lyxofuranosyl-nonan-one (216): A solution of aldehyde **135** (200 mg, 0.72) in dry THF (10 mL) was stirred at -0 °C under nitrogen atmosphere and 2.0 M solution of octylmagnesium bromide in diethyl ether (1.3 mmol, 620 µL) was slowly added. The reaction mixture was stirred at room temperature under nitrogen atmosphere for 3 hours, when a TLC check (Hex/AcOEt 1:1) attested the disappearance of the starting material. A Saturated Ammonium Chloride Solution (10 mL) and Et_2O (10 mL) were added to the mixture at 0 °C and left stirring for 15 minutes. The two layers were separated and the aqueous layer was extracted with Et_2O (2x10 mL). The combined organic layers were washed with brine (2x30 mL), dried with Na_2SO_4 and concentrated under reduced pressure to give a mixture of hydroxylamines. To a stirred solution of the crude mixture in dry CH_2Cl_2 (10 mL), Dess-Martin periodinane (436 mg, 1.0 mmol) was added at room temperature. The reaction mixture was stirred for 3 hours until a TLC control (Hex/AcOEt 10:1) attested the disappearance of the starting material. The mixture was extracted with $NaHCO_3$ saturated solution, dried over Na_2SO_4 and concentrated. The residue was purified by silica gel flash chromatography (Hex/AcOEt 13:1) to give

216 (225 mg, 058 mmol, 80%, R_f = 0.25) as a colorless oil.

216: colorless oil. $[\alpha]_D^{23}$ = + 23 (c =1.00, $CHCl_3$). ^{1}H-NMR (400 MHz, $CDCl_3$) δ = 7.36 – 7.26 (m, 5H, Ar), 5.20 (s, 1H, 1-H), 5.03 (t, J =6.0 Hz,1H, 3-H), 4.68 (d, J =12.0 Hz, 1H, H_a-OBn), 4.65 (d, J =8.0 Hz, 1H, 2-H), 4.52-4.49 (m, 2H, 4-H and H_b-OBn), 2.57 (ott, 2H, 1'H), 1.63 – 1.60 (m, 1H, 2'H), 1.41,(s, 3H, Me), 1.29 – 1.27 (m, 13H, 3'H-7'H and Me), 0.88 (t, J = 6.0 Hz, 3H, 8'$H_{a\text{-}b\text{-}c}$).^{13}C-NMR (100 MHz, $CDCl_3$) δ = 206.6 (d, 1C, *C*=O), 137.2 (s, 1C, Ar), 128.6 – 128.1 (d, 5C, Ar), 113.1 (s, acetal), 105.8 (d, C-1), 85.1 (d, C-2), 84.4 (d, C-4), 81.1 (d, C-3), 69.4 (t, Bn), 40.3 (t, 1C, C-1'), 32.0 – 22.8 (t, 6C, C-2' –C-7'; q, 2C, Me), 14.2 (q, 1C, C-8') ppm. MS (ESI): m/z (%) = 391.88 (100) $[M+H]^+$.$C_{23}H_{34}NO_5$ (390.52). calcd. C, 70.74; H, 8.78; found C, 70.70; H, 9.00.

Synthesis of benzyl 2,3-*O*-(1-methylethylidene)-D-lyxofuranosyl- heptadecan-9-ol (218): A solution of **216** (200 mg, 0.51) in dry THF (8 mL) was stirred at -0 °C under nitrogen atmosphere and 2.0 M solution of octylmagnesium bromide in diethyl ether (0.92 mmol, 460 µL) was slowly added. The reaction mixture was stirred at room temperature under nitrogen atmosphere for 16 hours, when a TLC check (Hex/AcOEt 10:1) attested the disappearance of the starting material. A Saturated Ammonium Chloride Solution (10 mL) and Et_2O (10 mL) were added to the mixture at 0 °C and left stirring for 15 minutes. The two layers were separated and the aqueous layer was extracted with Et_2O (2x10 mL). The combined organic layers were washed with brine (2x30 mL), dried with Na_2SO_4 and concentrated under reduced pressure. The residue was purified by silica gel flash chromatography (Hex/AcOEt 10:1) to give **218** (257 mg, 0,51 mmol, 100%, R_f = 0.35) as a colorless oil.

218: colorless oil. $[\alpha]_D^{23}$ = + 17 (c =2.00, $CHCl_3$). ^{1}H-NMR (400 MHz, $CDCl_3$) δ = 7.36 – 7.25 (m, 5H, Ar), 5.18 (s, 1H, 1-H), 4.87-4.85 (m, 1H, 3-H), 4.65-4.63 (m, 2H, 2-H and H_a-OBn), 4.49 (m, 1H, H_b-OBn), 3.6-3.85 (m, 1H, 4-H), 3.65(brs, OH), 1.66 – 1.57 (m, 4H, 1'H and 1''H), 1.49 (s, 3H, Me), 1.31 – 1.25 (m, 19H, 2'H-7'H, 2''H-7''H and Me), 0.89-0.85 (m, 6H, 8'$H_{a\text{-}b\text{-}c}$ and 8''$H_{a\text{-}b\text{-}c}$). ^{13}C-NMR (100 MHz, $CDCl_3$) δ = 137.4 (s, 1C, Ar), 128.6 – 128.0 (d, 5C, Ar), 112.9 (s, acetal), 104.7 (d, C-1), 85.4 (d, C-2), 80.9 (d, C-4), 80.7 (d, C-3), 69.2 (s, *C*-OH), 63.1 (t, Bn), 32.0 – 22.8 (t, 14C, C-1' –C-7' and C-1'' –C-7''; q, 2C, Me), 14.2 (q, 2C, C-8' and C-8'') ppm.

MS (ESI): m/z (%) = 505.99 (100) [M+H]$^+$.$C_{31}H_{52}NO_5$ (504.75). calcd. C, 73.77; H, 10.38; found C, 73.80; H, 10.00.

Synthesis of benzyl 2,3-*O*-(1-methylethylidene)-D-lyxofuranosyl-*N*,*N*-dibenzyl-carboxamide (220): A solution of **219** (200 mg, 0.72) in dry THF (20 mL) was stirred at -0 °C under nitrogen atmosphere and EDC (146 mg, 0.94 mmol) and HOBt (127 mg, 0.94 mmol) was added. The reaction mixture was stirred at 0 °C under nitrogen atmosphere for 1 hour. Then dibenzylamine (185 mg, 0.94 mmol) and Dipea (121 mg, 0.94 mmol) were added and the reaction mixture was stired at room temperature for 5 days, when a TLC check (CH_2Cl_2/MeOH 20:1) attested the disappearance of the starting material. A Saturated Ammonium Chloride Solution (10 mL) and CH_2Cl_2 (10 mL) were added to the mixture at 0 °C and left stirring for 15 minutes. The two layers were separated and the aqueous layer was extracted with CH_2Cl_2 (2x10 mL). The combined organic layers were washed with brine (2x30 mL), dried with Na_2SO_4 and concentrated under reduced pressure. The residue was purified by silica gel flash chromatography (Hex/AcOEt 5:1) to give **220** (181 mg, 0,38 mmol, 53%, R_f = 0.20) as a colorless oil.
220 colorless oil: $[\alpha]_D^{24}$ = + 33 (c =0.51, $CHCl_3$). ^{1}H-NMR (400 MHz, $CDCl_3$) δ = 7.38 – 7.23 (m, 15H, Ar), 5.30 (s, 1H, 1-H), 5.07 (t, J =6.0 Hz, 1H, 3-H), 4.91 (d, J = 4.0 Hz, 1H, 4-H), 4.82 (d, J =12.0 Hz, 1H, H_a-NBn), 4.68-4.63 (m, 3H, H_a-OBn, H_a-NBn and 2-H), 4.49-4.41 (m, 3H, H_b-OBn, H-N_bBn and H-N_bBn), 1.52 (s, 3H, Me), 1.33 (s, 3H, Me) ppm. ^{13}C-NMR (100 MHz, $CDCl_3$) δ = 167.0 (d, 1C, *C*=O), 137.1, 137.0, 136.0 (s, 3C, Ar), 128.9 – 127.2 (d, 15C, Ar), 113.6 (s, acetal), 105.0 (d, C-1), 84.4 (d, C-2), 80.7 (d, C-4), 80.4 (d, C-3), 69.4 (t, OBn), 49.1 (t, NBn), 48.3 (t, NBn), 26.1(q, 1C, Me,), 25.0 (q, 1C, Me,) ppm. MS (ESI): m/z (%) = 474.60 (100) [M+H]$^+$. $C_{29}H_{31}NO_5$ (473.55): calcd. C, 73.55; H, 6.60; N, 2.96; found C, 73.67; H, 6.70; N, 2.80.

Conclusion

We report the synthesis of two series of epimeric trihydroxypiperidines **147** and **151** alkylated at C-2 with both configurations, through a stereodivergent approach that relies on the stereoselective addition reaction of Grignard reagents to the D-mannose-derived nitrone **140**. The absence or the presence of a suitable Lewis acid allowed reversal of the selectivity of the addition, giving access to both diastereoisomers of the formed hydroxylamines **144** and **148**, respectively. An efficient final reductive ring-closure amination step allowed the synthesis of the trihydroxypiperidine skeleton, and final deprotection under acidic conditions led to the target compounds **147** and **151** in high yields and few synthetic steps from the starting materials. A careful spectroscopic analysis of the protected precursors of the final compounds **146** and **150** allowed us to determine the absolute configuration of the newly formed stereocenter and identify the more stable conformation, which were confirmed by X-ray and DFT analysis on compound **150e**. Biochemical characterization towards human glucocerebrosidase (GCase) and other lysosomal enzymes showed that compounds **147** and **151** behave as good GCase inhibitors with IC_{50} in the micromolar range. An interesting trend was found in the inhibitory activity potency: given the same alkyl chain length, the trihydroxypiperidines **151** *R*-configured at C-2 were 3- to 18-fold more active than the corresponding trihydroxypiperidines **147** *S*-configured at C-2. Kinetic analysis showed competitive inhibition for compounds **151**. Nearly all new compounds showed GCase activity rescue of 1.2- to 1.9-fold in fibroblasts derived from Gaucher patients bearing the N370/RecNcil mutation, independently on the configuration at C-2. More importantly, we identified the best chaperone **151a**, that was able to enhance GCase activity 1.9-fold at 50 µM in fibroblasts bearing the N370S mutation and, was also able to enhance GCase activity 1.8-fold in fibroblasts bearing the homozygous L444P mutation, which is a cell line resistant to most PCs. Considering that none of the therapeutic strategies available to date are effective in type II/III Gaucher disease, our results on L444P mutated fibroblasts are remarkable. Therefore, we demonstrated once again that the presence of a lipophilic chain plays a pivotal role for inhibition, while the shift of the chain in C-2 position in compound **151a**, compared to the analogous compounds with an eight carbon chain at either the endocyclic (**169**) or an exocyclic nitrogen (**167**), shows better properties as PC. The compound **151a,** due to its excellent PC activities, was further investigated *in vivo* study on animal models of PD (see *Chapter 4*). Moreover, a preliminary structure-activity relationships (SAR) was undertaken to identify those positions on the molecule that can be modified to improve some properties.

Finally, we report a molecular docking study in order to obtain structural information on the interactions between GCase and the newly synthesized alkyl trihydroxypiperidines **147** and **151**. Despite having a different configuration and substitution at C-5 compared to isofagomine (IFG, **2**), piperidines **151** with the *R* configuration at C-2 are able to interact within the enzyme cavity placing the piperidine moiety with the same orientation as IFG. Conversely, the length of the alkyl chain seems to influence its orientation within the enzyme cavity. Piperidines **147** with the *S* configuration at C-2 do not bind the active site of GCase with a unique orientation, which may reflect the lower inhibitory potency of this series.

The results included in this Section have been published. (F. Clemente, C. Matassini**,** A. Goti, A. Morrone, P. Paoli, F. Cardona, *ACS Med. Chem. Lett.* **2019**, *10*, 621-626. and F. Clemente, C. Matassini, C. Faggi, S. Giachetti, C. Cresti, A. Morrone, P. Paoli, A. Goti, M. Martínez-Bailén, F. Cardona, *Bioorg. Chem*. **2020**, *98*, 103740-103763.)

We also investigated the condensation/oxidation reaction with UHP in the presence of catalytic MTO starting from aldehyde **135** and several primary amines to obtain, in a simple and regioselective way, new carbohydrate-derivative nitrones. This strategy allowed to obtain with good yield the key intermediate **174a** to obtain trihydroxypiperidine 1,2-disubstituted. The synthetic strategy was based on the addition of octylMgBr onto nitrone **174a**, followed by intramolecular reductive amination. Access to both epimers at the newly created stererocentre was secured by carrying out the addition in the absence or presence of a Lewis acid. The addition reaction occurred with good yields and excellent stereoselectivity in both cases. The overall synthesis was achieved in 8 steps from low cost D-mannose and provided the final compounds **170** an **171** in 43% and 32% overall yield, respectively. The new compounds were investigated as potential inhibitor towards human lysosomal enzymes and as potential PC for GD in fibroblasts derived from Gaucher patients bearing the N370/RecNcil and L444P/L444P mutation. The newly synthesized trihydroxypiperidines **170** an **171** were potent inhibitor of GCase at 1 mM with the IC_{50} values equal to 100 µM and 15 µM, respectively. These data show that the presence of long alkyl chains in the *N* and C-*2* position afforded good GCase inhibitors. Moreover, **170** an **171** were selective inhibitors of the GCase enzyme with respect to other lysosomal enzymes. (α-mannosidase, β-mannosidase, α-galactosidase, β-galactosidase, α-fucosidase). Unfortunately, **170** an **171** did not enhance the intracellular activity of mutant GCase in N370S and L444P mutations.

With the aim to investigate the chain length on the biological properties, we report herein also two alternative synthetic strategies to obtain *N*-dodecyl trihydroxipiperidine **192**. In particular the stragey based on the key intermediate **174b**, obtained through the condensation / oxidation reaction with UHP and MTO starting from D-mannose derived aldehyde **135**, followed by reductive amination and subsequent acetonide deprotection, allowed to afford compound **192** with an overall yield on three steps of 48%.

Compound **192** was an excellent GCase inhibitor (IC_{50} = 3.4 μM), about 10-fold more active than the *N*-octyl piperidine analogue **169**, confirming that the presence of a long lipophilic alkyl chain plays a fundamental role in interacting with the GCase active site. Compound **192** was also able to recover the catalytic activity of the human enzyme bearing the N370/RecNcil mutation of a 1.28-fold at quite a low concentration (100 nM). However, compound **192** was toxic at slightly higher concentrations (50 μM), in agreement with previous reports, which showed that the cytotoxicity of alkylated imino- and azasugars increases upon increasing of the alkyl chain's length, in particular for chains above eight carbon atoms. The cmc analysis suggest that the toxicity of compounds **192** is independent from micelle formation.

With the aim of investigation the role of the stereochemistry at C-3 on the inhibition/pharmacological chaperoning activity of the target trihydroxypiperidines, we synthesized a series of trihydroxypiperidines and congeners with the "*all-cis*" configuration at the carbons bearing the hydroxy/amino groups. The reported syntheses exploited the reaction of the ketone intermediate **166**, which was functionalized at C=O through ketone reduction followed by alcohol alkylation (**175**, **208**), reductive amination (**176**), or *via* the stereoselective addition of various lithium acetylides (**177** and **178**, **211** and **212**). Interestingly, the newly synthesized compounds **175**, **176** and **178** showed moderate to good inhibition against human lysosomal β-glucosidase (GCase). For this enzyme, our data confirmed that the presence of an alkyl chain of at least eight carbon atoms is essential to impart GCase inhibitory activity. However, we showed that the alkyl chain can be placed at the C-3 position either maintaining the three hydroxyl groups (as in compound **178**), or *via* alkylation of the hydroxy group at C-3 (as in ether **175**). However, compound **176** failed to rescue the enzyme activity on cell lines likely due to its cytotoxicity. Nevertheless. The results of the Section were published in Molecules 2020 (M. G. Davighi, **F. Clemente**, C. Matassini , A. Morrone, A. Goti, M. Martínez Bailén, F. Cardona, Molecules. **2020**, 25, 4526-4549.

Finally, three different synthetic approaches to obtain 2,2-dioctyl trihydroxypiperidine **213** were explored. The third strategy, based on a one-pot conversion of tertiary amide into tertiary amines , is the most promising and will be pursued in the next future.

Chapter 4:
Test *in vivo* on animal models of Parkinson's Disease

4.1 Drosophila Melanogaster

4.1.1 Why Drosophila?

Drosophila melanogaster, as a non-mammalian animal, provides a simple, yet powerful, *in vivo* system for studying a range of genetic diseases.

There are many advantages of using Drosophila over other vertebrate models:

- They have a much shorter life cycle and generate large numbers of externally laid embryos (Figure 4.1). [220]

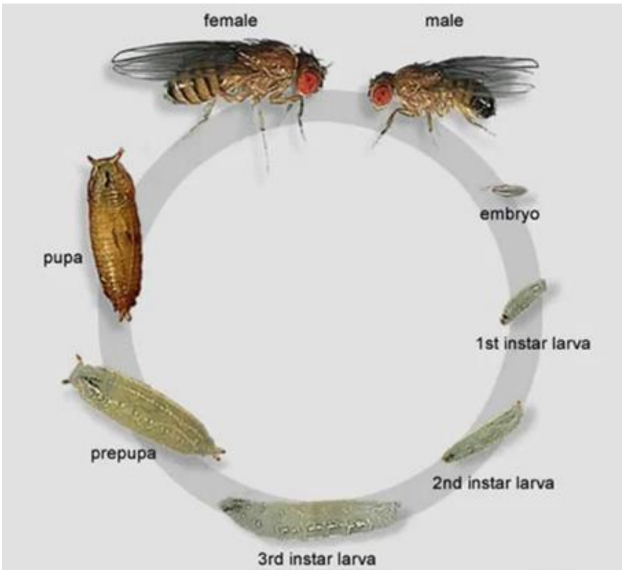

Day 0: Female lays eggs
Day 1: Eggs hatch
Day 2: First instar (one day in length)
Day 3: Second instar (one day in length)
Day 5: Third and final instar (two days in length)
Day 7: Larvae begin roaming stage. Pupariation (pupal formation) occurs 120 hours after egg laying
Day 11-12: Eclosion (adults emerge from the pupa case). Females become sexually mature 8-10 hours after eclosion
The generation time of Drosophila melanogaster varies with temperature. The above cycle is for a temperature of about 22°C.

Figure 4.1: Life cycle of Drosophila melanogaster

The reproductive cycle is complete in about 12 days at room temperature (25°C). Drosophila undergo a four-stage life cycle: egg, larva, pupa and fly (Figure 1). The female fruit flies lay between 750 and 1,500 eggs in her lifetime. After the egg is fertilized, the embryo emerges in ~24 hours. The embryo undergoes successive molts to become the first, second, and third larval stage. The larval stages are characterized by consumption of food and resulting growth, followed by the quiescent pupal stage, during which there is a re-organization of the body plan (metamorphosis) followed by the emergence of the adult fly. They live a month or more and then die (Figure 4.1).

- They are sexually dimorphic (males and females are different). [220]

Figure 4.2 shows the differences between females and males: females are slightly larger and display dark separated stripes at the posterior tip of their abdomen, which are merged in males (black arrows). Males have sex combs on the first pair of legs. Anal plates are darker and more complex in males and display a pin-like extension in females (white arrows).

- Drosophila has four pairs chromosomes. [220]

Flies have a pair of sex chromosomes (two X chromosomes for females, one X and one Y for males), together designated Chromosome 1, and three pairs of autosomes (non-sex chromosomes) identified 2 through 4. Chromosome 4 is the smallest and is also called the dot chromosome. It represents just ~2% of the fly genome (Figure 4.3).

- They acquire specific mutations which affect morphological changes in the adult flies.

These mutations affect anatomical landmark of flies such as sizes and positions of bristles, the sizes and shapes of eyes, wings and halteres, or the patterns of wing vein. These mutations can be used to study biological processes underlying body patterning and development (by addressing what the mutant phenotypes reveal about the normal gene function). On the other hand, these mutations provide important markers to be used during genetic crosses (Figure 4.4). An important genetic tool is the balancer chromosome. A balance chromosome contains alleles that are lethal when carried homozygous. It also contains a dominant marker of visible phenotype. The role of the balance is to maintain a homozygous lethal mutation. Strains building this mutation are kept in heterozygous state, where one of the chromosomes bears mutation and the other is a balance. The balance cannot take over the population since it is lethal if homozygous and it also enables easy recognition of flies.

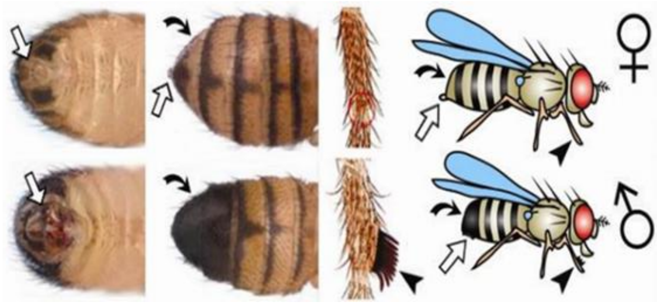

Figure 4.2: Differences between females and males in Drosophila.

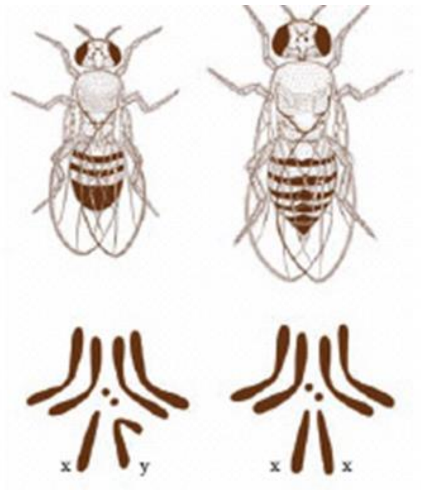

Figure 4.3: Drosophila chromosomes.

- Many Drosophila genes are homologous to human genes.
- They are easy and inexpensive to culture in laboratory conditions. [220]

Fly stocks are kept in glass or plastic vials which contain food (the main ingredients of which are corn flour, glucose, yeast and agar) at the bottom and are closed with cotton wool and they can easily be transferred to fresh vials for maintenance. These vials are usually stored in incubators with controlled temperature and humidity. Stock keeping is usually done at 18°C (generation time of about 1 month). It is good practice to keep one young and one two-week older vial of each stock. Every fortnight, freshly hatched flies from the month-old vial are flipped into a fresh vial, whilst the two-week-old vial should have produced larvae and serves as back-up. Such a routine allows you to spot any problems on time, such as infections (mites, mould, bacteria, viral infections). The equipment to analyse genetic markers and select virgins and males of the desired phenotype flies includes a binocular microscope with a light source, a CO_2 plate for anesthetization, a fly pusher and a morgue.

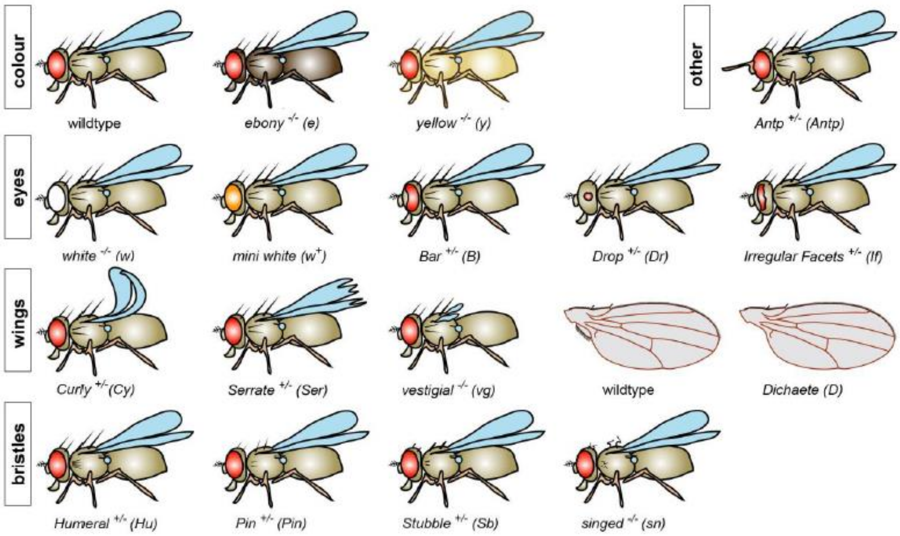

Figure 4.4: A few marker mutations commonly used for fly work.

4.1.2 *GBA*-associated Parkinson's Disease in Drosophila: *GBA* transgenic Drosophila model

Mutations in the *GBA* gene are associated with Parkinson's disease. This association has been established in patients with *GBA* mutation (see *Chapter 1.3.1.1*). To investigate *GBA* functions in PD, transgenic Drosophila expressing human WT, N370S and L444P were created. N370S and L444P transgenic flies exhibited significant decreased GCase activity by 82 and 75%, respectively, compared with *GBA* WT transgenic flies despite equivalent expression levels of *GBA* protein. [59] [88] Expression of the foreign gene is regulated by the Gal4/UAS system, a powerful tool to drive the expression of a chosen gene in a tissue-specific manner by exploiting a yeast transcriptional activation mechanism. This binary system is based on the properties of the yeast (*Saccharomyces cerevisiae*) GAL4 transcription factor, which activates transcription of its target genes by binding to specific cis-regulatory sites called UAS (Upstream Activation Sequence). The system is constituted of two independent parent transgenic lines, the GAL4 driver line in which the Gal4 gene is expressed in a tissue-specific pattern and the UAS responder line in which the gene of interest is under UAS control. Copulating of the UAS-containing responder flies with the GAL4 driver-containing flies results in progeny bearing the two components, in which the UAS-transgene is expressed in a transcriptional pattern by the GAL4 transcription factor (Figure 4.5). [221] [222]

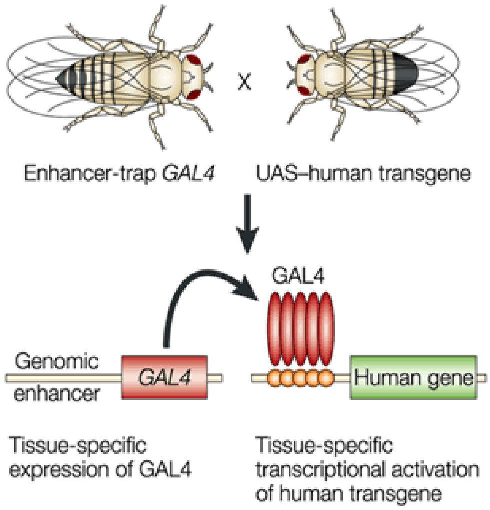

Figure 4.5: The Gal4/UAS system. [223]

Transgenic Drosophila expressing human *GBA* mutations, thanks to Gal4/UAS system, mimics the healthy carriers of GD. In this animal model there is no substrate accumulation in the lysosomes because the flies have their own *GBA* gene. The flies have two *GBA*1 homologs in the Drosophila melanogaster. Both of them received on chromosome 3 of the fly and are designated CG31148 (*GBA*1a) and CG31414 (*GBA*1b). The two genes encode proteins with about 31% identity and 50% similarity of the human GCase. Moreover, flies are powerful model to study the genetic pathways involved in normal development and in neuronal degenerative disease in general and PD in particular because the genetic pathways are conserved between Drosophila and mammals. Specifically, ERAD and UPR are well conserved among species. [224] [225] This type of model allows to evaluate the contribution of ER stress to disease pathogenesis in the absence of the well-known GCase - α-Syn bidirectional relationship for the reason that Drosophila does not have a homolog of α-Synuclein. Transgenic flies carrying N370S and L444P variants, due to presence of mutant GCase in the ER, presented UPR and increased level of ER stress and developed parkinsonian signs, manifested by death of dopaminergic cells, defective locomotion and a shorter life span. [59]

4.1.3 Rescue of parkinsonian signs in β-Glucosidase transgenic flies by our Pharmacological Chaperones for Gaucher Disease

We tested our best PCs, namely compounds **151a** and **167**, on transgenic flies expressing human WT GCase and carrying the mutant human L444P, thanks to Gal4/UAS system, for the partial rescue of Parkinsonians signs thanks to the collaboration with Prof. Mia Horowitz (Department of Cell Research and Immunology, Tel Aviv University, Israel) (Figure 4.6).

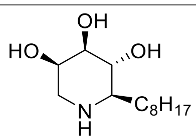 **151a**	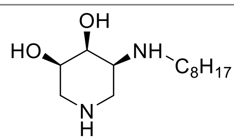 **167**
• GCase activity rescue on N370S mutated fibroblasts: 1.9-fold at 50 μM [158] • GCase activity rescue on L444P mutated fibroblasts: 1.8-fold at 100 μM [158]	• GCase activity rescue on N370S mutated fibroblasts: 1.5-fold at 100 μM [159] • not yet tested on GCase activity rescue on L444P mutated fibroblasts

Figure 4.6: PCs activity rescue on human fibroblasts bearing the N370S or the L444P mutations.

PCs have been tested on heterozygous Drosophila Melanogaster expressing human WT GCase and carrying the mutant human L444P (WtGCase/cyo; DdcGal4/sb and L444P/cyo; DdcGal4/sb), identified thanks to the presence of chromosome balancers. Flies expressing only transcription Gal4/UAS system are used as a control (Ddc-GAL4). Flies were grown as 10 flies (5 males and 5 females), per vials (total 100 flies) and were transferred to fresh food containing PC every other day. PCs, dissolved in water at different concentrations (100 μM or 1 mM), were added on the surface of the food.

PCs are competitive inhibitors of the target enzyme (see *Chapter 1*). High dosages of competitive inhibitor PCs may lead to the loss of target enzyme function due to inhibition. The side effects are addressed by administering PC therapy with breaks and avoid continuous treatment (on / off protocols). For this reason, the PCs are administered every other day.

The results on life span of the flies are shown in Figure 4.7. The treatment of transgenic flies expressing only transcription Gal4/UAS system at 1 mM concentration of compounds **151a** and **167** showed a significant reduction of life span most likely due to the inhibition of the endogenous GCase of the flies, while at the concentration of 100 µM there was no substantial difference with the untreated flies (Figure 4.7-A). The same trend on the life span of flies was shown for flies expressing human WT GCase at 1 mM and 100 µM concentration of compounds **151a** and **167** (Figure 4.7-B). In this case the reduction of the life span at 1 mM may be due not only to inhibition of endogenous GCase of the flies but also to inhibition of human GCase. Then we tested compounds **151a** and **167** on transgenic flies carrying the mutant human L444P at 100 µM. To our pleasure, these flies showed a significant increase in life span in comparison with untreated flies (Figure 4.7-C). However, there were no improvements in the locomotion behaviour in both strains of flies treatment with PCs (100 µM) with respect to untreated flies (see Experimental Section-climbing test). Further studies to verify the reduction of ER stress markers are underway.

A: Drosophila Melanogaster sco/cyo; sb/DdcGal4 as a control (Ddc-GAL4).

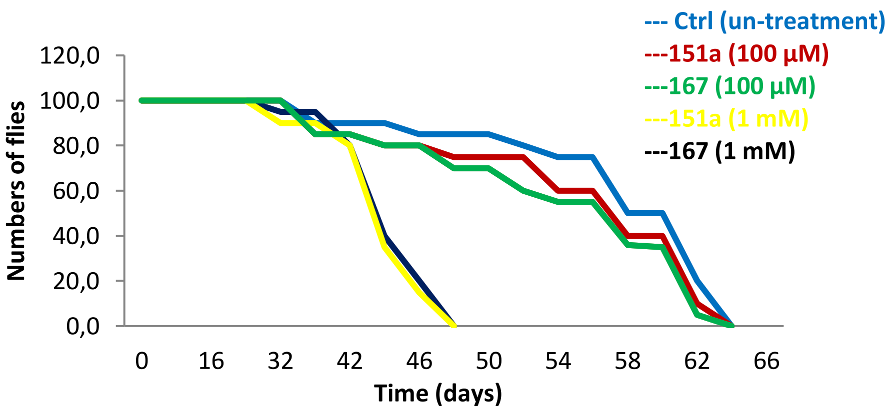

B: **Heterozygous Drosophila Melanogaster WtGCase/cyo; DdcGal4/sb**

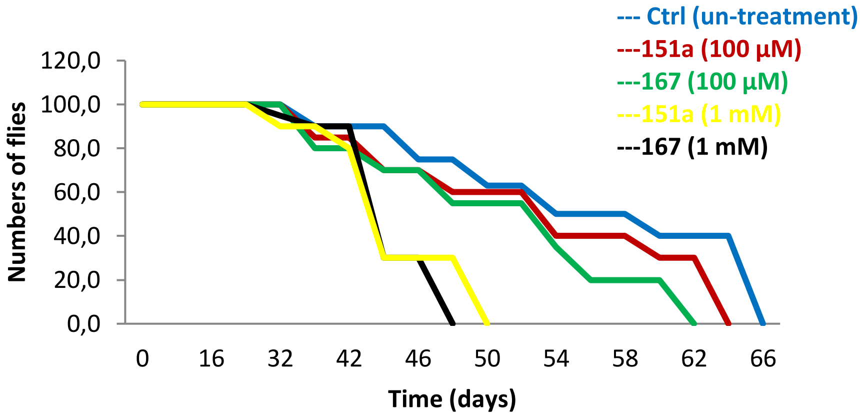

C: **Heterozygous Drosophila Melanogaster L444P/cyo ; DdcGal4/sb**

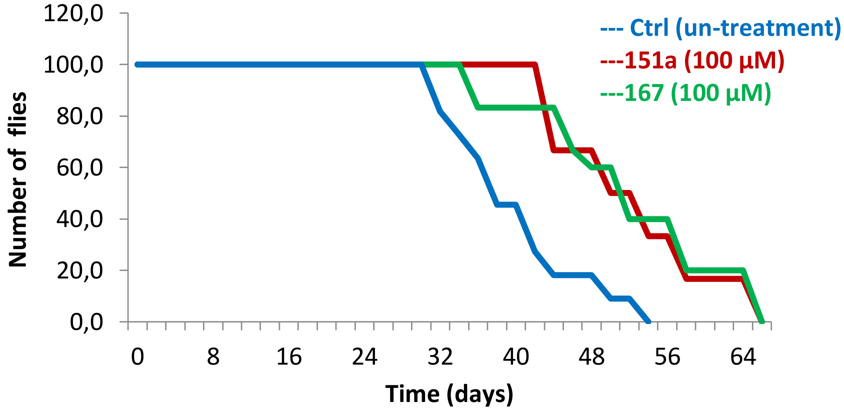

Figure 7: Overall survival rates of flies expressing only transcription Gal4/UAS system are used as a control (Ddc-GAL4) without (Ctrl) or with compounds **151a** and **167** at two different concentrations (1 mM and 100 µM) (A), human wild-type GCase without (Ctrl) or with compounds **151a** and **167** at two different concentrations (1 mM and 100 µM) (B) or expressing human L444P variant without (Ctrl) or with compounds **151a** and **167** at 100 µM concentration (C) tested on 100 flies. Flies were grown as 10 flies per vials and were transferred to fresh food every other day.

4.1.4 Experimental Section

Fly strains and maintenance.

Transgenic flies, harboring pUASTmycHisGCase and pUASTmycHisL444PGCase on the second chromosome were established by Bestgene (Chino Hills, CA, USA). Da-GAL4 driver line (No.55849) and Ddc-GAL4 driver line (No. 7009) were from

Bloomington Stock Center. Strains were maintained on standard cornmeal-molasses medium at 25 °C.

Survival assay.

For each fly strain, 10 vials, each containing 10 flies (5 males and 5 females), were maintained on food from day one post-eclosion. Fresh food was supplied every other day and deaths were recorded.

Climbing assays.

Climbing assays were performed by using a countercurrent apparatus developed initially for phototaxis experiments. Thirty flies were placed into the first chamber, tapped to the bottom, then given 30 sec to climb a distance of 10 cm. Flies that successfully climbed 10 cm or beyond in 30 sec were then shifted to a new chamber, and both sets of flies were given another opportunity to climb the 10-cm distance. This procedure was repeated a total of five times. After five trials, the number of flies in each chamber were counted. At least 60 flies were used for each genotype tested. Climbing ability was tested at days 2, 12 and 22 post-eclosion.

PC treatment.

PCs, dissolved in water at different concentrations (100 µM or 1 mM), were added on the surface of the food.

4.2 Thy1-aSyn mice

Thy1-αSyn Mice, a mouse model over-expressing full-length, human, wild-type alpha-synuclein under the Thy-1 promote, provides a powerful *in vivo* system for studying sporadic PD. This model reproduces many features of sporadic PD including progressive changes in dopamine release and striatal content, the deposition of α-synuclein (Lewy bodies), motor and nonmotor functions that are affected in pre-manifest and manifest phases of PD. [226] In our future projects compound **151a** will be tested on these model mice in order to evaluated the rescue of the GCase enzymatic activity in brain, motor functions and decrease of α-Syn aggregation thanks to the collaboration with Prof. G. Mannaioni, (Department of Neurosciences, Psychology, Drug Research and Child Health (NEUROFARBA), Division of Pharmacology and Toxicology, University of Florence).

4.2.1 Preliminary biological results on Wild-Type human fibroblasts

A growing evidence has been collected showing that targeting GCase pharmacologically might be a valid therapeutic strategy for Parkinson disease (PD), not only for those forms connected with *GBA* mutations, but also for sporadic forms of PD in the absence of GCase mutations (see *Chapter 1*). For this reason, we tested the ability of compound **151a** to rescue the GCase enzymatic activity in wild-type human fibroblasts from healthy donors and the results are shown in Figure 4.8. Remarkably, concentrations of **151a** between 50 and 100 µM were able to enhance GCase activities of 1.2–1.4- fold. [158]

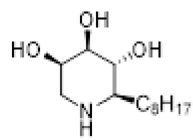

151a

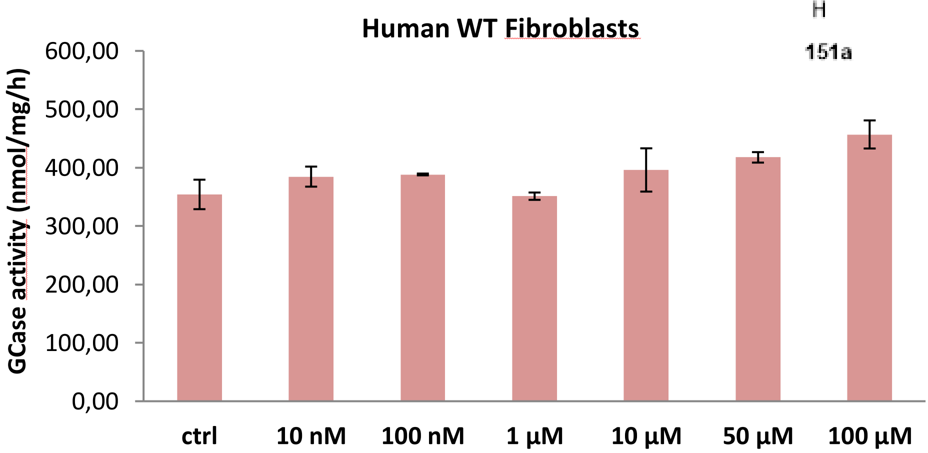

Figure 4.8: GCase activity in human fibroblasts derived from healthy donors measured after 4 days of incubation without (ctrl) or with compound **151a**.

These data compare well to those reported in the literature for IFG on WT human cells (1.3–1.4-fold enhancement at 25–30 µM) [189], and augur well for future applications using this compound to treat sporadic forms of PD. In order to evaluate the impact of our best chaperone **151a** on cell viability, an MTT test was carried out using WT fibroblasts, and the results are shown in Figure 4.9. A very low decrease in the MTT reduction rate was observed in WT fibroblasts but only at the highest concentrations and slightly increasing with time. [158]

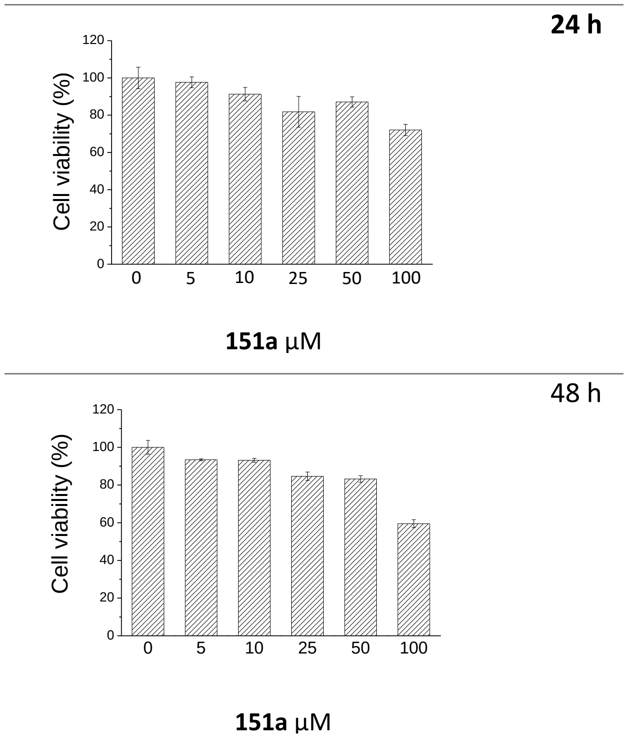

Figure 4.9: Viability assay. Wild-type fibroblasts were incubated for 24 and 48 h in the presence of compound **151a** at different concentrations. After this time, the viability of cells was evaluated using MMT assay. Obtained values were normalized with respect to control experiments. Data reported represent the mean value ± S.E.M. (n = 8).

4.2.2 Preliminary biological results on Wild-Type mice

Compound **151a** was tested on WT mice (wild type mouse-WTC57) in order to evaluated the optimal dose and vehicle of oral administration, together with the ability of compound **151a** to rescue the GCase activity in brain. The choice of oral administration is due to the advantages of PC based therapy (reduce hospitalization and the ability of PC to cross the blood brain barrier, see *Chapter 1*). Moreover, azasugars are not subjected to the first-pass metabolism. [73]

Three WT mice were treated with 100 mg/kg *per os* of compound **151a** (in warm aqueous solution for gavage) in a 1-day-on/2-day-off trial for 2 weeks. This protocol provoked the death of the animals. The mice showed severe ulcers of the gastrointestinal tract most likely due to the temperature of the administration vehicle. The same protocol carried out using 15% hydroalcoholic solution (for gavage) as solubilising agent caused anyway the death of the animals but no damage of the gastrointestinal system was found. Based on these results, we reduced ten-fold the administered dose using the same vehicle (15% hydroalcoholic solution for gavage). The low percentage of ethanol used as vehicle is unable to cause adverse effects caused by sub-chronic administration of ethanol. The treatment of 8 WT mice with 10 mg/kg *per os* of compound **151a** (in 15% hydroalcoholic solution for gavage), in a Monday-Wednesday-Friday trial for 2 weeks, didn't show a significant enhancement of GCase activity in brain compared to untreated mice (Figure 4.10).

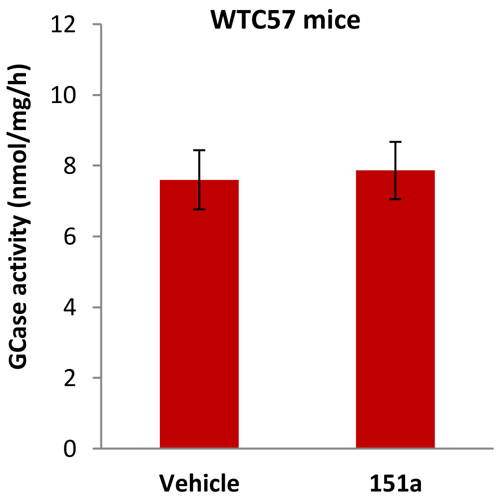

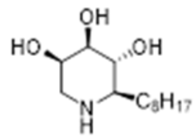

151a

Figure 4.10: GCase activity measured in brain homogenate derived from WT mice (WTC57, N=8 each condition) without (vehicle) or with 10 mg/kg of **151a** administered *per os* in 15% hydroalcoholic solution for gavage 3 days/week for 2 weeks.

Instead, the treatment of 8 WT mice with 30 mg/kg *per os* of compound **151a** (in 15% hydroalcoholic solution for gavage), in a Monday-Wednesday-Friday trial for 2 weeks, showed a significant enhancement (19%) of GCase activity in brain compared to untreated mice (Figure 4.11).

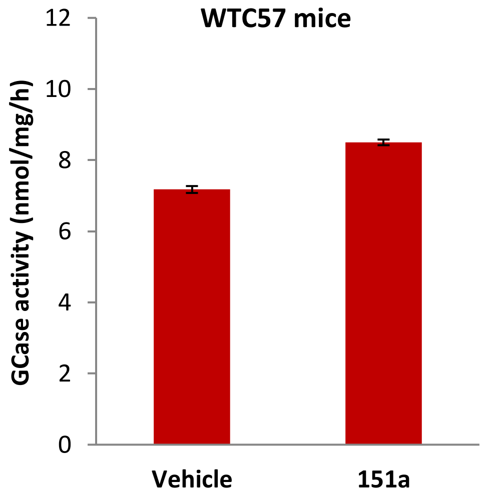

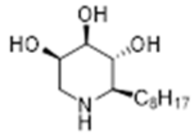

151a

Figure 4.11: GCase activity measured in brain homogenate derived from WT mice (WTC57, N=8 each condition) without (vehicle) or with 30 mg/kg of **151a** administered *per os* in 15% hydroalcoholic solution for gavage 3 days/week for 2 weeks.

The observation that the compound **151a** increase wild-type GCase activity *in vivo* suggests that **151a** can be a great candidate for the treatment for sporadic PD. The compound **151a** will be tested on Thy1-αSyn Mice model over-expressing full-length, human, wild-type alpha-synuclein in order to evaluated the rescue of the GCase enzymatic activity in brain, motor functions and decrease of α-Syn aggregation.

4.2.3 Experimental Section

Pharmacological chaperoning activity

Wild type fibroblasts were obtained from the "Cell line and DNA Biobank from patients affected by Genetic Diseases" (Gaslini Hospital, Genova, Italy).

Fibroblasts cells ($13.5\text{-}15.0\times10^4$) were seeded in T25 flasks with DMEM supplemented with fetal bovine serum (10%), penicillin/streptomycin (1%), and glutamine (1%) and incubated at 37 °C with 5% CO_2 for 24 h. The medium was removed, and fresh medium containing the azasugars was added to the cells and left for 4 days. The medium was removed, and the cells were washed with PBS and detached with trypsin to obtain cell pellets, which were washed four times with PBS, frozen and lysed by sonication in water. Enzyme activity was measured as reported above. Reported data are mean S.D. (n = 2).

Cytotoxicity tests

MTT test was carried out using human fibroblasts wild type at different concentrations. Fibroblasts were grown in the presence of Dulbecco's modified Eagle's medium supplemented with 10% fetal bovine serum (FBS), 1% glutamine, and 1% penicillin–streptomycin, at 37 °C in controlled atmosphere with 5% CO_2. For the experiments, cells were seeded at a density of 20,000 cells per well in 24-well plates and grown for 24 h (or 48 h) before adding compounds. Compounds were dissolved in water; then aliquots of these were diluted in the growth medium. To preserve sterility of solutions, these were filtered with 0.22 µm filters before adding to the dishes containing fibroblasts. Then, cells were incubated at 37 °C in 5% CO_2 for 24 h (or 48 h). After this time, the media were replaced with medium containing 0.5 mg/mL of 3-(4,5-dimethylthiazol-2-yl)-2,5-diphenyltetrazolium bromide (MTT); the cells were incubated for an additional 1 h at 37 °C in 5% CO_2. Finally, the number of viable cells was quantified by the estimation of their dehydrogenase activity, which reduces MTT to water-insoluble formazan. Growth medium was removed and substituted with 300 µL of DMSO to dissolve the formazan produced. The quantitation was carried out measuring the absorbance of samples at 570 nm with the iMark microplate absorbance reader (BIO RAD) in a 96-well format.

GCase activity assay.

Wild type human fibroblasts were disrupted by sonication, and a micro BCA protein assay kit (Sigma–Aldrich) was used to determine the total protein amount for the enzymatic assay, according to the manufacturer instructions. Enzyme activity was measured in a flat-bottomed 96-well plate. Fibroblasts homogenate (10 µL) and substrate 4-methylumbelliferyl-β-D-glucoside (3.33 mM, 20 µL, Sigma–Aldrich) in citrate/phosphate buffer (0.1:0.2, M/M, pH 5.8) containing sodium taurocholate (0.3%) and Triton X-100 (0.15%) at 37 °C were incubated for 1 h. The reaction was stopped by addition of sodium carbonate (200 µL; 0.5 M, pH 10.7) containing Triton X-100 (0.0025%), and the fluorescence of 4-methylumbelliferone released by β-glucosidase activity was measured in SpectraMax M2 microplate reader (λex=365 nm, λem=435 nm; Molecular Devices). GCase activity is given with respect to the control (no treatment). Data are mean SD (n = 3).

PC treatment of wild type mouse-WTC57: Four protocols

- 3 WT mice un-treated (control) and treated with 100 mg/kg *per os* of compound **151a** (in warm aqueous solution for gavage) in a 1-day-on/2-day-off trial for 2 weeks*.
- 3 WT mice un-treated (control) and treated with 100 mg/kg *per os* of compound **151a** (in 15% hydroalcoholic solution for gavage) in a 1-day-on/2-day-off trial for 2 weeks*.
- 8 WT mice un-treated (control) and treated with 10 mg/kg *per os* of compound **151a** (in 15% hydroalcoholic solution for gavage) in Monday-Wednesday-Friday trial for 2 weeks*.
- 8 WT mice un-treated (control) and treated with 30 mg/kg *per os* of compound **151a** (in 15% hydroalcoholic solution for gavage) in Monday-Wednesday-Friday trial for 2 weeks*.

*We deliberately chose to sacrifice the animals after a 15 days treatment.

GCase activity assay in the brain of mice.

Procedure for lysis of brain tissue using RIPA Lysis Buffer with protease and phosphatase inhibitors (Thermo Fisher Scientific). For each mouse 3 tissue samples from the brain were prepared.

Protease and phosphatase inhibitors were added to the RIPA Buffer immediately before use.

1. Tissue of interest was removed after the sacrifice: BRAIN, Pellet the cells by centrifugation at 2500 × g for 5 minutes. Supernatant was discarded.
2. Cells were washed twice in cold PBS. Pellet cells by centrifugation at 2500 × g for 5 minutes.
3. RIPA Buffer was added to the cell pellet. 1mL of RIPA buffer for 80 mg of tissue was used and the pellet was sonicated for 30 seconds with 50% pulse.
4. The mixture was shaked gently for 15 minutes on ice. The mixture was Centrifugated at ~14,000 × g for 15 minutes to pellet the cell debris.
5. Supernatant was transferred to a new tube for further analysis.

A micro BCA protein assay kit (Sigma–Aldrich) was used to determine the total protein amount for the enzymatic assay of the supernatant, according to the manufacturer instructions. RIPA Buffer is compatible with the BCA Protein Assay Kit. Enzyme activity was measured as reported above. Reported data are mean S.D. (n = 3).

Conclusion

Considering the excellent preliminary results of compound **151a** in modulating GCase activity not only for GD (see *Chapter 3*) but also for GD-related PD (see transgenic Drosophila Melanogaster expressing human WT GCase and carrying the mutant human L444P) and for the sporadic forms of PD that do not have the *GBA* mutation (see wild type mouse-WTC57), together with its straightforward synthesis starting from D-mannose with the high overall yield of 42% (see *Chapter 3*), it represents a promising target for future development. Further optimization of its physicochemical and pharmacokinetic properties will be the topic of future investigations.

Chapter 5:
Multivalency in β-glucosidase inhibition

Introduction

The multivalent effect (MVE) is defined as the increase of the biological response obtained with compounds possessing more than one bioactive unit linked to a common scaffold, compared to the sum of the contributions given by the individual bioactive molecules. However, the simultaneous presentation of multiple binding units may enhance the relative potency (rp) of the multivalent architectures with respect to the monovalent ligands simply due to the higher number of bioactive units.

Therefore, the MVE is defined as positive when the ratio rp/n is more than 1, where n represents the number of biological units grafted on the scaffold. [227] [228] The generally accepted phenomena which may account for the observed MVE involve:

1) *Statistical effect* (Figure 5.1-A), due to the enhancement of the local concentration of the active molecule in proximity of the binding site;

2) *Chelating effect* (Figure 5.1-B), involved when the enzyme presents more than one catalytic site;

3) *Secondary binding effect* (Figure 5.1-C), that may determine either a stronger binding of the inhibitor by non-specific interactions with non-catalytic subsites (Figure 5.1-C/a) or a steric hindrance that hampers access of the substrate to the catalytic site (Figure 5.1-C/b);

4) *Cluster effect*, when the association of several units of enzyme is favoured over one multivalent molecule (Figure 5.1-D/a), or with the formation of a crosslinked network if the enzyme also possesses a multimeric form (Figure 5.1-D/b). [228]-[230]

The wild-type or mutant GCase protein exists in a dimeric structure composed by four/two catalytically active 60 kD glycoprotein units. [231]-[234]

Due to its quaternary structure GCase is a very good candidate for multivalent interactions. GCase enzyme, considering its dimeric nature, can give an aggregative processes and the formation of stabilized inhibitor-enzyme networks (Figure 5.2) promoting a positive MV effect.

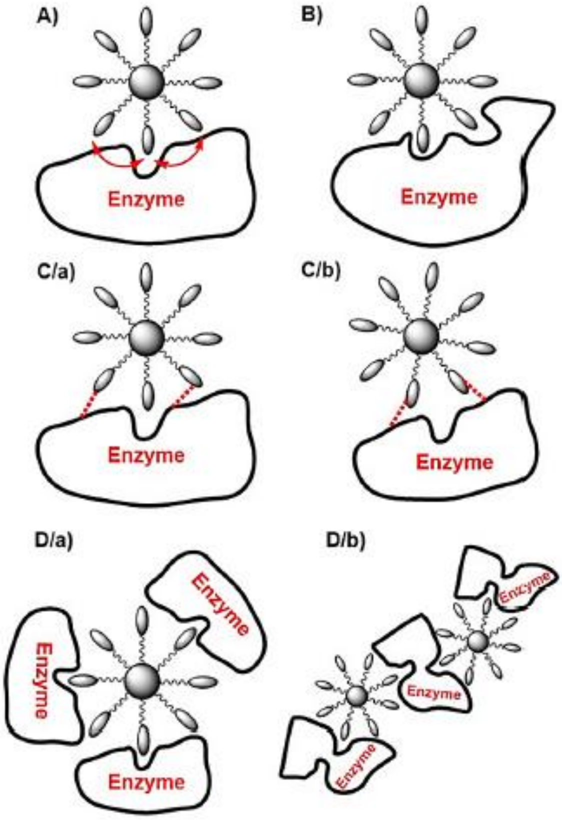

Figure 5.1: Proposed binding models accounting for the multivalent effect. [230]

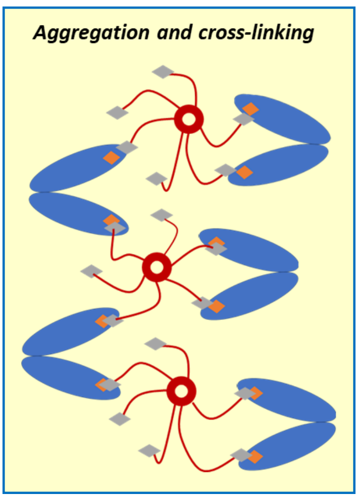

Figure 5.2: Possible binding mode for dimeric GCase, clustering effect.

The multivalent structural design was constructed with the double goal of developing novel pharmacological chaperones for GCase, while exploring the effect of multivalency on inhibition potency and selectivity. The main strategy used to achieve multivalent compounds is the click chemistry reaction CuAAC (copper-mediated azide-alkyne cycloaddition), the most common method reported in literature to date. CuAAC is a very versatile and fast synthetic way that allows to easily obtain multimeric compounds with a high valency degree. [235]-[237] In particular, the best results in terms of MVE towards GCase were obtained with a series of DNJ clusters based on cyclodextrin **223** (rp/n = 29 with respect to compound **222**) and DIX clusters based on pentaerythritol core **227** (rp/n = 2 with respect to compound **226**) (Figure 5.3). Moreover, the best MVE did not correspond to a good PC activity, since the best chaperones were identified in the tetravalent DNJ derivative **224** (3.3-fold mutant GCase residual activity increase at 10 µM) that showed no inhibitor activity. Furthermore, the trivalent acetyl-DNJ-derivative **225** provided the first evidences of the potential of pro-drugs in PCT (3.0-fold mutant GCase residual activity increase at 1 µM). The compound **225** improved permeability and cellular uptake, it showed higher enanchement in GCase activity derived from fibroblasts bearing N370S mutations than its corresponding deprotected analogue **224** (3.0-fold versus 2.4-fold) at a cellular concentration (1 µM) reduced by one order of magnitude (Figure 5.3). [238] [185]

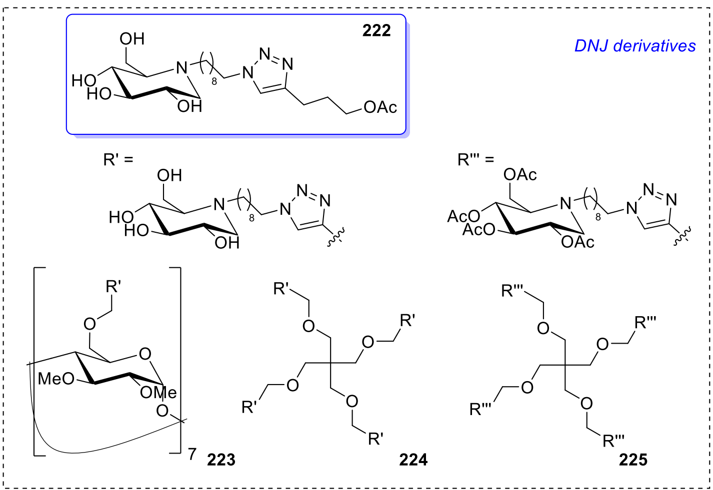

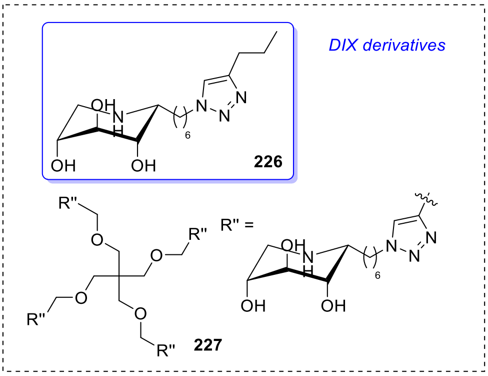

Figure 5.3: β-Glucosidases inhibitors and/or pharmacological chaperones.

Most of the procedures described in the literature for the synthesis of iminosugar-based clusters employ the copper-mediated azide-alkyne cycloaddition (CuAAC) reaction for the final conjugation step. However, a general drawback of the CuAAC strategy is the possibility of contamination by copper traces, which is likely considering the triazole properties for copper complexation [239] and the presence of several triazole moieties and other nitrogen atoms in these multivalent constructs.

In this context, and searching for new methodologies for the building of multivalent architecture by means of reactions that do not employ homogenous metal catalysis, we developed a new strategy based on the double reductive amination (DRA) reaction. The DRA reaction is a powerful tool to efficiently access polyhydroxipiperidines starting from dicarbonyl compounds, and this Chapter first reports some examples on this topic. Moreover, the synthesis of two divalent trihydroxypiperidines synthesized through this strategy is described and evaluated as human glycosidases inhibitors.

5.1 The Double Reductive Amination approach to the synthesis of polyhydroxypiperidines.

The DRA reaction on dicarbonyl compounds represents a straightforward tool to efficiently access the piperidine skeleton. The use, in most cases, of sugar-derived dicarbonyl substrates ensures the absolute configurations desired of the hydroxyl groups, while the variety of amines available as the nitrogen atom source guarantee the versatility of this method. We recently reported an exhaustive overview of this approach to the synthesis of polyhydroxypiperidines in Targets in Heterocyclic System Vol 23 (TARGETS IN HETEROCYCLIC SYSTEMS Chemistry and Properties (THS): C. Matassini, **F. Clemente**, F. Cardona, THE DOUBLE REDUCTIVE AMINATION APPROACH TO THE SYNTHESIS OF POLYHYDROXYPIPERIDINES", THS Volume 23 **2019**, *14*, 283-301. Editor: Orazio A. Attanasi, Pedro Merino, Domenico Spinelli; published by Società Chimica Italiana. DOI: https://www.soc.chim.it/it/libri _collane/ths/vol_23_2019.) Therefore, I report here only the most representative examples.

In 1994, the first synthesis of IFG as its hydrochloride salt was reported, employing ammonia as the nitrogen source in the DRA of pentadialdose **229** derived from Cerny epoxide (**228**). The key DRA step was achieved through catalytic hydrogenation at high pressure (35 atm), which led to monoprotected **230** in a remarkable 78% yield (Scheme 5.1). [240] The IFG is the compound that reached the most advanced stage in view of its use as PC for Gaucher disease (Phase II clinical trials, planned trademark Plicera®) to date.

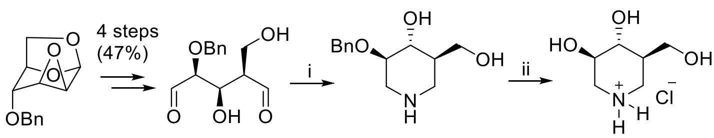

Scheme 5.1: Reactions and conditions: i) NH_3 (0.23 M), EtOH, H_2, Pd/C, 35 atm, 20°C, ii) HCl:H_2O, H_2, Pd/C, 1 atm.

In the early '90s Reitz and Baxter reported the total synthesis of 1-deoxynojirimycin (DNJ) [241] and its D-mannose configured analogue, 1-deoxymannojirimycin (DMJ), [242] by following the DRA approach of appropriate ketoaldehyde sugar substrates, poorly studied at that time, and without employing tedious protecting group manipulations. In this case, the DRA approach involved formation of a new stereocenter during the cyclization step.
Cyclization of the dicarbonyl intermediate **231** afforded **232** with an excellent diastereoselectivity (Scheme 5.2), which was ascribed to the strong stereocontrol played by the hydride addition in the reduction of the cyclic imine. Lower stereoselectivity was observed in the DRA step during the analogous

synthesis of DMJ.

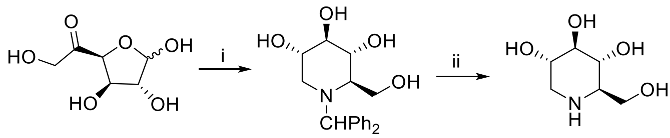

Scheme 5.2: Reactions and conditions: i) Ph_2CHNH_2, (0.8 equiv.), $NaBH_3CN$, MeOH, ii) H_2, $Pd(OH)_2/C$.

Starting from a 1,5-dicarbonyl intermediate obtained from lactose, D'Andrea, Guazzelli and co-workers investigated the role played by the employed amine in the selectivity of the DRA reaction, performed with $NaBH_3CN$ in MeOH at 60 °C. Indeed, the use of different quaternary ammonium salts (diversely hindered), selected amino-acids or hydroxylamine, resulted in different ratios of the final 1,6-dideoxynojirimycin derivatives, epimers at the newly formed stereocenter (namely 1,6-dideoxy-D-*galacto* and 1,6-dideoxy-L-*altro* nojirimycin derivatives). [243] Several iminosugar-amino acid hybrids in which the DNJ, the DMJ, the deoxygalactonojirimycin (DGJ) or the 1,5-dideoxy-1,5-iminoxylitol (DIX) skeleton is conjugated to properly protected amino acids were also accessed through the DRA approach exploiting the amine group of the amino acid side chain as the amine source. [244] [245] In addition, Overkleeft and co-workers made an impressive study on the synthesis of a collection of adamant-1-yl-methoxyfunctionalized DNJ derivatives as selective inhibitors of glucose metabolism. Their approach combined a Swern oxidation, performed to access the desired ketoaldehyde, with the DRA reaction carried out employing an excess of ammonium formate as the nitrogen source and $NaBH_3CN$ as the reducing agents in the DRA key step. [246] Very recently, the same authors applied the above mentioned oxidation-RA protocol on commercial (namely melibiose, maltose, cellobiose and lactose) and synthetic disaccharides, to access glycosylated 1-deoxynojirimycin derivatives. [247]

Martin and Saavedra also employed ammonium formate as the nitrogen source in their application of the DRA reaction to diketone substrates for the synthesis of β-homonojirimycin and β-homogalactonojirimycin analogues. [248] [249]

We envisaged that the "masked" dialdehyde **135** might be a versatile building block for the synthesis of natural 3,4,5-trihydroxypiperidines and related analogues through the DRA strategy. [174] Different aromatic and aliphatic amines were employed as the nitrogen source, and different conditions were screened to optimize the DRA step. For instance, the enantiomer of a natural compound **165** was accessed through acetonide deprotection of **62**. The DRA reaction on **135** was achieved with $BnNH_2$ as the amine source and H_2 in the presence of $Pd(OH)_2/C$ catalyst, affording **62** in excellent 69% yield over 4 steps (debenzylation, imine formation, imine reduction and RA over the anomeric carbon). However, this one-pot procedure suffered from scarce reproducibility with alkyl amines and better results were obtained using $NaBH_3CN$ as the reducing agent (in MeOH and in the presence of 3Å MS and CH_3COOH). This latter strategy required preliminary deprotection of aldehyde **135** by catalytic hydrogenation, but allowed the synthesis of several alkylated trihydroxipiperidines **233-236** and **169**. Functionalization of the α-position was achieved taking advantage of a highly stereoselective Strecker reaction on aldehyde **164** (or on its *O*-acetylated analogue **237**) and further conversion of the cyano group in compound **238** to access pipecolic acid analogues **239a-c** (Scheme 5.3). [183]

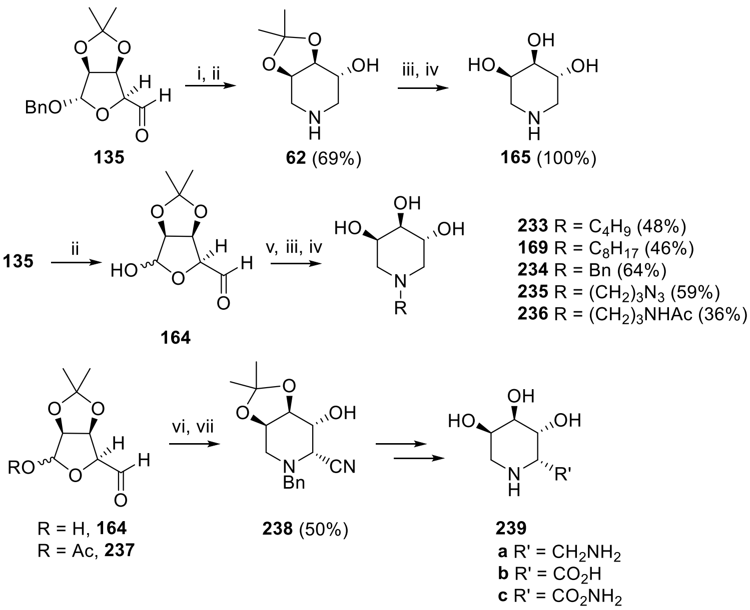

Scheme 5.3: Reactions and conditions: i) $BnNH_2$, MeOH, 3Å MS, r.t., 40 min, ii) H_2, $Pd(OH)_2/C$, MeOH, r.t., 25 h, iii) MeOH, 1M HCl, r.t., 18 h, iv) DOWEX 50WX8, v) RNH_2, $NaBH_3CN$, MeOH, 3Å MS, AcOH, r.t., 3-7 d, vi) $BnNH_2$, 3Å MS, TMSCN, dry CH_3CN, r.t., 18 h, vii) $NaBH_3CN$, AcOH, EtOH, r.t., 3 d.

Preliminar investigation of all these trihydroxypiperidines towards commercially available glycosidases did not identify any potent inhibitor. However, compound **169** later emerged as a potent human GCase inhibitor and a good PC, enabling rescue of GCase activity in Gaucher patients cell up to 1.5-fold. [159] More recently, a similar "masked" dialdehyde derived from D-ribose was employed by Martin and co-workers for the synthesis, through the DRA approach, of several *N*-alkylated trihydroxypiperidines with the *all-cis* configuration of the hydroxy groups. [250]

Finally, Crich and co-workers described for the first time an asymmetric strategy to access novel polyhydroxylated *N*-alkoxypiperidines, based on the ring-closing DRA of protected 1,5-dialdehydes with *O*-substituted hydroxylamines. [251] [252] Chirality was introduced *via* desymmetrization of cyclopentadiene (through highly enantioselective hydroboration with (-)-diisopinocampheylborane ((-)-Ipc$_2$BH), to give an optically enriched functionalized cyclopentene derivative **240**, followed by oxidative cleavage to yield the required dialdehyde **240** (Scheme 5.4). The DRA step was performed either in one-pot or in a two-step procedure which, through the diimmine **243**, gave higher yields of the target *N*-hydroxypiperidines **242**. [251] [252]

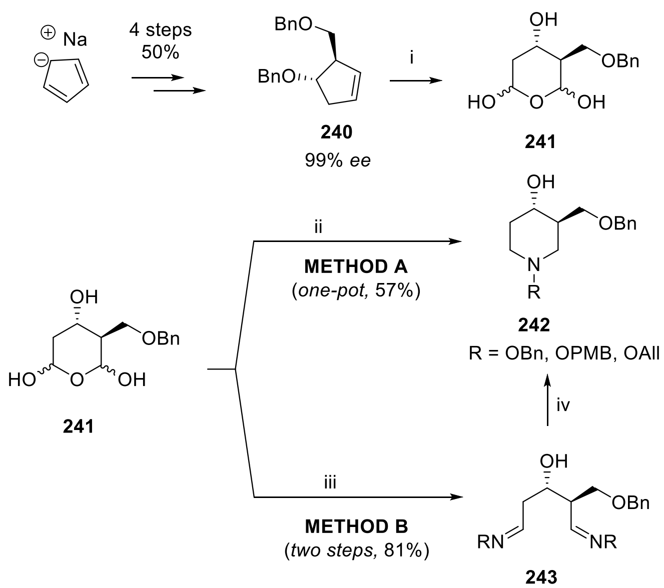

Scheme 5.4: Reactions and conditions: i) OsO_4, $NaIO_4$, dioxane:H_2O, ii) $RNH_2 \cdot HCl$ (1 equiv.), $NaBH_3CN$, AcOH, iii) $RNH_2 \cdot HCl$ (2.5 equiv.), iv) $NaBH_3CN$, AcOH.

Later on, Crich and co-workers adapted their asymmetric synthetic route to an iterative DRA reaction in order to obtain di- and trimeric hydroxylamine-based mimetics of β-(1→3)-glucans as potential immunomodulating agents. [253]

5.2 Synthesis and biological screening towards human lysosomal glycosidases of a divalent trihydroxypiperidine.

With the aim to access new divalent trihydroxypiperidines we explored the DRA reaction conditions describe above to obtain N-substituted piperidines [174] [175] starting from the "masked" dialdehyde **135** with ethylenediamine and hexamethylenediamine. The DRA reaction on the "masked" dialdehyde **135** was achieved with ethylenediamine or hexamethylenediamine as the amine sources, H_2 as reducting agent and $Pd(OH)_2/C$ as a catalyst in the presence of 3Å molecular sieves for 3-6 days (Scheme 5.5), affording dimeric trihydroxypiperidines **244** and **245** in excellent 69% and 54% yields, respectively, over 4 steps (debenzylation, imine formation, imine reduction and RA over the anomeric carbon). Acetonide deprotection gave piperidine **246** and **247** in excellent yields (Scheme 5.5).

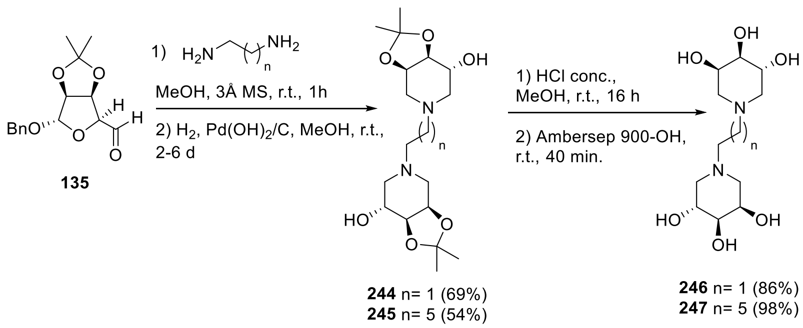

Schema 5.5: Synthesis of a divalent trihydroxypiperidines based on the double reductive amination.

Table XX: Inhibition percentage towards a panel of six lysosomal glycosidases in an extract from human leukocytes isolated from healthy donors, incubated with 1 mM concentration of compounds **246** and **247**.

	β-Glu	α-Gal	β-Gal	α-Man	β-Man	α-Fuc
165	50%	0%	0%	0%	0%	90%
246	17%	3%	34%	---	3%	12%
247	22%	9%	1%	1%	14%	50%

The inhibitory activity of compound **246** and **247** towards GCase was evaluated in leukocytes isolated from healthy donors at 1mM. A weak inhibition was observed for both divalent trihydroxypiperidines **246** and **247** (12% and 17%, respectively). Comparison of the activity of the bioactive unit (monovalent) **165** [159] with the two divalent compounds **246** and **247** obtained by combining the bioactive piperidine units through an aliphatic spacer of two different length (two and six carbon atoms, respectively) showed a reduction of the inhibitory activity. No multivalent effect was observed. One explanation for this result could be that the chain's length connecting the two bioactive units is not long enough to gain inhibitory activity towards GCase. For this reason, in the future we will perform the synthesis of a dimer bearing a longer spacer.
A biological screening of the two divalent compounds at 1 mM inhibitor concentration was performed also towards a panel of human lysosomal enzymes, namely α-fucosidase (α-Fuc), β-galactosidase (β-Gal), α-galactosidase (α-Gal), α-mannosidase (α-Man), β-mannosidase (β-Man) and β-glucosidase (β-Glu or GCase) in order to evaluate an increase in the inhibitory activity with respect to the monovalent **161**. Unfortunately, the data clearly show that there was a loss of inhibitory activity against the α-Fuc enzyme while there was no significant increase in enzyme inhibition against the other enzymes. A particular behaviour was observed for α- mannosidase, whereby compound **246** appears to function as an activator (increase in activity by 28%).

5.3 Experimental Section

General Experimental Procedures for the syntheses
Commercial reagents were used as received. All reactions were carried out under magnetic stirring and monitored by TLC on 0.25 mm silica gel plates (Merck F254). Column chromatographies were carried out on Silica Gel 60 (32–63 µm) or on silica gel (230–400 mesh, Merck). Yields refer to spectroscopically and analytically pure compounds unless otherwise stated. ^{1}H-NMR spectra were recorded on a Varian Gemini 200 MHz, a Varian Mercury 400 MHz or on a Varian INOVA 400 MHz instrument at 25 °C. ^{13}C-NMR spectra were recorded on a Varian Gemini 200 MHz or on a Varian Mercury 400 MHz instrument. Chemical shifts are reported relative to $CDCl_3$ (^{13}C: δ = 77.0 ppm), or to CD_3OD (^{13}C: δ = 49.0 ppm).

Integrals are in accordance with assignments, coupling constants are given in Hz. For detailed peak assignments 2D spectra were measured (COSY, HSQC, NOESY, and NOE as necessary). IR spectra were recorded with a IRAffinity-1S SHIMADZU system spectrophotometer. ESI-MS spectra were recorded with a Thermo Scientific™ LCQ fleet ion trap mass spectrometer. Elemental analyses were performed with a Thermo Finnigan FLASH EA 1112 CHN/S analyzer. Optical rotation measurements were performed on a JASCO DIP-370 polarimeter.

Synthesis of (*3R,4S,5R,3'R,4'S,5'R*)-1,1'-ethyl-di(5-hydroxy-3,4-*O*-(1-methylethylidene)-piperidine) (244): A solution of "masked" dialdehyde **135** (240 mg, 0.86 mmol) in dry MeOH (10 mL) was stirred in the presence of 3Å molecular sieves powder for 15 min, under nitrogen atmosphere and then ethylenediamine (24 µL, 0.36 mmol) was added. Reaction mixture was stirred for 1 hour under nitrogen atmosphere, then $Pd(OH)_2/C$ (120 mg) was added and left stirring under H_2 atmosphere for six days. The molecular sieves were removed by filtration through Celite and the filtrate was concentrated under vacuum. The crude mixture was purified by silica gel column chromatography (CH_2Cl_2/MeOH/ NH_4OH (6%) 15:1:0.1), affording **244** (93 mg, 0.25 mmol, R_f = 0.33) in 69% as waxy white solid.

244: waxy white solid. $[\alpha]_D^{23}$ = - 14.9 (c= 0.80 in MeOH). ^{1}H-NMR (400 MHz, CD_3OD) δ = 4.30-4.25 (m, 2H, 3-H and 3'-H), 4.87-4.82 (m, 2H, 4-H and 4'-H), 4.82-4.77 (m, 2H, 5-H and 5'-H), 2.97 (dd, J= 12.8, 2.6 Hz, 2H, 2-H_a and 2'-H_a), 2.75 (dd, J = 11.9, 2.8 Hz, 2H, 6-H_a and 6'-H_a), 2.59 (brs, 4H, 7-H and 7'-H), 2.56 (dd, J = 12.9, 3.3 Hz, 2H, 2-H_b and 2'-H_b), 2.19-2.11 (m, 2H, 6-H_b and 6'-H_b), 1.48 (s, 6H, Me), 1.33 (s, 6H, Me) ppm; ^{13}C-NMR (100 MHz, CD_3OD) δ = 108.8 (s, 2C, acetal), 78.5 (d, 2C, C-4 and C-4'), 73.0 (d, 2C, C-3 and C-3'), 68.8 (d, 2C, C-5 and C-5'), 56.3 (t, 4C, C-6 and C-6'), 54.2 (t, 2C, C-7 and C-7'), 54.0 (t, 2C, C-2 and C-2'), 27.1 (q, 2C, Me), 25.2 (q, 2C, Me) ppm; MS (ESI) m/z (%) = 373.26 (100) $[M+H]^+$, 395.31 (71) $[M+Na]^+$; IR (CD_3OD): 1221, 1244, 1379, 1462, 1564, 1595, 2630, 2938, , 2990, 3345 cm^{-1}. $C_{18}H_{32}N_2O_6$ (372.46): calcd. C, 58.05; H, 8.66; N, 7.52; found C, 58.00; H, 8.35; N, 7.65.

Synthesis of (*3R,4S,5R,3'R,4'S,5'R*)-1,1'-hexan-di(5-hydroxy-3,4-*O*-(1-

methylethylidene)-piperidine) (245): A solution of "masked" dialdehyde **135** (200 mg, 0.72 mmol) in dry MeOH (10 mL) was stirred in the presence of 3Å molecular sieves powder for 15 min, under nitrogen atmosphere and then hexanediamine (42 µL, 0.36 mmol) was added. Reaction mixture was stirred for 1 hour under nitrogen atmosphere, then $Pd(OH)_2/C$ (100 mg) was added and left stirring under H_2 atmosphere for two days. The molecular sieves were removed by filtration through Celite and the filtrate was concentrated under vacuum. The crude mixture was purified by silica gel column chromatography (gradient eluent from AcOEt:MeOH 10:1 to 5:1), affording **245** (167 mg, 0.40 mmol, R_f = 0.20 in AcOEt:MeOH 10:1) in 54% as pale yellow oil.

245: pale yellow oil. $[\alpha]_D^{23}$= - 47.3 (c= 1.00, MeOH). ^{1}H-NMR (400 MHz, CD_3OD) δ = 4.32-4.25 (m, 2H, 3-H and 3'-H), 3.86-3-76 (m, 4H, 5-H, 5'-H, 4-H and 4'-H), 3.02 (d, J= 12.7 Hz, 2H, 2-H_a and 2'-H_a), 2.78-2.69 (m, 2H, 6-H_a and 6'-H_a), 2.47-2.33 (m, 6H, 7-H, 7'-H, 2-H_b and 2'-H_b), 2.05-1.97 (m, 2H, 6-H_b and 6'-H_b), 1.59-1.51 (m, 4H, 8-H and 8'-H) 1.49 (s, 6H, Me), 1.42- 1-28 (m, 4H, 9-H and 9'-H), 1.34 (s, 6H, Me) ppm.^{13}C-NMR (100 MHz, CD_3OD) δ ppm= 110.1 (s, 2C, acetal), 80.3 (d, 2C, C-4 and C-4'), 74.3 (d, 2C, C-3 and C-3'), 70.5 (d, 2C, C-5 and C-5'), 59.2 (t, 2C, C-7 and C-7'), 57.8 (t, 2C, C-6 and C-6'), 55.1 (t, 2C, C-2 and C-2'), 28.5 (q, 2C, Me), 28.6 (t, 2C, C-9 and C-9'), 28.4 (t, 2C, C-8 and C-8'), 27.4 (q, 2C, Me). MS (ESI) m/z (%) = 429.21 (100) $[M+ H]^+$, 451.20 (16) $[M+Na]^+$. IR (CD_3OD): 1142, 1202, 1238, 1379, 1404, 1464, 1603, 2826, 2940, 3032, 3480, 3599, 3684 cm^{-1}. $C_{22}H_{40}N_2O_6$ (428.29): calcd. C, 61.66; H, 9.41; N, 6.54; found C, 61.70; H, 9.36; N, 6.22.

Synthesis of (*3R,4S,5R,3'R,4'S,5'R*)-1,1'-ethyl-di(3,4,5-trihydroxy-piperidine) (246): To a solution of **244** (15 mg, 0.04 mmol) in MeOH (3 mL), 12 M HCl (90 µL) was added and the mixture was stirred at room temperature for 16 hours. The crude mixture was concentrated to yield the deprotected compound as hydrochloride salt. The corresponding free amine was obtained by dissolving the residue in MeOH, then the strongly basic resin Ambersep 900-OH was added, and the mixture was stirred for 16 hours. The resin was removed by filtration and the crude product was triturated with CH_2Cl_2/MeOH/ NH_4OH (6%) 10:1:0.1 to afford pure piperidine **246** (10 mg, 0.03 mmol) as a waxy white solid in 86% yield.

246: waxy white solid. $[\alpha]_D^{23}$= – 30.1 (c= 0.40, MeOH). ^{1}H-NMR (400 MHz, D_2O) δ

= 3.81-3.77 (m, 2H, 3-H and 3'-H), 3.68-3.61 (m, 2H, 5-H and 5'-H), 3.32-3.26 (m, 2H, 4-H and 4'-H), 2.75-2.60 (m, 4H, 2-H_a , 2'-H_a , 6-H_a and 6'-H_a), 2.41-2.34 (m, 4H, 7-H- and 7'-H), 2.14 (m, 2H, 2-H_b and 2'-H_b), 1.98-1.87 (m, 2H, 6-H_b and 6'-H_b) ppm. ^{13}C-NMR (100 MHz, D_2O) δ = 73.7 (d, 2C, C-4 and C-4'), 67.7 (d, 2C, C-3 and C-3'), 67.6 (d, 2C, C-5 and C-5'), 56.8 (t, 2C, C-2 and C-2'), 56.0 (t, 2C, C-6 and C-6'), 53.5 (t, 2C, C-7 and C-7') ppm; MS (ESI) m/z (%) = 293.26 (100) $[M+H]^+$, 315.26 (26) $[M+Na]^+$. $C_{12}H_{24}N_2O_6$ (292.16): calcd. C, 49.30; H, 8.28; N, 9.58; found C, 49.15; H, 8.30; N, 9.13.

Synthesis of (*3R*,*4S*,*5R*,*3'R*,*4'S*,*5'R*)-1,1'- hexan-di(3,4,5-trihydroxy-piperidine) (247): To a solution of **245** (20 mg, 0.05 mmol) in MeOH (4 mL), 12 M HCl (100 µL) was added and the mixture was stirred at room temperature for 16 hours. The crude mixture was concentrated to yield the deprotected compound as hydrochloride salt. The corresponding free amine was obtained by dissolving the residue in MeOH, then the strongly basic resin Ambersep 900-OH was added, and the mixture was stirred for 16 hours. The resin was removed by filtration and the crude product was triturated with CH_2Cl_2/MeOH/ NH_4OH (6%) 10:1:0.1 to afford pure piperidine **247** (16 mg, 0.047 mmol) as a waxy white solid in 98% yield.

247: waxy white solid. $[\alpha]_D^{23}$= – 40 (c =0.75, MeOH). ^{1}H-NMR (400 MHz, CD3OD) δ ppm= 3.90 (brs, 2H, 3-H and 3'-H), 3.83-3.74 (m, 2H, 5-H and 5'-H), 3.44-3.36 (m, 2H, 4-H and 4'-H), 2.88-2.70 (m, 4H, 2-H_a , 2'-H_a , 6-H_a and 6'-H_a), 2.45-2.32 (m, 4H, 7-H- and 7'-H), 2.32-2.21 (m, 2H, 2-H_b and 2'-H_b), 2.08 (brs, 2H, 6-H_b and 6'-H_b), 1.59-1.45 (m, 4H, 8-H and 8'-H), 1.39-1.30 (m, 4H, 9-H and 9'-H). ^{13}C-NMR (100 MHz, CD_3OD) δ ppm= 75.3 (d, 2C, C-4 and C-4'), 69.5 (d, 2C, C-5 and C- 5'), 69.1 (d, 2C, C-3 and C-3'), 59.2 (t, 2C, C-7 and C-7'), 58.3 (t, 2C, C-6 and C-6'), 57.6 (t, 2C, C-2 and C-2'), 28.5 (t, 2C, C-9 and C-9'), 27.5 (t, 2C, C-8 and C-8'). MS (ESI) m/z (%) = 371.23 (100) $[M+ Na]^+$. $C_{16}H_{32}N_2O_6$ (348.44): calcd. C, 55.15; H, 9.26; N, 8.04; found C, 55.27; H, 9.19; N, 8.00.

Preliminary biological screening towards human lysosomal glycosidases

The effect of 1mM concentration of **246** and **247** was assayed towards seven lysosomal glycosidases namely: α-mannosidase, β-mannosidase, α-galactosidase, β-galactosidase, α-fucosidase, β-glucosidase from leukocytes isolated from healthy donors (controls) and α-glucosidase from lymphocytes isolated from healthy donors' flesh blood (controls). Isolated leukocytes or lymphocytes were disrupted by sonication, and a micro BCA protein assay kit (Sigma–Aldrich) was used to determine the total protein amount for the enzymatic assay, according to the manufacturer instructions.

α-Mannosidase activity was measured in a flat-bottomed 96-well plate. Azasugar solution (3 µL), 4.29 µg/µL leukocytes homogenate 1:10 (7 µL), and substrate 4-methylumbelliferyl-α-D-mannopyranoside (2.67 mM, 20 µL, Sigma–Aldrich) in Na phosphate/citrate buffer (0.2:0.1, M/M, pH 4.0) containing sodium azide (0.02%) were incubated at 37 °C for 1 h. The reaction was stopped by addition of sodium carbonate (200 µL; 0.5M, pH 10.7) containing Triton X-100 (0.0025 %), and the fluorescence 4-methylumbelliferone released by α-mannosidase activity was measured in SpectraMax M2 microplate reader (λex=365 nm, λem=435 nm; Molecular Devices). Inhibition is given with respect to the control (without azasugar). Data are mean SD (n=3).

β-Mannosidase activity was measured in a flat-bottomed 96-well plate. Azasugar solution (3 µL), 4.29 µg/µL leukocytes homogenate 1:10 (7 µL), and substrate 4-methylumbelliferyl-β-D-mannopyranoside (1.33 mM, 20 µL, Sigma–Aldrich) in Na phosphate/citrate buffer (0.2:0.1, M/M, pH 4.0) containing sodium azide (0.02%) were incubated at 37 °C for 1h. The reaction was stopped by addition of sodium carbonate (200 µL; 0.5M, pH 10.7) containing Triton X-100 (0.0025 %), and the fluorescence of 4-methylumbelliferone released by β-mannosidase activity was measured in SpectraMax M2 microplate reader (λex=365 nm, λem=435 nm; Molecular Devices). Inhibition is given with respect to the control (without azasugar). Data are mean SD (n=3).

α-Galactosidase activity was measured in a flat-bottomed 96-well plate. Azasugar solution (3 µL), 4.29 µg/µL leukocytes homogenate 1:3 (7 µL), and substrate 4-methylumbelliferyl α-D-galactopyranoside (1.47 mM, 20 µL, Sigma–Aldrich) in acetate buffer (0.1 M, pH 4.5) containing sodium azide (0.02%) were incubated at 37 °C for 1 h. The reaction was stopped by addition of sodium carbonate (200 µL; 0.5M, pH 10.7) containing Triton X-100 (0.0025 %), and the fluorescence 4-methylumbelliferone released by α-galactosidase activity was measured in SpectraMax M2 microplate reader (λex=365 nm, λem=435 nm; Molecular Devices). Inhibition is given with respect to the control (without azasugar). Data are mean SD (n=3).

β- Galactosidase activity was measured in a flat-bottomed 96-well plate. Azasugar solution (3 µL), 4.29 µg/µL leukocytes homogenate 1:10 (7 µL), and substrate 4-methylumbelliferyl β-D-galactopyranoside (1.47 mM, 20 µL, Sigma–Aldrich) in acetate buffer (0.1M, pH 4.3) containing NaCl (0.1M) and sodium azide (0.02%) were incubated at 37 °C for 1 h. The reaction was stopped by addition of sodium carbonate (200 µL; 0.5M, pH 10.7) containing Triton X-100 (0.0025 %), and the fluorescence 4-methylumbelliferone released by β-galactosidase activity was measured in SpectraMax M2 microplate reader (λex=365 nm, λem=435 nm; Molecular Devices). Inhibition is given with respect to the control (without azasugar). Data are mean SD (n=3).

α-Fucosidase activity was measured in a flat-bottomed 96-well plate. Azasugar solution (3 µL), 4.29 µg/µL leukocytes homogenate 1:3 (7 µL), and substrate 4-methylumbelliferyl α-L-fucopyranoside (1.51 mM, 20 µL, Sigma–Aldrich) in Na phosphate/citrate buffer (0.2:0.1, M/M, pH 5.5) were incubated at 37 °C for 1 h. The reaction was stopped by addition of sodium carbonate (200 µL; 0.5M, pH 10.7) containing Triton X-100 (0.0025 %), and the fluorescence 4-methylumbelliferone released by α- fucosidase activity was measured in SpectraMax M2 microplate reader (λex=365 nm, λem=435 nm; Molecular Devices). Inhibition is given with respect to the control (without azasugar). Data are mean SD (n=3).

α-Glucosidase activity was measured in a flat–bottomed 96 well plate. Azasugar solution (3 µL), 4.29 µg/µL lymphocytes homogenate (7µL) and 20 µL of substrate solution of 4-methylumbelliferyl-α-D-glucopyranoside (Sigma-Aldrich) in Na acetate buffer (0.2 M, pH 4.0) were incubated for 1 h at 37 °C. The reaction was stopped by the addition of a solution of sodium carbonate (200 µL; 0.5M, pH 10.7) containing Triton X-100 (0.0025 %), and the fluorescence of 4-methylumbelliferone released by α-glucosidase activity was measured in SpectraMax M2 microplate reader (λex=365 nm, λem=435 nm; Molecular Devices). Inhibition is given with respect to the control (without azasugar). Data are mean SD (n=3).

β-glucosidase activity was measured in a flat-bottomed 96-well plate. Azasugar solution (3 μL), 4.29 μg/μL leukocytes homogenate (7 μL), and substrate 4-methylumbelliferyl-β-D-glucoside (3.33 mM, 20 μL, Sigma–Aldrich) in citrate/phosphate buffer (0.1:0.2, M/M, pH 5.8) containing sodium taurocholate (0.3%) and Triton X-100 (0.15%) at 37 °C were incubated for 1 h. The reaction was stopped by addition of sodium carbonate (200 μL; 0.5M, pH 10.7) containing Triton X-100 (0.0025 %), and the fluorescence of 4-methylumbelliferone released by β-glucosidase activity was measured in SpectraMax M2 microplate reader (λex=365 nm, λem=435 nm; Molecular Devices). Percentage GCase inhibition is given with respect to the control (without azasugar). Data are mean SD (n=3)

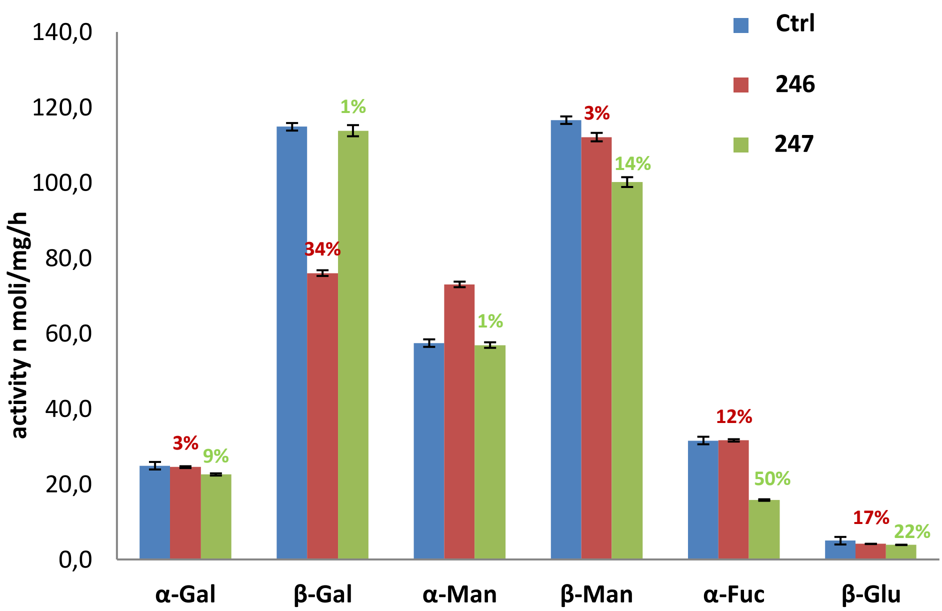

Inhibition percentage of lysosomal α-fucosidase (α-Fuc), β-galactosidase (β-Gal), α-galactosidase (α-Gal), α-mannosidase (α-Man), β-mannosidase (β-Man)and β-glucosidase (β-Glu or GCase) in an extract from human leukocytes isolated from healthy donors, incubated with 1 mM concentration of compounds **246** and **247**.

Conclusion

Our aim was to evaluate the biological activity of new multivalent systems against human GCase enzyme based on a trihydroxylated piperidine bioactive epitope, to find new selective inhibitors and, eventually, new pharmacological chaperones to use in the treatment of Gaucher disease. The synthesis of two new multivalent derivatives was efficiently carried out using a novel procedure that involves the double reduction amination (DRA) reaction as a key step. In particular, a key masked dialdehyde **135** intermediate was used in the DRA with an aliphatic primary diamine. The procedure is straightforward, simple, and does not used homogeneous metal catalysis, thus affording pure final compounds not contaminated by metal traces. The procedure allows, in a one-pot manner, the building of the piperidine ring and the connection of multiple piperidine epitopes through the covalent multivalent scaffold.

Unfortunally, preliminary biological assays of the divalent compounds **246** and **247** did not give the expected results. Further studies are underway within the research group to elongate the chain connecting the two bioactive epitopes. Moreover, we also plan to obtain trivalent and quadrivalent compounds by exploiting the DRA reaction starting from the key aldehyde **135** with branched tertiary or quaternary amines.

Chapter 6:
Synthesis of alkylated Azasugars: potential Pharmacological Chaperones for GM1 gangliosidosis and Morquio B diseases

Introduction

Two lysosomal storage diseases, GM1 gangliosidosis (GM1; MIM# 230500) and Morquio B disease (MBD; MIM# 253010), are caused by sequence alterations in a single gene, *GLB1*. They result in functional deficits of acid β-galactosidase (β-Gal; EC 3.1.2.23; MIM# 611458), an enzyme that cleaves terminal β-linked galactose residues from complex carbohydrates in the lysosomal compartment. Both diseases are inherited in an autosomal recessive manner. Depending on the mutations, degradation of one or the other of the β-galactosidase substrates is more or less impaired. If degradation of sphingolipidosis GM1-gangliosidosis is predominantly defective, the patients develop the symptomatology of GM1-gangliosidosis, while accumulation of keratan sulfate is an indication for Morquio disease type B. [254] [255]

GM1-gangliosidosis is considered a neurodegenerative disorder and is classified into three clinical subtypes: the severe infantile (type I; OMIM #230500), the juvenile (type II; OMIM #230600), and the milder adult (type III; OMIM #230650) forms. [256] The severe infantile form is fatal by the age of 1–2 years and mainly associated with severe progressive neurological symptoms (hypotonia, developmental regression by six months, seizures, cherry-red macula and severe gross motor decline) that manifest during early infancy. Patients with the juvenile form start to show symptoms at the age of 2–3 years as they retain some residual β-Gal enzymatic activity compared to those with the infantile form. Type II GM1-gangliosidosis is associated with slower progression of the neurological-related symptoms (ataxia, seizures, dysarthria, dysphagia, and hypotonia) and life expectancy is relatively higher as patients may live up to late childhood to early adolescence. Finally, type III GM1-gangliosidosis is the mildest with late onset (early to mid-adolescence) of the symptoms and higher life expectancy. Symptoms are mainly neuromuscular and may result in loss of independent ambulation (ataxia, dystonia, dysarthria). The estimated incidence of GM1 gangliosidosis is in the range of 1:100.000-200.000 live births. [256] [257]

Morquio B disease is characterized by marked skeletal abnormalities, corneal clouding, cardiac involvement, increased urinary excretion of keratan sulfate but no clinical signs of storage in neural tissues. [254] Morquio B disease is a rare disease with a prevalence of 1 in 250·000 live births. [257]

At present, only symptomatic and supportive therapies are available for patients with GM1 gangliosidosis and Morquio B. For GM1 only symptomatic treatment for some of the neurologic symptoms is available, but does not significantly alter the progression of the condition. For example, anticonvulsants may initially control seizures. Supportive treatments may include proper nutrition and hydration, and keeping the affected individual's airway open. [256] For Morquio B only physical therapy and surgical procedures, such as spinal fusion, may help with scoliosis and other bone and muscle issues. [258]

Therapies relying on pharmacological chaperones (PCs) may constitute a future option for the treatment of these lysosomal diseases. The potential of the galacto-configured iminosugar 1-deoxygalactonojirimycin (DGJ (**248**), Figure 6.1) as PC in human mutant fibroblasts associated with GM1 was already explored by Suzuki and co-workers. [259] The compound **248** was able to rescue the activity of mutant β-Gal in human fibroblasts from patients with GM1-gangliosidosis with the I51T and R201C mutations (3- and 7-fold, respectively), after culture with 1 mM DGJ for 4 days. The relatively high dose of iminosugar needed to have a relevant β-Gal activity enhancement and the lack of discrimination capabilities of DGJ between β- and α-galactosidases raised some concerns about unwanted side effects that jeopardized the progress of this approach into the clinics. [73] Several DGJ derivatives have been synthesized to enhance the compound specificity and affinity to galactosidases. In particular, previous studies have shown that the *N*-alkylated derivative of DGJ *N*-nonyl-DGJ (NN-DGJ, **249**, Figure 6.1) was able to rescue the intracellular activity of mutant β-Gal in GM1-gangliosidosis patient fibroblasts. [260] [261]

In addition, several azasugars exhibited lysosomal β-Gal inhibitory activity and PC properties which could treat GM1-gangliosidosis and Morquio disease type B. While 4-*epi*-isofagomine (**250**, Figure 6.1) showed moderate inhibition of human lysosomal β-Gal (IC_{50}= 1 µM) [262], the C-alkylated derivatives displayed a better activity in terms of inhibition and chaperoning activity. Demotz *et al.* identified *C*-pentyl-4-epi-isofagomine (**161;** Figure 6.1) as a highly potent (IC_{50}= 10 nM) and selective inhibitor of human lysosomal β-Gal. Moreover, **161** was able to half-maximal recover of β-Gal activity at 0.5 µM concentration. [170] [171] The nonyl analogous **251** was a potent inhibitor of lysosomal β-Gal (IC_{50}= 0.4 nM) and was more active than the pentyl derivative as a PC (half-maximal recovery of β-Gal activity was reached at 0.01 µM concentration), but it was a very potent inhibitor of lysosomal β-glucosidase (GCase, IC_{50}= 40 nM), an activity which may cause undesirable side-effects. [171] Moreover, the "*all-cis*" trihydroxypiperidines **252** and **253** (Figure 6.1) were good inhibitors of lysosomal β-Gal (to IC_{50}= 75 µM and IC_{50}= 44 µM, respectively) and were able to increase β-Gal activity in GM1 gangliosidosis patient fibroblasts up to 2-6-fold (at <100 µM concentration). [263]

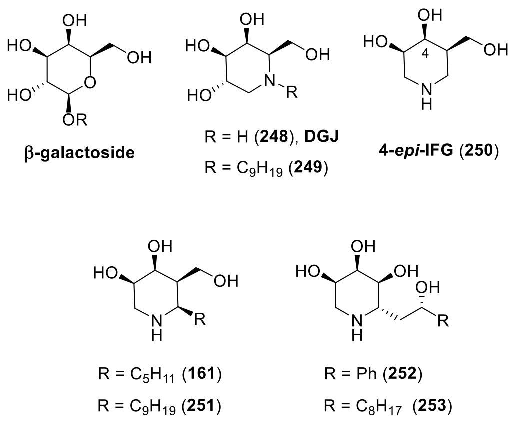

Figure 6.1: Structures of a general β-galactoside and of some imino- and azasugars inhibitors of β -Gal.

Based on these studies we decided to investigate the potential activity as β-Gal inhibitors of same "*all-cis*" trihydroxypiperidines synthesized in our laboratories [264] (Figure 6.2; *Chapter 3*).

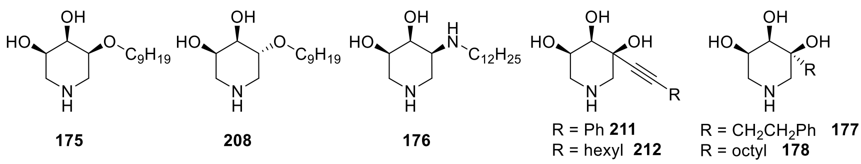

Figure 6.2. "*All-cis*" trihydroxypiperidines synthesized in our laboratories.

Unfortunately, none of the tested compounds inhibited β-Gal, apart from the *"all-cis"* ether **175** which showed only a 22% inhibition (Table 6.1). These data demonstrate that both the alkylation of the hydroxy or the exocyclic amine group, and the introduction of a substituent at C-3 of the trihydroxypiperidine skeleton dramatically affect β-Gal inhibition. Indeed, trihydroxypiperidines **252** and **253** (Figure 6.1), bearing the same "*all-cis"* hydroxy groups pattern, but with a chain at *C*-2, were potent β-Gal inhibitors [263]

Table 6.1: β-Gal inhibition in human leukocytes from healthy donors.

Entry	**Compounds**	**β-Gal** Inhibition [%][a]
1	**175**	22
2	**208**	0
3	**176**	0
4	**211**	0
5	**212**	4
6	**177**	0
7	**178**	0

[a] Percentage inhibition of β-Gal in human leukocytes extracts incubated with compounds (1 mM).

Based on the observation that the configuration of the three hydroxy groups and the position of the alkyl chain play a subtle role on the biological activity towards β-Gal, we decided to exploit our straightforward stereoselective synthesis of C-2 alkylated trihydroxypiperidines [158] to synthesize four novel *C*-2 pentyl trihydroxypiperidines **254**, **255**, **256** and **257** (Scheme 6.1), bearing two different stereochemical pattern at the hydroxy groups and a different absolute configuration at C-2. The choice of a pentyl alkyl chain (instead of a longer one) was made to avoid undesirable side-effects due to β-Glu inhibition. We envisage that the target compounds could be synthesized from two common intermediates **258** and **259** with a protecting group at the nitrogen atom, which could afford, respectively, both the trihydroxypiperidines **254** and **256** through simple O- and N-deprotection, and the "*all-cis*" trihydroxypiperidines **255** and **257,** with the opposite stereochemistry at C-3, through an oxidation-reduction sequence.

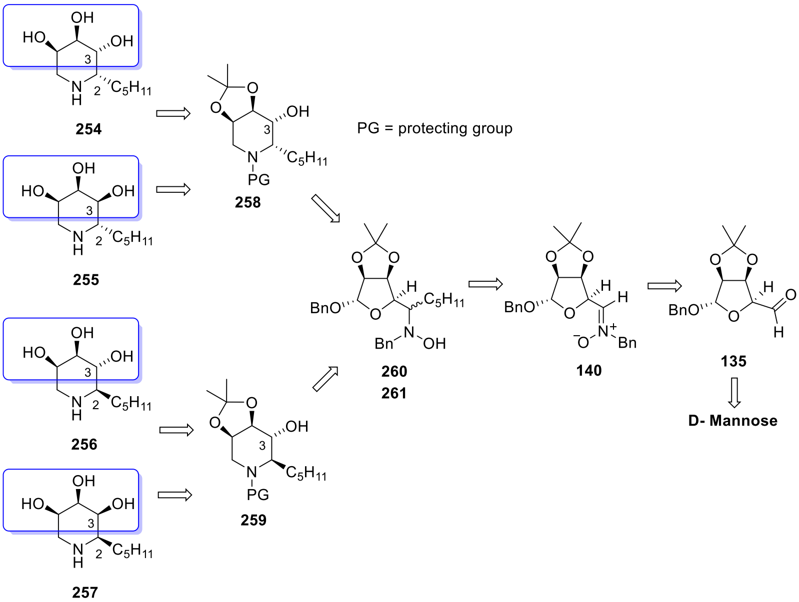

Scheme 6.1: Retrosynthetic stereodivergent strategy to yield C-2 pentyl trihydroxypiperidines **254**, **255**, **256** and **257**, starting the two common intermediates **258** and **259**, in turn obtained from D-mannose-derived nitrone **140**.

The piperidine intermediates **258** and **259** could be obtained *via* intramolecular reductive amination (RA) of hydroxylamines **260** and **261** with an *S* or *R* absolute configuration at the newly formed stereocenter, in turn derived from Grignard reagent additions onto nitrone **140** in the presence or absence of a suitable Lewis Acid (as thoroughly described in *Chapter 3*). The synthesis of nitrone **140** from aldehyde **135** from D-mannose was also previously reported [165] and described in *Chapter 3*. The stereodivergent retrosynthetic strategy employed for the preparation of the new compounds is shown in Scheme 6.1.

6.1 Synthesis of 2-pentyl trihydroxypiperidines

6.1.1 Results and discussions

6.1.1.1 Chemistry: synthesis and structural assignment

The addition of pentyl Grignard reagent to nitrone **140** without Lewis Acid in dry

THF at −78 °C for 3 hours afforded in good yield (70%, entry 1, Table 6.2) the corresponding hydroxylamines **260** and **261** as a 3.5:1 mixture in favour of the hydroxylamine **260** with the *S* absolute configuration at the newly formed stereocenter. The addition of $BF_3 \cdot Et_2O$ (1.0 equivalent) resulted in a reversal of stereochemistry, and the hydroxylamine **261** with an *R* absolute configuration at the newly formed stereocenter was formed with a *dr* = 5.0:1 (entry 2, Table 6.2).

Table 6.2: Addition of pentyl magnesium bromide to nitrone **140**.

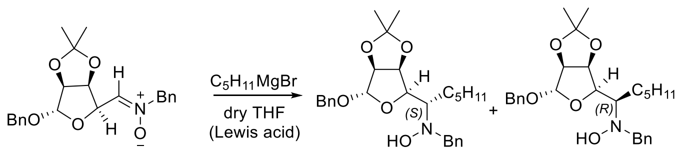

140 260 261

Entry	$C_5H_{11}MgBr$ equiv.	Lewis acid (1 equiv.)	Temp (°C)	Time (h)	260 : 261 ratio	Yield
1	1.8	none	-78	3	**3.5:1**	70%
2	1.8	$BF_3 \cdot Et_2O$	-30	2	**1:5**	75%

[a]Determined by integration of signals in the ^{1}H-NMR spectra of the crude reaction mixture.
[b]Determined on the basis of the total amount of *R* and *S* adducts recovered after purification by column chromatography.

In agreement with previous experiments with different Grignard reagents, the two hydroxylamines **260** and **261**, which were readily separable by flash column chromatography, were not stable to air and spontaneously partially oxidized to the corresponding nitrones **262** and **263** (Scheme 6.2). Also in this case, their characterization was only based on ^{1}H-NMR and MS analyses immediately after purification by column chromatography. Therefore, the complete characterization of pure nitrones **262** and **263** was carried out after oxidation of the hydroxylamines **260** and **261** with the hypervalent iodine reagent IBX [181] [182] in dry CH_2Cl_2, which provided the corresponding nitrones in excellent yields (Scheme 6.2). The hydroxylamine/nitrone mixtures were employed in the ring-closure reductive amination step with H_2 as a reducing agent (balloon), Pd/C as a catalyst and 2 equivalents of acetic acid in MeOH, affording the piperidines **264** and **265** in 2 days and excellent yields after treatment with a strongly basic anion exchange resin (Scheme 6.3).

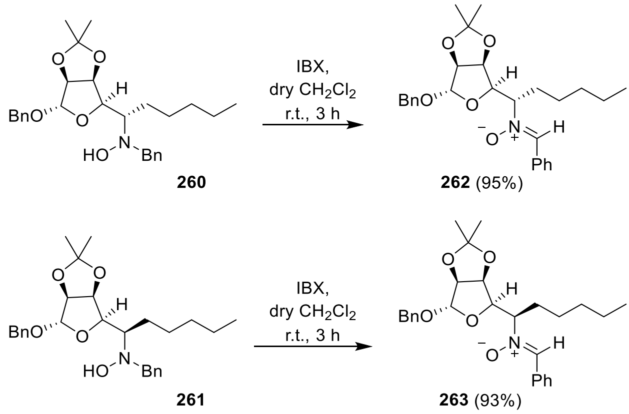

Scheme6.2: Oxidation of hydroxylamines **260** and **261** with IBX: synthesis of nitrones **262** and **263**.

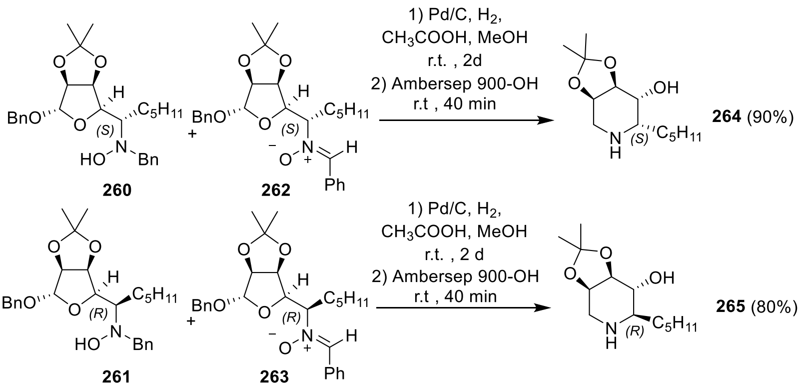

Scheme 6.3: The ring-closure reductive amination sequence.

Careful analysis of the ^{1}H-NMR, 2D-NMR and 1D-NOESY spectra carried out on piperidines **264** and **265** confirmed the stereochemical outcome of the Grignard addition as previously described in *Chapter 3*. The ^{1}H-NMR signals of the azasugar portion, together with their coupling constants, are shown in Tables 6.3 and 6.4 for piperidines **264** and **265**, respectively.

For compound **264**, 1D-NOESY spectra did not help to elucidate the structural assignment. However, its ^{1}H-NMR spectra showed small couplings constants for $^{3}J_{2\text{-}3}$, $^{3}J_{3\text{-}4}$ and $^{3}J_{4\text{-}5}$ (2.0–2.6 Hz, 2.6–3.2 Hz and 3.2-6.3 Hz, respectively). This pattern is in agreement with an *S* absolute configuration at C-2, with the piperidine displaying a preferred $^{1}C_{4}$ conformation in which the bulky R chain lies in the equatorial position and 3-H and 4-H are in an equatorial orientation (Figure6.4). In the 1D-NOESY spectra of compound **265**, strong NOE correlation peaks were observed between 2-H and 4-H, 4-H and 6-Hb and 2-H and 6-Hb, which confirmed the *R* configuration at C-2. Indeed, the axial orientation of 2-H derives from a preferred $^{4}C_{1}$ conformation which accommodates the bulky R chain again in an equatorial position (Figure 6.4). The higher coupling constant observed for the signals of 4-H in compound **265** compared to the same signal in **264** further confirmed an axial orientation of this proton with an *ax-ax* relationship with 3-H (J = 6.0 Hz).

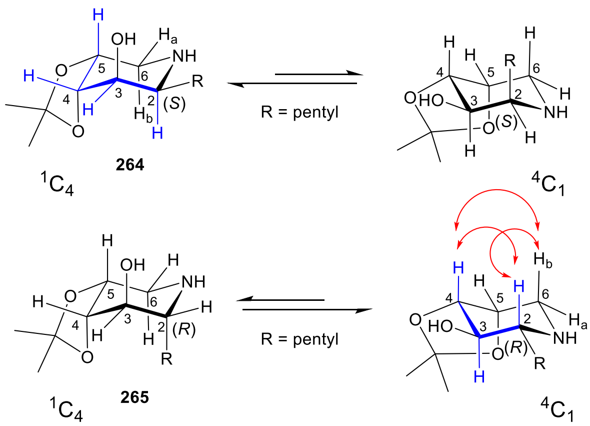

Figure 6.4: The two possible chair conformations of piperidines **264** and **265**. Dihedral angles between bonds analysed for the determination of the preferred conformation are shown in blue. Red double-ended arrows show the observed diagnostic NOE correlation peaks in the 1D-NOESY NMR spectra.

Table 6.3: ^{1}H-NMR chemical shifts (δ) and coupling constants (J) of the protons in the azasugar portion of compound **264**.

Comp. 264	**2H**		**3H**		**4H**		**5H**	
	δ (ppm)	^{2}J, ^{3}J (Hz)	δ (ppm)	^{2}J, ^{3}J (Hz)	δ (ppm)	^{2}J, ^{3}J (Hz)	δ (ppm)	^{2}J (Hz)

2.73 (td)	8.0 2.0	3.8 (t)	2.6	4.14 (dd)	5.2 3.2	4.19 (q)	6.3
6Ha		**6Hb**					
δ (ppm)	^2J, ^3J (Hz)	δ (ppm)	^2J, ^3J (Hz)				
3.05 (dd)	13.4 5.6	2.66 (dd)	13.2 7.6				

Table 6.4: ^{1}H-NMR chemical shifts (δ) and coupling constants (*J*) of the protons in the azasugar portion of compound **265**.

Comp. 265	**2H**	**6-Ha** and **3-H**	**4H**		**5H**	**6H$_b$**	
	δ (ppm)	δ (ppm)	δ (ppm)	^2J (Hz)	δ (ppm)	δ (ppm)	^2J (Hz)
	2.27 – 2.21 (m)	3.32-3.24 (m)	3.84 (t)	6.0	4.21-4.19 (m)	2.93	12

Final deprotection of the acetonide protecting groups under acidic conditions (aqueous HCl in MeOH) followed by basic treatment afforded the final trihydroxypiperidines **254** and **256** as free amines with good yields (Scheme 6.4).

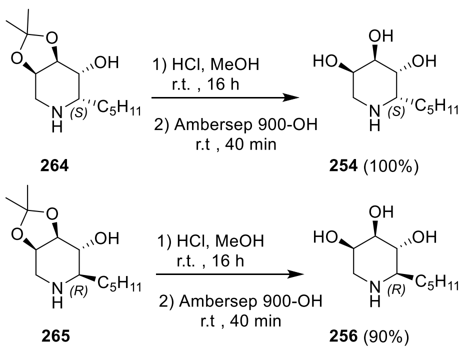

Scheme 6.4: The final deprotection step.

The inversion of configuration at C-3 in compound **255** and **257** was achieved through a protection-oxidation–reduction-deprotection sequence (Schemes 6.5

and 6.6).

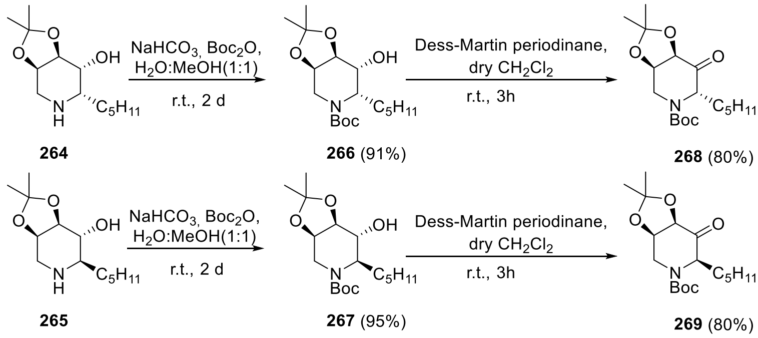

Scheme 6.5: Protection-oxidation sequence.

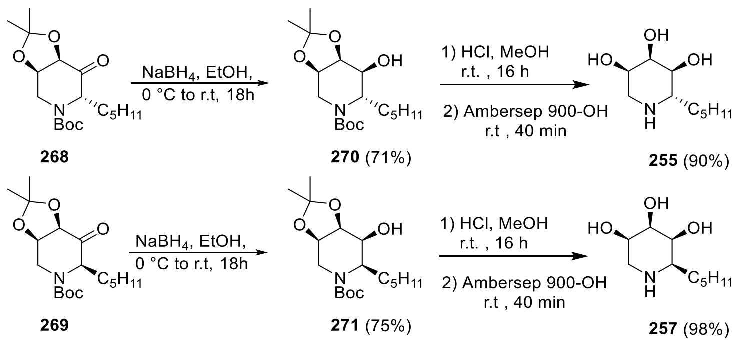

Scheme 6.6: Reduction-deprotection sequence.

Protection of alcohols **264** and **265** with the *tert*-butyloxycarbonyl group followed by oxidation with Dess Martin provided the key ketone intermediates **268** and **269** with good yields on two steps, 73% and 76% respectively (Scheme 6.5). The ketone intermediates underwent reduction in the presence of sodium boron hydride with good yields (Scheme 6.6). The high stereoselectivity observed in the reduction of **268** and **269** to **270** and **271**, respectively, by the hydride anion, derived from a favoured axial attack on the C-3 carbonyl group *anti* to the vicinal C=O bond, according to the Felkin–Anh model (Figure 6.4). [196] [197]
Final deprotection of the acetonide protecting groups in alcohols **270** and **271** under acidic conditions (aqueous HCl in MeOH), followed by basic treatment with excellent yields (90 % and 98%), afforded the final trihydroxypiperidines **254** and **256** as free amines with good yields (Scheme 6.6).

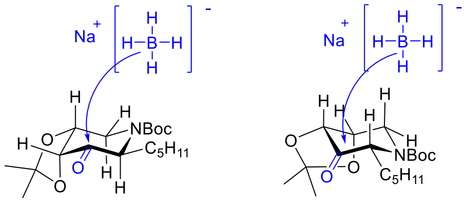

Figure 6.4: Favoured axial attack of the hydride anion on C=O bond.

The inversion of configuration at C-3 in compound **255** and **257** and their preferred conformation were established on the basis of careful analysis of their ^{1}H-NMR and 1D-NOESY spectra. In particular for compound **255,** a strong NOE correlation peak between 3-H and 5-H was observed (Figure 5) together with higher coupling constant observed for the signals of 3-H confirmed an axial orientation of this proton with an *ax-ax* relationship with 2-H (J= 8.0 Hz) (Table 5). This pattern is in agreement with an *S* absolute configuration at *C*-3, with the piperidine displaying a preferred conformation in which the bulky chain lies in the equatorial position and 2-H, 3-H and 5-H are in an *axial* orientation (Figure 5). 1D-NOESY studies for compound **257** showed a strong NOE peak between proton 2-H and 6-Hb and 4-H (Figure 5). Moreover the ^{1}H-NMR spectrum showed a large singlet for the proton 3-H, which is consistent with two *eq-ax* relationships with both 2-H and 4-H (Table 6). These evidences confirm the *S* stereochemistry at *C*-3 and a conformation in which the chain bulky is in equatorial position.

Table 6.5: ^{1}H-NMR chemical shifts (δ) and coupling constants (*J*) of the protons in the azasugar portion of compound **255**.

Comp. 255	2H		3H		4H	5H		6Ha and 6Hb	
	δ (ppm)	^2J (Hz)	δ (ppm)	^2J (Hz)	δ (ppm)	δ (ppm)	^2J (Hz)	δ (ppm)	^2J (Hz)
	2.64 (t)	8.8	3.12 (d)	8.0	3.95 (brs)	3.56 (t)	6.6	3.05 (dd)	7.6

Table 6.6: ^{1}H-NMR chemical shifts (δ) and coupling constants (*J*) of the protons in the azasugar portion of compound **257**.

Comp. 257	2H		3-H	4H	5H	6Ha		6H$_b$	
	δ (ppm)	^2J (Hz)	δ (ppm)	δ (ppm)	δ (ppm)	δ (ppm)	^2J (Hz)	δ (ppm)	^2J (Hz)
	2.44 (t)	6.8	3.73 (brs)	3.46 (brs)	3.79 (brs)	3.02 (d)	15.0	2.69	14.0

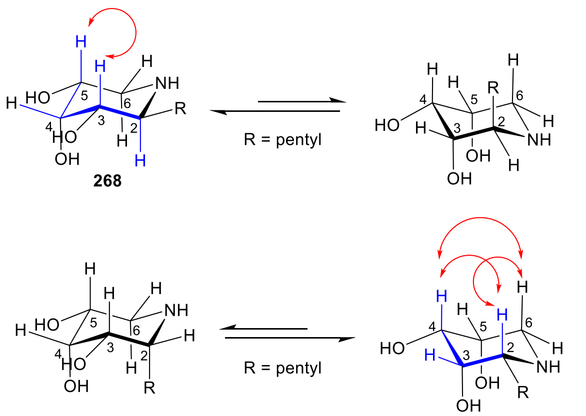

Figure 6.5: The two possible chair conformations of piperidines **255** and **257**. Dihedral angles between bonds analysed for the determination of the preferred conformation are shown in blue. Red double-ended arrows show the observed diagnostic NOE correlation peaks in the 1D-NOESY NMR spectra.

6.1.1.2 Preliminary biological screening towards human β-galactosidase and β-glucosidase.

Compounds **254**, **256**, **255** and **257** were first evaluated as human lysosomal β-Gal inhibitors at 1 mM in human leukocyte homogenates, and as human lysosomal β-Glucosidase (GCase) inhibitors at 1 mM in order to evaluate the selectivity of the new compounds. The results are shown in Table 6.7. Unfortunately, only compounds **254** and **256** showed 90% and 65% inhibitory activity towards β-Gal, respectively. These latter compounds showed a moderate IC_{50} (400 $\pm$ 15 μM and 1.15 $\pm$ 0.1 mM). The trihydroxypiperidines **254** with the *S* configuration at C-2 (Table 6.7, Entry 1) was more active than the corresponding epimeric trihydroxypiperidine **256** with the *R* configuration (Table 6.7, Entry 2). Therefore, the presence of a pentyl alkyl chain in trihydroxypiperidines **254** and **256** resulted beneficial for the inhibitory activity. Conversely, the opposite configuration at *C*-3 as in compounds **255** and **257** dramatically decreased β-Gal inhibition (down to 36% and 35%, respectively, regardless of the configuration of the chain in C-2) (Table 6.7, Entries 3 and 4 *vs* entries 1 and 2).

This result was somehow disappointing, since we expected that the "*all-cis*" configuration of the three hydroxy group could be beneficial to the inhibitory activity towards β-Gal. However, in consideration of literature data, potent PCs for β-Gal can be found among moderate to good inhibitors. [263] Therefore, in the next future, we will test the ability of our compounds to give enzymatic rescue on cell lines bearing the mutation.

None of the tested compounds strongly inhibited GCase (Table 6.7). These data confirm that the presence of a long alkyl chain is essential to impart GCase inhibition (see also *Chapter 3*).

Table 6.7. β-Gal and GCase inhibition in human leukocytes from healthy donors.

Entry	Compounds	β-Gal	GCase
		Inhibition [%][a]	Inhibition [%][a]
1	**254**	90	1
2	**256**	65	5
3	**255**	36	34
4	**256**	35	44

[a] Percentage inhibition of β-Gal or GCase in human leukocytes extracts incubated with compounds (1 mM).

6.1.2 Experimental Section

General Experimental Procedures for the syntheses

Commercial reagents were used as received. All reactions were carried out under magnetic stirring and monitored by TLC on 0.25 mm silica gel plates (Merck F254). Column chromatographies were carried out on Silica Gel 60 (32–63 μm) or on silica gel (230–400 mesh, Merck). Yields refer to spectroscopically and analytically pure compounds unless otherwise stated. ^{1}H-NMR spectra were recorded on a Varian Gemini 200 MHz, a Varian Mercury 400 MHz or on a Varian

INOVA 400 MHz instrument at 25 °C. ^{13}C-NMR spectra were recorded on a Varian Gemini 200 MHz or on a Varian Mercury 400 MHz instrument. Chemical shifts are reported relative to $CDCl_3$ (^{13}C: δ = 77.0 ppm), or to CD_3OD (^{13}C: δ = 49.0 ppm). Integrals are in accordance with assignments, coupling constants are given in Hz. For detailed peak assignments 2D spectra were measured (COSY, HSQC, NOESY, and NOE as necessary). IR spectra were recorded with a IRAffinity-1S SHIMADZU system spectrophotometer. ESI-MS spectra were recorded with a Thermo Scientific™ LCQ fleet ion trap mass spectrometer. Elemental analyses were performed with a Thermo Finnigan FLASH EA 1112 CHN/S analyzer. Optical rotation measurements were performed on a JASCO DIP-370 polarimeter.

Synthesis of benzyl-2,3-*O*-(1-methylethylidene)-β-L-gulofuranoside-5-(pentyl)-5-(*N*-benzyl-hydroxylamine) (260) and **benzyl-2,3-*O*-(1-methylethylidene)-α-D-mannofuranoside-5-(pentyl)-5-(*N*-benzyl- hydroxylamine) (261)**

- Method A: general procedure without Lewis acid

A solution of nitrone **140** (452 mg, 1.2 mmol) in dry THF (25 mL) was stirred at -78 °C under nitrogen atmosphere and pentylMgBr (1.8 mL, 2.2 mmol) was slowly added. The reaction mixture was stirred for 3 hours until a TLC control (PEt/AcOEt 1:1) attested the disappearance of the starting material. A 1M NaOH solution (10 mL) and Et_2O (10 mL) were added to the mixture at 0 °C and left stirring for 20 minutes. The two layers were separated and the aqueous layer was extracted with Et_2O (2x10 mL). The combined organic layers were washed with brine (2x30 mL), dried with Na_2SO_4 and concentrated under reduced pressure to give a mixture of hydroxylamines **260** and **261** (**260:261** ratio 3.5:1; the **260** :**261** ratio was determined by integration of ^{1}H-NMR signals of the crude reaction mixtures). The crude mixture was purified by silica gel column chromatography (gradient eluent from PEt/AcOEt 13:1 to 10:1) to give **260** (337 mg, 0.74 mmol, R_f = 0.35, PEt/AcOEt 10:1) and **261** (46 mg, 0.10 mmol, R_f = 0.25, PEt/AcOEt 10:1) corresponding to 70% total yield.

The secondary hydroxylamines **260** and **261** spontaneously oxidize to the corresponding nitrones **262** and **263**, so we could only perform ^{1}H-NMR and MS-ESI spectra immediately after their purification by column chromatography.

260: colourless oil. ^{1}H-NMR (400 MHz, $CDCl_3$) δ = 7.43-7.26 (m, 10H, Ar), 5.17 (s, 1H, 1-H), 4.79 (d, J=12.0 Hz, 1H, H_a-OBn), 4.71-4.70 (m, 1H, 3-H), 4.63 (d, J=8.0 Hz, 1H, 2-H), 4.58 (d, J=12.0 Hz, 1H, H_b-OBn), 4.43 (d, J=9.2 Hz, 1H, 4-H), 4.27 (d, J=14.0 Hz, 1H, H_a-NBn), 4.04 (d, J=14.0 Hz, 1H, H_b-NBn), 3.30-3.26 (m, 1H, 5-H), 1.54-1.51 (m, 4H, 1'H and 2'H) 1.45 (s, 3H, Me), 1.36-1.26 (m, 7H, Me, 3'H-5'H), 0.91 (t, J = 6.2 Hz, 3H, 5'$H_{a\text{-}b\text{-}c}$) ppm. $C_{27}H_{37}NO_5$: mass required m/z = 455.27; mass found - MS (ESI) m/z (%) = 478.21 (100) $[M+Na]^+$,456.15 (35) $[M+H]^+$.

261: colourless oil. ^{1}H-NMR (400 MHz, $CDCl_3$) δ = 7.37-7.24 (m, 10H, Ar), 5.07 (s, 1H, 1-H), 4.98 (bs, OH), 4.82-4.80 (m, 1H, 3-H), 4.66 (dd, J=12.0 Hz, 1H, H_a-OBn), 4.63 (d, J=5.6 Hz, 1H, 2-H), 4.50 (d, J=12.0 Hz, 1H, H_b-OBn), 4.33-4.31 (m, 1H, 4-H), 3.91 (s, 2H, $H_{a\text{-}b}$-NBn), 3.31 (q, J=6.0 Hz, 1H, 5-H), 1.78-1.72 (m, 2H, 1'H), 1.59-1.52 (m, 2H, 2'H), 1.43 (s, 3H, Me), 1.35-1.26 (m, 7H, Me , 3'H-5'H), 0.93 (t, J = 6.0 Hz, 3H, 5'$H_{a\text{-}b\text{-}c}$) ppm. $C_{27}H_{37}NO_5$: mass required m/z = 455.27; mass found - MS (ESI) m/z (%) = 478.19 (100) $[M+Na]^+$,456.15 (31) $[M+H]^+$.

- Method B: general procedure with Lewis acid

To a stirred solution of nitrone **140** (376 mg, 0.98 mmol) in dry THF (20 mL) at room temperature, boron trifluoride diethyl etherate (133 µL, 0.98 mmol) as Lewis acid was added and the resulting mixture was stirred at room temperature under nitrogen atmosphere for 15 minutes. The reaction mixture was cooled at -30 °C and pentylMgBr (1.5 mL, 1.76 mmol) was slowly added. The reaction mixture was stirred at -30 °C for 2 hours until a TLC control (PEt/AcOEt 1:1) attested the disappearance of the starting material. A 1M NaOH solution (10 mL) and Et_2O (10 mL) were added to the mixture at 0 °C and left stirring for 20 minutes. The two layers were separated and the aqueous layer was extracted with Et_2O (2x10 mL). The combined organic layers were washed with brine (2x30 mL) and dried with Na_2SO_4 and concentrated under reduced pressure to give a mixture hydroxylamines **260** and **261** (**260:261** ratio 1:5; the **260** :**261** ratio was determined by integration of ^{1}H-NMR signals of the crude reaction mixtures). The crude mixture was purified by silica gel column chromatography (gradient eluent from PEt/AcOEt 13:1 to 10:1) to give **260** (50 mg, 0.11 mmol, R_f = 0.35, PEt/AcOEt 10:1) and **261** (280 mg, 0.61 mmol, R_f = 0.25, PEt/AcOEt 10:1) corresponding to 75% total yield.

The secondary hydroxylamines **260** and **261** spontaneously oxidize to the corresponding nitrones **262** and **263**, so we could only perform ^{1}H-NMR and MS-ESI spectra immediately after their purification by column chromatography.

Synthesis of benzyl-2,3-*O*-(1-methylethylidene)-β-L-gulofuranoside-5-(pentyl)-5-(phenylmethanimine oxide) (262): To a stirred solution of hydroxylamine **260** (19.5 mg, 0.04 mmol) in dry CH_2Cl_2 (2 mL), IBX (2-Iodoxybenzoic acid contains stabilizer (45 wt. %)-Sigma-Aldrich) (40 mg, 0.06 mmol) was added and the resulting mixture was stirred under nitrogen atmosphere at room temperature for 3 h, when a TLC check (PEt/AcOEt 10:1) attested the disappearance of the starting material. Saturated solution of $NaHCO_3$ (4 mL) was added and the two layers were separated and the aqueous layer was extracted with CH_2Cl_2 (3x5 mL). The combined organic layers were washed with brine (2x6 mL) and concentrated after drying with Na_2SO_4. The residue was purified by silica gel flash column chromatography (PEt/AcOEt from 10:1) to give nitrone **262** (17.7 mg, 0.04 mmol, 98%, R_f = 0.25) as a straw yellow oil.

262: straw yellow oil. $[\alpha]_D^{25}$ = + 45 (c =1.00, $CHCl_3$). ^{1}H-NMR (400 MHz, $CDCl_3$) δ = 8.34-8.32 (m, 2H, *H*C=N and Ar), 7.46-7.43 (m, 4H, Ar), 7.30-7.23 (m, 5H, Ar), 5.01 (s, 1H, 1-H), 4.77-4.74 (m, 1H, 3-H), 4.67 (dd, J=5.6, 2.5 Hz, 1H, 2-H), 4.61-4.58 (m, 2H, H_a-Bn and 4-H), 4.33 (d, J=12.0 Hz, 1H, H_b-Bn), 4.06 (t, J= 10.2 Hz, 1H, 5-H), 2.17-2.11 (m, 1H, 1'H_a), 1.69-1.64 (m, 1H, 1'H_b), 1.50 (s, 3H, Me), 1.33-1.26 (m, 9H, Me and 2'H-5'H), 0.86 (t, J =7.0 Hz, 3H, 5'H_{a-b-c}) ppm. ^{13}C-NMR (50 MHz, $CDCl_3$) δ = 137.2 (s, 1C, Ar), 134.4 (d, 1C, Ar), 130.8 (s, 1C, Ar),130.2-127.9 (d, 10C, Ar and *C*=N), 112.6 (s, acetal), 104.5 (d, C-1), 85.4 (d, C-2), 79.7 (d, C-3), 79.1 (d, C-4), 76.7 (d, C-5), 68.8 (t, Bn), 31.5-22.6 (t, 4C, C-1'- C-4'and q, Me and q, Me), 14.2 (q, C-5') ppm. MS (ESI): m/z (%) = 928.62 (100) $[2M+Na]^+$, 476.16 (33) $[M+Na]^+$.IR ($CDCl_3$): ν = 974, 1080, 1107, 1209, 1456, 1582, 2243, 2858, 2932, 3032, 3065 cm^{-1}. $C_{27}H_{35}NO_5$ (453.58): calcd. C, 71.50; H, 7.78; N, 3.09; found C, 71.81; H, 7.53; N, 2.97.

Synthesis of benzyl-2,3-*O*-(1-methylethylidene)-α-D-mannofuranoside-5-(pentyl)-5-(phenylmethanimine oxide) (263): To a stirred solution of hydroxylamine **261** (22.2 mg, 0.05 mmol) in dry CH_2Cl_2 (2 mL), IBX (2-Iodoxybenzoic acid contains stabilizer (45 wt. %)-Sigma-Aldrich) (50 mg, 0.08 mmol) was added and the resulting mixture was stirred under nitrogen atmosphere at room temperature for 3 h, when a TLC check (PEt/AcOEt 10:1) attested the disappearance of the starting material. Saturated solution of $NaHCO_3$ (4 mL) was added and the two layers were separated and the aqueous layer was extracted with CH_2Cl_2 (3x5 mL). The combined organic layers were washed with brine (2x6 mL) and concentrated after drying with Na_2SO_4. The residue was purified by silica gel flash column chromatography (PEt/AcOEt from 10:1.2) to give nitrone **263** (22 mg, 0.05 mmol, 97%, R_f = 0.25) as a straw yellow oil.

263: straw yellow oil. $[\alpha]_D^{25}$ = + 80 (c =0.80, $CHCl_3$). ^{1}H-NMR (400 MHz, $CDCl_3$) δ = 8.27-8.25 (m, 2H, *H*C=N and Ar), 7.43-7.41 (m, 4H, Ar), 7.38-7.24 (m, 5H, Ar), 5.06 (s, 1H, 1-H), 4.70-4.68 (m, 1H, 3-H), 4.67 (d, J=12.0 Hz, 1H, H_a-Bn), 4.61 (d, J= 5.6 Hz,1H, 2-H), 4.49 (d, J=12 Hz, 1H, H_b-Bn), 4.47-4.46 (m, 1H, 4-H), 4.16 (t, J= 10.2 Hz, 1H, 5-H), 2.15-2.11 (m, 1H, 1'H_a), 1.84-1.78 (m, 1H, 1'H_b), 1.47 (s, 3H, Me), 1.42-1.24 (m, 6H, 2'H-4'H), 1.21 (s, 3H, Me), 0.85 (t, J= 6.0 Hz, 3H, 5'$H_{a\text{-}b\text{-}c}$) ppm. ^{13}C-NMR (100 MHz, $CDCl_3$) δ = 137.5 (s, 1C, Ar), 136.2 (d, 1C, Ar), 130.6 (s, 1C, Ar),130.5-127.9 (d, 10C, Ar and *C*=N), 112.6 (s, acetal), 105.5 (d, C-1), 85.3 (d, C-2), 80.1 (d, C-4), 79.4 (d, C-3), 74.7 (d, C-5), 69.2 (t, Bn), 31.7-22.7 (t, 4C, C-1'- C-4'and q, Me and q, Me), 14.2 (q, C-5') ppm. MS (ESI): m/z (%) = 928.62 (100) $[2M+Na]^+$, 476.18 (20) $[M+Na]^+$.IR ($CDCl_3$): ν = 974, 1080, 1107, 1209, 1456, 1582, 2243, 2860, 2932, 3032, 3065 cm^{-1}. $C_{27}H_{35}NO_5$ (453.58): calcd. C, 71.50; H, 7.78; N, 3.09; found C, 71.73; H, 7.58; N, 3.00.

Synthesis of (2*S*,3*R*,4*S*,5*R*)-3-hydroxy-4,5-*O*-(1-methylethylidene)-2-pentylpiperidine (264): To a mixture of hydroxylamine **262** (314 mg, 0.69 mmol in presence of nitrone **260)** in MeOH (35 mL), acid acetic (80 µL, 1.38 mmol) and Pd/C (160 mg) were added under nitrogen atmosphere. The mixture was stirred at room temperature under hydrogen atmosphere (balloon) for 2 days, until a control by ^{1}H-NMR spectroscopy attested the presence of acetate salt of 3-hydroxy-4,5-*O*-(1-methylethylidene)-2-pentylpiperidine piperidine **264**. The mixture was filtered through Celite® and the solvent was removed under reduced pressure. The corresponding free amine was obtained by dissolving the residue in MeOH, then the strongly basic resin Ambersep 900-OH was added, and the mixture was stirred for 40 minutes. The resin was removed by filtration and the crude product was purified on silica gel by flash column chromatography (CH_2Cl_2/MeOH/ NH_4OH (6%) 15:1:0.1) to afford 151 mg (0.62 mmol, 90% R_f = 0.30) of **264** as a white solid.

264: white solid m.p. 120-122 °C. $[\alpha]_D^{25}$ = + 36 (c =2.00, $CHCl_3$). ^{1}H-NMR (400 MHz, CD_3OD) δ = 4.19 (q, J = 6.3 Hz, 1H, 5-H), 4.14 (dd, J = 5.2, 3.2 Hz, 1H, 4-H), 3.80 (t, J = 2.6 Hz, 1H, 3-H), 3.05 (dd, *J* = 13.4, 5.6 Hz, 1H, 6-H_a), 2.73 (td, J=8.0, 2.0 Hz, 1H, 2-H), 2.66 (dd, J = 13.2, 7.6 Hz, 1H, 6-H_b), 1.53 (quint, J=7.0 Hz, 1H, 1'H_a), 1.47 (s, 3H, Me), 1.43-1.33 (m, 10H, 1'H_b, Me and 2'H-4'H), 0.92 (t, J = 7.0 Hz, 3H, 5'H_{a-b-c}) ppm. ^{13}C-NMR (50 MHz, CD_3OD) = 109.9 (s, acetal), 77.9 (d, C-4), 72.1 (d, C-5), 68.4 (d, C-3), 55.4 (d, C-2), 47.2 (t, C-6), 33.2-26.3 (t, 4C, C-1'- C-4'and q, Me, q, Me), 14.4 (q, C-5') ppm. MS (ESI): m/z (%) = 244.02 (100) $[M+H]^+$. IR (CD_3OD): ν = 1153, 1171, 1219, 1246, 1287, 1379, 1462, 2247, 2301, 2641, 2859, 2931, 3341 cm^{-1}. $C_{13}H_{25}NO_3$ (243.35): calcd. C, 64.16; H, 10.36; N, 5.76; found C, 64.14; H, 10.56; N, 5.60.

Synthesis of (2*R*,3*R*,4*S*,5*R*)-3-hydroxy-4,5-*O*-(1-methylethylidene)-2-pentylpiperidine (265): To a mixture of hydroxylamine **261** (150 mg, 0.33 mmol in presence of nitrone **263)** in MeOH (20 mL), acid acetic (38 µL, 0.66 mmol) and Pd/C (75 mg) were added under nitrogen atmosphere. The mixture was stirred at room temperature under hydrogen atmosphere (balloon) for 2 days, until a control by ^{1}H-NMR spectroscopy attested the presence of acetate salt of 3-hydroxy-4,5-*O*-(1-methylethylidene)-2-pentylpiperidine piperidine **265**. The mixture was filtered through Celite® and the solvent was removed under reduced pressure. The corresponding free amine was obtained by dissolving the residue in MeOH, then the strongly basic resin Ambersep 900-OH was added, and the mixture was stirred for 40 minutes. The resin was removed by filtration and the crude product was purified on silica gel by flash column chromatography (CH_2Cl_2/MeOH/ NH_4OH (6%) 15:1:0.1) to afford 72 mg (0.30 mmol, 90%, R_f = 0.30) of **265** as acolorless oil

265: colorless oil. $[\alpha]_D^{25}$ = – 32 (c =1.00, $CHCl_3$). ^{1}H-NMR (400 MHz, CD_3OD) δ = 4.21-4.19 (m, 1H, 5-H), 3.84 (t, J= 6.0 Hz, 1H, 4-H), 3.32-3.24 (m, 2H, 6-H_a and 3-H), 2.93 (d, J= 12.0 Hz, 1H, 6-H_b), 2.27-2.21 (m, 1H, 2-H), 1.83-1.78 (m, 1H, 1'H_a), 1.50 (s, 3H, Me), 1.37 (s, 3H, Me), 1.35-1.30 (m, 7H, 1'-H_b and 2'H-4'H), 0.92 (t, J = 6.0 Hz, 3H, 5'$H_{a,b,c}$) ppm. ^{13}C-NMR (100 MHz, CD_3OD) = 110.1 (s, acetal), 81.8 (d, C-4), 75.8 (d, C-3), 75.3 (d, C-5), 60.2 (d, C-2), 46.7 (t, C-6), 33.3-23.6 (t, 4C, C-1'-C-4'and q, Me, q, Me), 14.4 (q, C-5') ppm. ^{1}D-NOESY: Irradiation of 2-H gave a NOE at 4-H and 6-H_b, and irradiation of 4-H gave a NOE at 2-H and 6-H_b. MS (ESI): m/z (%) = 244.03 (100) $[M+H]^+$. IR (CD_3OD): ν = 1161, 1220, 1244, 1381, 2247, 2642, 2858, 2930, 3334 cm^{-1}. $C_{13}H_{25}NO_3$ (243.35): calcd. C, 64.16; H, 10.36; N, 5.76; found C, 64.24; H, 10.26; N, 5.42.

Synthesis of (2*S*, 3*R*, 4*R*, 5*R*)-2-pentylpiperidine-3,4,5-triol (254): A solution of **264** (30 mg, 0.12 mmol) in MeOH (4 mL) was left stirring with 12 M HCl (20 µL) at room temperature for 16 h. The crude mixture was concentrated to yield the hydrochloride salt of **264**. The corresponding free amine was obtained by dissolving the residue in MeOH, then the strongly basic resin Ambersep 900-OH was added, and the mixture was stirred for 40 minutes. The resin was removed by filtration and the crude product was purified on silica gel by flash column chromatography (CH_2Cl_2/MeOH/ NH_4OH (6%) 2:1:0.05) to afford 22 mg (0.11 mmol, 90%, R_f = 0.40) of **254** as free base, as a white solid.

254: white solid m.p. 125-127 °C. $[\alpha]_D^{25}$ = + 15 (c =1.00, CH_3OH). ^{1}H-NMR (400 MHz, CD_3OD) δ = 3.88-3.85 (m, 1H, 3-H), 3.83 (dd, J=8.0, 2.8 Hz, 1H, 5-H), 3.69-3.68 (m, 1H, 4-H), 2.80-2.79 (m, 1H, 2-H), 2.75 (d, J= 8.0 Hz, 2H, 6-H_{a-b}), 1.48-1.33 (m, 8H, 1'H-5'H), 0.91 (t, J= 6.0 Hz, 3H, 5'H_{a-b-c}) ppm. ^{13}C-NMR (100 MHz, CD_3OD) = 72.5 (d, C-3), 71.6 (d, C-4), 67.1 (d, C-5), 54.1 (d, C-2), 46.9 (t, C-6), 33.1, 31.6, 27.0, 23.7 (t, 4C, C-1' C-4'), 14.4 (q, C-5') ppm. MS (ESI): m/z (%) =204.07 (100) $[M+H]^+$. $C_{10}H_{21}NO_3$ (203.28): calcd. C, 59.09; H, 10.41; N, 6.89; found C, 59.00; H, 10.30; N, 6.80.

Synthesis of (2*R*, 3*R*, 4*R*, 5*R*)-2-pentylpiperidine-3,4,5-triol (256): A solution of **265** (30 mg, 0.12 mmol) in MeOH (4 mL) was left stirring with 12 M HCl (20 µL) at room temperature for 16 h. The crude mixture was concentrated to yield the hydrochloride salt of **256**. The corresponding free amine was obtained by dissolving the residue in MeOH, then the strongly basic resin Ambersep 900-OH was added, and the mixture was stirred for 40 minutes. The resin was removed by filtration and the crude product was purified on silica gel by flash column chromatography (CH_2Cl_2/MeOH/ NH_4OH (6%) 2:1:0.05) to afford 19 mg (0.09 mmol, 85%, R_f = 0.40) of **256** as free base, as a white solid.

256: white solid m.p. 74-76 °C. $[\alpha]_D^{25}$ = – 17 (c =0.50, CH_3OH). ^1H-NMR (400 MHz, CD_3OD) δ = 3.85 (bs, 1H, 5-H), 3.36-3.29 (m, 2H, 4-H and 3-H), 2.95 (d, J=14.0 Hz, 1H, 6-H_a), 2.67 (d, J=14.0 Hz, 1H, 6-H_b), 2.30-2.28 (m, 1H, 2-H), 1.87-1.82 (m, 1H, 1'H_a), 1.56-1.52 (m, 1H, 2'H_a), 1.34-1.33 (m, 6H, 1'H_b, 2'H_b, 3'H-4'H), 0.92 (t, J = 6.0 Hz, 3H, 5'$H_{a\text{-}b\text{-}c}$) ppm. ^{13}C-NMR (50 MHz, CD_3OD) = 76.7 (d, C-4), 73.9 (d, C-3), 70.7 (d, C-5), 61.7 (d, C-2), 50.8 (t, C-6), 33.4, 32.9, 26.3, 23.6 (t, 4C, C-1'and C-4'), 14.4 (q, C-5') ppm. MS (ESI): m/z (%) =204.06 (100) $[M+H]^+$. $C_{10}H_{21}NO_3$ (203.28): calcd. C, 59.09; H, 10.41; N, 6.89; found C, 59.11; H, 10.21; N, 6.79.

Synthesis of (2*S*,3*R*,4*S*,5*R*)-3-hydroxy-4,5-*O*-(1-methylethylidene)-*N*-Boc-2-pentylpiperidine (266): To a stirred solution of **264** (90 mg, 0.37 mmol) and $NaHCO_3$ (47 mg, 0.56 mmol) in H_2O (2.5 mL), MeOH (2.5 mL), and Boc_2O (121 mg, 0.56 mmol) were added. The mixture was stirred at room temperature for 48 hours until a TLC control (CH_2Cl_2/MeOH/ NH_4OH (6%) 10:1:0.1) attested the disappearance of the starting material. The mixture was concentrated and extracted with AcOEt (3x20 mL). The combined organic layers were washed with brine, dried over Na_2SO_4 and concentrated to give **266** (116 mg, 0.47 mmol, 91%) as a white solid.

266: white solid m.p. 86-88 °C. $[\alpha]_D^{25}$ = + 8.1 (c =2.00, $CHCl_3$). ^1H-NMR (400 MHz, $CDCl_3$) δ = 4.19 (brs, 1H, 5-H), 4.15-4.084 (m, 3H, 4-H, 2-H and 6-H_a), 3.92 (t, J= 6.0 Hz, 1H, 3-H), 3.14 (d, J = 14.4 Hz, 1H, 6-H_b), 2.81 (brs, 1H, OH), 1.70-1.65 (m, 1H, 1'H_a), 1.43 (s, 9H, *t*Bu), 1.41 (s, 3H, Me), 1.30 (s, 3H, Me), 1.29-1.25 (m, 7H, 1'H_b, 2'H-4'H), 0.85 (t, J = 6.0 Hz, 3H, 5'$H_{a\text{-}b\text{-}c}$) ppm. ^{13}C-NMR (100 MHz, $CDCl_3$) δ = 155.9 (s, N<u>C</u>OO), 109.1 (s, acetal), 79.9 (s, O<u>C</u>*t*Bu), 76.2 (d, C-4), 73.2 (d, C-5), 69.1 (d, C-3), 53.6 (d, C-2), 40.2, 39.7(t, C-6, two rotamers), 28.1 (q, 3C, *t*Bu), 31.8-22.7 (t, 4C, C-1'- C-4'and q, Me, q, Me), 14.1 (q, C-5') ppm. MS (ESI): m/z (%) = 708.84 (100) $[2M+Na]^+$, 366.09 (56) $[M+Na]^+$. IR ($CDCl_3$): ν = 950, 1124, 1454, 1685, 2922, 3604 cm^{-1}. $C_{18}H_{33}NO_5$ (343.46): calcd. C, 62.95; H, 9.68; N, 4.08; found C, 62.80; H, 10.00; N, 4.03.

Synthesis of (2*R*,3*R*,4*S*,5*R*)-3-hydroxy-4,5-*O*-(1-methylethylidene)-*N*-Boc-2-pentylpiperidine (266): To a stirred solution of **265** (190 mg, 0.78 mmol) and $NaHCO_3$ (98 mg, 1.17 mmol) in H_2O (3 mL), MeOH (3 mL), and Boc_2O (252 mg, 1.17 mmol) were added. The mixture was stirred at room temperature for 48 hours until a TLC control (CH_2Cl_2/MeOH/ NH_4OH (6%) 10:1:0.1) attested the disappearance of the starting material. The mixture was concentrated and extracted with AcOEt (3x20 mL). The combined organic layers were washed with brine, dried over Na_2SO_4 and the crude product was purified on silica gel by flash column chromatography (CH_2Cl_2/MeOH/ NH_4OH (6%) 15:1:0.1) to afford 171 mg (0.50 mmol, 95%, R_f = 0.34) of **266** as a white solid.

266: white solid m.p. 73-75 °C. $[\alpha]_D^{25}$ = – 19 (c =0.55, $CHCl_3$). ^{1}H-NMR (400 MHz, $CDCl_3$) δ = 4.38-4.28 (m, 1H, 5-H), 4.02-3.94 (m, 2H, 4-H and 6-H_a), 3.78-3.68 (m, 2H, 2-H and 3-H), 2.91 (brs, 1H, OH), 2.68 (brs, 1H, 6-H_b), 1.66 (brs, 2H, 1'H), 1.45 (s, 3H, Me),1.41 (s, 9H, *t*Bu), 1.31 (s, 3H, Me), 1.26-1.22 (m, 6H, 2'H-4'H), 0.84-0.83 (m, 3H, 5'$H_{a\text{-}b\text{-}c}$) ppm. ^{13}C-NMR (100 MHz, $CDCl_3$) δ = 155.4 (s, N<u>C</u>OO), 109.9 (s, acetal), 80.2 (s, O<u>C</u>*t*Bu), 78.3 (d, C-4), 72.3 (d, C-3), 70.8 (d, C-5), 56.4, 55.8 (d, C-2 two rotamers), 41.3, 40.6 (t, C-6, two rotamers), 28.4 (q, 3C, *t*Bu), 31.9-22.6 (t, 4C, C-1'- C-4'and q, Me, q, Me), 14.0 (q, C-5') ppm. MS (ESI): m/z (%) = 366.09 (100) $[M+Na]^+$, 708.84 (39) $[2M+Na]^+$. IR ($CDCl_3$): ν = 947, 1161, 1456, 1684, 2928, 3595 cm^{-1}. $C_{18}H_{33}NO_5$ (343.46): calcd. C, 62.95; H, 9.68; N, 4.08; found C, 62.88; H, 9.55; N, 4.00.

Synthesis of (2*S*,4*S*,5*R*)-3-oxo-4,5-*O*-(1-methylethylidene)-*N*-Boc-2-pentylpiperidine (**268**): Dess-Martin periodinane (216 mg, 0.51 mmol) was added to a solution of **264** (116 mg, 0.34 mmol) in dry CH_2Cl_2 (11 mL) at room temperature. The reaction mixture was stirred for 3 hours until a TLC control (CH_2Cl_2/MeOH/ NH_4OH (6%) 15:1:0.1) attested the disappearance of the starting material. The mixture was extracted with $NaHCO_3$ saturated solution, dried over Na_2SO_4 and concentrated. The residue was purified by silica gel flash chromatography (Hex/AcOEt 5:1) to give **268** (93 mg, 0.27 mmol, 80%, R_f = 0.41) as a white solid.

268: white solid m.p. 104-106 °C. $[\alpha]_D^{25}$ = + 32 (c =1.00, $CHCl_3$). ^{1}H-NMR (400 MHz, $CDCl_3$) δ = 4.75-4.64 (m, 1H, 2-H), 4.49-4.47 (m, 1H, 5-H), 4.39 (brs, 1H, 4-H), 4.29 (d, J= 6.4 Hz, 1H, 6-H_a), 2.95 (brs, 1H, 6-H_b), 1.78-1.71 (m, 1H, 1'H_a), 1.59-1.51 (m, 1H, 1'H_b), 1.44 (s, 9H, *t*Bu), 1.41 (s, 3H, Me), 1.30 (s, 3H, Me), 1.27-1.25 (m, 6H, 2'H-4'H), 0.83 (t, J= 6.0 Hz, 3H, 5'$H_{a\text{-}b\text{-}c}$) ppm. ^{13}C-NMR (100 MHz, $CDCl_3$) δ = 205.6 (s, C=O), 155.2 (s, N<u>C</u>OO), 111.6 (s, acetal), 80.6 (s, O<u>C</u>*t*Bu), 76.7 (d, C-4 or C-5), 76.6 (d, C-4 or C-5), 61.7,60.6 (d, C-2, two rotamers), 42.8, 41.5 (t, C-6, two rotamers), 28.4 (q, 3C, *t*Bu), 31.6-22.6 (t, 4C, C-1'- C-4'and q, Me, q, Me), 14.0 (q, C-5') ppm. MS (ESI): m/z (%) = 364.00 (100) $[M+Na]^+$. IR ($CDCl_3$): ν = 1159, 1217, 1256, 1370, 1410, 1456, 1692, 1744, 2927 cm^{-1}. $C_{18}H_{31}NO_5$ (341.45): calcd. C, 63.32; H, 9.15; N, 4.10; found C, 63.00; H, 9.25; N, 3.99.

Synthesis of (2*R*,4*S*,5*R*)-3-oxo-4,5-*O*-(1-methylethylidene)-*N*-Boc-2-pentylpiperidine (**269**): Dess-Martin periodinane (218 mg, 0.75 mmol) was added to a solution of **265** (171 mg, 0.50 mmol) in dry CH_2Cl_2 (15 mL) at room temperature. The reaction mixture was stirred for 3 hours until a TLC control (CH_2Cl_2/MeOH/ NH_4OH (6%) 15:1:0.1) attested the disappearance of the starting material. The mixture was extracted with $NaHCO_3$ saturated solution, dried over Na_2SO_4 and concentrated. The residue was purified by silica gel flash chromatography (Hex/AcOEt 4:1) to give **269** (137 mg, 0.40 mmol, 80%, R_f = 0.23) as a colourless oil.

269: colourless oil. $[\alpha]_D^{25}$ = + 41 (c =0.30, $CHCl_3$). ^{1}H-NMR (400 MHz, $CDCl_3$) δ = 4.88-4.79 (m, 1H, 5-H), 4.63-4.53 (m, 2H, 4-H and 6-H_a), 4.46-4.32 (m, 1H, 2-H), 2.66-2.64 (m, 1H, 6-H_b), 1.99 (brs, 1H, 1'H_a), 1.61-1.4 (m, 13H, 1'H_b, *t*Bu and Me), 1.38 (s, 3H, Me), 1.32-1.26 (m, 6H, 2'H-4'H), 0.89-0.88 (m, 3H, 5'$H_{a\text{-}b\text{-}c}$) ppm. ^{13}C-NMR (100 MHz, $CDCl_3$) δ = 206.6 (s, C=O), 154.8 (s, NCOO), 112.3 (s, acetal), 81.3 (s, OC*t*Bu), 79.2 (d, C-4), 74.3 (d, C-5), 63.0, 62.2 (d, C-2, two rotamers), 45.0, 43.5 (t, C-6, two rotamers), 28.4 (q, 3C, *t*Bu), 31.8-22.7 (t, 4C, C-1'- C-4'and q, Me, q, Me), 14.1 (q, C-5') ppm. MS (ESI): m/z (%) = 364.08 (100) $[M+Na]^+$. IR ($CDCl_3$): ν = 1159, 1217, 1256, 1369, 1410, 1456, 1692, 1744, 2928 cm^{-1}. $C_{18}H_{31}NO_5$ (341.45): calcd. C, 63.32; H, 9.15; N, 4.10; found C, 63.13; H, 9.10; N, 3.97.

Synthesis of (2*S*,3*S*,4*S*,5*R*)-3-hydroxy-4,5-*O*-(1-methylethylidene)-*N*-Boc-2-pentylpiperidine (270): A solution of **268** (60 mg, 0.18 mmol) in EtOH (1.4 mL) was cooled to 0°C and $NaBH_4$ (17 mg, 0.45 mmol) was added. The reaction mixture was allowed to warm to room temperature and stirred for 18 hours until a TLC control (Hex/EtOAc 4:1). Then, water (0.3 mL) and MeOH (0.8 mL) were added and mixture was stirred for 10 hours at room temperature and concentrated under reduced pressure. The crude product was purified by silica gel flash chromatography (CH_2Cl_2/MeOH 10:1) to give **270** (51 mg, 0.15 mmol, 71%, R_f = 0.50) as a white solid.

270: white solid m.p. 104-106 °C. $[\alpha]_D^{25}$ = + 6.5 (c =1.00, $CHCl_3$). ^1H-NMR (400 MHz, $CDCl_3$) δ = 4.42 (dd, J=8.0, 2.8 Hz, 1H, 4-H), 4.27 (brs, 1H, 3-H), 4.16-4.09 (m, 1H, 6-H_a), 3.92-3.78 (m, 1H, 2-H), 3.57 (t, J=7.4 Hz, 1H, 5-H), 2.74-2.70 (m, 1H, 6-H_b), 2.40-2.33 (m, 1H, OH), 1.72-1.67 (m, 1H, 1'H_a), 1.58-1.50 (m, 1H, 1'H_b), 1.43 (s, 9H, *t*Bu), 1.40 (s, 3H, Me), 1.32 (s, 3H, Me), 1.37-1.26 (m, 6H, 2'H-4'H), 0.84 (t, J= 6.6 Hz, 3H, 5'$H_{a\text{-}b\text{-}c}$) ppm. ^{13}C-NMR (100 MHz, $CDCl_3$) δ = 155.8 (s, N<u>C</u>OO), 109.5 (s, acetal), 79.8 (s, O<u>C</u>*t*Bu), 74.5 (d, C-4), 73.6 (d, C-3), 69.3 (d, C-5), 54.5, 53.6 (d, C-2 two rotamers), 42.7, 41.6 (t, C-6, two rotamers), 28.5 (q, 3C, *t*Bu), 32.2-22.7 (t, 4C, C-1'- C-4'and q, Me, q, Me), 14.1 (q, C-5') ppm. MS (ESI): m/z (%) = 366.09 (100) $[M+Na]^+$, 708.83 (30) $[2M+Na]^+$. IR ($CDCl_3$): ν = 955, 1157, 1416, 1684, 2918, 3620 cm^{-1}. $C_{18}H_{33}NO_5$ (343.46): calcd. C, 62.95; H, 9.68; N, 4.08; found C, 62.88; H, 9.55; N, 4.00.

Synthesis of (2*R*,3*S*,4*S*,5*R*)-3-hydroxy-4,5-*O*-(1-methylethylidene)-*N*-Boc-2-pentylpiperidine (271): A solution of **269** (70 mg, 0.21 mmol) in EtOH (1.4 mL) was cooled to 0°C and $NaBH_4$ (20 mg, 0.53 mmol) was added. The reaction mixture was allowed to warm to room temperature and stirred for 18 hours until a TLC control (Hex/EtOAc 4:1). Then, water (0.3 mL) and MeOH (0.8 mL) were added and mixture was stirred for 10 hours at room temperature and concentrated under reduced pressure. The crude product was purified by silica gel flash chromatography (CH_2Cl_2/MeOH 10:1) to give **271** (54 mg, 0.16 mmol, 75%, R_f = 0.50) as a white solid.

271: white solid m.p. 71-73 °C. $[\alpha]_D^{25}$ = – 20 (c =0.65, $CHCl_3$). ^1H-NMR (400 MHz, $CDCl_3$) δ = 4.27 (brs, 1H, 6-H_a), 4.13 (t, J=7.6 Hz, 1H, 5-H), 4.07-4.05 (m, 2H, 4-H and 3-H), 3.85-3.81 (m, 1H, 2-H), 3.08-2.97 (m, 1H, 6-H_b), 2.45 (brs, 1H, OH), 1.77-1.75 (m, 1H, 1'H), 1.51 (s, 3H, Me), 1.43 (s, 9H, *t*Bu), 1.35 (s, 3H, Me), 1.28-1.23 (m, 6H, 2'H-4'H), 0.87 (brs, 3H, 5'$H_{a\text{-}b\text{-}c}$) ppm. ^{13}C-NMR (100 MHz, $CDCl_3$) δ = 154.9(s, N<u>C</u>OO), 109.5 (s, acetal), 80.1 (s, O<u>C</u>*t*Bu), 75.4 (d, C-4 or C-3), 71.6 (d, C-5), 66.5 (d, C-4 or C-3), 53.9 (d, C-2), 41.3, 40.2 (t, C-6, two rotamers), 28.0 (q, 3C, *t*Bu), 31.9-22.8 (t, 4C, C-1'- C-4'and q, Me, q, Me), 14.1 (q, C-5') ppm. MS (ESI): m/z (%) = 366.00 (100) $[M+Na]^+$, 708.84 (40) $[2M+Na]^+$. IR ($CDCl_3$): ν = 954, 1157, 1416, 1684, 2918, 3620 cm^{-1}. $C_{18}H_{33}NO_5$ (343.46): calcd. C, 62.95; H, 9.68; N, 4.08; found C, 62.90; H, 9.65; N, 4.16.

Synthesis of (2*S*,3*S*,4*R*,5*R*)-2-pentylpiperidine-3,4,5-triol (255): A solution of **270** (45 mg, 0.13 mmol) in MeOH (6 mL) was left stirring with 12 M HCl (30 µL) at room temperature for 16 h. The crude mixture was concentrated to yield the hydrochloride salt of **270**. The corresponding free amine was obtained by dissolving the residue in MeOH, then the strongly basic resin Ambersep 900-OH was added, and the mixture was stirred for 40 minutes. The resin was removed by filtration to afford 25 mg (0.12 mmol, 95%) of **255** as free base, as a white solid.

255: white solid m.p. 130-132 °C. $[\alpha]_D^{25}$ = + 41 (c =0.80, CH_3OH). ^{1}H-NMR (400 MHz, CD_3OD) δ = 3.95 (brs,1H, 4-H), 3.56 (t, J= 6.6 Hz, 1H, 5-H), 3.12 (d, J=8.0 Hz, 1H, 3-H), 2.74 (d, J= 7.6 Hz, 2H, 6-H_{a-b}), 2.64 (t, J= 8.8 Hz, 1H, 2-H), 1.80 (t, J= 11.8 Hz, 1H, 1'H_a), 1.51-1.49 (m, 1H, 2'H_a), 1.34-1.22 (m, 6H, 1'H_b, 2'H_b and 3'H-5'H), 0.92 (t, J= 6.6 Hz, 3H, 5'H_{a-b-c}) ppm. ^{13}C-NMR (100 MHz, CD_3OD) = 74.2 (d, C-3), 73.2 (d, C-4), 70.3 (d, C-5), 55.4 (d, C-2), 46.5 (t, C-6), 33.4, 32.8, 26.4, 23.7 (t, 4C, C-1' C-4'), 14.4 (q, C-5') ppm. MS (ESI): m/z (%) = 226.10 (100) $[M+]^+$. $C_{10}H_{21}NO_3$ (203.28): calcd. C, 59.09; H, 10.41; N, 6.89; found C, 59.12; H, 10.23; N, 6.41.

Synthesis of (2*R*,3*S*,4*R*,5*R*)-2-pentylpiperidine-3,4,5-triol (257): A solution of **271** (24 mg, 0.07 mmol) in MeOH (3 mL) was left stirring with 12 M HCl (15 µL) at room temperature for 16 h. The crude mixture was concentrated to yield the hydrochloride salt of **271**. The corresponding free amine was obtained by dissolving the residue in MeOH, then the strongly basic resin Ambersep 900-OH was added, and the mixture was stirred for 40 minutes. The resin was removed by filtration to afford 14 mg (0.07 mmol, 98%) of **257** as free base, as pale yellow oil.

257: pale yellow oil. $[\alpha]_D^{25}$ = – 40 (c =0.50, CH_3OH). ^{1}H-NMR (400 MHz, CD_3OD) δ = 3.79 (bs, 1H, 5-H), 3.73 (bs, 1H, 3-H), 3.46 (bs, 1H, 4-H), 3.02 (d, J= 15.0 Hz, 1H, 6-H_a), 2.69 (d, J= 14.0 Hz, 1H, 6-H_b), 2.44 (t, J= 6.8 Hz, 1H, 2-H), 1.58-1.53 (m, 1H, 1'H_a), 1.51-1.44 (m, 1H, 2'H_a), 1.43-1.29 (m, 6H, 1'H_b, 2'H_b, 3'H-4'H), 0.92 (t, J = 6.0 Hz, 3H, 5'H_{a-b-c}) ppm. ^{13}C-NMR (100 MHz, CD_3OD) = 72.6 (d, C-3), 71.3 (d, C-4), 71.7 (d, C-5), 60.0 (d, C-2), 51.6 (t, C-6), 33.2, 32.7, 26.7, 23.7 (t, 4C, C-1'and C-4'), 14.4 (q, C-5') ppm. MS (ESI): m/z (%) =204.12 (100) $[M+H]^+$. $C_{10}H_{21}NO_3$ (203.28): calcd. C, 59.09; H, 10.41; N, 6.89; found C, 59.17; H, 10.11; N, 6.70.

Biological screening towards human lysosomal β-galactosidase (β-Gal) and β-glucosidase (GCase)

The new compounds were screened at 1 mM concentration towards β-galactosidase (β-Gal) and β-glucosidase (GCase) in leukocytes isolated from healthy donors (controls). Isolated leukocytes were disrupted by sonication, and a micro BCA protein assay kit (Sigma–Aldrich) was used to determine the total protein amount for the enzymatic assay, according to the manufacturer's instructions.

- Human lysosomal β-galactosidase (β-Gal) activity

β-Gal activity was measured in a flat-bottomed 96-well plate. Azasugar solution (3 µL), 4.29 µg/µL leukocytes homogenate 1:10 (7 µL), and substrate 4-methylumbelliferyl β-D-galactopyranoside (1.47 mM, 20 µL, Sigma–Aldrich) in acetate buffer (0.1M, pH 4.3) containing NaCl (0.1M) and sodium azide (0.02%) were incubated at 37 °C for 1 h. The reaction was stopped by addition of sodium carbonate (200 µL; 0.5M, pH 10.7) containing Triton X-100 (0.0025%), and the fluorescence 4-methylumbelliferone released by β-galactosidase activity was measured in SpectraMax M2 microplate reader (λex=365 nm, λem=435 nm; Molecular Devices). Inhibition is given with respect to the control (without azasugar). Percentage β-Gal inhibition is given with respect to the control (without compound). Data are mean SD (n=3).

- Human lysosomal β-glucosidase (GCase) activity

GCase activity was measured in a flat-bottomed 96-well plate. Compound solution (3 µL), 4.29 µg/µL leukocytes homogenate (7 µL), and substrate 4-methylumbelliferyl-β-D-glucoside (3.33 mM, 20 µL, Sigma–Aldrich) in citrate/phosphate buffer (0.1:0.2, M/M, pH 5.8) containing sodium taurocholate (0.3%) and Triton X-100 (0.15%) at 37 °C were incubated for 1 h. The reaction was stopped by addition of sodium carbonate (200 µL; 0.5M, pH 10.7) containing Triton X-100 (0.0025 %), and the fluorescence of 4-methylumbelliferone released by β-glucosidase activity was measured in SpectraMax M2 microplate reader (λex=365 nm, λem=435 nm; Molecular Devices). Percentage GCase inhibition is given with respect to the control (without compound). Data are mean SD (n=3).

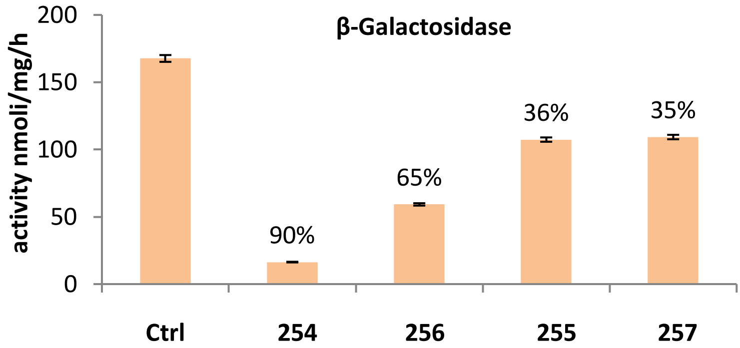

Percentage of β-Gal inhibition of the whole collection of compounds in human leukocytes extracts incubated with azasugars at 1 mM concentration.

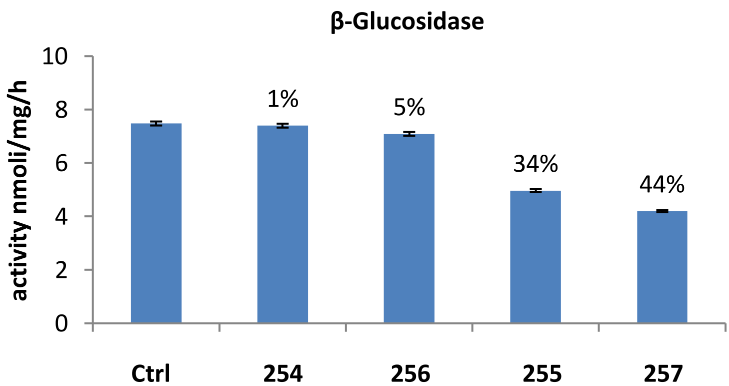

Percentage of GCase inhibition of the whole collection of compounds in human leukocytes extracts incubated with azasugars at 1 mM concentration.

For compounds showing GCase inhibitory activity higher than 60% at 1 mM concentration, the IC_{50} values were determined by measuring the initial hydrolysis rate with 4-methylumbelliferyl β-D-galactopyranoside (1.47 mM).
Data obtained were fitted to the following equation using the Origin Microcal program.

$$\frac{Vi}{Vo} = \frac{Max - Min}{1 + \left(\frac{x}{IC_{50}}\right)^{slope}} + Min$$

where V_i/V_o, represent the ratio between the activity measured in the presence of the inhibitor (V_i) and the activity of the control without the inhibitor (V_0), "x" the inhibitor concentration, Max and Min, the maximal and minimal enzymatic activity observed, respectively.

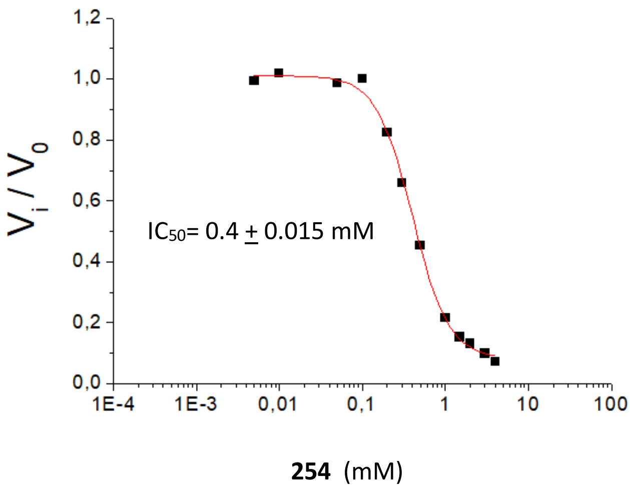

IC_{50} of compound **254** towards β-Gal

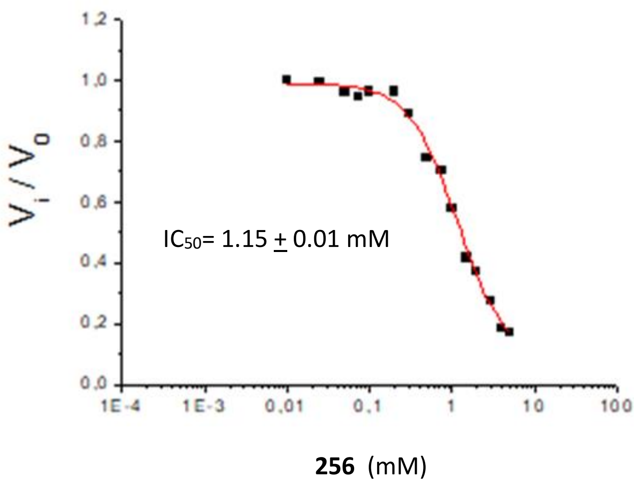

IC_{50} of compound **256** towards β-Gal

Conclusion

In summary, with the aim of searching for new human lysosomal β-Gal inhibitors, we synthesized a series of trihydroxypiperidines with a C-2 pentyl chain with both configurations, together with their epimers at C-3 bearing the "*all-cis*" configuration at the carbons bearing the hydroxy groups. The synthesis exploited the reaction of nitrone intermediate **140** derived from aldehyde **135**, followed by RA, to obtain *C*-2 pentyl trihydroxypiperidines. The inversion of configuration at *C*-3 in compound was achieved through an oxidation–reduction sequence. Unfortunately, none of the reported compounds showed β-Gal inhibition. However, these data give useful pointers, suggesting that the presence of pentyl alkyl chain is beneficial for β-Gal inhibitory activity, but the inversion of hydroxyl group at *C*-3 dramatically decreases β-Gal inhibition. Regarding GCase inhibition, the presence of a long alkyl chain in inhibitors was confirmed to be essential for the activity.

List of abbreviations

AcOEt	Ethyl acetate
ATF6	Activating transcription factor 6
BBB	Blood-brain barrier
Boc	*Tert*-butyloxycarbonyl
CBE	Conduritol B epoxide
cmc	Critical micellar concentration
CSG	Ceramide-specific glucosyltransferase
CuAAC	Copper-mediated azide-alkyne cycloaddition
DHA	Dihydroxyacetone
DIX	1,5-dideoxy-1,5-iminoxylitol
DMF	*N*,*N*-Dimethylformamide
DMJ	1-deoxymannojirimycin
DMP	Dess Martin periodinane
DNJ	Deoxynojirimycin
DRA	Double Reductive Amination
equiv.	Equivalents
ER	Endoplasmic reticulum
ERAD	Endoplasmic-reticulum-associated protein degradation
ERS	Endoplasmic reticulum stress
ERT	Enzyme replacement therapy
FCC	Flash column chromatography
FSA	Fructose 6-phosphate aldolase
GCase or β-Glu	β-glucosidase
GD	Gaucher disease
GlcCer	Glucosylceramide
HA	Hydroxyacetone
HB	Hydroxybutanone
Hex	Hexane
HNJ	Homonojirimycin
IBX	Hypervalent iodine reagent
IFG	Isofagomine
IRE1	Inositol-requiring protein 1
LSDs	Lysosomal Storage Disorders
M6-P	Mannose 6-phosphate
MTT	3-(4,5-dimethylthiazol-2-yl)-2,5-diphenyltetrazolium bromide

MVE	Multivalent effect
NB-DNJ	*N*-Butyldeoxynojirimycin
PC	Pharmacological chaperone
PCT	Pharmacological Chaperone Therapy
PD	Parkinson's Disease
PERK	Protein kinase R (PKR)-like endoplasmic reticulum kinase
PEt	Petroleum ether
QC	Quality control
RA	Reductive Amination
RhamT	Rhamnosyltransferase
rp	Relative potency
S2P	Site-2 protease
SRT	Substrate reduction therapy
TESH	Triethylsilane
TFA	Trifluoroacetic acid
UPR	Unfolded protein response
WT	Wild type
α-Fuc	α-fucosidase
α-Gal	α-galactosidase
α-Glu	α-glucosidase
α-Man	α-mannosidase
α-Syn	α-synuclein
β-Gal	β-galactosidase
β-Man	β-mannosidase

References

[1] F. M. Platt, A. D'Azzo, B. L. Davidson, E. F. Neufeld, C. J. Tifft, *Nat. Rev. Dis. Prim*. **2018**, *4*, 27-51.
[2] A. R. A. Marques, P. Saftig, *J. Cell Sci*. **2019**, *132*, jcs221739.
[3] B. McInnes, M. Potier, N. Wakamatsu, S. B. Melancon, M. H. Klavins, S. Tsuji, D. J. Mahuran, *J. Clin. Invest*. **1992**, *90*, 306-314.
[4] S. C. Garman, D. N. Garboczi, J. *Mol. Biol*. **2004**, *337*, 319-335.
[5] I. Ron, M. Horowitz, *Hum. Mol. Genet*. **2005**, *14*, 2387-2398.
[6] S. Zhang, R. Bagshaw, W. Hilson, Y. Oho, A. Hinek, J. T. Clarke, J. W. Callahan, *Biochem. J*. **2000**, *348*, 621-632.
[7] G. Parenti, G. Andria, A. Ballabio, *Annu. Rev. Med*. **2015**, *66*, 471-486.
[8] L. Ellgaard, A. Helenius, *Curr.Opin.CellBiol*. **2001**, *13*, 431-437.
[9] T. Anelli, R. Sitia, *EMBO J*. **2008**, *27*, 315-327.
[10] D. N. Hebert, M. Molinari, *Physiol. Rev*. **2007**, *87*, 1377-1408.
[11] M. F. Coutinho, M. J. Prata, S. Alves, *Mol. Genet. Metab*. **2012**, *105*, 542-550.
[12] W. Peter, R. David, *Science*. **2011**, *334*, 1081-1086.
[13] P. Giancarlo, A. Generoso, K. J. Valenzano, *Mol Ther*. **2015**, *7*, 1138-1148.
[14] M. Filocamo, A. Morrone, *Hum. Genomics*. **2011**, *5*, 156-169.
[15] R. O. Brady, *Annu Rev Med*. **2006**, *57*, 283-296.
[16] F. M. Platt, M. Jeyakumar, *Acta Paediatr Suppl*. **2008**, *97*, 88-93.
[17] F. M. Platt, G. R. Neises, R. A. Dwek, T. D. Butters, *J. Biol. Chem*. **1994**, *269*, 8362-8365.
[18] P. Giraldo, P. Alfonso, K. Atutxa, M. A. Fernandez-Galan, A. Barez, R. Franco, D. Alonso, A. Martin, P. Latre, M. Pocov, *Haematologica*. **2009**, *94*, 1771-1775.
[19] K. A. Lyseng-Williamson, *Drugs*. **2014**, *74*, 61-74.
[20] R. Schiffmann, E. J. Fitzgibbon, C.Harris, C.De Vile, E. H. Davies, L. Abel, I. N. van Schaik, W. Benko, M. Timmons, M. Ries, A. Vellodi, *Ann. Neurol*. **2008**, *64*, 514-522.
[21] P. K. Mistry, M. Balwani, H. N. Baris, H. B. Turkia, T. A. Burrow, J. Charrow, G. F. Cox, S. Danda, M. Dragosky, G. Drelichman, A. El-Beshlawy, C. Fraga, S. Freisens, S. Gaemers, E. Hadjiev, S. P. Kishnani, E. Lukina, P. Maison-Blancheq, A. M. Martins, G. Pastores, M. Petakov, M. J. Peterschmitt, H. Rosenbaum, B. Rosenbloom, L. H. Underhill, T. M. Cox, *Blood Cell Mol. Dis*. **2018**, *71*, 71-74.
[22] A. C. Muntau, J. Leandro, M. Staudigl, F. Mayer, S. W. Gersting, *J. Inherit. Metab. Dis.* **2014**, *37*, 505-523.
[23] E. M. Sànchez-Fernàndez, J. M. G. Fernàndez, C. O. Mellet, *Chem. Commun*. **2016**, *52*, 5497-5515.

[24] M. Convertino, J. Das, N. V. Dokholyan, *ACS Chem. Biol*. **2016**, *11*, 1471-1489.
[25] D. M. Pereira, P. Valentao, P. B. Andrade, *Chem. Sci*. **2018**, *9*, 1740-1752.
[26] R. E. Boyd, G. Lee, P. Rybczynski, E. R. Benjamin, R. Khanna, B. A. Wustman, K. J. Valenzano, *J. Med. Chem*. **2013**, *56*, 2705-2725.
[27] G. J. Kornhaber, M. B. Tropak, G. H. Maegawa, S. J. Tuske, S. J. Coales, D. J. Mahuran, Y. Hamuro, *ChemBioChem*. **2008**, *9*, 2643-2649.
[28] C. Porto, A. Pisani, M. Rosa, E. Acampora, V. Avolio, M. R. Tuzzi, B. Visciano, C. Gagliardo, S. Materazzi, G. La Marca, G. Andria, G, Parenti, *J. Inherit Metab. Dis*. **2012**, *35*, 513-520.
[29] C. Porto, M. Cardone, F. Fontana, B. Rossi, M. R. Tuzzi, A. Tarallo, M. V. Barone, G. Andria, G. Parenti, *Molecular Therapy* **2009**, *17*, 964-971.
[30] E. R Benjamin, R. Khanna, A Schilling, J. J. Flanagan, L. J. Pellegrino, N. Brignol, Y. Lun, D. Guillen, B. E. Ranes, M.Frascella, R. Soska, J. Feng, L. Dungan, B. Young, D. J. Lockhart, K. J. Valenzano, *Molecular Therapy* **2012**, *20*, 717-726.
[31] J. Shen, N. J. Edwards, Y. Bin Hong, G. J. Murray, *Biochem. Biophys. Res. Commun.* **2008**, *369*, 1071-1075.
[32] J. Charrow, H. C. Andersson, P. Kaplan, E. H. Kolodny, P. Mistry, G. Pastores, B. E. Rosenbloom, C. R. Scott, R. S. Wappner, N. J. Weinreb, A. Zimram, *Arch. Intern. Med*. **2000**, *160*, 2835-2843.
[33] G. A. Grabowski (Ed.), Advances in Gaucher Disease: Gaucher Disease: Basic and Clinical Perspectives, Future Medicine Ltd, Unitec House, 2 Albert Place, London N3 1QB, UK, **2013**.
[34] G. A. Grabowski, S. Gatt, M. Horowitz, *Crit. Rev. Biochem. Mol. Biol*. **1990**, *25*, 385-414.
[35] H. Dvir, M. Harel, A. A. McCarthy, L. Toker, I. Silman, A. H. Futerman, *EMBO Rep*. **2003**, *4*, 703-709.
[36] G. A. Grabowski, *Lancet*. **2008**, *372*, 1263-1271.
[37] L. M. de Lau, M. M. Breteler, *Lancet Neurology*. **2006**, *5*, 525-535.
[38] L. V. Kalia, A. E. Lang, *Lancet*. **2015**, *386*, 896-912.
[39] M. Zaaroor, A. Sinai, D. Goldsher, A. Eran, M. Nassar, I. Schlesinger, J Neurosurg **2018**, *128*, 202-210.

[40] M. H. Polymeropoulos, C. Lavedan, E. Leroy, S. E. Ide, A. Dehejia, A. Dutra, B. Pike, H. Root, J. Rubenstein, R. Boyer, E. S. Stenroos, S. Chandrasekharappa, A. Athanassiadou, T. Papapetropoulos, W. G. Johnson, A. M. Lazzarini, R. C. Duvoisin, G. Di Iorio, L. I. Golbe, R. L. Nussbaum, *Science*. **1997**, *276*, 2045-2047.
[41] A. B. Singleton, M. Farrer, J. Johnson, A. Singleton, S. Hague, J. Kachergus, M. Hulihan, T. Peuralinna, A. Dutra, R. Nussbaum, S. Lincoln, A. Crawley, M. Hanson, D. Maraganore, C. Adler, M. R. Cookson, M. Muenter, M.

Baptista, D. Miller, J. Blancato, J. Hardy, K. Gwinn-Hardy, *Science*. **2003**, *302*, 841-841.

[42] O. Neudorfer, N. Giladi, D. Elstein, A. Abrahamov, T. Turezkite, E. Aghai, A. Reches, B. Bembi, A. Zimran, *QJM*. **1996**, *89*, 691695.

[43] J. Mitsui, I. Mizuta, A. Toyoda, R. Ashida, Y.Takahashi, J. Goto, Y. Fukuda, H. Date, A. Iwata, M. Yamamoto, N. Hattori, M. Murata, T. Toda, S. Tsuji, *Arch. Neurol.* **2009**, *66*, 571-577.

[44] J. Aharon-Peretz, H. Rosenbaum, R. Gershoni-Baruch, *N Engl J Med*. **2004**, *351*, 1972-1879.

[45] A. Lwin, E. Orvisky, O. Goker-Alpan, M. E. LaMarca, E. Sidransky, *Mol Genet Metab*. **2004**, 81, 70-73.

[46] O. Goker-Alpan, G. Lopez, J. Vithayathil, J. Davis, M. Hallett, E. Sidransky, *Arch Neurol*. **2008**, *65*, 1353-1360.

[47] J. Bras, C. Paisan-Ruiz, R. Guerreiro, M. H. Ribeiro, A. Morgadinho, C. Januario, E. Sidransky, C. Oliveira, A. Singleton, *Neurobiol Aging*. **2009**, *30*, 1515-1532.

[48] E. Sidransky, M. A. Nalls, J. O. Aasly, J. Aharon-Peretz, G. Annesi, E. R. Barbosa , *et al*. *N Engl J Med*. **2009**, *361*, 1651-1712».

[49] P. Giraldo, J. L.Capablo, P. Alfonso, B. Garcia-Rodriguez, P. Latre, P. Irun, A. Saenz de Cabezon, M. Pocovi, *J Inherit Metab Dis*. **2011**, *34*, 781-788.

[50] K. Kalinderi, S. Bostantjopoulou, C. Paisan-Ruiz, Z. Katsarou, J. Hardy, L. Fidani, *Neurosci Lett*. **2009**, *452*, 87-96.

[51] A. Velayati, W. H. Yu, E. Sidransky, *Curr. Neurol. Neurosci. Rep*. **2010**, *10*, 190-198.

[52] L. Alvarez-Erviti, M. C. Rodriguez-Oroz, J. M. Cooper, C. Caballero, I. Ferrer, J. A. Obeso, A. H. V. Schapira, *Arch. Neurol*. **2010**, *67*, 1464-1472.

[53] D. C. Schondorf, M. Aureli, F. E. McAllister, C. J. Hindley, F. Mayer, B. Schmid, S. P. Sardi, M. Valsecchi, S. Hoffmann, L. K. Schwarz , U. Hedrich, D. Berg, L. S. Shihabuddin, J. Hu, J. Pruszak, S. P. Gygi, S. Sonnino, T. Gasser, M. Deleidi, *Nat Commun*. **2014**, *5*, 4028-4038.

[54] H. J. R. Fernandes, E. M. Hartfield, H. C. Christian, E. Emmanoulidou, Y. Zheng, H. Booth, H. Bogetofte, C. Lang, B. J. Ryan, S. P. Sardi, J. Badger, J. Vowles, S. Evetts, G. K. Tofaris, K. Vekrellis, K. Talbot, M. T. Hu, W. James, S. A. Cowley, R. Wade-Martins, *Stem Cell Reports*. **2016**, *6*, 342-356.

[55] J. Magalhaes, M. E. Gegg, A. Migdalska-Richards, M. K. Doherty, P. D. Whitfield, A. H. V. Schapira, *Hum Mol Genet*. **2016**, *25*, 3432-3445.

[56] E. J. Bae, N. Y. Yang, M. Song, C. S. Lee, J. S. Lee, B. C. Jung, H. J. Lee, S. Kim, E. Masliah, S. P. Sardi, L. Seung-Jae, *Nat Commun*. **2014**, *5*, 4755-4770.

[57] K. J. Kinghorn, S. Gronke, J. I. Castillo-Quan, N. S. Woodling, L. Li, E. Sirka, M. Gegg, K. Mills, J. Hardy, I. Bjedov, L. Partridge, *J Neurosci*. **2016**, *36*, 11654-11670.

[58] Y. H. Xu, Y. Sun, H. Ran, B. Quinn, D. Witte, G. A. Grabowski, *Mol Genet Metab*. **2011**, *102*, 436-447.
[59] G. Maor, O. Cabasso, O. Krivoruk, J. Rodriguez, H. Steller, D. Segal, M. Horowitz, *Hum Mol Genet*. **2016**, *25*, 2712-2727.
[60] M. E. Gegg, L. Sweet, B. H. Wang, L. S. Shihabuddin, S. P. Sardi, A. H. V. Schapira, *Mov. Disord*. **2015**, *30*, 1085-1094.
[61] S. P. Sardi, P. Singh, S. H. Cheng, L. S. Shihabuddin, M. G. Schlossmacher, *Neurodegenerative Dis.* **2012**, *10*, 195-202.
[62] B. S. Kilpatrick, J. Magalhaes, M. S. Beavan, A. McNeill, M. E. Gegg, M. W. J. Cleeter, D. Bloor-Young, G. C. Churchill, M. R. Duchen, A. H. Schapira, S. Patel, *Cell Calcium.* **2016**, *59*, 12-20.
[63] J. R. Mazzulli, Y. H. Xu, Y. Sun, A. L. Knight, P. J. McLean, G. A. Caldwell, E. Sidransky, G. A. Grabowski, D. Krainc, *Cell*. **2011**, *146*, 37-52.
[64] L. D. Osellame, A. A. Rahim, I. P. Hargreaves, M. E. Gegg, A. Richard-Londt, S. Brandner, S. N. Waddington, A. H. V. Schapira, M. R. Duchen, *Cell Metab*. **2013**, *17*, 941-953.
[65] H. Li, A. Ham, T. C. Ma, S-H. Kuo, E. Kanter, D. Kim, H. S. Ko, Y. Quan, S. P.Sardi, A. Li, O. Arancio, U. J. Kang, D. Sulzer, G. Tang, *Autophagy*. **2019**, *15*, 113-130.
[66] M. Suzuki, N. Fujikake, T. Takeuchi, A. Kohyama-Koganeya, K. Nakajima, Y. Hirabayashi, K. Wada, Y. Nagai, *Hum. Mol. Genet*. **2015**, *24*, 6675-6686.
[67] E. M. Rocha, G. A. Smith, E. Park, H. Cao, E. Brown, P. Hallett, O. Isacson, *Ann Clin Transl Neurol*. **2015**, *2*, 433–438.
[68] Y. V. Taguchi, J. Liu, J. Ruan, J. Pacheco, X. Zhang, J. Abbasi, J. Keutzer, P. K. Mistry, S. S Chandra, *J Neurosci*. **2017**, *37*, 9617-9631.
[69] G. Liu, M. Chen, N. Mi, W. Yang, X. Li, P. Wang, N. Yin, Y. Li, F. Yue, P. Chan, *Neurobiol Aging*. **2015**, *36*, 2649-2659.
[70] K. E. Murphy, A. M. Gysbers, S. K. Abbott, N. Tayebi, W. S. Kim, E. Sidransky, A. Cooper, B. Garner, G. M. Halliday, *Brain*. **2014**, *137*, 834-848.
[71] E. Colla, P. Coune, Y. Liu, O. Pletnikova, J. C. Troncoso, T. Iwatsubo, B. L. Schneider, M. K. Lee, *J Neurosci*. **2012**, *32*, 3306-3320.
[72] A. Bellucci, L. Navarria, M. Zaltieri, E. Falarti, S. Bodei, S. Sigala, L. Battistin, M. Spillantini, C. Missale, P. Spano, *J Neurochem*. **2011**, *116*, 588–605.
[73] P. Compain, O.R. Martin (Eds.), Iminosugars: From Synthesis to Therapeutic Applications, Wiley VCH, New York, **2007**.
[74] Y. Sun, H. Ran, B. Liou, B. Quinn, M. Zamzow, W. Zhang, J. Bielawski, K. Kitatani, K. D. R. Setchell, Y. A. Hannun, G.A. Grabowski, *PlosOne*. **2011**, *6*, e19037.
[75] P. Alfonso, S. Pampin, J. Estrada, J. C. Rodriguez-Rey, P. Giraldo, J. Sancho, M. Pocovi, *Blood Cells Mol*. *Dis.* **2005**, *35*, 268-276.

[76] A. R. Sawker, W.-C. Cheng, E. Beutler, C. H. Wong, W. E. Balch, J. W. Kelly, *Proc. Natl. Acad. Sci*. **2002**, *99*, 15428-15433.
[77] B. Brumshtein, H. M. Greenblatt, T. D. Butters, Y. Shaaltlel, D. Avlezer, I. Silman, A. H. Futerman, J. L. Sussman, *J. Biol. Chem*. **2007**, *282*, 29052-29058.
[78] C. Kuriyama, O. Kamiyama, K. Ikeda, F. Sanae, A. Kato, I. Adachi, T. Imahori, H. Takahata, T. Okamoto, N. Asano, *Bioorg. Med. Chem*. **2008**, *16*, 7330-7336.
[79] N. Asano, K. Ikeda, L. Yu, A. Kato, K. Takebayashi, I. Adachi, I. Kato, H. Ouchi, H. Takahata, G. W. J. Fleet, Tetrahedron Asymmetry. **2005**, *16*, 223-229.
[80] X. Zhu, K. A. Sheth, S. Li, H.-H. Chang, J.-Q. Fan, *Angew. Chem. Int. Ed. Engl*. **2005**, *44*, 7450-7453.
[81] H. H. Chang, N. Asano, S. Ishii, Y. Ichikawa, J. Q. Fan, *FEBS J.* **2006**, 4082-4092.
[82] R. A. Steet, S. Chung, B. Wustman, A. Powe, H. Do, S. A. Kornfeld, *Proc. Natl. Acad. Sci*. U.S.A. **2006**, *103*, 13813-13818.
[83] Amicus Therapeutics, Inc.: WO2005046612 (**2005**).
[84] T. Hill, M. B. Tropak, D. Mahuran, S. W. Withers, *ChemBioChem*. **2011**, *12*, 2151-2154.
[85] P. Compain, O. R. Martin, C. Boucheron, G. Godin, L. Yu, K. Ikeda, N. Asano, *ChemBioChem*. **2006**, *7*, 1356-1359.
[86] S. Pushpakom, F. Iorio, P. A. Eyers, K. J. Escott, S. Hopper, A. Wells, A. Doig, T. Guilliams, J. Latimer, C. McNamee, A. Norris, P. Sanseau, D. Cavalla, M. Pirmohamed, *Nat Rev Drug Discov*. **2019**, *18*, 41-58.
[87] D. Athauda, T. Foltynie, *CNS Drugs*. **2018**, *32*, 747-761.
[88] T. Suzuki, M. Shimoda, K. Ito, S. Hanai, H. Aizawa, T. Kato, K. Kawasaki, T. Yamaguchi, H. D. Ryoo, N. Goto-Inoue, M. Setou, S. Tsuji, N. Ishida, *PLoS One.* **2013**, *8*, e69147.
[89] A. Sanchez-Martinez, M. Beavan, M. E. Gegg, K. Y. Chau, A. J. Whitworth, A. H. V. Schapira, *Sci Rep*. **2016**, *6*, 31380-31392.
[90] A. Migdalska-Richards, L. Daly, E. Bezard, A. H. V. Schapira, *Ann Neurol.* **2016**, *80*, 766-775.
[91] F. Richter, S.M. Fleming, M. Watson, V. Lemesre, L. Pellegrino, B. Ranes, C. Zhu, F. Mortazavi, C. K. Mulligan, P. C. Sioshansi, S. Hean, K. De La Rosa, R. Khanna, J. Flanagan, D. J. Lockhart, B. A. Wustman, S. W. Clark, M. F. Chesselet, *Neuronotherapeutics*. **2014**, *11*, 840-856.
[92] R. P. Tripathi, S. S. Verma, J. Pandey, V. K. Tiwari, *Curr. Org. Chem*. **2008**, *12*, 1093-1115.
[93] C. Claver, I. Penafiel, M. Urrutigoity, P. Kalck In Science of Synthesis, Catalytic Reduction in Organic Synthesis, Vol. 2, (Ed.: J. G. De Vries), Thieme, **2018**.

[94] E. W. Baxter, A. B. Reitz, *Organic Reaction*. **2001**, *59*, 1-714.
[95] R. F. Borch, M. D. Bernstein, H, D, Durst, *J. Am. Che. Soc*. **1971**, *93*, 2897-2904.
[96] E. Podyacheva, O. I. Afanasyev, A. A. Tsygankov, M. Makarova, D. Chusov, *Synthesis*. **2019**, *51*, 2667-2677.
[97] R. O. Hutchins, M. K. Hutchins, M. L. Crawley, *e-EROS Encyclopedia of Reagents for Organic Synthesis*. **2007**, 1-9.
[98] G. W. Gribble, A. F. Abdel-Magid, *e-EROS Encyclopedia of Reagents for Organic Synthesis*. **2007**, 1-11.
[99] O. I. Afanasyev, E. Kuchuk, D. L. Usanov, D. Chusov, *Chem. Rev*. **2019**, *119*, 11857-11911.
[100] B. G. Winchester, *Tetrahedron: Asymmetry*. **2009**, *20*, 645-651.
[101] T. M. Gloster, G. J. Davies, *Org. Biomol. Chem*. **2010**, *8*, 305-320.
[102] A. E. Stütz, T. M. Wrodnigg, *Adv. Carbohydr. Chem. Biochem*. **2011**, *66*, 187-298.
[103] G. Horne, *Top. Med. Chem*. **2014**, *12*, 23-51.
[104] N. F. Bras, N. M. F. S. A. Cerqueira, M. J. Ramos, P. A. Fernandes, *Expert Opin. Ther. Pat*. **2014**, *24*, 857-874.
[105] G. Horne, F. X. Wilson, J. Tinsley, D. H. Williams, R. Storer, *Drug Discov*. **2011**, *16*, 107-118.
[106] R. A. Dwek, T. D. Butters, F. M. Platt, N. Zitzmann, *Nat. Rev. Drug Discov*. **2002**, *1*, 65–75.
[107] L. J. Scott, C. M. Spencer, *Drugs*. **2000**, *59*, 521-549.
[108] T. D. Butters, R. A. Dwek, F. M. Platt, *Chem. Rev.* **2000**, *100*, 4683-4696.
[109] T. M. Cox, J. M. F. G. Aerts, G. Andria, M. Beck, N. Belmatoug, B. Bembi, R. Chertkoff, S. Vom Dahl, D. Elstein, A. Erikson, M. Giralt, R. Heitner, C. Hollak, N. Hrebicek, S. Lewis, A. Mehta, G. M. Pastores, A. Rolfs, M. C. Sa Miranda, A. Zimran, *J. Inherit. Metab. Dis*. **2003**, *26*, 513-526.
[110] G. M. Pastores, N. L. Barnett, E. H. Kolodny, *Clinical Therapeutics*. **2005**, *27*, 1215-1227.
[111] E. H. McCafferty, L. J. Scott, *Drugs*. **2019**, *79*, 543-554.
[112] H. Yoda, *Curr. Org. Chem*. **2002**, *6*, 223-243.
[113] T. Ayad, Y. Genisson, M. Baltas, *Curr. Org. Chem*. **2004**, *8*, 1211-1233.
[114] S. G. Pyne, M. Tang, *Curr. Org. Chem*. **2005**, *9*, 1393-1418.
[115] B. G. Davis, *Tetrahedron: Asymmetry*. **2009**, *20*, 652-671.
[116] A. Brandi, F. Cardona, S. Cicchi, F. M. Cordero, A. Goti, *Chem. Eur. J*. **2009**, *15*, 7808-7821.
[117] B. L. Stocker, E. D. Dangerfield, A. L. Win-Mason, G. W. Haslett, M. S. M. Timmer, *Eur. J. Org. Chem*. **2010**, *9*, 1615-1637.
[118] T. Ritthiwigrom, C. W. G. Au, S. G. Pyne, *Curr. Org. Synth*. **2012**, *9*, 583-612.
[119] R. Lahiri, A. A. Ansari, Y. D. Vankar, *Chem. Soc. Rev*. **2013**, *42*, 5102-5118.

[120] A. Wood, K. L. Prichard, Z. Clarke, T. A. Houston, G. W. J. Fleet, N. I. Simone, *Eur. J. Org. Chem*. **2018**, 6812-6829.
[121] K. L. Prichard, N. O'Brien, M. Ghorbani, A. Wood, E. Barnes, A. Kato, T. A. Houston, M. I. Simone, *Eur. J. Org. Chem*. **2018**, 6830-6842.
[122] C. Dehoux-Baudoin, Y. Génisson, *Eur. J. Org. Chem*. **2019**, 4765-4777.
[123] K. Prichard, D. Campkin, N. O'Brien, A. Kato, G. W. J. Fleet, M. I. Simone, *Chem. Biol. Drug Des*. **2018**, *92*, 1171-1197.
[124] P .R. Markad, D. P. Sonawane, S. Ghosh, B. A. Chopade, N. Kumbhar, T. Louat, J. Herman, M. Waer, P. Herdewijn, D. D. Dhavale, *Bioorg. Med. Chem*. **2014**, *22*, 5776-5782.
[125] D. D. Dhavale, K. S. Ajish Kumar, V. D. Chaudhari, T. Sharma, S. G. Sabharwal, J. PrakashaReddy, *Org. Biomol. Chem*. **2005**, *3*, 3720-3726.
[126] J. A. Castillo, J. Calveras, J. Casas, M. Mitjans, M. P. Vinardell, T. Parella, T. Inoue, G. A. Sprenger, J. Joglar, P. Clapés, *Org. Lett.* **2006**, *8*, 6067–6070.
[127] A. L. Concia, C. Lozano, J. A. Castillo, T. Parella, J. Joglar, P. Clapés, Chem. Eur. J. 2009, 15, 3808–3816.
[128] M. Sugiyama, Z. Hong, P. H. Liang, S. M. Dean, L. J. Whalen, W. A. Greenberg, C.-H. Wong, *J. Am. Chem. Soc*. **2007**, *129*, 14811–14817.
[129] C. Nicolas, R. Pluta, M. Pasternak-Suder, O. R. Martin, J. Mlynarski, *Eur. J. Org. Chem*. **2013**, *7*, 1296-1305.
[130] S. Baś, R. Kusy, M. Pasternak-Suder, C. Nicolas, J. Mlynarski, O. R. Martin, *Org. Biomol. Chem*. **2018**, *16*, 1118-1125.
[131] G. Masson, P. Compain, O.R. Martin, *Org. Lett*. **2000**, *2*, 2971-2974.
[132] G. Godin, P. Compain, G. Masson, O. R. Martin, *J. Org. Chem*. **2002**, *67*, 6960-6970.
[133] A. Bordier, P. Compain, O. R. Martin, K. Ikeda, N. Asano, *Tetrahedron Asymmetry*. **2003**, *14*, 47-51.
[134] G. Godin, P. Compain, O. R. Martin, *Org. Lett*. **2003**, *5*, 3269-3272.
[135] F. Oulaïdi, E. Gallienne, P. Compain, O. R. Martin, *Tetrahedron Asymmetry*. **2011**, *22*, 609-612.
[136] A. Biela-Banaš, E. Gallienne, S. Front, O. R. Martin, *Tetrahedron Lett*. **2014**, *55*, 838-841.
[137] Y. Ichikawa, Y. Igarashi, M. Ichikawa, Y. Suhara, *J. Am. Chem. Soc*. **1998**, *120*, 3007-3018.
[138] Y. Igarashi, M. Ichikawa, Y. Ichikawa, *Bioorg. Med. Chem. Lett*. **1996**, *6*, 553-558.
[139] M. Ichikawa, Y. Igarashi, Y. Ichikawa, *Tetrahedron Lett*. **1995**, *36*, 1767-1770.
[140] G. Le Bouc, C. Thomassigny, C. Greck, *Tetrahedron: Asymmetry*. **2006**, *17*, 2006-2014.
[141] C. M. Pedersen, M. Bols, *Org. Biomol. Chem*. **2017**, *15*, 1164-1173.

[142] R. Lucas, P. Balbuena, J. C. Errey, M. A. Squire, S. S. Gurcha, M. McNeil, G. S. Besra, B. G. Davis, *ChemBioChem*. **2008**, *9*, 2197-2199.

[143] M. R. McNeil, P. J. Brennan, *Res. Microbiol*. **1991**, *142*, 451-46.

[144] S. Dharuman, Y. Wang, D. Crich, *Carbohydrate Res*. **2016**, *419*, 29-32.

[145] Y. Blériot, D. Gretzke, T. M. Krülle, T. D. Butters, R. A. Dwek, R. J. Nash, N. Asano, G. W. J. Fleet, *Carbohydrate Research*. **2005**, *340*, 2713-2718.

[146] N. J. Pawar, V. S. Parihar, S. T. Chavan, R. Joshi, P. V. Joshi, S. G. Sabharwal, V. G. Puranik, D. D. Dhavale, *J. Org. Chem*. **2012**, *77*, 7873-7882.

[147] N. T. Patil, S. John, S. G. Sabharwal, D. D. Dhavale, *Bioorg. Med. Chem*. **2002**, *10*, 2155-2160.

[148] A. F. G. Glawar, S. F. Jenkinson, S. J. Newberry, A. L. Thompson, S. Nakagawa, A. Yoshihara, K. Akimitsu, K. Izumori, T. D. Butters, A. Kato, G. W. J. Fleet, *Org. Biomol. Chem*. **2013**, *11*, 6886-6899.

[149] S. Mirabella, G. Fibbi, C. Matassini, C. Faggi, A. Goti, F. Cardona, *Org. Biomol. Chem*. **2017**, *15*, 9121-9126.

[150] F. Cardona, A. Goti, C. Parmeggiani, P. Parenti, M. Forcella, P. Fusi, L. Cipolla, S. M. Roberts, G. J. Davies, T. M. Gloster, *Chem. Commun*. **2010**, *46*, 2629-2631.

[151] C. Bonaccini, M. Chioccioli. C. Parmeggiani, F. Cardona, D. Lo Re, G. Soldaini, P. Vogel, C. Bello, A. Goti, P. Gratteri, *Eur. J. Org. Chem*. **2010**, 5574-5585.

[152] D. Bini, M. Forcella, L. Cipolla, P. Fusi, C. Matassini, F. Cardona, *Eur. J. Org. Chem*. **2011**, 3995-4000.

[153] C. Parmeggiani, F. Cardona, L. Giusti, H.-U. Reissig, A. Goti, *Chem. Eur. J*. **2013**, *19*, 10595-10604.

[154] G. D'Adamio, A. Sgambato, M. Forcella, S. Caccia, C. Parmeggiani, M. Casartelli, P. Parenti, D. Bini, L. Cipolla, P. Fusi, F. Cardona, *Org. Biomol. Chem*. **2015**, *13*, 896-892.

[155] G. D'Adamio, M. Forcella, P. Fusi, P. Parenti, C. Matassini, X. Ferhati, C. Vanni, F. Cardona, *Molecules***. 2018**, *23*, 436-453.

[156] X. Ferhati, C. Matassini, M. G. Fabbrini, A. Goti, A. Morrone, F. Cardona, A. J. Moreno-Vargas, P. Paoli, *Bioorg. Chem*. **2019**, *87*, 534-549.

[157] F. Clemente, C. Matassini, A. Goti, A. Morrone, P. Paoli, F. Cardona, *ACS Med. Chem. Lett*. **2019**, *10*, 621-626.

[158] F. Clemente, C. Matassini, C. Faggi, S. Giachetti, C. Cresti, A. Morrone, P. Paoli, A. Goti, M. Martínez Bailén, F. Cardona, *Bioorg. Chem*. **2020**, *98*, 103740-103763.

[159] C. Parmeggiani, S. Catarzi, C. Matassini, G. D'Adamio, A. Morrone, A. Goti, P. Paoli, F. Cardona, *ChemBioChem*. **2015**, *16*, 2054-2064.

[160] M. Lombardo, C. Trombini, *Synthesis*. **2000**, 759-774.

[161] P. Merino, *C. R. Chim*. **2005**, *8*, 775-788.

[162] P. Merino, S. Franco, F. L. Merchan, T. Tejero, *Synlett*. **2000**, 442-454.

[163] P. Merino, S. Anoro, S. Franco, J. M. Gascon, V. Martin, F. L. Merchan, J. Revuelta, T. Tejero, V. Tuñon, *Synth. Commun*. **2000**, *30*, 2989-3021.

[164] E. Marca, I. Delso, T. Tejero, J. T. Vázquez, R. L. Dorta, P. Merino, *Tetrahedron Lett*. **2009**, *50*, 7152-7155.

[165] C. Parmeggiani, C. Matassini, F. Cardona, A. Goti, *Synthesis*. **2017**, *49*, 2890-2900.

[166] J. Blanz, P. Saftig, *J. Neurochem*. **2016**, *139*, 198-215.

[167] E. D. Goddard-Borger, B. Fiege, E. M. Kwan, S. G. Withers, *ChemBioChem*. **2011**, *12*, 1703-1711.

[168] L. F. Mackenzie, Q. Wang, R. A. J. Warren, S. G. Withers, *J. Am. Chem. Soc*. **1998**, *120*, 5583-5584.

[169] B. L. Cantarel, P. M. Coutinho, C. Rancurel, T. Bernard, V. Lombard, B. Henrissat, *Nucleic Acid Res.* **2009**, *37*, 233-238.

[170] S. Front, A. Biela-Banás, P. Burda, D. Ballhausen, K. Higaki, A. Caciotti, A. Morrone, J. Charollais-Thoenig, E. Gallienne, S. Demotz, O. R. Martin, *Eur. J. Med. Chem*. **2017**, *126*, 160-170.

[171] S. Front, S. Almeida, V. Zoete, J. Charollais-Thoenig, E. Gallienne, C. Marmy, V. Pilloud, R. Martin, T. Wood, O. R. Martin, S. Demotz, *Bioorg. Med. Chem*. **2018**, *26*, 5462-5469.

[172] G. D'Adamio, A. Goti, C. Parmeggiani, E. Moreno-Clavijo, I. Robina, F. Cardona, *Eur. J. Org. Chem*. **2011**, 7155-7162.

[173] D. Martella, F. Cardona, C. Parmeggiani, F. Franco, J.A. Tamayo, I. Robina, E. Moreno-Clavijo, A. J. Moreno-Vargas, A. Goti, *Eur. J. Org. Chem*. **2013**, 4047-4056.

[174] C. Matassini, S. Mirabella, A. Goti, F. Cardona, *Eur. J. Org. Chem*. **2012**, *21*, 3920-3924.

[175] C. Matassini, S. Mirabella, X. Ferhati, C. Faggi, I. Robina, A. Goti, E. M. Clavijo, A. J. M. Vargas, F. Cardona, *Eur. J. Org. Chem*. **2014**, *25*, 5419-5432.

[176] P. Merino, E. Castillo, F. L. Merchán, T. Tejero, *Tetrahedron: Asymmetry*. **1997**, *8*, 1725-1729.

[177] P. Merino, E. Castillo, S. Franco, F. L. Merchán, T. Tejero, *Tetrahedron*. **1998**, *54*, 12301-12322.

[178] A. Dondoni, S. Franco, F. Junquera, F.L. Merchán, P. Merino, T. Tejero, V. Bertolasi, *Chem. Eur. J.* **1995**, *1*, 505–520.

[179] A. Dondoni, F. Junquera, F. L. Merchán, P. Merino, M.-C. Scherrmann, T. Tejero, *J. Org. Chem.* **1997**, *62*, 5484-5496.

[180] F.-E. Chen, J.-F. Zhao, F.J. Xiong, B. Xie, P. Zhang, *Carbohydr. Res*. **2007**, *342*, 2461-2464.

[181] C. Matassini, C. Parmeggiani, F. Cardona, A. Goti, *Org. Lett*. **2015**, *17*, 4082-4085.

[182] C. Matassini, F. Cardona, *Chimia*. **2017**, *71*, 558-561.
[183] C. Matassini, S. Mirabella, A. Goti, I. Robina, A.J. Moreno-Vargas, F. Cardona, Beilstein J. Org. Chem. **2015**, *11*, 2631-2640.
[184] J.-Q. Fan, *Trends Pharmacol. Sci*. **2003**, *24*, 355-369.
[185] A. Joosten, C. Decroocq, J. de Sousa, J.P. Schneider, E. Etamé, A. Bodlenner, T. D. Butters, P. Compain, *ChemBioChem*. **2014**, *15*, 309-319.
[186] A. Yu, A. R. Sawkar, L. J. Whalen, C.-H. Wong, J. W. Kelly, *J. Med. Chem*. **2007**, *50*, 94-100.
[187] L. Yu, K. Ikeda, A. Kato, I. Adachi, G. Godin, P. Compain, O. Martin, N. Asano, *Bioorg. Med. Chem*. **2006**, *14*, 7736-7744.
[188] D. L. Ston, N. Tayebi, E. Orvisky, B. Stubblefield, V. Madike, E. Sidransky, *HumanMutat*. **2000**, *15*, 181-188.
[189] Y. Sun, B. Liou, Y.-H. Xu, B. Quinn, W. Zhang, R. Hamler, K. D. R. Setchell, G. A. Grabowski, *J. Biol. Chem*. **2012**, *287*, 4275-4287.
[190] R. Khanna, E. R. Benjamin, L. Pellegrino, A. Schilling, B. A. Rigat, R. Soska, H. Nafar, B. E. Ranes, J. Feng, Y. Lun, A. C. Powe, D. J. Palling, B. A. Wustman, R. Schiffmann, D. J. Mahuran, D. J. Lockhart, K. J. Valenzano, *FEBS J*. **2010**, *277*, 1618-1638.
[191] E. D. Goddard-Borger, M. B. Tropak, S. Yonekawa, C. Tysoe, D. J. Mahuran, S. G. Withers, J. *Med. Chem*. **2012**, *55*, 2737-2745.
[192] A. J. Olson, *J. Comput. Chem*. **2009**, *16*, 2785-2791.
[193] R. L. Lieberman, B. A. Wustman, P. Huertas, A. C. Jr. Powe, C. W. Pine, R. Khanna, M. G. Schlossmacher, D. Ringe, G. A. Petsko, *Nat. Chem. Biol*. **2007**, *3*, 101-107.
[194] A. Kato, I. Nakagome, S. Nakagawa, Y. Koike, R. J. Nash, I. Adachi, S. Hirono, *Bioorg. Med. Chem*. **2014**, *22*, 2435-2441.
[195] A. Kato, I. Nakagome, K. Sato, A. Yamamoto, I. Adachi, R.J. Nash, G. W. J. Fleet, Y. Natori, Y. Watanabe, T. Imahori, Y. Yoshimura, H. Takahatae, S. Hirono, *Org. Biomol. Chem*. **2016**, *14*, 1039-1048.
[196] N. T. Anh, O. Eisenstein, *Nouv. J. Chim*. **1977**, *1*, 61-70.
[197] J. P. Battioni, W. Chodkiewicz, *Chem. Inf*. **1978**, *9*, 320-328.
[198] F. Cardona, M. Bonanni, G. Soldaini, A. Goti, *ChemSusChem*. **2008**, *1*, 327-332.
[199] W. A. Herrmann, R. W. Fischer, D. W. Marz, *Angew. Chem*. **1991**, *103*, 1706-1709.
[200] W. A. Herrmann, R. W. Fischer, D. W. Marz, *Angew. Chem. Int. Ed. Engl*. **1991**, *30*, 1638-1641.
[201] W. A. Herrmann, R. W. Fischer, M. U. Rauch, W. Scherer, *J. Mol. Catal*. **1994**, *86*, 243-266.
[202] W. A. Herrmann, F. E. Klhn, *Acc. Chem. Res*. **1997**, *30*, 169-180.
[203] J. H. Espenson, *Chem. Commun*. **1999**, 479-488.
[204] G. Soldaini, F. Cardona, A. Goti, *Org. Lett*. **2005**, *7*, 725-728.

[205] M. R. Stammer, J. B. F. N. Engberts, T. J. de Boer, *Rec. Trav. Chim.* **1970**, *89*, 169-174.

[206] S. Cicchi, M. Bonanni, F. Cardona, J. Revuelta, A. Goti, *Org. Lett*. **2003**, 5, 1773-1776.

[207] C. Matassini, M. Bonanni, M. Marradi, S. Cicchi, A. Goti, *Eur. J. Inorg. Chem*. **2020**, 1106-1113.

[208] H.R. Mellor, F. M. Platt, R. A Dwek, T.D. Butters, *Biochem. J.* **2003**, *374*, 307-314.

[209] F. Clemente, C. Matassini, F. Cardona, *Eur. J. Org. Chem*. **2020**, 4447-4462.

[210] C. Santos, F. Stauffert, S. Ballereau, C. Dehoux, F. Rodriguez, A. Bodlenner, P. Compain, Y. Génisson, *Bioorg. Med. Chem*. **2017**, *25*, 1984-1989.

[211] N. Lamb, S. R. Abrams, *Can. J. Chem*. **1990**, *68*, 1151-1162.

[212] F. Rocquet, J.-P. Battioni, M.-L. Capmau, W. Chodkiewicz, *C. R. Acad. Sci*. **1969**, *268*, 1449-1452.

[213] K. Ando, K. N. Houk, J. Busch, A. Menassé, U. Séquin, *J. Org. Chem*. **1998**, *63*, 1761-1766.

[214] M. Cherest, H. Felkin, *Tetrahedron Lett*. **1968**, 2199-2204.

[215] F. Oulaidi, S. Front-Deschamps, E. Gallienne, E. Lesellier, K. Ikeda, N. Asano, P. Compain, O. R. Martin, *ChemMedChem*. **2011**, *6*, 353-361.

[216] H. R. Mellor, J. Nolan, L. Pickering, M.R. Wormald, F. M. Platt, R. A. Dwek, G. W. J. Fleet, T. D. Butters *Biochem. J.* **2002**, *366*, 225-233.

[217] K.-J. Xiao, J.-M. Luo, K.-Y. Ye, Y. Wang, P.-Q. Huang, *Angew. Chem. Int. Ed*. **2010**, *49*, 3037-3040.

[218] M. S. DeClue, K. K. Baldridge, P. Kast, D. Hilvert, *J. Am. Chem. Soc*. **2006**, *128*, 2043-2051.

[219] S. Handa, H. G. Floss, *ChemComm*. **1997**, *2*, 153-154.

[220] M. Demerec, B. P. Kaufman, Drosophila Guide: Introduction to the genetics and cytology of Drosophila melanogaster. Dept. Genet., Cold Spring Harbor, New York., **1943**.

[221] J. A. Fischer, E. Giniger, T. Maniatis, M. Ptashne, *Nature*. **1988**, *332*, 853-856.

[222] J. B. Duffy, *Genesis*. **2002**, *34*, 1-15.

[223] M. M. K. Muqit, M. B. Feany, *Nature Reviews Neuroscience*. **2002**, *3*, 237-243.

[224] B. Lu, *Apoptosis*. **2009**, *14*, 1008-1028.

[225] R. J. West, R. Furmston, C. A. Williams, C. J. Elliott, *Parkinsons Dis*. **2015**, 381281-381292.

[226] M.-F. Chesselet, F. Richter , C. Zhu, I. Magen, M. B. Watson, S. R. Subramaniam, *Neurotherapeutics*. **2012**, *9*, 297-314.

[227] J. Diot, M.I. García-Moreno, S.G. Gouin, C. Ortiz-Mellet, K. Haupy, J. Kovensky, *Org. Biomol. Chem.* **2009**, *7*, 357–363.
[228] N. Kanfar, E. Bartolami, R. Zelli, A. Marra, J.-Y. Winum, S. Ulrich, P. Dumy, *Org. Biomol. Chem*. **2015**, *13*, 9894-9906.
[229] S.-K. Choi, Synthetic Multivalent Molecules: Concepts And Biomedical Applications, John Wiley & Sons, Inc., Hoboken, New Jersey, **2004**.
[230] C. Matassini, C. Parmeggiani, F. Cardona, A. Goti, *Tetrahedron Letters.* **2016**, *57*, 5407-5415.
[231] F. Y. Choy, M. Woo, M. Potier, *Biochim. Biophys. Acta*. **1986**, *870*, 76-81.
[232] G. Dawson, J. C. Ellory, *Biochem. J.* **1985**, *226*, 283-288.
[233] P. G. Pentchev, R. O. Brady, S. R. Hibbert, A. E. Gal, D. Shapiro, *J. Biol. Chem*. **1973**, *248*, 5256-5261.
[234] P. M. Strasberg, J. A. Lowden, *J. Chromatogr*. **1983**, *261*, 419-422.
[235] H. C. Kolb, M. G. Finn, K. B. Sharpless, *Angew. Chem. Int. Ed*. **2001**, *40*, 2004-2021.
[236] C. W. Tornöe, C. Christensen, M. Meldal, *J. Org. Chem*. **2002**, *67*, 3057-3064.
[237] V. C. Rostovtsev, L. G. Green, V. V. Fokin, K. B. Sharpless, *Angew. Chem. Int. Ed*. **2002**, *41*, 2596-2599.
[238] C. Decroocq, D. Rodriguez-Lucena, K. Ikeda, N. Asano, P. Compain, *ChemBioChem*. **2012**, *13*, 661-664.
[239] C. Ornelas, J. Broichhagen, M. Week, *J. Am. Chem. Soc*. **2010**, *132*, 3923-3931.
[240] T. M. Jespersen, M. Bols, *Tetrahedron*. **1994**, *50*, 13449-13460.
[241] A. B. Reitz, E. W. Baxter, *Tetrahedron Lett*. **1990**, *31*, 6777-6780.
[242] E. W. Baxter, A. B. Reitz, *Bioorg. Med. Chem. Lett*. **1992**, *2*, 1419-1422.
[243] D. Cuffaro, M. Landi, F. D'Andrea, L. Guazzelli, *Carbohydrate Res*. **2019**, *482*, 107744-107751.
[244] A. J. Steiner, A. E. Stütz, C. A. Tarling, S. G. Withers, T. M. Wrodnigg, *Aust. J. Chem*. **2009**, *62*, 553-557.
[245] A. J. Steiner, A. E. Stütz, C. A. Tarling, S. G. Withers, T. M. Wrodnigg, *Carbohydr. Res*. **2007**, *342*, 1850-1858.
[246] T. Wennekes, R. J. B. H. N. van den Berg, W. Donker, G. A. van der Marel, A. Strijland, J. M. F. G. Aerts, H. S. Overkleeft, *J. Org. Chem*. **2007**, *72*, 1088-1097.
[247] B. Liu, J. van Mechelen, R. J. B. H. N. van den Berg, A. M. C. H. van den Nieuwendijk, J. M. F. G. Aerts, G. A. van der Marel, J. D. C. Codée, H. S. Overkleeft, *Eur. J. Org. Chem*. **2019**, 118-129.
[248] O. R. Martin, O. M. Saavedra, *Tetrahedron Lett*. **1995**, *36*, 799-802.
[249] O. R. Martin, O. M. Saavedra, F. Xie, L. Liu, S. Picasso, P. Vogel, H. Hizu, N. Asano, *Bioorg. Med. Chem*. **2001**, *9*, 1269-1278.

[250] S. Front, E. Gallienne, J. Charollais-Thoenig, S. Demotz, O. R. Martin, *ChemMedChem*. **2016**, *11*, 133-141.
[251] G. Malik, X. Guinchard, D. Crich, *Org. Lett*. **2012**, *14*, 596-599.
[252] G. Malik, A. Ferry, X. Guinchard, T. Cresteil, D. Crich, *Chem. Eur. J*. **2013**, *19*, 2168-2179.
[253] A. Ferry, G. Malik, X. Guinchard, V. Větvička, D. Crich, *J. Am. Chem. Soc*. **2014**, *136*, 14852-14857.
[254] Y Suzuki, A. Oshima, E. Namba, β-Galactosidase deficiency (β-galactosidosis) GM1 gangliosidosis and Morquio B disease, in: C.R. Scriver, A.L. Beaudet, W.S. Sly, D. Valle (Eds.), The Metabolic and Molecular Bases of Inherited Disease, McGraw-Hill, New York, **2001**.
[255] A. Caciotti, M. A. Donati, T. Bardelli, A. d'Azzo, G. Massai, L. Luciani, E. Zammarchi, A. Morrone, *Am. J. Pathol*. **2005**, *167*, 1689-1698.
[256] N. Brunetti-Pierri, F. Scaglia, *Mol. Genet. Metab*. **2008**, *94*, 391-396.
[257] A. Caciotti, S.C. Garman, Y. Rivera-Colòn, E. Procopio, S. Catarzi, L. Ferri, C. Guido, P. Martelli, R. Parini, D. Antuzzi, R. Battini, M. Sibilio, A. Simonati, E. Fontana, A. Salviati, G. Akinci, C. Cereda, C. Dionisi-Vici, F. Deodato, A. d'Amico,, A. d'Azzo, E. Bertini, M. Filocamo, M. Scarpa, M. di Rocco, C.J. Tifft, F. Ciani, S. Gasperini, E. Pasquini, R. Guerrini, M.A. Donati, A. Morrone, *Biochim. Biophys. Acta*. **2011**, *1812*, 782-790.
[258] C. Prat, O. Lemaire, J. Bret, L. Zabraniecki, B. Fournié, *Joint Bone Spine*. **2008**, *75*, 495-498.
[259] L. Tominaga, Y. Ogawa, M. Taniguchi, K. Ohno, J. Matsuda, A. Oshima, Y. Suzuki, E. Nanba, *Brain Dev.* **2001**, *23*, 284-287.
[260] J. Matsuda, O. Sukuzi, A. Oshima, Y. Yamamoto, A. Noguchi, K. Takimoto, M. Itoh, Y. Matsuzaki, Y. Yasuda, S. Ogawa, Y. Sakata, E. Nanba, K. Higaki, Y. Ogawa, L. Tominaga, K. Ohno, H. Iwasaki, H. Watanabe,, Y. Suzuki, *Proc. Natl. Acad. Sci*. **2003**, *100*, 15912-15917.
[261] . A. Rigat, M. B. Tropak, J. Buttner, E. Crushell, D. Benedict, J. W. Callahan, D. R. Martin, D. J. Mahuran, *Mol. Genet. Metab*. **2012**, *107*, 203-212.
[262] A. Biela-Banas, F. Oulaidi, S. Front, E. Gallienne, K. Ikeda-Obatake, N. Asano, D. A. Wenger, O. R. Martin. *ChemMedChem*. **2014**, *9*, 2647-2652.
[263] A. Siriwardena, D.P. Sonawane, O. P. Bande, P. R. Markad, S. Yonekawa, M. B. Tropak, S. Ghosh, B. A. Chopade, D. J. Mahuran, D. D. Dhavale, *J. Org. Chem*. **2014**, *79*, 398-4404.
[264] M. G. Davighi, F. Clemente, C. Matassini , A. Morrone, A. Goti, M. Martínez Bailén, F. Cardona, *Molecules*. **2020**, *25*, 4526-4549.

Part of this PhD thesis has been the object of publications and communications at conferences.

Publications

1. M. G. Davighi, **F. Clemente**, C. Matassini , A. Morrone, A. Goti, M. Martínez Bailén, F. Cardona, "Synthesis of "All-Cis" Trihydroxypiperidines from a Carbohydrate-Derived Ketone: Hints for the Design of New β-Gal and GCase Inhibitors". *Molecules*. **2020**, 25, 4526-4549. DOI:10.3390/molecules25194526. (IF: 3.267)
2. **F. Clemente**, C. Matassini, C. Faggi, S. Giachetti, C. Cresti, A. Morrone, P. Paoli, A. Goti, M. Martínez-Bailén F. Cardona, "Glucocerebrosidase (GCase) activity modulation by 2-alkyl trihydroxypiperidines: inhibition and pharmacological chaperoning". *Bioorg. Chem*. **2020**, *98*, 103740-103763. DOI: 10.1016/j.bioorg.2020.103740, (IF 4.831)
3. **F. Clemente**, C. Matassini, F. Cardona, "The Reductive Amination Routes to the Synthesis of Piperidine Iminosugars". *Eur. J. Org. Chem.* **2020**, DOI: 10.1002/ejoc.201901840. (IF 2.889)
4. **F. Clemente**, C. Matassini, A. Goti, A. Morrone, P. Paoli, F. Cardona,"Stereoselective synthesis of C-2 alkylated trihydroxypiperidines: effect of the chain length and the configuration at C-2 on their activity as Pharmacological Chaperones for Gaucher Disease", *ACS Med. Chem. Lett,* **2019**, *10*, 621-626. DOI:10.1021/acsmedchemlett.8b00602. (IF 3.975)

Chapters on Scientific Books

1. TARGETS IN HETEROCYCLIC SYSTEMS - Chemistry and Properties (THS): C. Matassini, **F. Clemente**, F. Cardona, "*THE DOUBLE REDUCTIVE AMINATION APPROACH TO THE SYNTHESIS OF POLYHYDROXYPIPERIDINES*", *THS Volume 23* (**2019**), cap. 14, pag. 283-301. Editori: Orazio A. Attanasi, Pedro Merino, Domenico Spinelli; pubblicato dalla Società Chimica Italiana. DOI: https://www.soc.chim.it/it/libri_collane/ths/vol_23_2019.

Communications

1. **F. Clemente**, C. Matassini, A. Goti and F. Cardona, Grignard addition onto a carbohydrate-derived nitrone en route to the synthesis of 2-substituted trihydroxypiperidines : a straightforward access to potential Pharmacological Chaperones for Gaucher disease, XXVIII International Conference on Organometallic Chemistry (Co.G.I.C.O.), Florence (Italy), 15-20/07/2018, P-CO-01.
2. **F. Clemente**, C. Matassini, M. Martínez Bailén A. Goti and F.Cardona, Stereoselective access to 8-membered iminosugars by means of allylic

organometallic reagents additions to a carbohydrate-derived aldehyde and osmium-catalyzed tethered aminohydroxylation, XXII International Conference on Organic Synthesis–22-ICOS, Florence (Italy), 16-21/09/2018, P-460.

3. **F. Clemente,** 2-substituted trihydroxy piperidines with opposite configurations as new potential pharmacological chaperones for Gaucher disease, PhDday[9], Florence (Italy), 31/05/2018, PO-4.
4. **F. Clemente**, C. Matassini, A. Goti and F.Cardona, Design, synthesis and evaluation as potential Pharmacological Chaperones for Gaucher disease of 2-substituted trihydroxy piperidines, Merck – Elsevier Young Chemist Symposium–MEYCS (XVIII edition), Rimini (Italy),19-21/11/2018, PO-7.
5. **F. Clemente**, Trihydroxypiperidines differently substituted with lipophilic alkyl chains as pharmacological chaperones for Gaucher Disease, PhDday[10], Florence (Italy), 23/05/2019, PO-17
6. **F. Clemente**, C. Matassini, A. Goti, F. Cardona, Stereoselective synthesis of C-2 alkylated trihydroxypiperidines: effect of the chain length and the configuration at C-2 on their activity as Pharmacological Chaperones for Gaucher Disease, XXXIX Convegno Nazionale della Divisione di Chimica Organica della Società Chimica Italiana (CDCO19), Torino 8-12/09/2019, OC-02.

Communications as co-author

1. C. Matassini, **F. Clemente**, A. Goti, F. Cardona "Diversely functionalized trihydroxypiperidines as novel pharmacological chaperones for Gaucher Disease: a dual synthetic strategy from the carbohydrate pool", Fourth China-Italy Bilateral Symposium on Organic Chemistry (CISOC4), Bologna, 16-17/04/2019, JOC (Junior Oral Communication) 4.